

**Physical and Chemical Treatment of Oil Sands Process-Affected  
Water with Polyaluminum Chloride and Potassium Ferrate(VI)**

by

Chengjin Wang

A thesis submitted in partial fulfillment of the requirements for the degree of

Doctor of Philosophy  
in  
Environmental Engineering

Department of Civil and Environmental Engineering  
University of Alberta

© Chengjin Wang, 2016

## ABSTRACT

This study investigated the application of polyaluminum chloride (PACl) and potassium ferrate(VI) for the treatment of oil sands process-affected water (OSPW). In addition, the performance of potassium ferrate(VI) was compared with other oxidation processes, including UV/hydrogen peroxide (H<sub>2</sub>O<sub>2</sub>), and ozonation with and without hydroxyl radical ( $\cdot$ OH) scavenger. The comparison of the performance not only involved the removal of naphthenic acids (NAs) and aromatics, but also the oxidation of sulfur and nitrogen containing species.

PACls are commonly used in water treatment with the most effective species reported to be Al<sub>13</sub>. In this research, PACl with 83.6% Al<sub>13</sub> was synthesized using the slow base titration method and compared with a commercially available PACl in terms of aluminum species distribution, coagulation/flocculation (CF) performance, floc morphology, and contaminant removal. Both coagulants were effective in removing suspended solids, achieving over 96% turbidity removal at all applied coagulant doses (0.5-3.0 mM Al). The removal efficiencies of metals varied among different metals depending on their pK<sub>a</sub> values. Metal cations with pK<sub>a</sub> values (Fe, Al, Ga, and Ti) below OSPW pH of 6.9-8.1 (dose dependent) were removed by more than 90%, while metal cations with higher pK<sub>a</sub> values (K, Na, Ca, Mg and Ni) had removals of less than 40%. NAs were not removed due to their low molecular weights, negative charges, and hydrophilic characteristics at the OSPW pH. At the highest applied coagulant dose of 3.0 mM Al, the synthetic PACl reduced *Vibrio fischeri* inhibition effect to 43.3±3.0% from 49.5±0.4% in raw OSPW. In contrast, no reduction of toxicity was found for OSPW treated with

the commercial PACl. Based on water quality and floc analyses, the dominant CF mechanism for particle removal during OSPW treatment was considered to be enmeshment in the precipitates (i.e., sweep flocculation).

Potassium ferrate(VI) showed high selectivity in oxidizing the organic fraction of OSPW. It preferentially removed two-ring and three-ring fluorescing aromatics at doses <100 mg/L Fe(VI), and one-ring aromatics were removed only at doses  $\geq$ 100 mg/L Fe(VI). Ferrate(VI) oxidation achieved 64.0% and 78.4% removal of classical NAs (NAs with two oxygen atoms) at the dose of 200 mg/L and 400 mg/L Fe(VI), respectively, and NAs with high carbon number and ring number were removed preferentially.  $^1\text{H}$  nuclear magnetic resonance ( $^1\text{H}$  NMR) spectra indicated that the oxidation of fluorescing aromatics resulted in the opening of some aromatic rings. Electron paramagnetic resonance (EPR) analysis detected the signals of organic radical intermediates, indicating that one-electron transfer is one of the probable mechanisms in the oxidation of NAs.

The efficiency of three different oxidation processes, including UV/H<sub>2</sub>O<sub>2</sub> oxidation, ferrate(VI) oxidation, and ozonation with and without ·OH scavenger tert-butyl alcohol (TBA) on the removal of organic compounds in OSPW was investigated and compared. UV/H<sub>2</sub>O<sub>2</sub> oxidation occurred through radical reaction and photolysis, transforming one-ring, two-ring, and three-ring fluorescing aromatics simultaneously and achieving 42.4% of classical NA removal at 2.0 mM H<sub>2</sub>O<sub>2</sub> and 950 mJ/cm<sup>2</sup> UV dose. Ferrate(VI) oxidation exhibited high selectivity as mentioned above. At 2.0 mM Fe(VI), 46.7% of classical NAs was removed. Ozonation achieved almost complete removal of fluorescing aromatics,

sulfur-containing NAs (NAs+S), and classical NAs (97.1% removal) at the utilized O<sub>3</sub> dose of 2.0 mM. Both molecular ozone reaction and ·OH reaction were important pathways in transforming the organics in OSPW as supported by the ozonation performance with and without TBA. All the three oxidation processes reduced the acute toxicity towards *Vibrio fischeri* and on goldfish primary kidney macrophages (PKMs), with ozonation being the most efficient process. Fourier transform ion cyclotron resonance mass spectrometry (FTICR-MS) analyses revealed that O<sub>x</sub> species (species containing no other heteroatoms except oxygen) were the dominant species among the organic species (i.e., O<sub>x</sub>; O<sub>x</sub>S<sub>y</sub>: sulfur-containing species; O<sub>x</sub>N<sub>y</sub>: nitrogen-containing species; and O<sub>x</sub>S<sub>y</sub>1N<sub>y</sub>2: sulfur and nitrogen containing species) in OSPW, accounting for 82.3% and 51.3% of the total species detected in negative and positive electrospray ionization (ESI) mode, respectively. The oxidation processes transformed the distribution profiles of O<sub>x</sub>, O<sub>x</sub>S<sub>y</sub>, and O<sub>x</sub>N<sub>y</sub> fractions, with the most significant changes occurring to O<sub>x</sub>S<sub>y</sub>. It was also noted that the selectivity of the oxidants impacted the transformation patterns, especially embodied by different performance by different oxidants detected in negative ESI mode on transforming O<sub>2</sub> to O<sub>3</sub> and/or O<sub>4</sub> and on transforming O<sub>2</sub>S to O<sub>3</sub>S and/or O<sub>4</sub>S.

## PREFACE

This thesis is an original work by Chengjin Wang, who designed and conducted the experiments, collected and analyzed the data, as well as prepared the manuscripts, under the supervision of Dr. Mohamed Gamal El-Din. Some colleagues also contributed to manuscript edits, sample analysis, or chemical preparation, and some of them were co-authors of the manuscripts submitted for publication. Some of the analyses were done in other departments of the University of Alberta, or research institutes in Edmonton, as specified below.

Chapter 2 of this thesis has been published as “Wang, C., Alpatova, A., McPhedran, K.N. and Gamal El-Din, M. (2015) Coagulation/flocculation process with polyaluminum chloride for the remediation of oil sands process-affected water: Performance and mechanism study. *Journal of Environmental Management* 160, 254-262”. Dr. Alpatova and Dr. McPhedran contributed to the manuscript edits. Surface analyses of the flocs were conducted in the Alberta Centre for Surface Engineering and Science (ACSES) at the University of Alberta and National Institute for Nanotechnology (NINT). Zeta potential and particle size were analyzed in Dr. Hongbo Zeng’s research laboratory in the Department of Chemical and Materials Engineering at the University of Alberta, while X-ray powder diffraction (XRD) analysis was done in Alberta Innovates Technology Futures. Finally, naphthenic acid (NA) quantification was conducted by Ms. Nian Sun in Dr. Gamal El-Din’s research group.

Chapter 3 has been published as “Wang, C., Klammerth, N., Huang, R., Elnakar, H. and Gamal El-Din, M. (2016) Oxidation of oil sands process-affected water by potassium ferrate(VI). *Environmental Science & Technology* 50(8), 4238-4247”. Dr. Klammerth contributed to the manuscript edits; Dr. Huang contributed to naphthenic acid analysis; and Mr. Elnakar contributed to the potassium ferrate(VI) preparation. Identification and quantification of model compounds and reaction byproducts and nuclear magnetic resonance (NMR) analysis were done in the NMR laboratory in the Department of Chemical and Materials Engineering at the University of Alberta. Electron paramagnetic resonance (EPR) analysis was conducted in Dr. Joel Weiner’s laboratory in the Department of Biochemistry Faculty of Medicine & Dentistry at the University of Alberta; and toxicity analysis on goldfish primary kidney macrophages was done in Dr. Miodrag Belosevic’s laboratory in the Department of Biological Sciences at the University of Alberta.

Chapter 4 has been published as “Wang, C., Klammerth, N., Messele, S. A., Singh, A., Belosevic, M., and Gamal El-Din, M., Comparison of UV/hydrogen peroxide, potassium ferrate(VI), and ozone in oxidizing the organic fraction of oil sands process-affected water (OSPW). *Water Research* 100, 476-485”. Dr. Klammerth and Dr. Messele contributed to manuscript edits, while Dr. Belosevic and Dr. Singh contributed to the toxicity analysis on goldfish primary kidney macrophages. NMR analysis and toxicity analysis on goldfish primary kidney macrophages were done in the same laboratories as specified for Chapter 3. NA

concentration was quantified by Dr. Rongfu Huang in Dr. Gamal El-Din's research group.

A version of Chapter 5 has been submitted to Environmental Science & Technology as “Wang, C., Huang, R., Klammerth, N., Chelme-Ayala, P., and Gamal El-Din, M., Analyses of the organic fractions in raw and oxidized oil sands process-affected water with Fourier transform ion cyclotron resonance mass spectrometry (FTICR-MS) and ultra-performance liquid chromatography time-of-flight mass spectrometry (UPLC-TOF-MS)”. Dr. Huang contributed to UPLC-TOF-MS analysis, while Dr. Klammerth and Dr. Chelme-Ayala contributed to manuscript edits. FTICR-MS analysis was carried out in the Department of Chemical and Materials Engineering at the University of Alberta.

## ACKNOWLEDGEMENTS

First, I would like to thank my supervisor Dr. Mohamed Gamal El-Din for the inspiring academic guidance and generous financial support, without which this thesis is not possible. I cherish the research experience under Dr. Gamal El-Din's supervision and the experience working as his teaching assistant, during which I benefited from his broad knowledge and professional manner.

I also would like to thank Dr. Tong Yu sincerely for offering me an opportunity to work with him. I appreciate all his kind help.

My sincere gratitude also goes to the project managers and postdoctoral fellows in Dr. Gamal El-Din's research group, who helped me revise research proposals, conference posters and presentations, paper manuscripts, and the thesis. They are Dr. Nikolaus Klamerth, Dr. Pamela Chelme-Ayala, Dr. Kerry N. McPhedran, Dr. Alla Alpatova, Dr. Yanyan Zhang, Dr. Rongfu Huang, Dr. Selamawit Ashagre Messele, and Dr. Vanessa Incani.

I also thank the technicians in Dr. Gamal El-Din's research group: Mrs. Maria Demeter and Ms. Nian Sun, who were bothered by me routinely when I worked in the laboratory. I also appreciate all the help and support I received from my friends and colleagues.

I would like to extend my appreciation to Dr. Hongbo Zeng, Dr. Bin Yan, Mr. Mark Miskolzie, Ms. Nupur Dabral, Dr. Dimitre Karpuzov, Dr. Anqiang He, Dr. Shihong Xu, Mr. Paul Concepcion, Ms. Xin (Jean) Zhang, Mr. Guangcheng Chen, Dr. Randy Whittal, Ms. Jing Zheng, Dr. Joel Weiner, and Dr. Richard Rothery

from the University of Alberta and Mr. Philip Chong from Alberta Innovates Technology Futures for their help on sample analyses.

I am very grateful for sponsors of this research, including Alberta Water Research Institute, the Helmholtz-Alberta Initiative, and a Natural Sciences and Engineering Research Council of Canada (NSERC) Senior Industrial Research Chair (IRC) in Oil Sands Tailings Water Treatment through the support by Syncrude Canada Ltd., Suncor Energy Inc., Shell Canada, Canadian Natural Resources Ltd., Total E&P Canada Ltd., EPCOR Water Services, IOWC Technologies Inc., Alberta Innovates - Energy and Environment Solution, and Alberta Environment and Parks.

Finally, I express my deep gratitude to my family for their patience and support.

*To my parents*

*To my wife Fan, and to my son Samuel*

# TABLE OF CONTENTS

1 GENERAL INTRODUCTION AND RESEARCH OBJECTIVES.....	1
1.1 Background.....	1
1.2 OSPW composition.....	3
1.2.1 Particulate matter in OSPW.....	3
1.2.2 Dissolved organic matter in OSPW.....	4
1.2.3 Metals and anions in OSPW.....	6
1.3 Scope of research and objectives.....	7
1.3.1 PACl.....	8
1.3.2 Potassium ferrate(VI).....	9
1.3.3 Research objectives.....	10
1.4 Thesis organization.....	12
1.5 References.....	15
2 COAGULATION/FLOCCULATION PROCESS WITH POLYALUMINUM CHLORIDE FOR THE REMEDIATION OF OIL SANDS PROCESS- AFFECTED WATER: PERFORMANCE AND MECHANISM STUDY.....	27
2.1 Introduction.....	27
2.2 Materials and methods.....	30
2.2.1 OSPW and chemicals.....	30
2.2.2 Coagulation and flocculation test.....	31
2.2.3 Water quality analysis.....	32
2.2.4 Coagulants, flocs and particle analysis.....	33
2.3. Results and discussion.....	36
2.3.1 Raw OSPW water quality.....	36
2.3.2 Characterization of synthetic and commercial PACl.....	39

2.3.3 Coagulation performance.....	41
2.3.3.1 Turbidity removal .....	41
2.3.3.2 Organic matter removal .....	45
2.3.3.3 Metals.....	49
2.3.3.4 Acute toxicity on <i>Vibrio fischeri</i> .....	50
2.3.4 Floc analysis after sedimentation.....	52
2.4 Conclusions.....	56
2.5 References.....	58
3 OXIDATION OF OIL SANDS PROCESS-AFFECTED WATER BY POTASSIUM FERRATE(VI) .....	64
3.1 Introduction.....	64
3.2 Materials and methods .....	67
3.2.1 OSPW and chemicals.....	67
3.2.2 Experimental design.....	67
3.2.2.1 OSPW Study .....	67
3.2.2.2 Water Quality Analysis for the OSPW Study .....	68
3.2.2.3 Model Compound Study .....	71
3.3 Results and discussion .....	72
3.3.1 Analyses of raw OSPW .....	72
3.3.3 Organic matter removal .....	76
3.3.3.1 Removal of aromatics .....	76
3.3.3.2 Removal of NAs .....	79
3.3.4 Removal mechanisms .....	83
3.3.4.1 Oxidation vs coagulation.....	83
3.3.4.2 Oxidative species .....	85

3.3.4.3 Oxidation mechanisms of aromatics and NAs.....	87
3.3.4.4 Electron paramagnetic resonance analysis.....	88
3.3.4.5 Model compound study.....	89
3.3.5 Toxicity .....	92
3.3.6 pH adjustment .....	95
3.3.7 Environmental implications .....	97
3.4 References.....	98
<b>4 COMPARISON OF UV/HYDROGEN PEROXIDE, POTASSIUM FERRATE(VI), AND OZONE IN OXIDIZING THE ORGANIC FRACTION OF OIL SANDS PROCESS-AFFECTED WATER (OSPW).....</b>	<b>109</b>
4.1 Introduction.....	109
4.2 Materials and methods .....	112
4.2.1 OSPW and chemicals.....	112
4.2.2 Experimental design.....	113
4.3 Results and discussion .....	118
4.3.1 SFS analysis .....	118
4.3.3 Quantification of NAs by UPLC-TOF-MS.....	123
4.3.3.1 Classical NAs.....	123
4.3.3.2 NAs+O and NAs+O <sub>2</sub> .....	127
4.3.5 Toxicity .....	139
4.3.6 Cost comparison.....	142
4.4 Conclusions.....	144
References.....	146
<b>5 ANALYSES OF THE ORGANIC FRACTIONS IN RAW AND OXIDIZED OIL SANDS PROCESS-AFFECTED WATER WITH FOURIER TRANSFORM ION CYCLOTRON RESONANCE MASS SPECTROMETRY AND ULTRA-</b>	

PERFORMANCE LIQUID CHROMATOGRAPHY TIME-OF-FLIGHT MASS SPECTROMETRY .....	157
5.1 Introduction.....	157
5.2 Materials and methods .....	160
5.2.1 Raw OSPW and chemicals .....	160
5.2.2 Experimental design.....	160
5.2.3 FTICR-MS analysis .....	161
5.2.4 UPLC-TOF-MS analysis .....	162
5.3 Results and discussion .....	163
5.3.1 FTICR-MS results.....	164
5.3.1.1 Transformation of O <sub>x</sub> species.....	164
5.3.1.3 Transformation of sulfur-containing species .....	173
5.3.1.4 Transformation of nitrogen-containing species .....	176
5.3.2 UPLC-TOF-MS results .....	178
5.3.2.1 Total ion chromatograms (TICs) .....	178
5.3.2.2 Negative mode results.....	180
5.3.2.3 Positive mode results .....	185
5.3.3 Environmental significance .....	188
5.4 References.....	189
6 CONCLUSIONS AND RECOMMENDATIONS .....	196
6.1 Thesis overview .....	196
6.2 Conclusions.....	197
6.2.1 New findings on OSPW composition.....	198
6.2.2 Coagulation and flocculation with PACl .....	199
6.2.3 Ferrate(VI) oxidation .....	200

6.2.4 Comparison experiment with ferrate(VI), UV/H <sub>2</sub> O <sub>2</sub> , and ozonation.	201
6.2.5 FTICR-MS vs UPLC-TOF-MS.....	202
6.3 Recommendations.....	203
APPENDIX A. STANDARD CURVE FOR ALUMINUM SPECIES QUANTIFICATION BY <sup>27</sup> AL NMR.....	206
APPENDIX B. XRD SPECTRUM OF THE MINERALS IN RAW OSPW.....	208
APPENDIX C. IN VITRO ASSAY ON GOLDFISH PRIMARY KIDNEY MACROPHAGES .....	209
APPENDIX D. MEASUREMENT OF THE MODEL COMPOUND CONCENTRATION AND IDENTIFICATION OF THE END PRODUCTS IN THE FERRATE(VI) STUDY .....	211
APPENDIX E. ESTIMATION OF THE MOLAR RATIO OF AROMATIC ORGANIC MATTER OVER TOTAL NA <sub>S</sub> .....	217
APPENDIX F. RELATIVE ABUNDANCE OF THE DETECTED SPECIES IN RAW AND OXIDIZED OSPW .....	219
BIBLIOGRAPHY.....	223

## LIST OF TABLES

Table 2.1 Water quality analysis of raw OSPW (n = 3; mean±standard deviation)	37
Table 2.2 Characteristics of synthetic and commercial PACl	40
Table 4.1 Water quality of raw OSPW	113
Table 4. 2 Summary of NA removal by different oxidation processes	129
Table 4.3 Assumptions for cost estimate	142
Table 4.4 CapEx <sup>a</sup> and OpEx <sup>b</sup> analyses for the oxidation processes (chemical dose: 2.0 mM)	143
Table A1 HPLC solvent gradient for the measurement of model compound concentration	212
Table A2 HPLC solvent gradient for detecting oxidation products of CHPA	212
Table A3 HPLC solvent gradient for detecting oxidation products of CHA and ADA	213
Table A4 Estimation of molar ratio of aromatics over organic acids	218
Table A5 Relative abundance of O <sub>x</sub> , O <sub>x</sub> S <sub>y</sub> , and O <sub>x</sub> N <sub>y</sub> out of total organic species detected by FTICR-MS in negative ESI mode	219
Table A6 Relative abundance of O <sub>x</sub> , O <sub>x</sub> S <sub>y</sub> , and O <sub>x</sub> N <sub>y</sub> out of total organic species detected by FTICR-MS in positive ESI mode	219
Table A7 Relative abundance of specific O <sub>x</sub> species out of total O <sub>x</sub> species detected by FTICR-MS in negative ESI mode	219
Table A8 Relative abundance of specific O <sub>x</sub> species out of total O <sub>x</sub> species detected by FTICR-MS in positive ESI mode	220
Table A9 Relative abundance of specific O <sub>x</sub> S <sub>y</sub> species out of total O <sub>x</sub> S <sub>y</sub> species detected by FTICR-MS in negative ESI mode	220
Table A10 Relative abundance of specific O <sub>x</sub> S <sub>y</sub> species out of total O <sub>x</sub> S <sub>y</sub> species detected by FTICR-MS in positive ESI mode	220
Table A11 Relative abundance of specific O <sub>x</sub> N <sub>y</sub> species out of total O <sub>x</sub> N <sub>y</sub> species detected by FTICR-MS in negative ESI mode	221

Table A12 Relative abundance of specific $O_xN_y$ species out of total $O_xN_y$ species detected by FTICR-MS in positive ESI mode .....	221
Table A13 Relative abundance of specific $O_x$ species out of total $O_x$ species detected by UPLC-TOF-MS in negative ESI mode .....	221
Table A14 Relative abundance of specific $O_x$ species out of total $O_x$ species detected by UPLC-TOF-MS in positive ESI mode .....	222

## LIST OF FIGURES

Figure 2.1 (a) SEM image of raw OSPW solids, (b) distribution of main minerals in OSPW, and (c) particle size distribution in OSPW .....	38
Figure 2.2 <sup>27</sup> Al NMR spectra of (a) synthetic PACl and (b) commercial PACl (Note: aluminum concentration in each coagulant solution was 0.05 M; aluminum concentration in the internal standard was 0.1 M).....	40
Figure 2.3 Changes in (a) turbidity, (b) zeta potential, (c) pH, (d) TOC, (e) DOC and (f) UV <sub>254</sub> at different applied PACl doses (Note: error bars indicate mean±SD with n=3).....	42
Figure 2.4 Flocs formed in the CF process with (a) synthetic PACl and (b) commercial PACl during the flocculation process (coagulant dose: 0.5 mM Al) 44	
Figure 2.5 Representative SEM image of the flocs formed upon synthetic PACl treatment (coagulant dose of 2.0 mM Al).....	44
Figure 2.6 SEM images of flocs and element distribution maps of aluminum and silicon measured with EDS: (a) SEM image of the flocs formed with synthetic PACl, (b) Si distribution on synthetic PACl flocs, (c) Al distribution on synthetic PACl flocs, (d) SEM image of the flocs formed with commercial PACl, (e) Si distribution on commercial PACl flocs, and (f) Al distribution on commercial PACl flocs (coagulant dose: 2.0 mM Al).....	45
Figure 2.7 Concentration of NAs species in (a) raw OSPW, (b) synthetic PACl-treated OSPW (applied dose: 3.0 mM Al), and (c) commercial PACl-treated OSPW (applied dose: 3.0 mM Al) (Note: z number is a negative even number and -z indicates the deficiency of hydrogen compared with saturated acyclic organic molecules).....	48
Figure 2.8 Representative metal removal (%) by PACl vs pK <sub>a</sub> of the metal cations at an applied coagulant dose of 1.5 mM Al. (Note: error bars indicate mean±SD with n=3).....	50
Figure 2.9 Acute toxicity to <i>Vibrio fischeri</i> of raw OSPW and PACl-treated OSPW (Note: error bars indicate mean±SD with n=3).....	51
Figure 2.10 Representative SEM images of the frozen flocs formed at a coagulant does of 2.0 mM Al for synthetic PACl (a and c) and commercial PACl (b and d) .....	52
Figure 2.11 Element distribution on the surface of raw OSPW solids and flocs analyzed by EDS at a representative coagulant dose of 2.0 mM Al: (a) carbon (C), aluminum (Al), silicon (Si) and oxygen (O); and (b) sodium (Na), chlorine (Cl), magnesium (Mg), calcium (Ca), iron (Fe), and potassium (K).....	54

Figure 2.12 XPS survey spectra of (a) raw OSPW solids, (b) flocs formed with synthetic PACl and (c) flocs formed with commercial PACl (coagulant dose: 2.0 mM Al).....	55
Figure 2.13 Positive mode SIMS spectra of the (a) raw OSPW solids, (b) synthetic PACl flocs, and (c) commercial PACl flocs (scan area: 500 $\mu\text{m}$ $\times$ 500 $\mu\text{m}$ ; coagulant dose: 2.0 mM Al) (Note: consult discussion for information on areas highlighted with dashed ovals) .....	56
Figure 3.1 Spectroscopic analyses of raw OSPW: (a) $^1\text{H}$ NMR spectrum (the numbers below the scale are the integrated peak area for each fraction with a total of 100), (b) FT-IR spectrum, (c) UV-Visible light absorption spectrum, and (d) SFS.....	73
Figure 3.2 Change of (a) residual ferrate(VI) concentration and (b) pH with reaction time, and (c) final pH of oxidized OSPW at different doses of ferrate(VI) .....	76
Figure 3.3 (a) $^1\text{H}$ NMR spectra for 200 mg/L Fe (VI)-treated OSPW (the numbers besides the peaks indicate the relative peak area when the DMSO solvent peak was set to be 100 as internal standard) and (b) SFS of raw and treated OSPW ...	77
Figure 3.4 Ion mobility spectra for (a) raw OSPW, (b) ferrate(VI)-treated OSPW (200 mg/L), and (c) ferrate(VI)-treated OSPW (400 mg/L); classical NAs distribution in (d) raw OSPW, (e) ferrate(VI)-treated OSPW (200 mg/L) and (f) ferrate(VI)-treated OSPW (400 mg/L); and classical NAs removal with respect to (g) carbon number and (h) -z number .....	79
Figure 3.5 Concentration of NAs+O in (a) raw OSPW, (b) 200 mg/L Fe(VI)-treated OSPW, (c) 400 mg/L Fe(VI) treated-OSPW; and concentration of NAs+O <sub>2</sub> in (d) raw OSPW, (e) 200 mg/L Fe(VI)-treated OSPW, and (f) 400 mg/L Fe(VI)-treated OSPW.....	81
Figure 3.6 Raw OSPW and 200 mg/L ferrate(VI)-treated OSPW (pH adjusted to 2.5) .....	83
Figure 3.7 Ferrate(VI) vs ferric in OSPW treatment: (a) SFS of raw OSPW and ferric-treated OSPW, (b) UV <sub>254</sub> removal, (c) AEF removal, and (d) inhibition effect on <i>Vibrio fischeri</i> .....	85
Figure 3.8 Distribution diagram of Fe(VI) species.....	86
Figure 3.9 EPR spectrum of the reaction mixture of OSPW, 100 mg/L Fe(VI) and 10g/L POBN .....	88
Figure 3.10 Model compound degradation by ferrate(VI) (dose: 200 mg/L Fe(VI)) at different reaction time (Note: initial concentration of each model compound is 60 mg/L).....	90

Figure 3.11 (a) Acute toxicity to *Vibrio fischeri* of raw OSPW and ferrate(VI)-treated OSPW (Note: error bars indicate mean±SD with n=3); (b) Nitrite production by PKMs exposed to medium control, raw OSPW, and OSPW treated with ferrate (VI) with the dose of 25 mg/L and 100 mg/L Fe(VI). Positive and negative controls were heat killed *A. salm onicida* and culture medium, respectively. Nitric oxide production was determined using the Griess reaction and RNI concentration was determined using RNI standard curve. Data are represented as RNI production by macrophages from separate cultures established from three individual fish. Statistical analysis was done using one-way ANOVA with a Dunnett's post hoc test. Asterisks (\*) indicate statistically significant increases ( $p < 0.05$ ) of RNI production in treated compared to raw OSPW ..... 93

Figure 3.12 (a) Integrated peak area of SFS at different ferrate(VI) dose; (b) Linear relationship between inhibition effect and integrated peak area in the SFS ..... 94

Figure 3.13 Oxidation performance by ferrate(VI) at initial pH 6: (a) SFS, (b) SFS peak area, (c) NAs distribution (dose: 200 mg/L Fe(VI)), and (d) inhibition effect on *Vibrio fischeri* (For comparison reason, oxidation performance by ferrate(VI) at natural pH was replotted in b and d) ..... 96

Figure 4.1 Quasi-collimated beam UV apparatus 115

Figure 4.2 Absorption spectra of the raw OSPW and 2.0 mM H<sub>2</sub>O<sub>2</sub> in Milli-Q water, and irradiance spectrum of the medium pressure mercury lamp ..... 116

Figure 4.3 SFS of raw OSPW and OSPW oxidized by UV/H<sub>2</sub>O<sub>2</sub> (a), ferrate(VI) (b), O<sub>3</sub> with and without TBA (c and d) ..... 119

Figure 4.4 Ion mobility spectra for raw OSPW (a), UV-treated OSPW (no H<sub>2</sub>O<sub>2</sub>) (b), UV/H<sub>2</sub>O<sub>2</sub>- treated OSPW (c, d), ferrate(VI)-treated OSPW (e, f), O<sub>3</sub>-treated OSPW with and without TBA (g, h, i, and j)..... 122

Figure 4.5 Classical NAs distribution in raw OSPW (a), UV treated OSPW (b), ferrate(VI)-treated OSPW (c,d), UV/H<sub>2</sub>O<sub>2</sub>- treated OSPW (e, f), and O<sub>3</sub>-treated OSPW with and without TBA (g, h, i and j)..... 124

Figure 4.6 Classical NA removal with respect to carbon number (a) and -z number (b)..... 125

Figure 4.7 NAs+O distribution in raw OSPW (a), UV treated OSPW (b), ferrate(VI)-treated OSPW (c,d), UV/H<sub>2</sub>O<sub>2</sub>- treated OSPW (e, f), and O<sub>3</sub>-treated OSPW with and without TBA (g, h, i and j)..... 130

Figure 4.8 NAs+O distribution in raw OSPW and treated OSPW with respect to carbon number (a) and -z number (b)..... 131

Figure 4.9 NAs+O<sub>2</sub> distribution in raw OSPW (a), UV treated OSPW (b), ferrate(VI)-treated OSPW (c,d), UV/H<sub>2</sub>O<sub>2</sub>- treated OSPW (e, f), and O<sub>3</sub>-treated OSPW with and without TBA (g, h, i and j)..... 132

Figure 4.10 NAs+O<sub>2</sub> distribution in raw OSPW and treated OSPW with respect to carbon number (a) and -z number (b)..... 133

Figure 4.11 <sup>1</sup>H NMR spectra (a) and <sup>13</sup>C NMR spectra (b) for the organics in raw OSPW and treated OSPW (Note: the numbers besides the peaks indicate the relative peak area as the DMSO solvent peak was set to be 100 as internal standard, and the numbers in the brackets are the peak reduction relative to the corresponding raw OSPW peak area)..... 135

Figure 4.12 (a) Inhibition effect on *Vibrio fischeri* caused by raw OSPW and OSPW treated with UV/H<sub>2</sub>O<sub>2</sub> ferrate (VI) and ozone, (b) Nitrite production by PKMs exposed to medium control, raw OSPW, and OSPW treated with UV/H<sub>2</sub>O<sub>2</sub>, ferrate (VI), and ozone (data for ozonation with TBA is not shown due to the interference on inhibition effect from TBA). Positive and negative controls were heat killed *A. salmon icida* and culture medium, respectively. Nitric oxide production was determined using the Griess reaction and RNI concentration was determined using RNI standard curve. Data are represented as mean ± SEM RNI production by macrophages from separate cultures established from three individual fish (n = 3). Statistical analysis was done using one-way ANOVA with a Dunnett's post hoc test. Asterisks (\*) indicate statistically significant increases (p <0.05) of RNI production in treated compared to raw OSPW ..... 140

Figure 5.1 Fractions of organics in raw and treated OSPWs detected by FTICR-MS: relative abundance of O<sub>x</sub>, O<sub>x</sub>S<sub>y</sub>, and O<sub>x</sub>N<sub>y</sub> out of the total organic species detected in negative ESI mode (a) and positive ESI mode (b), and relative abundance of O, O<sub>2</sub>, O<sub>3</sub>, O<sub>4</sub>, O<sub>5</sub>, O<sub>6</sub>, O<sub>7</sub>, and O<sub>8</sub> species out of the total O<sub>x</sub> species detected in negative ESI mode (c) and positive ESI mode (d), and relative abundance of S, OS, O<sub>2</sub>S, O<sub>3</sub>S, O<sub>4</sub>S, O<sub>5</sub>S, O<sub>6</sub>S, S<sub>2</sub>, OS<sub>2</sub>, O<sub>2</sub>S<sub>2</sub>, O<sub>4</sub>S<sub>2</sub>, and O<sub>6</sub>S<sub>2</sub> species out of the total sulfur containing species detected by FTICR-MS in negative ESI mode (e) and positive ESI mode (f) 165

Figure 5.2 Relative abundance of ON, O<sub>2</sub>N, O<sub>3</sub>N, O<sub>4</sub>N, O<sub>5</sub>N, O<sub>x</sub>N<sub>2</sub> species out of total nitrogen containing species in raw and treated OSPWs measured by FTICR-MS in negative ESI mode (a) and positive ESI mode (b)..... 166

Figure 5.3 Carbon number and -z number distribution of O<sub>2</sub> species in raw OSPW (a,b), ferrate(VI)-treated OSPW (c,d), UV/H<sub>2</sub>O<sub>2</sub>-treated OSPW (e,f), ozonated OSPW (g,h), and ozonated TBA-spiked OSPW (i,j) detected by FTICR-MS in negative and positive ESI modes ..... 168

Figure 5.4 Carbon number and -z number distribution of total O<sub>x</sub> species in raw OSPW (a,b), ferrate(VI)-treated OSPW (c,d), UV/H<sub>2</sub>O<sub>2</sub>-treated OSPW (e,f),

ozonated OSPW (g,h), and ozonated TBA-spiked OSPW (i,j) detected by FTICR-MS in negative and positive ESI modes.....	169
Figure 5.5 DCM extracted organic fractions of OSPW .....	170
Figure 5.6 Carbon number and -z number distribution of O <sub>x</sub> N species in raw OSPW (a), ferrate(VI)-treated OSPW (b), UV/H <sub>2</sub> O <sub>2</sub> -treated OSPW (c), ozonated OSPW (d), and ozonated TBA-spiked OSPW (e) detected by FTICR-MS in positive ESI mode.....	177
Figure 5.7 TICs of the raw OSPW acquired in negative and positive ESI modes (a), and the retention time distribution of the species detected by UPLC-TOF-MS in negative ESI mode (b) and positive ESI mode (c).....	179
Figure 5.8 Concentrations of O <sub>x</sub> species in raw OSPW and treated OSPW detected by UPLC-TOF-MS in negative ESI mode (a), and relative abundance of O <sub>x</sub> species detected in positive ESI mode (b) .....	181
Figure 5.9 Carbon number and -z number distribution of O <sub>2</sub> species in raw OSPW (a,b), ferrate(VI)-treated OSPW (c,d), UV/H <sub>2</sub> O <sub>2</sub> -treated OSPW (e,f), ozonated OSPW (g,h), and ozonated TBA-spiked OSPW (i,j) detected by UPLC-TOF-MS in negative and positive ESI mode.....	182
Figure 5.10 Carbon number and -z number distribution of total O <sub>x</sub> species in raw OSPW (a,b), ferrate(VI)-treated OSPW (c,d), UV/H <sub>2</sub> O <sub>2</sub> -treated OSPW (e,f), ozonated OSPW (g,h), and ozonated TBA-spiked OSPW (i,j) detected by UPLC-TOF-MS in negative and positive ESI mode.....	183
Figure 5.11 The difference of relative abundance of O <sub>x</sub> species with different carbon number detected with negative mode FTICR-MS and UPLC-TOF-MS in raw OSPW (a), OSPW treated by ferrate(VI) (b), UV/H <sub>2</sub> O <sub>2</sub> (c), ozonation without TBA (d), and ozonation with TBA (e) ( $\Delta_{\text{Relative abundance}} = \text{Relative abundance detected with FTICR-MS} - \text{Relative abundance detected with UPLC-TOF-MS}$ , and the relative abundance is out of the total O <sub>x</sub> species. Only results based on major species O <sub>2</sub> , O <sub>3</sub> , O <sub>4</sub> , and O <sub>5</sub> were plotted).....	184
Figure 5.12 The difference of relative abundance of O <sub>x</sub> species with different -z number detected with negative mode FTICR-MS and UPLC-TOF-MS in raw OSPW (a), OSPW treated by ferrate(VI) (b), UV/H <sub>2</sub> O <sub>2</sub> (c), ozonation without TBA (d), and ozonation with TBA (e) ( $\Delta_{\text{Relative abundance}} = \text{Relative abundance detected with FTICR-MS} - \text{Relative abundance detected with UPLC-TOF-MS}$ ,	

and the relative abundance is out of the total O <sub>x</sub> species. Only results based on major species O <sub>2</sub> , O <sub>3</sub> , O <sub>4</sub> , and O <sub>5</sub> were plotted).....	186
Figure 5.13 Correlation between relative abundance of O <sub>x</sub> species detected by UPLC-TOF-MS and FTICR-MS (for each sample, the relative abundance of O <sub>2</sub> , O <sub>3</sub> , O <sub>4</sub> , O <sub>5</sub> , and O <sub>6</sub> out of total O <sub>x</sub> species was used).....	187
Figure A1 Relative peak area of Al <sup>3+</sup> versus its concentration (the peak area was relative to AlO <sub>2</sub> <sup>-</sup> peak area which was set to be 100; AlO <sub>2</sub> <sup>-</sup> solution was in the inner NMR tube with 3 mm OD and the Al(NO <sub>3</sub> ) <sub>3</sub> solution was in the outer NMR tube with 5 mm OD)	206
Figure A2 <sup>27</sup> Al NMR spectra for Al(NO <sub>3</sub> ) <sub>3</sub> standard samples: (a) 0.0142 mM Al; (b) 0.0284 mM Al; (c) 0.0568 mM Al; and (d) 0.1136 mM Al (NaAlO <sub>2</sub> was used as internal standard, and its peak area was set to be 100 in each spectrum).....	207
Figure A3 XRD spectrum of the minerals in raw OSPW .....	208
Figure A4 Extracted-ion chromatogram (EIC) of (a) model compound cyclohexanecarboxylic acid (C <sub>7</sub> H <sub>12</sub> O <sub>2</sub> , CHA), product 1 (C <sub>7</sub> H <sub>12</sub> O <sub>3</sub> , blue color), and product 2 (C <sub>7</sub> H <sub>10</sub> O <sub>3</sub> , red color) in ferrate(VI) oxidized CHA solution (200 mg/L Fe(VI), 180 min); product peaks were replotted with new scale in (b) for product 1 (C <sub>7</sub> H <sub>12</sub> O <sub>3</sub> ), and (c) for product 2 (C <sub>7</sub> H <sub>10</sub> O <sub>3</sub> ) (The peak composition regarding the m/z ratios was also provided in the inlaid figures for each peak).	214
Figure A5 Extracted-ion chromatogram (EIC) of (a) model compound cyclohexanepentanoic acid (C <sub>11</sub> H <sub>20</sub> O <sub>2</sub> , CHPA), product 1 (C <sub>11</sub> H <sub>20</sub> O <sub>3</sub> ), and product 2 (C <sub>11</sub> H <sub>18</sub> O <sub>3</sub> ) in ferrate(VI) oxidized CHPA solution (200 mg/L Fe(VI), 180 min); product peaks were replotted with new scale in (b) for product 1 (C <sub>11</sub> H <sub>20</sub> O <sub>3</sub> ), and (c) for product 2 (C <sub>11</sub> H <sub>18</sub> O <sub>3</sub> ) (The peak composition regarding the m/z ratios was also provided in the inlaid figures for each peak).....	215
Figure A6 Extracted-ion chromatogram (EIC) of (a) model compound 1,3-adamantanedicarboxylic acid (C <sub>12</sub> H <sub>16</sub> O <sub>4</sub> , ADA), product 1 (C <sub>12</sub> H <sub>16</sub> O <sub>5</sub> ), and product 2 (C <sub>12</sub> H <sub>14</sub> O <sub>5</sub> ) in ferrate(VI) oxidized ADA solution (200 mg/L Fe(VI), 180 min); product peaks were replotted in (b) for product 1 (C <sub>12</sub> H <sub>16</sub> O <sub>5</sub> ), and (c) for product 2 (C <sub>12</sub> H <sub>14</sub> O <sub>5</sub> ) (The peak composition regarding the m/z ratios was also provided in the inlaid figures for each peak) .....	216

# 1 GENERAL INTRODUCTION AND RESEARCH OBJECTIVES

## 1.1 Background

Oil sands, also known as bituminous sands, are “sands deposits impregnated with dense, viscous petroleum” (Speight 2000). The largest oil sands deposits are located in Alberta, Canada, with an estimated reserve of 1.7-2.5 trillion of barrels of bitumen in the ground of the Athabasca area (60-70% of the total reserve in Alberta), the neighbouring Peace River area (~15%) and Cold Lake area (~15%) (Hirsch 2005, Mackinnon and Zubot 2013, Speight 2000). Alberta’s first commercial bitumen production from oil sands started in 1967, and expanded fast in recent years (Sobkowicz 2010). In 2014, 2.3 million barrels/day of bitumen were produced from Alberta oil sands, supplying 2.5% of the global oil consumption (Alberta Government 2015).

Oil sands composition varies with location and depth, containing 1-20% (by weight) of bitumen, 1-10% of formation water, and the rest are mainly minerals such as sands, clays, and slits (Mackinnon and Zubot 2013). The bitumen is extracted from oil sands by surface mining for deposits near the surface (30-75m) and by *in-situ* extraction for those much deeper in the ground (Hirsch 2005). Briefly, for surface mining, the oil sands are excavated by giant trucks and brought to a crusher and slurry operation; for *in-situ* extraction, steam or solvent is injected into the oil sands deposits to loosen the thick bitumen, and then it will be drawn to surface (Hirsch 2005). Current hot-water bitumen recovery and the following upgrading use about 2 to 2.5 m<sup>3</sup> water for one m<sup>3</sup> crude oil production

(Zubot 2010), generating large amount of slurries, which will settle in the tailing ponds into three layer: the course sands at the bottom, the fine tailings in the middle, named fluid fine tailing (FFT) or mature find tailing (MFT), and a water layer at the top (Mackinnon and Zubot 2013). The top water layer, also known as oil sands process-affected water (OSPW), has been intensively studied in the water treatment area for its reuse and possible discharge into the environment. The toxicity of OSPW has been reported on model plant *Arabidopsis thaliana* (Leishman et al. 2013), bacterium *Vibrio fischeri* (Wang et al. 2013, Zhang et al. 2015), microalgae *Pseudokirchneriella subcapitata* (Debenest et al. 2012), fishes including fathead minnow (He et al. 2012), walleye (Marentette et al. 2015), goldfish (Hagen et al. 2012, Klamerth et al. 2015), and Japanese medaka (Alharbi et al. 2016), and mammals such as the mouse (Garcia-Garcia et al. 2011, Wang et al. 2013) and Wistar rat (Rogers et al. 2002), which warrants the current non-release policy on the OSPW and prompts extensive studies on OSPW treatment.

Different water treatment processes have been studied to remove pollutants from the OSPW and to reduce the toxicity, including (1) physical treatments such as coagulation/flocculation (CF) with alum (Pourrezaei et al. 2011b), adsorption by activated carbon (Islam et al. 2016), petroleum coke (Pourrezaei et al. 2014, Zubot et al. 2012) and graphite (Moustafa et al. 2014), and filtration with different types of membrane (Alpatova et al. 2013, Alpatova et al. 2015, Dong et al. 2014); (2) chemical treatments such as chlorine oxidation (Shu et al. 2014), ozonation (Gamal El-Din et al. 2011), and various advanced oxidation processes (AOPs) including UV/chlorine (Shu et al. 2014), UV/H<sub>2</sub>O<sub>2</sub> (Afzal et al. 2012),

peroxydisulfate oxidation (Drzewicz et al. 2012), solar photocatalytic degradation (Leshuk et al. 2016), and combined ozonation and ultrasonication (Headley et al. 2015a); and (3) various biological treatments with different microorganisms and reactors (Huang et al. 2015a, Hwang et al. 2013, Islam et al. 2014, Quesnel et al. 2015, Shi et al. 2015, Xue et al. 2016, Zhang et al. 2015).

## **1.2 OSPW composition**

OSPW is a type of water with high salinity and alkalinity, and it contains varieties of metals, anions, and organic compounds as well as suspended particles (Bauer 2013). The complexity of the water quality is mainly caused by the ore leaching, chemical addition during the extraction and upgrading processes, bitumen leftover, chemical addition for tailing amendments, and is further impacted by physical, chemical and microbial activities in the tailing ponds (Mackinnon and Zubot 2013). The following sections present a summary of some major components in OSPW, including suspended particles, organic matters, and salts (i.e., metals and anions).

### **1.2.1 Particulate matter in OSPW**

After settling in the tailing ponds, the total suspended solid (TSS) in the top layer OSPW is <0.1% (by weight) (Mackinnon and Zubot 2013). For example, Wang et al. (2013) reported a concentration of TSS of 124 mg/L. Depending on the sources of OSPW and the aging time, the particles in raw OSPW give the water a turbidity of 25-200 NTU (Dong et al. 2014, Kim et al. 2013, Pourrezaei et al. 2011b, Wang et al. 2015). The particles in raw OSPW have variable shapes and sizes and the X-ray powder diffraction (XRD) results indicate that the mineral species in OSPW

are dominated by quartz (60%) and clay minerals including kaolinite (25%) and illite (15%) (Wang et al. 2015). The distribution of minerals in OSPW is consistent with the mineral distribution in MFT and fine minerals in the oil sands (Chalaturnyk et al. 2002). For example, the dominant mineral in oil sands is quartz, and the major clay components of the McMurray Formation are kaolinite and illite (fine micas) which account for 40%-70% and 30%-45% of clay, respectively (Chalaturnyk et al. 2002). Particle size in raw OSPW ranges from 0.2  $\mu\text{m}$  to 1.0  $\mu\text{m}$ , with the average particle being around 0.5  $\mu\text{m}$  (Wang et al. 2015). The surface of these particles is negatively charged, with the reported zeta potential being -40 mV (Pourrezaei et al. 2011b). The small sizes and negative surfaces of these particles contribute to their stability in OSPW which makes them difficult to remove in the various treatment processes.

### **1.2.2 Dissolved organic matter in OSPW**

The composition of the organic fraction of OSPW is very complex, and the identification and quantification of the species in it are ongoing research topics (Headley et al. 2015b, Huang et al. 2015b). So far, it has been reported that the organic fraction of OSPW contains naphthenic acids (NAs), sulfur and nitrogen containing species, and aromatic compounds including trace amount of polyaromatic hydrocarbon (PAH) (Jones et al. 2013, Mohamed et al. 2013, Quagraine et al. 2005, Zhang et al. 2015). NAs refers to a mixture of alkyl-substituted acyclic and cycloaliphatic carboxylic acids, with a general formula  $\text{C}_n\text{H}_{2n+z}\text{O}_x$ , where n indicates the number of carbon atoms, z specifies the hydrogen deficiency, and x is the number of oxygen atoms (Jones et al. 2013,

Mohamed et al. 2013). These acids are thought to be derived from hydrocarbons via natural biodegradation pathways such as  $\alpha$ - and  $\beta$ -oxidation of alkyl substituents (Lengger et al. 2013). So far focus of OSPW treatment has been put on removing classical NAs (NAs with  $x=2$ ) (Garcia-Garcia et al. 2011, Wang et al. 2015, Zhang et al. 2015) which have been reported to be “the most acutely toxic chemical classes in OSPW” (Morandi et al. 2015). NAs with more oxygens (oxy-NAs,  $x>2$ ) are reported to be less toxic than the classical NAs due to the increase of hydrophilicity after oxidation (i.e., less affinity to cell membrane) (Frank et al. 2009, Frank et al. 2008, He et al. 2010). The total concentrations of NAs can be measured with the Fourier transform infrared spectroscopy (FT-IR) method, and the distribution of each NA species can be measured with high resolution mass spectrometry (HR-MS), such as ultra-performance liquid chromatography time-of-flight mass spectrometry (UPLC-TOF-MS) (Pourrezaei et al. 2011a), Orbitrap-MS (Pereira et al. 2013) and Fourier transform ion cyclotron resonance mass spectrometry (FTICR-MS) (Barrow et al. 2015, Headley et al. 2015a). For classical NAs, it has been reported that their concentration in OSPW ranged from 9 to 43 mg/L (Alpatova et al. 2014, Islam et al. 2014, Pourrezaei et al. 2011a), and two to three rings compounds, including five and six carbon member rings, or a combination of the two, dominated in the NAs mixture (Zubot 2010).

However, these “NAs-centered” ideas have been challenged by studies incorporating other organic species into the research scope thanks to the application of high resolution mass spectrometry. For example, Scarlett et al. (2013) suggested that aromatics in OSPW are at least as toxic as NAs. On the

other hand, a recent study by Alharbi et al. (2016) concluded that NAs “did not appear to be the cause of the inhibition” of the ATP-binding cassette (ABC) transport proteins; instead, sulfur and nitrogen containing species detected in positive ionization mode might be the inhibitors. Similarly, Quesnel et al. (2015)’s research attributed the reduced toxicity towards *S. pombe* cells to the removal of O<sub>3</sub>S species. These diverse and sometimes controversial conclusions from OSPW toxicity studies warranted the inclusion of aromatics, and sulfur and nitrogen-containing species in evaluating the OSPW remediation processes in future studies. At the same time, more research is needed from the analytical perspective to elucidate the molecular structure of these sulfur and nitrogen containing species.

### **1.2.3 Metals and anions in OSPW**

Due to the use of saline water, the leaching of ore and the addition of NaOH in the bitumen extraction process, large amounts of sodium remain in OSPW (Mikula et al. 1996). The reported concentrations of sodium in OSPW range from 700-1000 mg/L (Wang 2011, Zubot 2010). Potassium, magnesium, and aluminum which are the main cations in the minerals of oil sands, and calcium which is added as coagulant to condition the solids in the tailing ponds, exist in OSPW at relatively high concentration of 8-20 mg/L as reported by Wang (2011) and Pourrezaei et al. (2011). Other metals ions including iron, zinc, barium, copper, vanadium and nickel are also detected. With a large amount of organic compounds in OSPW, metal-organic matter complexes are supposed to exist in OSPW.

The major anions in OSPW are chloride (390-970 mg/L), sulphate (300-500 mg/L) and bicarbonate (alkalinity value: 600-800 mg/L as CaCO<sub>3</sub>) (Pourrezaei et al. 2011a, Zubot 2010). Since the pH is a function of alkalinity for a given pCO<sub>2</sub> (Stumm and Morgan 1996), the high concentration of bicarbonate is the buffer to stabilize OSPW pH within a range of 8.5-9.0.

### **1.3 Scope of research and objectives**

The low biodegradability of OSPW prompts extensive studies on physical and chemical treatments of OSPW. However, two promising chemicals, polyaluminum (PACl) as coagulant and potassium ferrate(VI) as oxidant, have not been investigated in OSPW remediation. This research is aimed to fill this gap by working on the application of PACl in the CF process and the application of potassium ferrate(VI) in the oxidation process for OSPW treatment. Moreover, very few studies have done a well-defined performance comparison among different oxidation processes, especially a direct comparison between selective oxidation and unselective oxidation has not been carried out. To reduce this knowledge gap, the selective oxidation performance of potassium ferrate(VI) is compared with other oxidation processes, including UV/H<sub>2</sub>O<sub>2</sub>, and ozonation with and without ·OH scavenger. The comparison of the performance not only involves the removal of NAs and aromatics, but also the oxidation of sulfur and nitrogen containing species, measured by FTICR-MS in both negative and positive ESI modes, which fills another knowledge gap regarding how sulfur and nitrogen containing species are transformed by different oxidation processes. At last, the FTICR-MS results are compared with UPLC-TOF-MS results in the two ESI

modes, overcoming the knowledge gap that no such comparison of these analytical techniques has been reported. The following is the rationale why the two reagents, PACl and potassium ferrate(VI), are to be studied for OSPW remediation.

### 1.3.1 PACl

PACl contains a mixture of monomeric and polymeric aluminum-containing cations, including  $\text{Al}^{3+}$ ,  $\text{Al}_2(\text{OH})_2^{4+}$ ,  $\text{Al}_8(\text{OH})_{20}^{4+}$ ,  $\text{AlO}_4\text{Al}_{12}(\text{OH})_{24}(\text{H}_2\text{O})_{12}^{7+}$  and other polymeric aluminum species, the distribution of which differs among different PACl products (Burgess 1978, Crittenden et al. 2012, Siefert 2000). Many studies have shown that  $\text{Al}_{13}$  is the most efficient species amongst PACl coagulants (Gao et al. 2005). Although disputes still exist on the structure of  $\text{Al}_{13}$  molecule, Keggin structure is currently one of the most widely accepted models. In Keggin structure, there is one core tetrahedral  $\text{AlO}_4$  group in the center of the molecule, which is surrounded by 12 six-coordinated (with  $\text{H}_2\text{O}$ ,  $\text{OH}^-$ , or  $\text{O}^{2-}$ ) aluminum atoms. The resulting  $\text{Al}_{13}$  cation has a positive valence of 7 (Holleman et al. 2001). As a coagulant, the high positive charge of this poly-cation leads to high charge neutralization capacity and strong ability to compress the electric double layer (Schultz-Hardy rule) (Crittenden et al. 2012). Moreover, the OH function groups on the molecule provide adsorption sites for metal and organic matters (Siefert 2000, Stumm and Morgan 1996). With the oxygen bridge, this pre-hydrolyzed Keggin structure is stable and resistant to pH change (Tang 2006). Current industrial PACl usually has an  $\text{Al}_{13}$  percentage lower than 40%, while

higher percentage products (>80%  $Al_{13}$ ) can be synthesized in the laboratory (Wang et al. 2011).

Compared with conventional metal coagulants such as  $AlCl_3$  and alum, PACl has advantages in terms of both particulate and organic compounds removal (Gao et al. 2005, Hu et al. 2006). Using the same dose in term of total aluminum, PACl with high percentage of  $Al_{13}$  increased the zeta potential much more than  $AlCl_3$  over a pH range of 7-10 (Yan et al. 2008). On the other hand, higher humic acids removal was achieved with PACl than with  $AlCl_3$  at pH from 7 to 9 (Wu et al. 2012). Another study with modified PACl showed higher dissolved organic carbon (DOC) removal than with alum at pH above 7 (Stewart et al. 2009). All these advantages with PACl might be due to the high percentage of  $Al_{13}$ , because  $Al_{13}$  sustained positive charges with the Keggin structure while  $AlCl_3$  or alum was hydrolyzed into negatively charged  $Al(OH)_4^-$  (Wu et al. 2012). These studies provided theoretical support for the application of PACl to treat OSPW, which has a typical pH range of 8.5-9.0.

### **1.3.2 Potassium ferrate(VI)**

Ferrate(VI) compounds have been tested as oxidant/coagulant/disinfectant in water and wastewater treatment and as the cathode material in “super-iron battery” configuration (Jiang 2014, Licht and Yu 2008). Potassium ferrate(VI) is the most widely used ferrate(VI) product in water and wastewater treatment as it is easier to be purified than other ferrate(VI) salts such as sodium ferrate(VI) (Delaude and Laszlo 1996).

The redox potential of ferrate(VI) ions at acidic pH condition is the strongest among all oxidants/disinfectants ( $E_0=+2.20V$ ) (Alsheyab et al. 2009); at basic pH condition, it becomes a mild oxidant with  $E_0$  value equal to 0.6-0.7 V (Alsheyab et al. 2009, Ghernaout and Naceur 2011). Ferrate(VI) preferentially targets electron-rich moieties (ERM) such as amines, primary and secondary alcohols (Green 2001). Reactions with other organic compounds without such ERMs (e.g. ibuprofen) were also reported but with lower rate constants (Sharma and Mishra 2006). With the transformation of the organic matter in OSPW, toxicity might also be reduced. Therefore, this selective ferrate(VI) oxidation might be a unique way to untangle the toxicity effect of NAs and the aromatics in OSPW by preferentially targeting some active aromatics. After oxidation, ferrate(VI) is usually reduced to ferric at the pH range of most water and wastewater, which can further provide the coagulation function. The coagulation function of the ferric products makes ferrate(VI) a green agent because iron will deposit in the sediment after treatment instead of leaving a high residual concentration in the water.

### **1.3.3 Research objectives**

The objectives of the study on PACl (Chapter 2) are as follows: (1) to test and compare two PACl products for their efficiency in CF treatment of OSPW (i.e., removal of turbidity, organics, metals, NAs, and ultraviolet (UV) absorbing compounds quantified as UV light absorbance at the wavelength of 254 nm ( $UV_{254}$ ); (2) to investigate the impact of PACl CF process on OSPW toxicity using *Vibrio fischeri*; and (3) to elucidate the contaminant removal mechanisms based on water quality and floc analyses.

The objectives of the study on ferrate(VI) oxidation of the organic fraction (Chapter 3) are as follows: (1) to test the efficiency of potassium ferrate(VI) in oxidizing organic matters including NAs and aromatics in OSPW; (2) to test the efficiency of potassium ferrate(VI) in reducing the toxicity towards *Vibrio fischeri* and goldfish primary kidney macrophages (PKMs); (3) to explore the removal mechanisms by comparing the performance of potassium ferrate(VI) and ferric chloride, carrying out the electron paramagnetic resonance (EPR) analysis, and conducting model compound study; and (4) to investigate the effect of initial pH adjustment on the efficiency of the oxidation process.

The objectives of the comparison study on ferrate(VI), UV/H<sub>2</sub>O<sub>2</sub>, and ozonation (Chapter 4) are as follows: (1) to compare the oxidation processes including UV/H<sub>2</sub>O<sub>2</sub>, potassium ferrate(VI), and ozone (with and without ·OH scavenger tert-butyl alcohol (TBA)) in transforming NAs and aromatics in OSPW; (2) to compare the efficiency of toxicity reduction by different processes *Vibrio fischeri* and goldfish PKMs; and (3) to explore the oxidation mechanisms behind the performance differences, mainly from the perspective of oxidation selectivity.

The objectives of analyses of the organic fractions in raw and oxidized OSPW with FTICR-MS and UPLC-TOF-MS in negative and positive electrospray ionization modes (Chapter 5) are as follows: (1) to investigate the abundance of organic species in raw OSPW and oxidized OSPW, including NAs, sulfur and nitrogen containing species, and other unidentified species; (2) to compare the performance of the different oxidation processes in species transformation; and (3) to compare the impact of different analytical techniques (UPLC-TOF-MS versus

FTICR-MS) and different ionization modes (negative versus positive) on the speciation of the organic compounds.

By accomplishing these research objectives, this research study will provide a comprehensive performance evaluation and deep mechanism explanation of PACl CF process and ferrate(VI) oxidation process. Also, a well-defined performance comparison of different oxidation processes will provide valuable information on the advantages and disadvantages of each process, and will generate valuable information for future process selection on OSPW treatment. At the end, the application of FTICR-MS in both negative and positive mode will reveal a comprehensive picture of the composition of the organic fraction in OSPW, and provide new dimensions, besides NAs, to evaluate the treatment performances.

#### **1.4 Thesis organization**

This thesis consists of six chapters. Chapter 1 is a general introduction to the research background and objectives. Specifically, it covers a brief review of the oil sands production, OSPW quality, PACl and ferrate(VI) characteristics, research objectives, and thesis organization. The experimental methodologies, results, and discussions are presented in Chapters 2-5. At the end, a concluding chapter summarizing the major findings of this thesis is included as Chapter 6.

Chapter 2 presents the CF studies with synthetic PACl and commercial PACl. Synthetic PACl with high percentage of  $Al_{13}$  was prepared in the laboratory, and the aluminum species distribution in both synthetic PACl and commercial PACl was characterized by  $^{27}Al$  nuclear magnetic resonance (NMR). Performance

evaluation of these two types of PACl was done based on different parameters including turbidity, pH, zeta potential, total organic carbon (TOC), DOC, UV<sub>254</sub>, NAs concentration, metals' concentrations, and acute toxicity towards *Vibrio fischeri*. In order to elucidate the removal mechanisms, the flocs were characterized with scanning electron microscope (SEM), energy dispersive X-ray spectroscopy (EDS), X-ray photoelectron spectroscopy (XPS), and secondary ion mass spectrometry (SIMS).

Chapter 3 investigates the oxidation of NAs and aromatics in OSPW by potassium ferrate(VI). Synchronous fluorescence spectra (SFS), ion mobility spectra (IMS), <sup>1</sup>H and <sup>13</sup>C NMR, and UPLC-TOF-MS were employed to characterize the removal of NAs and/or aromatics. The selectivity of ferrate(VI) oxidation was specially studied from the perspective of preferential removal of fluorescing aromatics with two and three rings and NAs with high carbon number and ring number. Electron paramagnetic resonance (EPR) analysis was done to detect signals of organic radical intermediates. In addition, OSPW toxicity before and after treatment was analyzed with *Vibrio fischeri* and goldfish PKMs. At the end of the study, structure-reactivity study with model compounds cyclohexanecarboxylic acid (CHA), cyclohexanepentanoic acid (CHPA), 1,3-adamantanedicarboxylic acid (ADA) was included.

Chapter 4 compares the efficiencies of four different oxidation processes, including UV/H<sub>2</sub>O<sub>2</sub> oxidation, ferrate(VI) oxidation, and ozonation with and without ·OH scavenger TBA on the transformation of organic fractions in OSPW. The selective oxidation by ferrate(VI) and molecular ozone was compared with

the indiscriminating oxidation via the generation of  $\cdot\text{OH}$  in UV/H<sub>2</sub>O<sub>2</sub> process. Both NAs and aromatics removals were covered with the analytical techniques such as SFS, IMS, <sup>1</sup>H and <sup>13</sup>C NMR, and UPLC-TOF-MS, and the toxicity of raw and treated OSPW on *Vibrio fischeri* and goldfish PKMs was investigated.

Chapter 5 extends the performance investigation of the four oxidation processes covered in Chapter 4 (UV/H<sub>2</sub>O<sub>2</sub> oxidation, ferrate(VI) oxidation, and ozonation with and without  $\cdot\text{OH}$  scavenger TBA) to a more comprehensive scope, incorporating species with heteroatoms of oxygen, sulfur, and nitrogen. The relative abundance of specific organic species and/or fractions and the oxidative transformation of these species and/or fractions were characterized semi-quantitatively with FTICR-MS and UPLC-TOF-MS in negative and positive ESI modes. In addition, analytical techniques FTICR-MS versus UPLC-TOF-MS were also compared based on the distribution of oxygen containing species (i.e., species without sulfur and nitrogen).

Chapter 6 is a general conclusion of the research presented in Chapters 2-5. Moreover, recommendations for future work are also included in this chapter. Some of the experimental methodologies, together with supplementary figures and tables, are provided in the Appendix sections.

## 1.5 References

- Alberta Government (2015) 2014-2015 Energy annual report, Edmonton, Alberta.
- Alharbi, H.A., Saunders, D.M.V., Al-Mousa, A., Alcorn, J., Pereira, A.S., Martin, J.W., Giesy, J.P. and Wiseman, S.B. (2016) Inhibition of ABC transport proteins by oil sands process affected water. *Aquatic Toxicology* 170, 81-88.
- Alpatova, A., Kim, E.-S., Dong, S., Sun, N., Chelme-Ayala, P. and Gamal El-Din, M. (2014) Treatment of oil sands process-affected water with ceramic ultrafiltration membrane: Effects of operating conditions on membrane performance. *Separation and Purification Technology* 122(0), 170-182.
- Alpatova, A., Kim, E.-S., Sun, X., Hwang, G., Liu, Y. and Gamal El-Din, M. (2013) Fabrication of porous polymeric nanocomposite membranes with enhanced anti-fouling properties: Effect of casting composition. *Journal of Membrane Science* 444, 449-460.
- Alpatova, A., Meshref, M., McPhedran, K.N. and Gamal El-Din, M. (2015) Composite polyvinylidene fluoride (PVDF) membrane impregnated with Fe<sub>2</sub>O<sub>3</sub> nanoparticles and multiwalled carbon nanotubes for catalytic degradation of organic contaminants. *Journal of Membrane Science* 490, 227-235.
- Alsheyab, M., Jiang, J.Q. and Stanford, C. (2009) On-line production of ferrate with an electrochemical method and its potential application for wastewater treatment - A review. *Journal of Environmental Management* 90(3), 1350-1356.

- Barrow, M.P., Peru, K.M., McMartin, D.W. and Headley, J.V. (2015) Effects of extraction pH on the fourier transform ion cyclotron resonance mass spectrometry profiles of Athabasca oil sands process water. *Energy & Fuels, in progress.*
- Bauer, A.E. (2013) Identification of oil sands naphthenic acid structures and their associated toxicity to *Pimephales promelas* and *Oryzias latipes*. M.S., University of Waterloo, Waterloo, Ontario.
- Burgess, J. (1978) *Metal ions in solution*, Ellis Horwood, Chichester.
- Chalaturnyk, R.J., Don Scott, J. and Özüm, B. (2002) Management of oil sands tailings. *Petroleum Science and Technology* 20(9-10), 1025-1046.
- Debenest, T., Turcotte, P., Gagne, F., Gagnon, C. and Blaise, C. (2012) Ecotoxicological impacts of effluents generated by oil sands bitumen extraction and oil sands lixiviation on *Pseudokirchneriella subcapitata*. *Aquatic Toxicology* 112-113, 83-91.
- Delaude, L. and Laszlo, P. (1996) A novel oxidizing reagent based on potassium ferrate(VI). *Journal of Organic Chemistry* 61(18), 6360-6370.
- Dong, S., Kim, E.-S., Alpatova, A., Noguchi, H., Liu, Y. and Gamal El-Din, M. (2014) Treatment of oil sands process-affected water by submerged ceramic membrane microfiltration system. *Separation and Purification Technology* 138(0), 198-209.
- Frank, R.A., Fischer, K., Kavanagh, R., Burnison, B.K., Arsenault, G., Headley, J.V., Peru, K.M., Van, D.K.G. and Solomon, K.R. (2009) Effect of

- carboxylic acid content on the acute toxicity of oil sands naphthenic acids. *Environmental Science & Technology* 43(2), 266-271.
- Frank, R.A., Kavanagh, R., Kent Burnison, B., Arsenault, G., Headley, J.V., Peru, K.M., Van Der Kraak, G. and Solomon, K.R. (2008) Toxicity assessment of collected fractions from an extracted naphthenic acid mixture. *Chemosphere* 72(9), 1309-1314.
- Gao, B., Chu, Y., Yue, Q., Wang, B. and Wang, S. (2005) Characterization and coagulation of a polyaluminum chloride (PAC) coagulant with high Al<sub>13</sub> content. *Journal of Environmental Management* 76(2), 143-147.
- Garcia-Garcia, E., Ge, J.Q., Oladiran, A., Montgomery, B., Gamal El-Din, M., Perez-Estrada, L.C., Stafford, J.L., Martin, J.W. and Belosevic, M. (2011) Ozone treatment ameliorates oil sands process water toxicity to the mammalian immune system. *Water Research* 45(18), 5849-5857.
- Gheraout, D. and Naceur, M.W. (2011) Ferrate(VI): In situ generation and water treatment - A review. *Desalination and Water Treatment* 30(1-3), 319-332.
- Green, J. R. (2011), Potassium ferrate. In *Encyclopedia of Reagents for Organic Synthesis*, John Wiley & Sons Inc., New York.
- Hagen, M.O., Garcia-Garcia, E., Oladiran, A., Karpman, M., Mitchell, S., Gamal El-Din, M., Martin, J.W. and Belosevic, M. (2012) The acute and sub-chronic exposures of goldfish to naphthenic acids induce different host defense responses. *Aquatic Toxicology* 109, 143-149.
- He, Y., Patterson, S., Wang, N., Hecker, M., Martin, J.W., Gamal El-Din, M., Giesy, J.P. and Wiseman, S.B. (2012) Toxicity of untreated and ozone-

- treated oil sands process-affected water (OSPW) to early life stages of the fathead minnow (*Pimephales promelas*). *Water Research* 46(19), 6359-6368.
- He, Y., Wiseman, S.B., Zhang, X., Hecker, M., Jones, P.D., Gamal El-Din, M., Martin, J.W. and Giesy, J.P. (2010) Ozonation attenuates the steroidogenic disruptive effects of sediment free oil sands process water in the H295R cell line. *Chemosphere* 80(5), 578-584.
- Headley, J.V., Kumar, P., Dalai, A., Peru, K.M., Bailey, J., McMartin, D.W., Rowland, S.M., Rodgers, R.P. and Marshall, A.G. (2015a) Fourier transform ion cyclotron resonance mass spectrometry characterization of treated Athabasca oil sands processed waters. *Energy & Fuels* 29(5), 2768-2773.
- Headley, J.V., Peru, K.M. and Barrow, M.P. (2015b) Advances in mass spectrometric characterization of naphthenic acids fraction compounds in oil sands environmental samples and crude oil—a review. *Mass Spectrometry Reviews, In progress*.
- Hirsch, T. (2005) *Treasure in the sand : an overview of Alberta's oil sands resources*. Canada West Foundation, Calgary, Alberta.
- Holleman, A.F., Wiber, E. and Wiberg, N. (2001) *Holleman-Wiberg's Inorganic Chemistry*, Academic Press, California.
- Hu, C., Liu, H., Qu, J., Wang, D. and Ru, J. (2006) Coagulation behavior of aluminum salts in eutrophic water: Significance of Al<sub>13</sub> species and pH control. *Environmental Science & Technology* 40(1), 325-331.

- Huang, C., Shi, Y., Gamal El-Din, M. and Liu, Y. (2015a) Treatment of oil sands process-affected water (OSPW) using ozonation combined with integrated fixed-film activated sludge (IFAS). *Water Research* 85, 167-176.
- Huang, R., McPhedran, K.N. and Gamal El-Din, M. (2015b) Ultra performance liquid chromatography ion mobility time-of-flight mass spectrometry characterization of naphthenic acids species from oil sands process-affected water. *Environmental Science & Technology* 49(19):11737-45
- Hwang, G., Dong, T., Islam, M.S., Sheng, Z., Perez-Estrada, L.A., Liu, Y. and Gamal El-Din, M. (2013) The impacts of ozonation on oil sands process-affected water biodegradability and biofilm formation characteristics in bioreactors. *Bioresource Technology* 130, 269-277.
- Islam, M.S., Dong, T., Sheng, Z., Zhang, Y., Liu, Y. and Gamal El-Din, M. (2014) Microbial community structure and operational performance of a fluidized bed biofilm reactor treating oil sands process-affected water. *International Biodeterioration & Biodegradation* 91(0), 111-118.
- Islam, M.S., Zhang, Y., McPhedran, K.N., Liu, Y. and Gamal El-Din, M. (2016) Mechanistic investigation of industrial wastewater naphthenic acids removal using granular activated carbon (GAC) biofilm based processes. *Science of The Total Environment* 541, 238-246.
- Jiang, J. (2014) Advances in the development and application of ferrate(VI) for water and wastewater treatment. *Journal of Chemical Technology & Biotechnology* 89(2), 165-177.

- Jones, D., Scarlett, A.G., West, C.E., Frank, R.A., Gieleciak, R., Hager, D., Pureveen, J., Tegelaar, E. and Rowland, S.J. (2013) Elemental and spectroscopic characterization of fractions of an acidic extract of oil sands process water. *Chemosphere* 93(9), 1655-1664.
- Kim, E.-S., Liu, Y. and Gamal, E.-D.M. (2013) An *in-situ* integrated system of carbon nanotubes nanocomposite membrane for oil sands process-affected water treatment. *Journal of Membrane Science* 429, 418-427.
- Klamerth, N., Moreira, J., Li, C., Singh, A., McPhedran, K.N., Chelme-Ayala, P., Belosevic, M. and Gamal El-Din, M. (2015) Effect of ozonation on the naphthenic acids' speciation and toxicity of pH-dependent organic extracts of oil sands process-affected water. *Science of The Total Environment* 506–507(0), 66-75.
- Leishman, C., Widdup, E.E., Quesnel, D.M., Chua, G., Gieg, L.M., Samuel, M.A. and Muench, D.G. (2013) The effect of oil sands process-affected water and naphthenic acids on the germination and development of *Arabidopsis*. *Chemosphere* 93(2), 380-387.
- Lengger, S.K., Scarlett, A.G., West, C.E. and Rowland, S.J. (2013) Diamondoid diacids ('O<sub>4</sub>' species) in oil sands process-affected water. *Rapid Communications in Mass Spectrometry* 27(23), 2648-2654.
- Leshuk, T., Wong, T., Linley, S., Peru, K.M., Headley, J.V. and Gu, F. (2016) Solar photocatalytic degradation of naphthenic acids in oil sands process-affected water. *Chemosphere* 144, 1854-1861.

- Licht, S.; Yu, X. (2008) Recent Advances in Fe(VI) Synthesis. In *Ferrates*, American Chemical Society; Vol. 985, pp 2-51.
- Mackinnon, M.; Zubot, W., (2013) Chapter 10: Water management. In *Handbook on theory and practice of bitumen recovery from Athabasca oil sands Volume II: Industrial practices*, Czarnecki, J.; Masliyah, J.; Xu, Z.; Dabros, M., Eds. Kingsley Knowledge Publishing: Alberta.
- Marentette, J.R., Frank, R.A., Hewitt, L.M., Gillis, P.L., Bartlett, A.J., Brunswick, P., Shang, D. and Parrott, J.L. (2015) Sensitivity of walleye (*Sander vitreus*) and fathead minnow (*Pimephales promelas*) early-life stages to naphthenic acid fraction components extracted from fresh oil sands process-affected waters. *Environmental Pollution* 207, 59-67.
- Mikula, R.J., Kasperski, K.L., Burns, R.D. and MacKinnorr, M.D. (1996) Nature and fate of oil sands fine tailings. *Advances in Chemistry Series* 251, 718-723.
- Mohamed, M.H., Wilson, L.D., Peru, K.M. and Headley, J.V. (2013) Colloidal properties of single component naphthenic acids and complex naphthenic acid mixtures. *Journal of Colloid and Interface Science* 395(0), 104-110.
- Morandi, G.D., Wiseman, S.B., Pereira, A., Mankidy, R., Gault, I.G.M., Martin, J.W. and Giesy, J.P. (2015) Effects-directed analysis of dissolved organic compounds in oil sands process-affected water. *Environmental Science & Technology* 49(20), 12395-12404.
- Moustafa, A.M.A., McPhedran, K.N., Moreira, J. and Gamal El-Din, M. (2014) Investigation of Mono/competitive adsorption of environmentally relevant

ionized weak acids on graphite: impact of molecular properties and thermodynamics. *Environmental Science & Technology* 48(24), 14472-14480.

Crittenden, J.C., Trussell, R.R., Hand, D.W., Howe, K.J. and Tchobanoglous, G. (2012) *MWH's water treatment: principles and design*, Wiley, New Jersey.

Pereira, A.S., Islam, M.S., Gamal El-Din, M. and Martin, J.W. (2013) Ozonation degrades all detectable organic compound classes in oil sands process-affected water; an application of high-performance liquid chromatography/obitrap mass spectrometry. *Rapid Communications in Mass Spectrometry* 27(21), 2317-2326.

Pourrezaei, P., Alpatova, A., Khosravi, K., Drzewicz, P., Chen, Y., Chelme-Ayala, P. and Gamal El-Din, M. (2014) Removal of organic compounds and trace metals from oil sands process-affected water using zero valent iron enhanced by petroleum coke. *Journal of Environmental Management* 139(0), 50-58.

Pourrezaei, P., Drzewicz, P., Wang, Y., Gamal El-Din, M., Perez-Estrada, L.A., Martin, J.W., Anderson, J., Wiseman, S., Liber, K. and Giesy, J.P. (2011a) The impact of metallic coagulants on the removal of organic compounds from oil sands process-affected water. *Environmental Science & Technology* 45(19), 8452-8459.

Pourrezaei, P., Drzewicz, P., Wang, Y., Gamal El-Din, M., Perez-Estrada, L.A., Martin, J.W., Anderson, J., Wiseman, S., Liber, K. and Giesy, J.P. (2011b) The impact of metallic coagulants on the removal of organic compounds

from oil sands process-affected water. *Environmental Science & Technology* 45(19), 8452-8459.

Quagraine, E.K., Peterson, H.G. and Headley, J.V. (2005) *In situ* bioremediation of naphthenic acids contaminated tailing pond waters in the Athabasca oil sands region - Demonstrated field studies and plausible options: A review. *Journal of Environmental Science and Health - Part A Toxic/Hazardous Substances and Environmental Engineering* 40(3), 685-722.

Quesnel, D.M., Oldenburg, T.B.P., Larter, S.R., Gieg, L.M. and Chua, G. (2015) Biostimulation of oil sands process-affected water with phosphate yields removal of sulfur-containing organics and detoxification. *Environmental Science & Technology* 49(21), 13012-13020.

Rogers, V.V., Wickstrom, M., Liber, K. and MacKinnon, M.D. (2002) Acute and subchronic mammalian toxicity of naphthenic acids from oil sands tailings. *Toxicological Sciences* 66(2), 347-355.

Scarlett, A.G., Reinardy, H.C., Henry, T.B., West, C.E., Frank, R.A., Hewitt, L.M. and Rowland, S.J. (2013) Acute toxicity of aromatic and non-aromatic fractions of naphthenic acids extracted from oil sands process-affected water to larval zebrafish. *Chemosphere* 93(2), 415-420.

Sharma, V. and Mishra, S. (2006) Ferrate(VI) oxidation of ibuprofen: A kinetic study. *Environmental Chemistry Letters* 3(4), 182-185.

Shi, Y., Huang, C., Rocha, K.C., Gamal El-Din, M. and Liu, Y. (2015) Treatment of oil sands process-affected water using moving bed biofilm reactors:

- With and without ozone pretreatment. *Bioresource Technology* 192(0), 219-227.
- Siefert, K.S. (2000) Polyaluminum chlorides. In *Kirk-Othmer encyclopedia of chemical technology*, John Wiley & Sons Inc., New York.
- Sobkowicz, J. (2010) History and developments in the treatment of oil sands fine tailings. In *Tailings and mine waste 2010*, The Organizing Committee of the 14th International Conference on Tailings and Mine Waste, Eds. CRC Press, Florida.
- Speight, J.G. (2000) *Kirk-Othmer encyclopedia of chemical technology*, John Wiley & Sons Inc., New York.
- Stewart, T.A., Trudell, D.E., Alam, T.M., Ohlin, C.A., Lawler, C., Casey, W.H., Jett, S. and Nyman, M. (2009) Enhanced water purification: A single atom makes a difference. *Environmental Science & Technology* 43(14), 5416-5422.
- Stumm, W. and Morgan, J.J. (1996) *Aquatic chemistry: chemical equilibria and rates in natural waters*, John Wiley & Sons Inc., New York.
- Tang, H. (2006) *Inorganic polymer flocculation theory and the flocculants*, China Architecture & Building Press, Beijing.
- Wang, C., Alpatova, A., McPhedran, K.N. and Gamal El-Din, M. (2015) Coagulation/flocculation process with polyaluminum chloride for the remediation of oil sands process-affected water: Performance and mechanism study. *Journal of Environmental Management* 160, 254-262.

- Wang, D., Wang, S., Huang, C. and Chow, C.W.K. (2011) Hydrolyzed Al(III) clusters: Speciation stability of nano-Al<sub>13</sub>. *Journal of Environmental Sciences* 23(5), 705-710.
- Wang, N., Chelme-Ayala, P., Perez-Estrada, L., Garcia-Garcia, E., Pun, J., Martin, J.W., Belosevic, M. and Gamal El-Din, M. (2013) Impact of ozonation on naphthenic acids speciation and toxicity of oil sands process-affected water to *Vibrio fischeri* and mammalian immune system. *Environmental Science & Technology* 47(12), 6518-6526.
- Wang, Y. (2011) Application of coagulation-flocculation process for treating oil sands process-affected water. M.Sc., University of Alberta, Edmonton, Alberta.
- Wu, Z., Zhang, P., Zeng, G., Zhang, M. and Jiang, J. (2012) Humic acid removal from water with polyaluminum coagulants: effect of sulfate on aluminum polymerization. *Journal of Environmental Engineering* 138(3), 293-298.
- Xue, J., Zhang, Y., Liu, Y. and Gamal El-Din, M. (2016) Treatment of oil sands process-affected water (OSPW) using a membrane bioreactor with a submerged flat-sheet ceramic microfiltration membrane. *Water Research* 88, 1-11.
- Yan, M., Wang, D., Yu, J., Ni, J., Edwards, M. and Qu, J. (2008) Enhanced coagulation with polyaluminum chlorides: Role of pH/alkalinity and speciation. *Chemosphere* 71(9), 1665-1673.

- Zhang, Y., McPhedran, K.N. and Gamal El-Din, M. (2015) Pseudomonads biodegradation of aromatic compounds in oil sands process-affected water. *Science of The Total Environment* 521-522, 59-67.
- Zubot, W., MacKinnon, M.D., Chelme-Ayala, P., Smith, D.W. and Gamal El-Din, M. (2012) Petroleum coke adsorption as a water management option for oil sands process-affected water. *Science of The Total Environment* 427-428, 364-372.
- Zubot, W.A. (2010) Removal of naphthenic acids from oil sands process water using petroleum coke. M.Sc., University of Alberta, Edmonton, Alberta.

## 2 COAGULATION/FLOCCULATION PROCESS WITH POLYALUMINUM CHLORIDE FOR THE REMEDIATION OF OIL SANDS PROCESS-AFFECTED WATER: PERFORMANCE AND MECHANISM STUDY<sup>1</sup>

### 2.1 Introduction

The recovery of bitumen through the oil sands mining operations in northern Alberta, Canada, has rapidly increased in recent years with over 2 million barrels per day of oil being produced in 2013 (Alberta Government 2014). The hot-water bitumen recovery, and following upgrading processes, use about 3 m<sup>3</sup> of water for each m<sup>3</sup> of crude oil production (Holowenko et al. 2002) which generates large volumes of oil sands process-affected water (OSPW). OSPW is highly saline water with a range of organic and inorganic constituents, including metals, anions, organic compounds, and suspended particles (Allen 2008). Some metals and organic compounds make OSPW toxic with known negative impacts on aquatic organisms including algae, fish, invertebrates and mammals (Garcia-Garcia et al. 2011, He et al. 2011, Pourrezaei et al. 2011, Wiseman et al. 2013). Due to this toxicity, OSPW is currently stored in tailing ponds near mining sites awaiting adequate treatment prior to being released into receiving environments (Speight 2000).

---

<sup>1</sup> A version of this chapter has been published: Wang, C., Alpatova, A., McPhedran, K.N. and Gamal El-Din, M. (2015) Coagulation/flocculation process with polyaluminum chloride for the remediation of oil sands process-affected water: Performance and mechanism study. *Journal of Environmental Management* 160, 254-262.

The coagulation/flocculation (CF) process is widely used as a pretreatment to other processes including advanced oxidation, membrane filtration, adsorption, or ion exchange processes (Alpatova et al. 2014, Crittenden et al. 2012, Pourrezaei et al. 2011). Commonly used coagulants are trivalent aluminum salts,  $\text{Al}^{3+}$  (e.g., alum; polyaluminum chloride: PACl), iron salts,  $\text{Fe}^{3+}$  (e.g., ferric sulphate; ferric chloride), and organic polymers (e.g., cationic polydiallyldimethylammonium chloride (polyDADMAC); polyacrylamide) (AWWA 1999). Using the CF process for OSPW treatment has recently been investigated using alum alone and/or organic polymers (Alpatova et al. 2014, Pourrezaei et al. 2011). Pourrezaei et al. (2011) found that at an optimum dose of 250 mg/L alum the turbidity and total organic carbon (TOC) removals during OSPW treatment were 90% and 10%, respectively. However, the CF treatment process has been shown to increase the toxicity of treated waters (Al-Mutairi 2006, Fort and Stover 1995, Pourrezaei et al. 2011). Pourrezaei et al. (2011) showed that the toxicity of the alum-treated OSPW towards *Chironomus dilutes* (75% survival) increased as compared to raw OSPW (100% survival), while the addition of polyDADMAC made the treated water even more toxic (42.5% survival). For aluminum-based coagulants, the toxicity increase might be attributed to the monomeric aluminum ions ( $\text{Al}^{3+}$ ), which are more available to the organisms than polymeric aluminum compounds (Bard et al. 2009, Stumm and Morgan 1996). The overall performance of aluminum-based coagulants has been reported with PACl resulting in higher removals of turbidity, metals and organic matter as compared to alum, especially at  $\text{pH} > 8$  (Stewart et al. 2009, Wu et al. 2012). The residual aluminum concentration in the treated water

was also found to be lower using PACl versus other aluminum-based coagulants (Kimura et al. 2013). Therefore, a CF process with PACl is considered a potentially feasible process for OSPW pretreatment, which might lead to higher pollutant removal and better toxicity performance (i.e., less/no impact or even reduced toxicity) as compared with other coagulants.

PACl is a mixture of  $\text{Al}^{3+}$  and polymeric aluminum cations including,  $\text{Al}_2(\text{OH})_2^{4+}$ ,  $\text{Al}_8(\text{OH})_{20}^{4+}$ ,  $\text{AlO}_4\text{Al}_{12}(\text{OH})_{24}(\text{H}_2\text{O})_{12}^{7+}$  and other species (Crittenden et al. 2012, Yang et al. 2011). The compound  $\text{AlO}_4\text{Al}_{12}(\text{OH})_{24}(\text{H}_2\text{O})_{12}^{7+}$  is generally referred to as  $\text{Al}_{13}$  and has been reported as the most effective PACl species in the CF process (Bottero et al. 1980, Gao et al. 2005).  $\text{Al}_{13}$  is a pre-hydrolyzed coagulant with high positive charge ( $\text{Al}_{13}^{7+}$ ) making it less sensitive to pH changes and thus sustain charge neutralization capacity even in basic conditions, as compared to  $\text{Al}^{3+}$  (Hu et al. 2006). Although the physical structure of  $\text{Al}_{13}$  molecule is still debated, the Keggin structure is currently the most widely accepted model (Holleman et al. 2001). The adsorption of pollutants, especially metals, might be promoted due to the presence of hydroxyl functional groups found in the Keggin structure (Burgess 1978). Commercially available PACl products usually contain less than 40% of  $\text{Al}_{13}$  because of their relatively high total aluminum concentration and relatively low basicity. However, products with >80%  $\text{Al}_{13}$  have been synthesized previously with lower total aluminum concentrations and higher basicity (Wang et al. 2004, Wang et al. 2011). Given that  $\text{Al}_{13}$  is the most effective PACl species for the CF process, the use of a synthesized PACl may

have better performance for OSPW treatment versus the commercially available product.

This study is the first to consider PACl for the treatment of OSPW. To investigate PACl treatment, comparisons were made between a PACl synthesized in our laboratory having a high  $Al_{13}$  percentage and a commercial PACl with relatively low  $Al_{13}$  percentage. The objectives of this study were as follows: (1) to test and compare two PACl products for their efficiency in OSPW treatment (i.e., turbidity, organics removals, metals, naphthenic acids, and  $UV_{254}$ ); (2) to investigate the impact of PACl coagulants on OSPW toxicity using *Vibrio fischeri*; and (3) to elucidate contaminant removal mechanisms based on water quality and floc analyses.

## **2.2 Materials and methods**

### **2.2.1 OSPW and chemicals**

Raw OSPW was collected from an active oil sands tailings pond in Fort McMurray, Alberta, Canada, and was preserved at 4 °C in a cold storage room prior to use. Sodium hydroxide (NaOH) and aluminum chloride ( $AlCl_3$ ) used in PACl synthesis, were purchased from Sigma-Aldrich (St. Louis, MO, USA). All working solutions were prepared in 18 M $\Omega$  Milli-Q water (Millipore Corp., Bedford, MA, USA).

PACl with high  $Al_{13}$  content was prepared using the modified slow base titration method at room temperature ( $23\pm 1.0$  °C) (Wang et al. 2002, Wu et al. 2012). A 187.5 mL of 0.5 M NaOH solution was added to 75.0 mL of 0.5 M  $AlCl_3$  solution

(OH/Al molar ratio of 2.5) at a rate of 1.5 mL/min controlled by a Master Flex L/S peristaltic pump (Cole-Parmer, Chicago, IL, USA). After titration, the PACl solution was diluted to a concentration of 0.1 M as Al and aged for 24 hours to allow structure rearrangement prior to use in experiments (Wang et al. 2011). The commercial PACl was provided by Cleartech Industries Inc. (Edmonton, AB, Canada) and used as received.

### **2.2.2 Coagulation and flocculation test**

A Phipps & Bird PB-700<sup>TM</sup> JarTester (Richmond, VA, USA) was used to perform the jar tests using 2L of OSPW at a room temperature ( $23\pm 1.0^{\circ}\text{C}$ ). Coagulants were added to the jars immediately after the start of rapid mixing. After flocculation and sedimentation, 200 mL of the supernatant was collected using a syringe from about 2 cm below the water surface. In order to optimize the mixing time and rapid and slow mixing speeds, a  $2^4$  factorial design study was carried out at the dose of 1.0 mM Al, with two rapid mixing times (20 s and 120 s), two rapid mixing speeds (80 rpm and 220 rpm), two slow mixing times (30 min and 120 min), and two slow mixing speeds (15 rpm and 30 rpm). Based on the TOC and turbidity removals in the initial study, the condition used for all the current experiments included 30 s rapid mixing at 80 rpm, 30 min of slow mixing at 15 rpm, and 60 min of settling. After CF optimization, triplicate jar tests for each PACl were performed with doses including 0.5, 1.0, 1.5, 2.0, 2.5, and 3.0 mM Al. The 3.0 mM Al was chosen as a maximum value given that higher doses may not be feasible for full-scale treatment processes due to cost considerations (Crittenden et al. 2012).

### 2.2.3 Water quality analysis

Treated water samples were preserved in amber glass bottles at 4 °C prior to analysis of each sample in triplicate (unless otherwise stated). The pH was measured using an Accumet Research AR20 pH/conductivity meter (Fisher Scientific, Ottawa, ON, Canada) and turbidity was measured with an Orbeco-Hellige 965 Digital Nephelometric Turbidimeter (Orbeco Analytical Systems Inc., Sarasota, FL, USA). The color was determined using EPA Method 110.2; alkalinity according to the Standard Method 2320-B (APHA 2005); and chemical oxygen demand (COD) by the Standard Colorimetric Method 5220-D (APHA 2005). A 0.45 µm nylon filter (Supelco Analytical, Bellefonte, PA, USA) was used to filter OSPW samples prior to determining soluble COD and DOC (TOC was measured without filtration) (Apollo 9000 TOC Combustion Analyzer, FOLIO Instruments Inc., Kitchener, ON, Canada); and UV<sub>254</sub> with a UV/visible spectrophotometer (Varian Inc., Santa Clara, CA, USA). An Elan 6000 ICP mass spectrometer (PerkinElmer, Waltham, MA, USA) was used to quantify the concentration of metals after the samples were filtered through 0.45 µm nylon filter (Supelco Analytical, Bellefonte, PA, USA).

Naphthenic acids (NAs) were quantified by ultra performance liquid chromatography (Waters Corp., Milford, MA, USA) equipped with a Phenyl BEH column (15x1 mm, 1.7 µm) (Waters Corp., Milford, MA, USA). The detection of NAs was performed with a high resolution Synapt G2 HDMS mass spectrometer (Waters Corp., Milford, MA, USA) equipped with an electrospray ionization source (Waters Corp., Milford, MA, USA) operating in the negative ion mode.

The Waters UPLC system was controlled by MassLynx<sup>®</sup> 4.1 software (Waters Corp., Milford, MA). Tuning and calibration were performed using standard solutions of leucine enkephalin and sodium formate, respectively. Target Lynx<sup>®</sup> 4.1 software was used for data analysis of the target compounds. A mobile phase consisted of: A, 10 mM ammonium acetate solution prepared in the Optima-grade water and B, 10 mM ammonium acetate in 50% methanol: 50% acetonitrile, both Optima-grade. Gradient elution was as follows: 1% B for the first 2 min then ramped to 60% B by 3 min, to 70% B by 7 min, to 95% B by 13 min, followed by a hold until 14 min and finally returned to 1% B, followed by a further 5.8 min re-equilibration time. The flow was set at 100 $\mu$ L/min and the column temperature was set at 50°C. The temperature of the samples was 4°C. The total NAs were reported based on their carbon number and hydrogen deficiency (-z number).

Acute toxicity towards *Vibrio fischeri* was measured with the Microtox<sup>®</sup> 81.9% screening test protocol. Particle size analysis of raw OSPW was performed with a Malvern Zetasizer Nano (Malvern Instruments, Worcestershire, UK) instrument, while zeta potential analysis (Malvern Instruments, Worcestershire, UK) was done with OSPW sampled immediately after the rapid mixing phase. The difference in coagulants' performance was tested with two-way analysis of variance (ANOVA) run within Microsoft Excel at a 95% confidence interval.

#### **2.2.4 Coagulants, flocs and particle analysis**

Given the extensive samples created by using two coagulants at various concentrations some analyses were completed at representative doses as noted in figure captions and discussion below. The aluminum species in both PACl

products were identified by  $^{27}\text{Al}$  nuclear magnetic resonance (NMR) (Gao et al. 2005). The  $^{27}\text{Al}$  NMR spectra were acquired with 3 channel Agilent/Varian Unity Inova Spectrometer (Agilent Technologies, CA, USA) operating at 399.952 MHz ( $^1\text{H}$  resonance frequency, or a magnetic field of 9.4T).  $^{27}\text{Al}$  resonance frequency was 104.214 MHz. A switchable broad band probe was used for all experiments. 90 degree pulse was determined to be 9.75  $\mu\text{s}$ ; however for all experiments a reduced flip angle of 30 degrees or 3.25  $\mu\text{s}$  was used to avoid relaxation issues. Other key parameters were as follows: acquisition time = 1.0s, relaxation delay = 0.1 s, spectral width = 62598 Hz or 600 ppm, and scans = 2000. Software VNMRJ 3.2A was used to process the data. To quantify the aluminum species, 3 mm OD (outside diameter) NMR tube was inserted into 5 mm OD NMR tube, with the sample solution in the 5 mm OD tube and internal  $\text{NaAlO}_4$  standard in the 3 mm OD tube. These two tubes were loaded for analysis together. The NMR spectra for four standard samples and the standard curve to quantify the aluminum species were provided in Appendix A.

Two different floc types prepared for analysis in this study included dry flocs and wet flocs. After the settling process, dry flocs were prepared from material sampled from the bottom of the jars using pasteur pipettes, and freeze-dried with a LABCONCO freeze dry system (Kansas City, MO, USA). Dry flocs were analyzed by surface elemental analysis using energy-dispersive X-ray spectroscopy (EDS), X-ray photoelectron spectroscopy (XPS), and secondary ion mass spectrometry (SIMS). A scanning electron microscope (SEM) (VEGA3, Tescan Inc., Cranberry, PA, USA) coupled with EDS detector (Oxford

Instruments, Abingdon, UK) was used to take images and analyze the distribution of elements on the floc surfaces. The XPS instrument (Kratos Axis 165, Kratos Analytical, Kyoto, Japan) was equipped with a monochromatic Al K $\alpha$  source ( $h\nu = 1486.6$  eV) and operated at a pressure below  $3 \times 10^{-8}$  Pa.. SIMS was conducted with an ION-TOF IV instrument (GmbH, Münster, Germany) to detect atoms and molecular fragments sputtered from the floc surface. The X-ray diffraction (XRD) analysis for semi-quantification of mineral species in OSPW was performed with a Siemens D5000 X-ray diffractometer (Munich, Germany).

Wet flocs were sampled from the bottom of the jars with pasteur pipettes after settling and frozen *in situ* to  $-16$  °C on an Emitech K25X Peltier cooling stage (Quorum Technologies, Kent, UK). The SEM analysis for flocs was performed with an Hitachi H-3000N VPSEM (Hitachi Ltd., Tokyo, Japan) microscope in order to evaluate the floc structure. This freezing process was used instead of a more typical drying process given that water is an important component of the floc structure and the drying process remove this water with subsequent changes to the floc structure. To our knowledge this is the first time that a freezing process has been used for the analysis of flocs formed during coagulation using the SEM. The EDS analysis of the wet flocs was done with the Oxford EDS detector (Oxford Instruments, Abingdon, UK).

## 2.3. Results and discussion

### 2.3.1 Raw OSPW water quality

Due to the addition of caustic soda during the bitumen extraction process, the raw OSPW was slightly alkaline with pH of  $8.4 \pm 0.2$  (Table 1). The raw OSPW was characterised by high turbidity ( $135 \pm 12$  NTU), organic content ( $211.0 \pm 8.0$  mg/L as COD) and high alkalinity ( $776.9 \pm 7.6$  mg/L as  $\text{CaCO}_3$ ). Among metals present in OSPW, sodium was the most abundant species at  $840.6 \pm 1.7$  mg/L. The predominant anion species were chloride and sulphate at  $641.2 \pm 27.4$  mg/L and  $274.7 \pm 40.0$  mg/L, respectively. Both the DOC/TOC and soluble COD/COD ratios of 0.80 and 0.81, respectively, indicate that about 20% of the OSPW organic matter is found as particulate matter or attached to particles. Specific  $\text{UV}_{254}$  absorbance (SUVA) of OSPW was  $1.2 \pm 0.1$   $\text{L}/\text{mg}\cdot\text{m}^{-1}$ , which suggests a low aromaticity of the dissolved organic fraction of OSPW (AWWA 1999). The concentration of all NAs was  $12.1 \pm 0.8$  mg/L, which is within, but at the lower end of, the reported range of 9-43 mg/L in previous studies (Alpatova et al. 2014, Islam et al. 2014, Pourrezaei et al. 2011). This lower value may be due to the sample being taken from an active settling basin in which the OSPW constituents have not been concentrated extensively through OSPW recycling.

**Table 2.1** Water quality analysis of raw OSPW (n = 3; mean ± standard deviation)

<b>Parameter</b>	<b>Value</b>
pH	8.4±0.2
Turbidity (NTU)	135±12
Zeta potential (mV)	-41.3±0.2
Alkalinity (mg/L)	776.9±7.6
Color (CU)	11.3±1.3
Chloride (mg/L)	641.0±27.4
Sulfate (mg/L)	274.7±40.0
<i>Organic parameters</i>	
COD (mg/L)	211.0±8.0
Soluble COD (mg/L)	170±1.5
Soluble COD/COD	0.81
TOC (mg/L)	56.3±6.0
DOC (mg/L)	45.3±5.0
DOC/TOC	0.80
UV <sub>254</sub> (cm <sup>-1</sup> )	0.494±0.018
SUVA <sup>a</sup> (L/mg·m <sup>-1</sup> )	1.2±0.1
Naphthenic acids (NAs) (mg/L)	12.1±0.8
<i>Metals (mg/L)</i>	
Sodium (Na)	840.6±1.7
Calcium (Ca)	10.1±0.1
Potassium (K)	14.7±0.1
Titanium (Ti)	0.09±0.03
Gallium (Ga)	0.001±0.000
Iron (Fe)	1.0±0.0
Aluminum (Al)	2.1±0.0
Nickel (Ni)	0.01±0.00
Manganese (Mn)	0.02±0.01
Magnesium (Mg)	8.6±0.1

<sup>a</sup> Specific UV<sub>254</sub> absorbance (SUVA)=100\*(UV<sub>254</sub>/DOC)

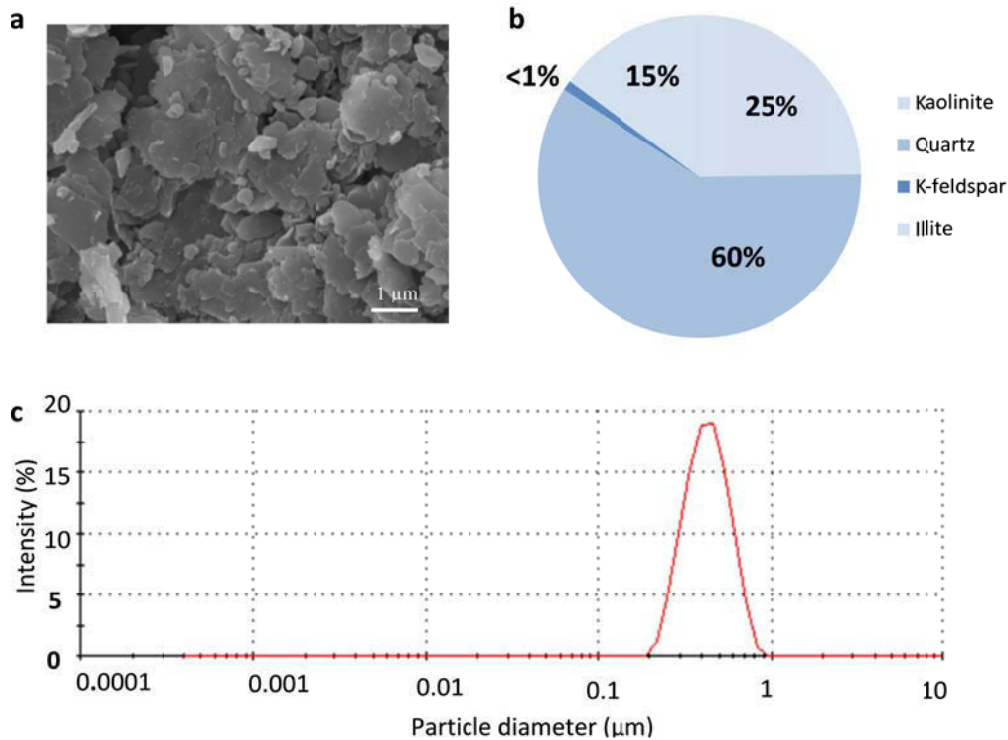


**Figure 2.1** (a) SEM image of raw OSPW solids, (b) distribution of main minerals in OSPW, and (c) particle size distribution in OSPW

The particles in raw OSPW have variable shapes and sizes (Figure 2.1a) and the XRD results (Figure 2.1b, and the XRD spectrum is provided in Appendix B) indicated that the mineral species in OSPW were dominated by quartz (60%) and clay minerals including kaolinite (25%) and illite (15%). The distribution of minerals in OSPW was consistent with the mineral distribution in mature fine tailings (MFT) taken from the bottom portions of the OSPW settling basins and fine minerals found in the actual oil sands being extracted (Chalaturnyk et al. 2002, Masliyah et al. 2011). Most of the particles in raw OSPW were in the size range from 0.2 μm to 1.0 μm, with an average particle size of 0.5 μm (Figure 2.1c). This range was lower than that in MFT where the particles larger than 2 μm

were predominant (Li et al. 2015). The larger particle sizes would be expected in the settled MFT versus the smaller, unsettled particles found in OSPW. The surface of these particles was negatively charged, with an average zeta potential of  $-41.3 \pm 0.2$  mV (Table 2.1). The small sizes and negative surfaces of these particles contribute to their stability in OSPW which makes them difficult to remove in the various treatment processes.

### **2.3.2 Characterization of synthetic and commercial PACl**

The  $^{27}\text{Al}$  NMR spectra of synthetic and commercial PACl were shown in Figure 2.2, with  $\text{Al}^{3+}$  detected at 0 ppm,  $\text{Al}_{13}$  at 63 ppm, and the  $\text{AlO}_2^-$  at 80 ppm (Wang et al. 2011). Using the summation of the peak areas at 63 ppm and 0 ppm, it was found that 83.6% and 30.5% of the aluminum atoms existed as  $\text{Al}_{13}$  in the synthetic and commercial PACl, respectively (Table 2). There are several explanations for the ability to achieve a higher percentage of  $\text{Al}_{13}$  in synthesized PACl versus the commercial PACl. Synthetic PACl had a higher basicity (0.83) as compared to commercial PACl (0.43) which provides abundant hydroxide ions to polymerize the monomeric aluminum ions. In addition, the synthetic PACl solution was more dilute at 0.1 M versus commercial PACl at 4.6 M that reduces the opportunity of further polymerization of  $\text{Al}_{13}$  to other species. Other factors such as aging time may also have an impact on the distribution of aluminum species, but are not further discussed currently due to lack of availability of this information for the commercial PACl.

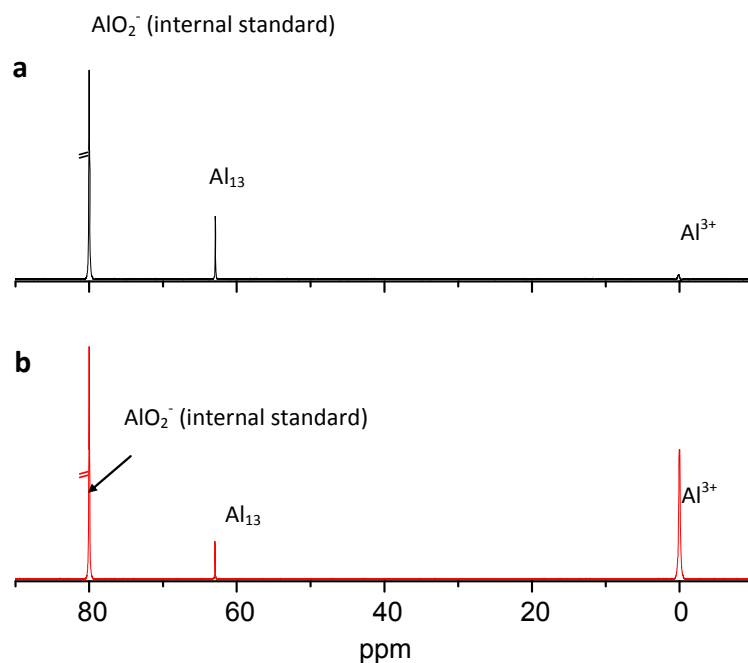


Figure 2.2  $^{27}\text{Al}$  NMR spectra of (a) synthetic PACl and (b) commercial PACl (Note: aluminum concentration in each coagulant solution was 0.05 M; aluminum concentration in the internal standard was 0.1 M)

**Table 2.2** Characteristics of synthetic and commercial PACl

Coagulant Synthetic		Commercial	
Concentration of Al (M)		0.1	4.62
% Aluminum species measured with $^{27}\text{Al}$ NMR	$\text{Al}_m^a$	5.4	49.4
	$\text{Al}_{13}$	83.6	30.5
	$\text{Al}_{\text{other}}^b$	11.0	11.1
pH		4.3-4.4	<1 <sup>c</sup>
Basicity <sup>d</sup>		0.83	0.43

<sup>a</sup>  $\text{Al}_m$ : monomeric aluminum

<sup>b</sup>  $\text{Al}_{\text{other}}$ : aluminum species other than for  $\text{Al}_m$  and  $\text{Al}_{13}$ .

<sup>c</sup> Provided by Cleartech Industries Inc. (Edmonton, AB, Canada).

<sup>d</sup> Basicity =  $[\text{OH}^-]/[\text{Al}^{3+}]/3$ , in which  $[\text{OH}^-]/[\text{Al}^{3+}]$  is the molar ratio of hydroxide to metal ion, and 3 is the charge of aluminum ion.

### 2.3.3 Coagulation performance

#### 2.3.3.1 Turbidity removal

Both PACl coagulants achieved high turbidity removal (> 96%) regardless of the applied dose (Figure 2.3a). This high removal indicates the excellent ability of PACl to remove turbidity of OSPW using either synthetic or commercial products. A similar trend was found by Pourrezaei et al. (2011) using alum at 0.3 to 2.0 mM Al with removals >90% after coagulation/flocculation regardless of the dose. Despite having similar turbidity removals, there were significant differences between these two PACl products with regards to zeta potential with synthetic PACl promoting a greater increase in OSPW zeta potential than the commercial PACl (Figure 2.3b) that can be attributed to the higher proportion of  $Al_{13}$  species in the synthetic PACl. The effect of  $Al_{13}$  species in increasing zeta potential outweighed pH effect; despite the higher reduction of pH for the commercial PACl (Figure 2.3c) the synthetic PACl had a greater impact on the zeta potential. The OSPW particles were negatively charged regardless of the applied PACl dose for the commercial PACl reaching a maximum of -15 mV at 3.0 mM Al. In contrast, the particles gained a positive charge at the highest applied PACl dose of 3.0 mM Al for the synthetic PACl. Overall, the observed results suggest that the total charge neutralization of raw OSPW is difficult to achieve.

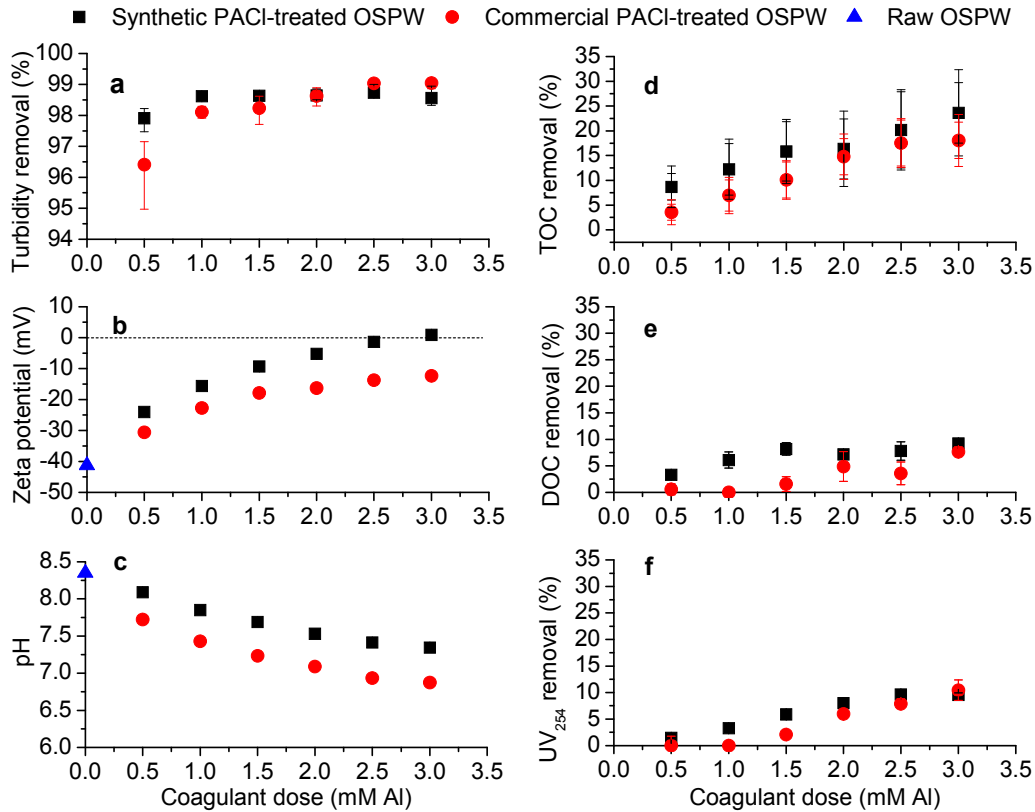


**Figure 2.3** Changes in (a) turbidity, (b) zeta potential, (c) pH, (d) TOC, (e) DOC and (f) UV<sub>254</sub> at different applied PACI doses (Note: error bars indicate mean  $\pm$  SD with n=3)

There are two main mechanisms for the removal of particles by PACI in the CF process including charge neutralization and sweep flocculation (or enmeshment in precipitate). Given the high turbidity removal, in conjunction with highly negative zeta potentials, it is hypothesized that the charge neutralization mechanism of particle removal did not play a significant role in the OSPW treatment process. For example, at 0.5 mM Al over 96% of the turbidity was removed for synthetic and commercial PACI despite having zeta potentials of -24.0 mV and -30.6 mV, respectively. At these potentials the particle collision is not well promoted given it

is recommended that the zeta potential should be greater than -20 mV for particle removal (Crittenden et al. 2012). However, to further understand the mechanisms of particle removal, subsequent analyses considered included floc visualization (Figure 2.4), SEM (Figure 2.5) and EDS (Figure 2.6). Voluminous precipitates were formed upon OSPW treatment with both PACls, even at the lowest applied doses of 0.5 mM Al, which created essential conditions for sweep flocculation (Figure 2.4). It has been shown that precipitates are formed rapidly for waters with high alkalinity and multivalent anion concentrations, as for the current OSPW, where particles are trapped before they can collide as necessary for removal by charge neutralization (AWWA 1999). Moreover, enmeshment in the precipitate mechanism is not influenced by the particle properties, thus even negative charged particles can be entrapped in precipitates (Crittenden et al. 2012). SEM images of the frozen flocs indicate that the particles were dispersed in the flocs with no obvious clusters found (Figure 2.5). In addition, the EDS data showed that OSPW quartz and clay particles were as evenly distributed as aluminum for both synthetic and commercial PACl samples (Figure 2.6), which indicates that these particles did not aggregate into larger clusters. Given the excellent conditions for sweep flocculation, coupled with no evidence of particle clusters, we conclude that sweep flocculation was the main removal mechanism.

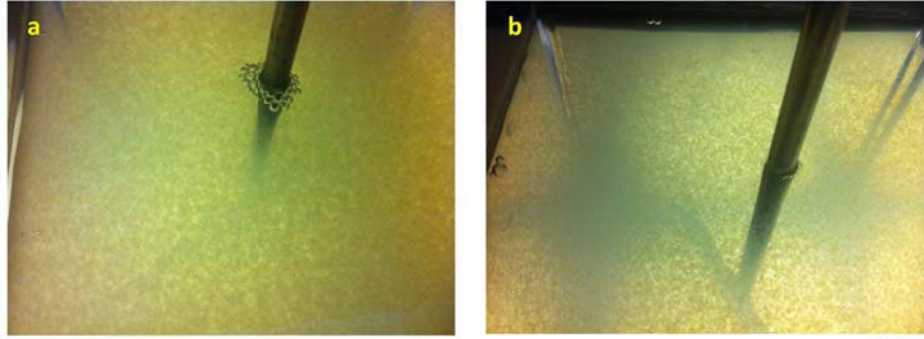


**Figure 2.4** Floccs formed in the CF process with (a) synthetic PACl and (b) commercial PACl during the flocculation process (coagulant dose: 0.5 mM Al)

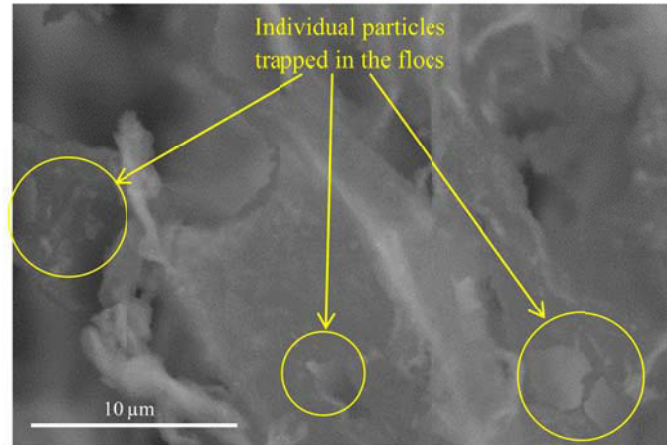


**Figure 2.5** Representative SEM image of the floccs formed upon synthetic PACl treatment (coagulant dose of 2.0 mM Al)

It is interesting to note that, based on the zeta potential shown in Figure 2.3b, charge neutralization was occurring but did not contribute appreciably to the particle settling and removal. This can be explained by the inability of entrapped particles in sweep flocculation to freely aggregate even when neutralized. However, even though the charge neutralization is not considered to be important

for the particle removal in OSPW, in the following section this effect is found to facilitate the adsorption of dissolved organic matter.

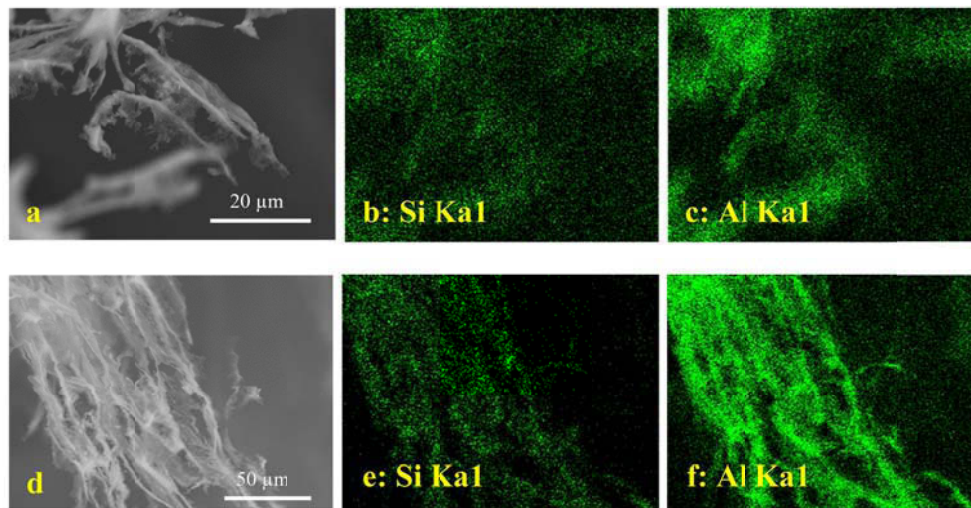


**Figure 2.6** SEM images of flocs and element distribution maps of aluminum and silicon measured with EDS: (a) SEM image of the flocs formed with synthetic PACl, (b) Si distribution on synthetic PACl flocs, (c) Al distribution on synthetic PACl flocs, (d) SEM image of the flocs formed with commercial PACl, (e) Si distribution on commercial PACl flocs, and (f) Al distribution on commercial PACl flocs (coagulant dose: 2.0 mM Al)

#### 2.3.3.2 Organic matter removal

Figures 2.3d, 2.3e and 2.3f show the removal efficiency (%) of TOC (a), DOC (b), and  $UV_{254}$  (c) for both PACl coagulants. TOC and DOC are used to determine the total organic matter and dissolved organic matter, respectively, while  $UV_{254}$  is typically used as a surrogate for monitoring the presence of aromatic or conjugated double-bond compounds (Sawyer et al. 2003). Overall, the removal efficiencies increased with the increase in applied coagulant dose for both coagulants. For synthetic PACl, the TOC removal increased from  $8.7 \pm 3.0\%$  at 0.5

mM Al to  $23.6 \pm 7.0\%$  at 3.0 mM Al; while for commercial PACl removals increased from  $3.6 \pm 2.1\%$  at 0.5 mM Al to  $18.1 \pm 4.4\%$  at 3.0 mM Al. The efficiency of TOC removal was not significantly different for synthetic and commercial PACls at any applied coagulant dose ( $p > 0.05$ ) (Figure 2.3d). The efficiency for removal of DOC and  $UV_{254}$  absorbance (both  $< 10\%$ ) was much lower than TOC removal for both coagulants (Figures 2.3e and 2.3f). This decreased efficiency can be attributed to the unfavorable adsorption of the DOC to the amorphous flocs due to the hydrophilic characteristics of the floc surface and the electrostatic repulsion of the DOC when in anionic form. Given the similar removal patterns, the  $UV_{254}$  removal can be attributed directly to the DOC removal of the OSPW. The synthetic PACl performed better in removing DOC and  $UV_{254}$ -absorbing compounds. This improved performance was likely due to the higher charge neutralization capacity of synthetic PACl that provided a higher reduction in the electrostatic repulsion between flocs and the dissolved organic molecules, thus facilitated their adsorption. The advantage of synthetic PACl was more obvious at applied doses lower than 2.0 mM Al, where the zeta potential in the commercial PACl-treated OSPW was too negative to have dissolved organic matter adsorbed onto the flocs.

Among the organic OSPW compounds, the NAs have been shown to be toxic to algae, fish, invertebrates and mammals, making them a main concern for removal during OSPW treatment (He et al. 2012, Jones et al. 2011, Kannel and Gan 2012). However, currently no NAs were removed using either of the PACl products even at the highest 3.0 mM Al doses (Figure 2.7). The reasoning behind the negligible

removal of NAs can be explained as follows. In the CF process, dissolved organic matter is mostly removed through physical and/or chemical adsorption (Crittenden et al. 2012). Physical adsorption only effectively works for compounds with high molecular weight that can overcome the electrostatic repulsion to become adsorbed. As shown in Figure 2.7, the carbon number of NAs in OSPW ranged from 9 to 20 where their molecular weights would be in the range of 150 to 350 Da. This range is too small for the anionic NAs to overcome the electrostatic repulsion between them and the negatively charged flocs; thus, no NAs removal through physical adsorption would be expected. Secondly, it is also unlikely that NAs can be removed through chemical adsorption. Although the hydroxide functional groups on the floc surfaces are potential adsorption sites for the formation of hydrogen bonds with the NAs, this adsorption is insignificant given the polar flocs surface will preferentially form hydrogen bonds with water molecules. In addition, the electrostatic repulsion and the hydrogen bonding with water also make the coordinative interaction between flocs surface and organic ions ineffective (Crittenden et al. 2012, Faust and Aly 1998). There is a potential to improve the removal of NAs through floc adsorption by further decreasing the OSPW pH and at the same time increasing the hydrophobicity of the floc surface. Decreasing pH will lead to a reduction in the repulsive forces between NAs and the flocs, thus promoting their aggregation. On the other hand, increasing hydrophobicity of the flocs (e.g. by adding polymers) will promote the adsorption process once the NAs and flocs are in close proximity to each other. However,

further research is needed to determine the impacts of reducing OSPW pH and adding polymers on the overall CF process and on the NAs removals.

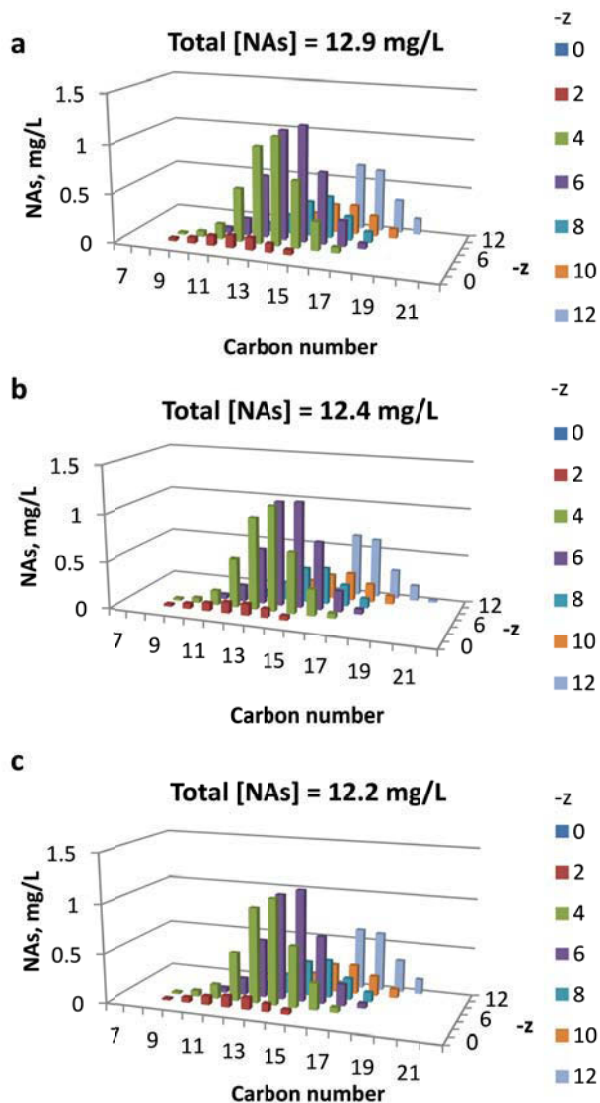


**Figure 2.7** Concentration of NAs species in (a) raw OSPW, (b) synthetic PACl-treated OSPW (applied dose: 3.0 mM Al), and (c) commercial PACl-treated OSPW (applied dose: 3.0 mM Al) (Note: z number is a negative even number and -z indicates the deficiency of hydrogen compared with saturated acyclic organic molecules)

### 2.3.3.3 Metals

The removal efficiency was variable among the metals with similar efficiencies found for synthetic and commercial PACl (Figure 2.8). Overall, individual metal removals were constant at all the applied dose ranges (0.5-3.0 mM Al), with more than 90% removal achieved for Fe, Al, Ga, and Ti, while other metals including K, Na, Ca, Mg, and Ni were removed to a lesser extent (0 to 40% removals) (data not shown). In order to elucidate the removal mechanisms, the metal removal efficiencies were plotted as a function of the  $pK_a$  values of their corresponding cations (Figure 2.8). The efficiency of metals removal was well-correlated to the  $pK_a$  values with metal cations having  $pK_a$  values lower than the treated OSPW pH (Fe, Al, Ga, and Ti) being removed to a higher extent and those with higher  $pK_a$  values (K, Na, Ca, Mg and Ni) showing lower removals. It is expected that metal cations with low  $pK_a$  values were readily hydrolysed and were more likely to complex with the functional groups on the surface of flocs (e.g., hydroxyl groups on the amorphous precipitate and carboxylic functional groups on the particulate organic matter) (Schindler and Stumm 1987). On the other hand, metal cations with high  $pK_a$  values often exist in mobile aqua ion forms that reduced their ability to be adsorbed through the complexation process (Stumm and Morgan 1996). Additionally, the tertiary surface complex formation mechanism (metal ions form complexes with ligands already adsorbed to the flocs surface) may also contribute to the removal of the metals (Stumm and Morgan 1996).

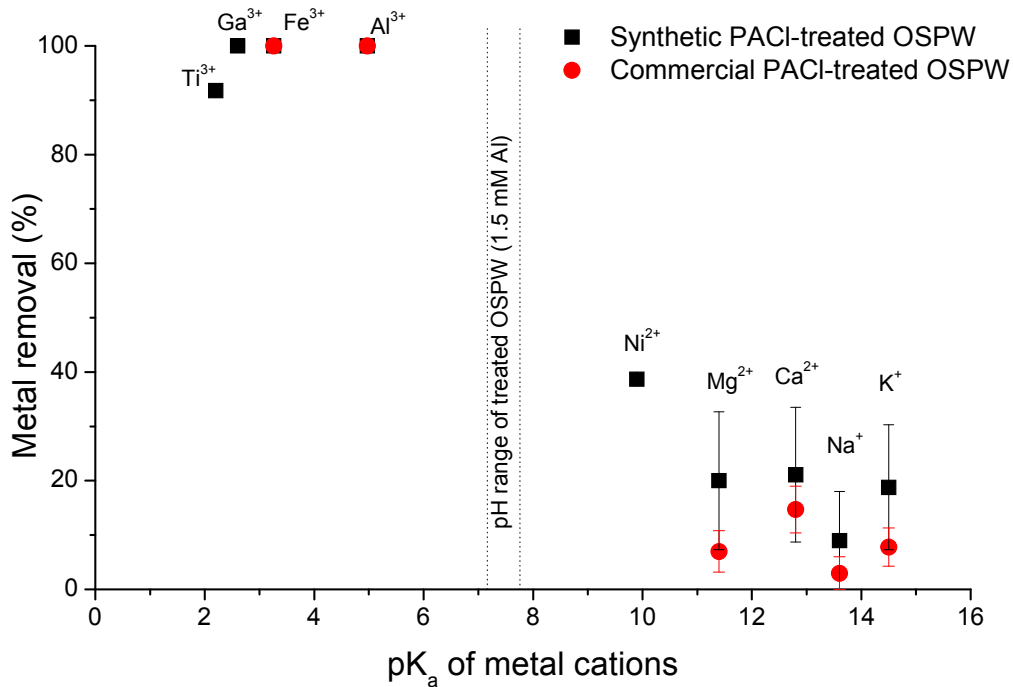


**Figure 2.8** Representative metal removal (%) by PACl vs  $pK_a$  of the metal cations at an applied coagulant dose of 1.5 mM Al. (Note: error bars indicate mean  $\pm$  SD with  $n=3$ )

#### 2.3.3.4 Acute toxicity on *Vibrio fischeri*

Figure 2.9 shows the inhibition effect of the raw and treated OSPW on *V. fischeri* as measured by the Microtox<sup>®</sup> 81.9% screening test. The inhibition level of raw OSPW was  $49.5 \pm 0.4\%$ , which was marginally higher than previously reported values of 40-42% (Shu et al. 2014) and 45% (Afzal et al. 2012) for other OSPW samples. Given the OSPW samples are variable, it is expected that the toxicities will vary from pond to pond. Overall, the addition of PACl did not cause any additional toxicity to *V. fischeri*. In fact, the synthetic PACl at the highest applied coagulant dose of 3.0 mM Al caused a decrease in the OSPW toxicity to

43.3±3.0%. Given the results of previous studies (Pourrezaei et al. 2011), it was expected the OSPW toxicity would increase with increasing coagulant addition. However, it was noted that the residual Al concentration in all treated OSPW samples was found to be below the detection limit of 0.02 mg/L, which is much lower than Al concentration in raw OSPW (2.1±0.02 mg/L) (Table 1). In addition, since an increase in removal of organic compounds was observed with increasing PACl doses, it is likely that the synthetic coagulant promoted removal of organic fraction(s) which are responsible for OSPW toxicity.

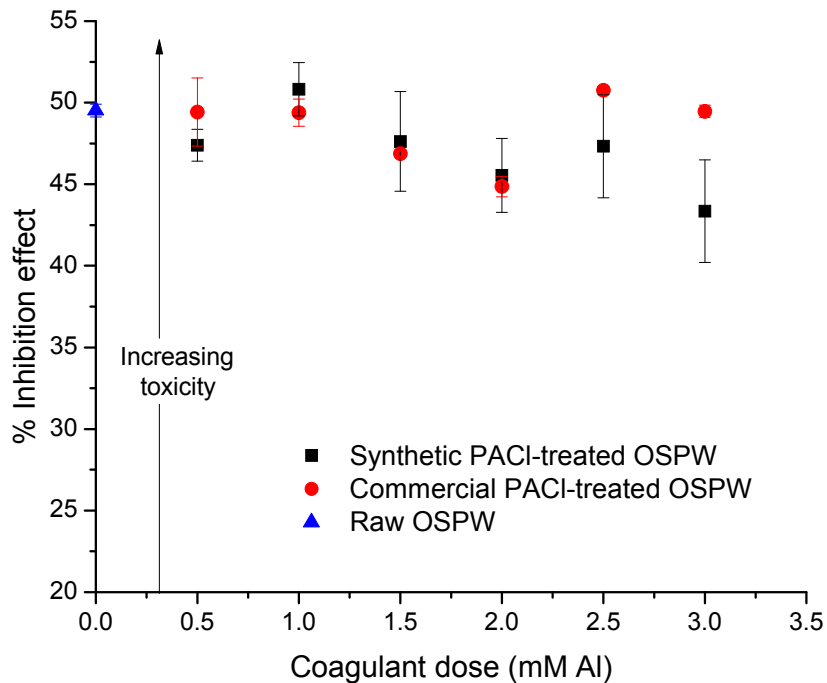


**Figure 2.9** Acute toxicity to *Vibrio fischeri* of raw OSPW and PACl-treated OSPW (Note: error bars indicate mean ± SD with n=3)

### 2.3.4 Floc analysis after sedimentation

The surface analysis was performed on the flocs sampled from the sediments after the CF process for both PACl coagulants (Figure 2.5 and Figure 2.10). The frozen flocs revealed fluffy structures, with clays and sands trapped within these flakes. As explained previously, this voluminous floc structure provided optimum conditions for trapping particles even though the surface charge of the particles were only partially neutralized. Once trapped, the particles could not move as freely as in the raw OSPW, making further aggregation difficult. Thus, the compact aggregation of clay or sand particles in OSPW was not observed.

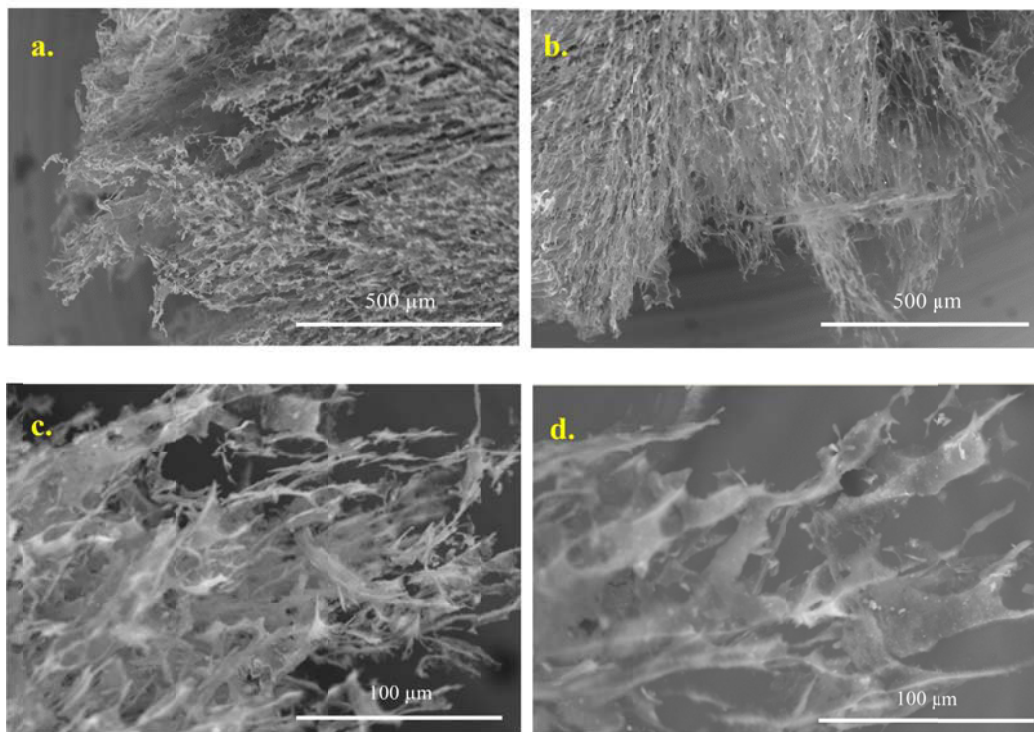
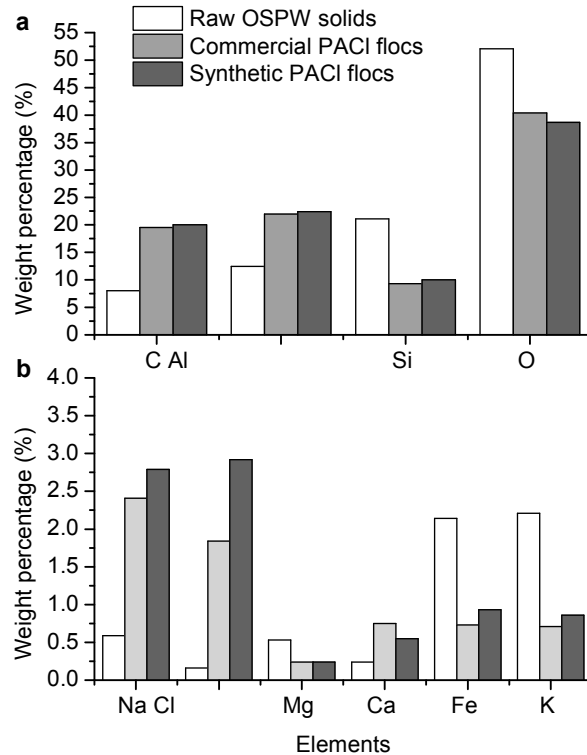


**Figure 2.10** Representative SEM images of the frozen flocs formed at a coagulant dose of 2.0 mM Al for synthetic PACl (a and c) and commercial PACl (b and d)

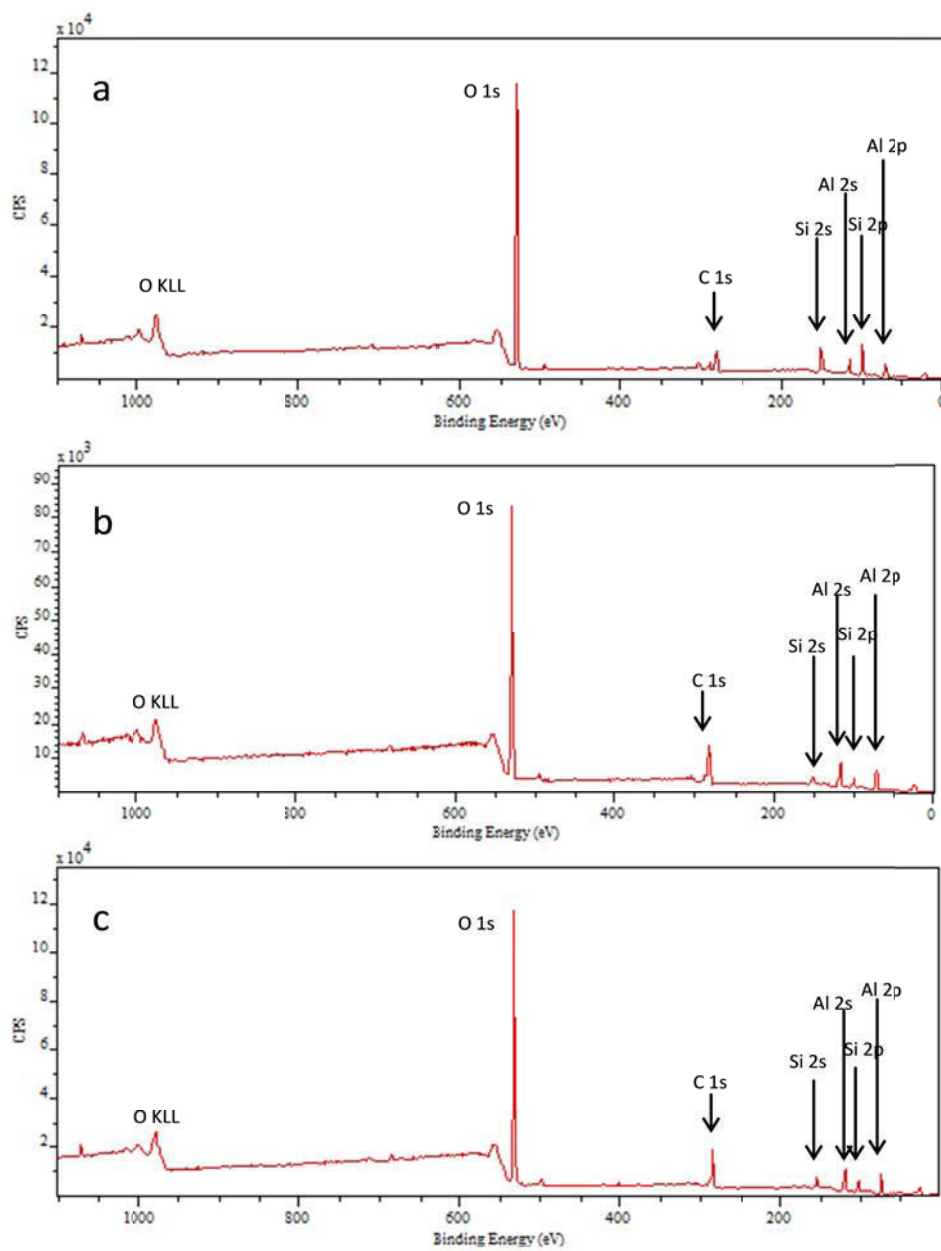
The distribution of all measured elements based on total weight percentages found on the flocs after CF for both coagulants and for the surfaces of raw OSPW solids was evaluated by EDS analysis (Figure 2.11). In both raw OSPW solids and flocs, Al, O, Si and C were the most abundant elements (Figure 2.11a), while Na, Mg, Cl, K, Ca and Fe were found at relatively low concentrations (Figure 2.11b). The percentage of carbon on the floc surfaces increased as compared to that on the raw OSPW solids which indicates that organic compounds were being removed in the CF process. Compared with the element distribution on the surface of the raw OSPW solids, the weight proportions of quartz and major clay elements including Si, K, Mg and Fe decreased on the floc surfaces, while the major coagulant elements of Al and Cl increased due to the addition of PACl coagulants. XPS spectra further confirmed the dominance of Al, Si, C and O atoms with peaks found at binding energies of 74.0 eV( $Al_{2p}$ ), 154.0 eV( $Si_{2s}$ ), 284.0-289.0 eV( $C_{1s}$ ), and 532.0 eV( $O_{1s}$ ), respectively (Figure 2.12).

Figure 2.13 shows positive mode SIMS spectra of the raw OSPW solids and dry flocs formed in the CF process for: (a) raw OSPW; (b) synthetic PACl; and (c) commercial PACl. Overall, the organic fragments in the SIMS spectra for raw OSPW solids were less abundant as compared to either PACl coagulant (e.g., dashed ovals). The relatively weaker peak intensities of organic fragments ( $CH_3$ ,  $CH_3O$ ,  $C_3H_6$ ,  $C_3H_7$  and  $C_4H_9$ ) were observed for the raw OSPW solids (Figure 2.13a) versus the dry PACl flocs (Figures 2.13b and 2.13c). As well, the appearance of new organic fragments (i.e., aliphatic hydrocarbon fragments  $C_4H_{10}$ ,  $C_5H_7$  and benzene ring structure fragments  $C_6H_6$  and  $C_7H_7$ ) on the surface of the

dry flocs indicates removal of dissolved organic matter. The SIMS spectra of the two dry floc samples were comparable to each other (Figures 2.13b and 2.13c), which is consistent with the results shown for these two coagulants with regards to turbidity, TOC and metal removals.



**Figure 2.11** Element distribution on the surface of raw OSPW solids and flocs analyzed by EDS at a representative coagulant dose of 2.0 mM Al: (a) carbon (C), aluminum (Al), silicon (Si) and oxygen (O); and (b) sodium (Na), chlorine (Cl), magnesium (Mg), calcium (Ca), iron (Fe), and potassium (K)



**Figure 2.12** XPS survey spectra of (a) raw OSPW solids, (b) flocs formed with synthetic PACl and (c) flocs formed with commercial PACl (coagulant dose: 2.0 mM Al)

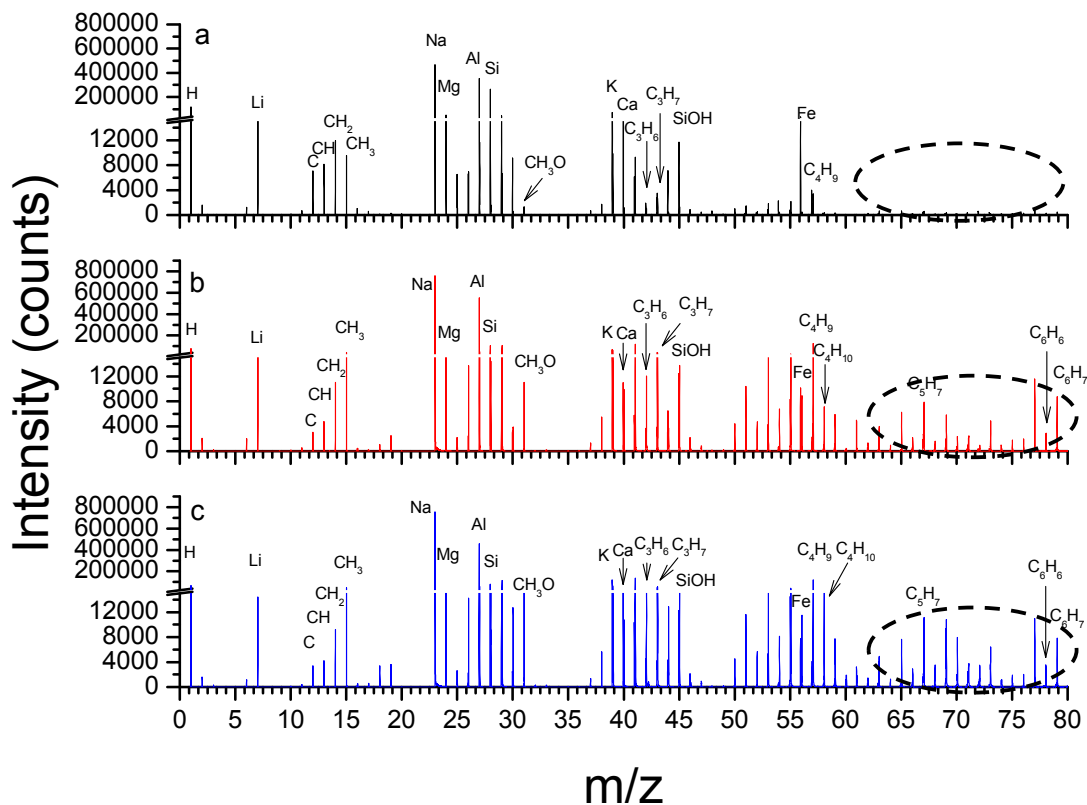


**Figure 2.13** Positive mode SIMS spectra of the (a) raw OSPW solids, (b) synthetic PACl flocs, and (c) commercial PACl flocs (scan area: 500  $\mu\text{m}$   $\times$  500  $\mu\text{m}$ ; coagulant dose: 2.0 mM Al) (Note: consult discussion for information on areas highlighted with dashed ovals)

## 2.4 Conclusions

This study was the first comprehensive investigation of the CF treatment process for OSPW using commercial and synthesized PACl. According to  $^{27}\text{Al}$  nuclear magnetic resonance analysis, the percentage of  $\text{Al}_{13}$  in the synthetic and commercial PACl was 83.6% and 30.5% of total aluminum atoms, respectively. Both coagulants were effective in removing suspended solids from OSPW, achieving more than 96% turbidity removal at the applied coagulants dose range of 0.5-3.0 mM Al with the dominant particle removal mechanism determined to

be sweep flocculation. For dissolved organic matter, the DOC and UV<sub>254</sub> removals for synthetic PACl were slightly better at low doses (< 2.0 mM Al) than commercial PACl, which was attributed to the higher charge neutralization capacity of synthetic PACl reducing the electrostatic repulsion and facilitating adsorption. NAs were not removed given their low molecular weights as compared to the removed particulates, and due to their negative charge and hydrophilic characteristics in the alkaline environment of OSPW. Metals with low pK<sub>a</sub> values (Fe, Al, Ga, and Ti) were almost completely removed during the CF processes due to complexation with the floc surface functional groups, while metals with high pK<sub>a</sub> (K, Na, Ca, Mg and Ni) had removals less than 40%. The CF performance data and proposed flocculation mechanisms were further supported by floc analysis including SEM, EDS, XPS and SIMS.

## 2.5 References

- Afzal, A., Drzewicz, P., Perez-Estrada, L.A., Chen, Y., Martin, J.W. and Gamal El-Din, M. (2012) Effect of molecular structure on the relative reactivity of naphthenic acids in the UV/H<sub>2</sub>O<sub>2</sub> advanced oxidation process. *Environmental Science & Technology* 46(19), 10727-10734.
- Al-Mutairi, N.Z. (2006) Coagulant toxicity and effectiveness in a slaughterhouse wastewater treatment plant. *Ecotoxicology and Environmental Safety* 65(1), 74-83.
- Alberta Government (2014) 2013-2014 Energy annual report, Edmonton, Alberta, Canada.
- Allen, E.W. (2008) Process water treatment in Canada's oil sands industry: I. Target pollutants and treatment objectives. *Journal of Environmental Engineering and Science* 7(2), 123-138.
- Alpatova, A., Kim, E.-S., Dong, S., Sun, N., Chelme-Ayala, P. and Gamal El-Din, M. (2014) Treatment of oil sands process-affected water with ceramic ultrafiltration membrane: Effects of operating conditions on membrane performance. *Separation and Purification Technology* 122(0), 170-182.
- APHA (2005) Standard methods for the examination of water and wastewater. Eaton A.D., Clesceri L.S., Rice E.W., Greenberg A.E., Franson M.A.H. (Eds) 21<sup>st</sup> edition, American Public Health Association (APHA), American Water Works Association (AWWA), and the Water Environment Federation (WEF), Washinton D.C.

- AWWA (1999) Water quality and treatment: a handbook of community water supplies, American Water Works Association (AWWA), McGraw-Hill, New York.
- Bard, S.M., Gagnon, G.A., Mortula, M. and Walsh, M.E. (2009) Aluminum toxicity and ecological risk assessment of dried alum residual into surface water disposal. *Canadian Journal of Civil Engineering* 36, 127.
- Bottero, J.Y., Cases, J.M., Fiessinger, F. and Polrier, J.E. (1980) Studies of hydrolyzed aluminum chloride solutions. 1. Nature of aluminum species and composition of aqueous solutions. *Journal of Physical Chemistry* 84(22), 2933-2939.
- Burgess, J. (1978) Metal ions in solution, Ellis Horwood, Chichester.
- Chalaturnyk, R.J., Don Scott, J. and Özü, B. (2002) Management of oil sands tailings. *Petroleum Science and Technology* 20(9-10), 1025-1046.
- Crittenden, J.C., Trussell, R.R., Hand, D.W., Howe, K.J. and Tchobanoglous, G. (2012) MWH's water treatment: principles and design, Wiley, New Jersey.
- Faust, S.D. and Aly, O.M. (1998) Chemistry of Water Treatment, CRC Press, Florida.
- Fort, D.J. and Stover, E.L. (1995) Impact of toxicities and potential interactions of flocculants and coagulant aids on whole effluent toxicity testing. *Water Environment Research* 67(6), 921-925.
- Gao B., Chu Y., Yue Q., Wang, B., and Wang S. (2005) Characterization and coagulation of a polyaluminum chloride (PAC) coagulant with high Al13 content. *Journal of Environmental Management* 76(2), 143-147.

- Garcia-Garcia, E., Ge, J.Q., Oladiran, A., Montgomery, B., Gamal El-Din, M., Perez-Estrada, L.C., Stafford, J.L., Martin, J.W. and Belosevic, M. (2011) Ozone treatment ameliorates oil sands process water toxicity to the mammalian immune system. *Water Research* 45(18), 5849-5857.
- He, Y., Patterson, S., Wang, N., Hecker, M., Martin, J.W., Gamal El-Din, M., Giesy, J.P. and Wiseman, S.B. (2012) Toxicity of untreated and ozone-treated oil sands process-affected water (OSPW) to early life stages of the fathead minnow (*Pimephales promelas*). *Water Research* 46(19), 6359-6368.
- He, Y., Wiseman, S.B., Hecker, M., Zhang, X., Wang, N., Perez, L.A., Jones, P.D., Gamal El-Din, M., Martin, J.W. and Giesy, J.P. (2011) Effect of ozonation on the estrogenicity and androgenicity of oil sands process-affected water. *Environmental Science & Technology* 45(15), 6268-6274.
- Holleman, A.F., Wiber, E. and Wiberg, N. (2001) Holleman-Wiberg's Inorganic chemistry, Academic Press, California.
- Holowenko, F.M., MacKinnon, M.D. and Fedorak, P.M. (2002) Characterization of naphthenic acids in oil sands wastewaters by gas chromatography-mass spectrometry. *Water Research* 36(11), 2843-2855.
- Hu, C., Liu, H., Qu, J., Wang, D. and Ru, J. (2006) Coagulation behavior of aluminum salts in eutrophic water: Significance of  $Al_{13}$  species and pH control. *Environmental Science and Technology* 40(1), 325-331.
- Islam, M.S., Dong, T., Sheng, Z., Zhang, Y., Liu, Y. and Gamal El-Din, M. (2014) Microbial community structure and operational performance of a fluidized

- bed biofilm reactor treating oil sands process-affected water. *International Biodeterioration & Biodegradation* 91(0), 111-118.
- Jones, D., Scarlett, A.G., West, C.E. and Rowland, S.J. (2011) Toxicity of individual naphthenic acids to *Vibrio fischeri*. *Environmental Science & Technology* 45(22), 9776-9782.
- Kannel, P.R. and Gan, T.Y. (2012) Naphthenic acids degradation and toxicity mitigation in tailings wastewater systems and aquatic environments: A review. *Journal of Environmental Science and Health, Part A* 47(1), 1-21.
- Kimura, M., Matsui, Y., Kondo, K., Ishikawa, T.B., Matsushita, T. and Shirasaki, N. (2013) Minimizing residual aluminum concentration in treated water by tailoring properties of polyaluminum coagulants. *Water Research* 47(6), 2075-2084.
- Li, M., Barbour, S.L. and Si, B.C. (2015) Measuring solid percentage of oil sands mature fine tailings using the dual probe heat pulse method. *Journal of Environmental Quality* 44(1), 293-298.
- Masliyah, J.H., Xu, Z. and Czarnecki, J.A. (2011) *Handbook on theory and practice of bitumen recovery from Athabasca oil sands*, Kingsley Publishing Services, Alberta.
- Pourrezaei, P., Drzewicz, P., Wang, Y., Gamal El-Din, M., Perez-Estrada, L.A., Martin, J.W., Anderson, J., Wiseman, S., Liber, K. and Giesy, J.P. (2011) The impact of metallic coagulants on the removal of organic compounds from oil sands process-affected water. *Environmental Science & Technology* 45(19), 8452-8459.

- Sawyer, C., McCarty, P. and Parkin, G. (2003) Chemistry for environmental engineering and science, McGraw-Hill Education, New York.
- Schindler, P.W. and Stumm, W. (1987) Aquatic surface chemistry: chemical processes at the particle-water interface. Stumm, W. (ed), pp. 83-110, John Wiley and Sons, New York.
- Shu, Z., Li, C., Belosevic, M., Bolton, J.R. and Gamal El-Din, M. (2014) Application of a solar UV/chlorine advanced oxidation process to oil sands process-affected water remediation. *Environmental Science and Technology* 48(16), 9692-9701.
- Speight, J.G. (2000) Kirk-Othmer encyclopedia of chemical technology, John Wiley & Sons, Inc.
- Stewart, T.A., Trudell, D.E., Alam, T.M., Ohlin, C.A., Lawler, C., Casey, W.H., Jett, S. and Nyman, M. (2009) Enhanced water purification: A single atom makes a difference. *Environmental Science & Technology* 43(14), 5416-5422.
- Stumm, W. and Morgan, J.J. (1996) Aquatic chemistry: chemical equilibria and rates in natural waters, Wiley, New York.
- Wang, D., Sun, W., Xu, Y., Tang, H. and Gregory, J. (2004) Speciation stability of inorganic polymer flocculant-PACl. *Colloids and Surfaces A: Physicochemical and Engineering Aspects* 243(1-3), 1-10.
- Wang, D., Tang, H. and Gregory, J. (2002) Relative importance of charge neutralization and precipitation on coagulation of kaolin with PACl:

- Effect of sulfate ion. *Environmental Science & Technology* 36(8), 1815-1820.
- Wang, D., Wang, S., Huang, C. and Chow, C.W.K. (2011) Hydrolyzed Al(III) clusters: Speciation stability of nano-Al<sub>13</sub>. *Journal of Environmental Sciences* 23(5), 705-710.
- Wiseman, S.B., He, Y., Gamal El-Din, M., Martin, J.W., Jones, P.D., Hecker, M. and Giesy, J.P. (2013) Transcriptional responses of male fathead minnows exposed to oil sands process-affected water. *Comparative Biochemistry and Physiology Part C: Toxicology & Pharmacology* 157(2), 227-235.
- Wu, Z., Zhang, P., Zeng, G., Zhang, M. and Jiang, J. (2012) Humic acid removal from water with polyaluminum coagulants: Effect of sulfate on aluminum polymerization. *Journal of Environmental Engineering* 138(3), 293-298.
- Yang, Z., Gao, B., Cao, B., Xu, W. and Yue, Q. (2011) Effect of OH<sup>-</sup>/Al<sup>3+</sup> ratio on the coagulation behavior and residual aluminum speciation of polyaluminum chloride (PAC) in surface water treatment. *Separation and Purification Technology* 80(1), 59-66.

## 3 OXIDATION OF OIL SANDS PROCESS-AFFECTED WATER BY POTASSIUM FERRATE(VI)<sup>2</sup>

### 3.1 Introduction

The oil sands deposits of Alberta are estimated to contain around 2 trillion barrels of oil (Hirsch 2005, Mackinnon and Zubot 2013). In 2013, 2.09 million barrels per day of bitumen was produced from Alberta oil sands (Alberta Government 2014). Current extraction processes, including hot-water extraction in surface mining and steam heating with *in-situ* methods, consume large quantities of water (Mackinnon and Zubot 2013). The wastewater generated during the extraction and the following upgrading process, commonly referred as oil sands process-affected water (OSPW), contains suspended solids, metals, salts, and organic matter which pose environmental risks when released into the environment (Allen 2008). The organic matter in OSPW consists of classical naphthenic acids (NAs), oxidized naphthenic acids (oxy-NAs), heteroatomic NAs, aromatics (phenols, polycyclic aromatic hydrocarbons (PAHs), and benzene, toluene, ethylbenzene, and xylenes (BTEX)), and other organic compounds (Allen 2008, Grewer et al. 2010, Mackinnon and Zubot 2013). Classical NAs refer to a mixture of alkyl-substituted acyclic and cycloaliphatic carboxylic acids, with a general formula  $C_nH_{2n+z}O_2$ , where n indicates the number of carbon atoms, and z (zero or a negative even

---

<sup>2</sup> A version of this chapter has been published: Wang, C., Klammerth, N., Huang, R., Elnakar, H. and Gamal El-Din, M. (2016) Oxidation of oil sands process-affected water by potassium ferrate(VI). *Environmental Science & Technology* 50(8), 4238-4247.

integer) specifies the hydrogen deficiency (Brient et al. 2000) due to the formation of double bonds and/or rings. Oxy-NAs refer to oxidized NAs with general formula  $C_nH_{2n+z}O_x$  ( $x \geq 3$ ) (Grewer et al. 2010). In addition, NAs containing heteroatoms (mainly sulfur: S-NAs) (Barrow et al. 2010, Headley et al. 2011, Headley et al. 2009, Headley et al. 2012, Nyakas et al. 2013, Wang et al. 2013) and aromatic NAs (Reinardy et al. 2013, Scarlett et al. 2013) have been reported to exist in OSPW. NAs are usually the main concern in OSPW treatment due to their high concentration and the potential environmental impact. Aromatics in OSPW attracted less attention due to their relatively low concentration.

Organic fractions extracted from OSPW were reported to be toxic to yellow perch (Nero et al. 2006) and fathead minnows (Kavanagh et al. 2012), and to affect germination and development of plants like *Arabidopsis* (Leishman et al. 2013). As organic matter in OSPW is a complex mixture, the contribution from each specific organic fraction to the total toxicity is not clear. Therefore, more research is needed to untangle the complicated toxicity effect. Recent studies have examined different organic fractions of OSPW extracted at different pH (Klamerth et al. 2015), other studies used fractionation procedures to separate the organic fractions in OSPW into NAs and aromatics (Frank et al. 2008, Scarlett et al. 2013). Jones et al. (2011) employed model NAs, which had been identified in OSPW, to investigate their toxicity. These methods confirmed that both NAs fraction and aromatic fraction contributed to the toxicity of OSPW and Scarlett et al. (2013) also suggested that aromatics in OSPW were at least as toxic as NAs. Another possible way to untangle the toxicity effect of NAs and the aromatics

might be found in the selective oxidation process, during which some electron-rich aromatics might be preferentially oxidized than the electron-poor NAs.

Potassium ferrate(VI) is a selective oxidant and has been tested as oxidant/coagulant/disinfectant in water and wastewater treatment and as the cathode material in “super-iron battery” configuration (Jiang 2014, Licht and Yu 2008). At acidic pH conditions, the redox potential of ferrate(VI) is the one of the highest among all the oxidants ( $E_0=2.20$  V); at the basic pH conditions, it decreases to 1.4 V for  $\text{HFeO}_4^-$  and 0.6-0.7V for  $\text{FeO}_4^{2-}$  (Alsheyab et al. 2009, Ghernaout and Naceur 2011, Ninane et al. 2008). Ferrate(VI) preferentially targets electron-rich moieties (ERM) such as amines, primary and secondary alcohols (Green 2001); reactions with other organic compounds without such ERMs (e.g. ibuprofen) were also reported but with lower rate constants (Sharma and Mishra 2006). At the pH range of most water and wastewater, ferrate(VI) is usually reduced to ferric, which can further provide the coagulation function. The coagulation function of the ferric products makes ferrate(VI) a green agent because iron will deposit in the sediment after treatment instead of leaving a high residual concentration in the water.

This paper is the first to investigate the application of potassium ferrate(VI) in OSPW treatment. The objectives of this study are: (1) to test the efficiency of potassium ferrate(VI) in oxidizing organic matters including NAs and aromatics in OSPW; (2) to test the efficiency of potassium ferrate(VI) in reducing toxicity; (3) to explore the removal mechanisms by comparing the performance of potassium ferrate(VI) and ferric chloride, carrying out the electron paramagnetic

resonance (EPR) analysis, and conducting model compound study; and (4) to investigate the effect of initial pH adjustment on the efficiency of the oxidation process.

## **3.2 Materials and methods**

### **3.2.1 OSPW and chemicals**

Raw OSPW was collected from an active oil sands tailings pond in Fort McMurray, Alberta, Canada, and was preserved at 4°C in a cold storage room prior to use. Potassium ferrate(VI) with purity of 92% was prepared by wet method (Thompson et al. 1951). Ferric chloride (reagent grade) was purchased from Sigma-Aldrich (St. Louis, MO, USA), and sodium bicarbonate and sodium thiosulfate were purchased from Fisher Scientific (Fair Lawn, NJ, USA). The model compounds, cyclohexanecarboxylic acid ( $C_7H_{12}O_2$ ) (98%) and cyclohexanepentanoic acid ( $C_{11}H_{20}O_2$ ) (98%), were purchased from Sigma-Aldrich (St. Louis, MO, USA). 1,3-adamantanedicarboxylic acid ( $C_{12}H_{16}O_4$ ) (>95%) was purchased from Tokyo Chemical Industry (TCI) (Tokyo, Japan). All other chemicals were of analytical grade unless specified otherwise.

### **3.2.2 Experimental design**

#### *3.2.2.1 OSPW Study*

The investigated ferrate(VI) dose was between 1 and 400 mg/L calculated as iron. Dry potassium ferrate(VI) was added into 200 mL OSPW under rapid mixing with RT 15 power IKAMAG<sup>®</sup> magnetic stirrers (IKA Works, Inc., Wilmington, NC, USA). After 3 hours, rapid mixing was stopped, and sodium thiosulfate was

added to quench the residual ferrate(VI). The treated OSPW was then filtered through 0.45  $\mu\text{m}$  nylon filter (Supelco Analytical, Bellefonte, PA, USA) and preserved in amber glass bottles. During the reaction, pH was monitored, and OSPW samples (0.5 mL) were taken at different times to measure residual ferrate(VI) concentration by spectrophotometry at 510 nm, with a molar absorption coefficient  $\epsilon_{510\text{nm}} = 1150 \text{ M}^{-1}\text{cm}^{-1}$  (Luo et al. 2011). As a comparison, experiments with ferric chloride were conducted in a similar way with same iron concentrations. All experiments were done in triplicates.

#### *3.2.2.2 Water Quality Analysis for the OSPW Study*

pH was monitored using an Accumet Research AR20 pH/conductivity meter (Fisher Scientific, Ottawa, ON, Canada).  $\text{UV}_{254}$  absorbance was measured with a UV-Vis spectrophotometer (Varian Inc., Santa Clara, CA, USA). Synchronous fluorescence spectra (SFS) of the filtered water were recorded with Varian Cary Eclipse fluorescence spectrometer (Mississauga, ON, Canada). Excitation wavelengths ranged from 200 to 600 nm, and emission wavelengths were recorded from 218 to 618 nm. Scanning speed was 600nm/min and the photomultiplier (PMT) voltage was 800 mV. Regarding the different response factors (i.e., different quantum yields) of different fluorescing aromatics under UV irradiance, the quantification of the removal of these aromatics based on the peak area is not adopted in this study.

Naphthenic acids (NAs) were quantified by ultra-performance liquid chromatography time-of-flight mass spectrometry (UPLC TOF-MS). The injection solution was prepared with 500  $\mu\text{L}$  sample, 100  $\mu\text{L}$  of 4.0 mg/L internal

standard (myristic acid-1-<sup>13</sup>C) in methanol, and 400  $\mu$ L methanol to reach a final sample volume of 1 mL. Raw OSPW was used as the control sample for quality control. Chromatographic separations were performed using a Waters UPLC Phenyl BEH column (1.7  $\mu$ m, 150 mm  $\times$  1 mm), with mobile phases of 10 mM ammonium acetate in water (A) and 10 mM ammonium acetate in 50/50 methanol/acetonitrile (B). The elution gradient was 0–2 min, 1% B; 2–3 min, increased from 1% to 60% B; 3–7 min, increased to 70% B; 7–13 min, 95% B; 13–14 min, 1% B and hold 1% B until 20 min to equilibrate column with a flow rate of 100  $\mu$ L/min. The column temperature was set at 50  $^{\circ}$ C and the sample temperature at 10  $^{\circ}$ C. Samples were analyzed with a high-resolution time-of-flight mass spectrometer (Synapt G2, Waters Corp., Milford, MA, USA) with the electrospray ionization (ESI) source operating in negative ion mode and TOF analyzer in high-resolution mode. The negative ESI has been commonly used to determine naphthenic acids species based on previous comprehensive studies of OSPW (Huang et al. 2015, Martin et al. 2010, Sun et al. 2014). The data acquisition process was controlled using MassLynx (Waters Corp., Milford, MA, USA) and data extraction from spectra was performed using TargetLynx (Waters Corp., Milford, MA, USA). The identification of NAs (O<sub>2</sub>) and oxy-NAs are based on the empirical formula C<sub>n</sub>H<sub>2n+z</sub>O<sub>x</sub> (x=2, 3, 4, 5) with n ranging from 7 to 26 and z from 0 to -18. And the quantification of each NA species was done by comparing its peak area with that of the internal standard. The UPLC-TOF-MS quantification method was developed previously and has been verified in a number of publications (Huang et al. 2015, Ross et al. 2012, Sun et al. 2014,

Wang et al. 2013) as a semi-quantification method, given the full quantification method is not currently available due to the lack of individual NA standard compounds. The method for acquisition of ion mobility (IM) spectra was the same as described by Wang et al. (2013).

<sup>1</sup>H nuclear magnetic resonance (NMR) spectra were acquired with 3-channel Agilent/Varian Unity Inova Spectrometer (Agilent Technologies, Santa Clara, CA, USA) at 399.950 MHz. 200 mL water sample was used for each analysis. The pH of the water was adjusted to 2.0-2.5 with 6 M sulphuric acid, and then the organic fraction was extracted with 50 mL dichloromethane (DCM). Then the extract was evaporated to dryness through the air drying process. The dried organic fraction was then reconstituted in 1 mL deuterated dimethyl sulfoxide (DMSO) and transferred into the NMR tubes for analysis. The extracted organic matter was reconstituted in 1 mL deuterated dimethyl sulfoxide (DMSO) and transferred into 5 mm OD (outside diameter) NMR tubes for analysis. Key parameters of the instrument were set as follows: <sup>1</sup>H resonance frequency: 399.950 MHz; pw30 (i.e. 30 degree pulse): 3.3 ms; acquisition time: 5s; spectral width: 10000 Hz or 25 ppm; transmitter offset: 989.9 Hz; relaxation delay: 0.1 s. The data were process with software VNMRJ 4.2A.

Fourier transform infrared (FT-IR) spectra were acquired with PerkinElmer Spectrum 100 FT-IR Spectrometer (PerkinElmer Life and Analytical Sciences, Woodbridge, ON, CA). The samples for FT-IR analysis were prepared as follows: the pH of 100 mL OSPW was adjusted to 2.0, and the organic fraction was extracted with 50 mL carbon tetrachloride (Sigma-Aldrich, St. Louis, MO, USA),

and the extract was evaporated to dryness, reconstituted in 5 mL CCl<sub>4</sub> and injected into the KBr cell for analysis.

The electron paramagnetic resonance (EPR) signals were obtained with Bruker Elexsys E500 spectrometer (Billerica, MA, USA).  $\alpha$ -(4-Pyridyl N-oxide)-N-tert-butyl nitron (POBN) (Sigma-Aldrich, St. Louis, MO, USA) was used as the spin trap. All the spectra were obtained at 150 K using a liquid nitrogen dewar with the following settings: temperature = 150 K, center field = 336 G, sweep width = 20 G, microwave frequency = 9.436 GHz, modulation frequency = 100 kHz, and power = 20 mW.

Acute toxicity towards *Vibrio fischeri* was measured with the Microtox<sup>®</sup> 81.9% screening test protocol. *In vitro* toxicity assessment was done using goldfish primary kidney macrophages (PKMs), and detailed procedure is provided in Appendix C and can also be found in Shu et al. (2014).

### 3.2.2.3 Model Compound Study

Three naphthenic acid model compounds, cyclohexanecarboxylic acid (CHA, C<sub>7</sub>H<sub>12</sub>O<sub>2</sub>), cyclohexanepentanoic acid (CHPA, C<sub>11</sub>H<sub>10</sub>O<sub>2</sub>), 1,3-adamantanedicarboxylic acid (ADA, C<sub>12</sub>H<sub>16</sub>O<sub>4</sub>) were selected to study their degradation kinetics and analyze degradation by-products with ferrate(VI) oxidation. Sodium bicarbonate buffer (1.18 g/L, pH adjusted to 8.5) with a single NA model compound concentration of 60 mg/L was used as the model mixture. The buffer solution was prepared to simulate the 600 mg/L (as CaCO<sub>3</sub>) alkalinity in OSPW. The dose of ferrate(VI) applied was 200 mg/L Fe(VI) and the

experiment was conducted by adding solid ferrate(VI) under rapid mixing as described in the OSPW study. Samples were taken at 0 min, 2 min, 5 min, 10 min, 20 min, 30 min, 45 min, 60 min, 90 min, 120 min, and 180 min, and immediately quenched with sodium thiosulfate. The concentrations of the model compounds after ferrate(VI) oxidation were measured with Agilent 1100 binary HPLC coupled with G1946D MSD mass spectrometer (Santa Clara, CA, USA). End products were identified with Agilent 1200 HPLC coupled with Agilent 6220 oaTOF mass spectrometer (Santa Clara, CA, USA). Mass spectrometry was performed in the negative scan/SIM (selected-ion monitoring) mode. Detailed information about the instruments and the setups is provided in the Appendix D.

### **3.3 Results and discussion**

#### **3.3.1 Analyses of raw OSPW**

Organic matter in OSPW contains both aromatic and aliphatic organic compounds. Analyses of OSPW by various analytical methods ( $^1\text{H}$  NMR, SFS, UV-Vis, FT-IR) show a variety of different signals like aromatic and aliphatic hydrogen, and acid groups.  $^1\text{H}$  NMR spectrum provides the information about the structures and functional groups of the organic matter in OSPW by detecting the chemical shift of protons in different environments. The  $^1\text{H}$  NMR spectrum (Figure 3.1) clearly shows three different resonances of hydrogen atoms bonded in organic molecules: at 0.3-2.2 ppm are the hydrogen atoms attached to aliphatic carbons, at 6.5-8.0 ppm are the hydrogen atoms on aromatic rings, and at 11.4-12.5 ppm are the hydrogen atoms in carboxyl functional groups (Clayden et al. 2012). No peak is

detected from 4.5 to 5.5 ppm, which represents hydrogens attached to aliphatic carbon-carbon double bonds (Clayden et al. 2012). The aromatic hydrogen peak is

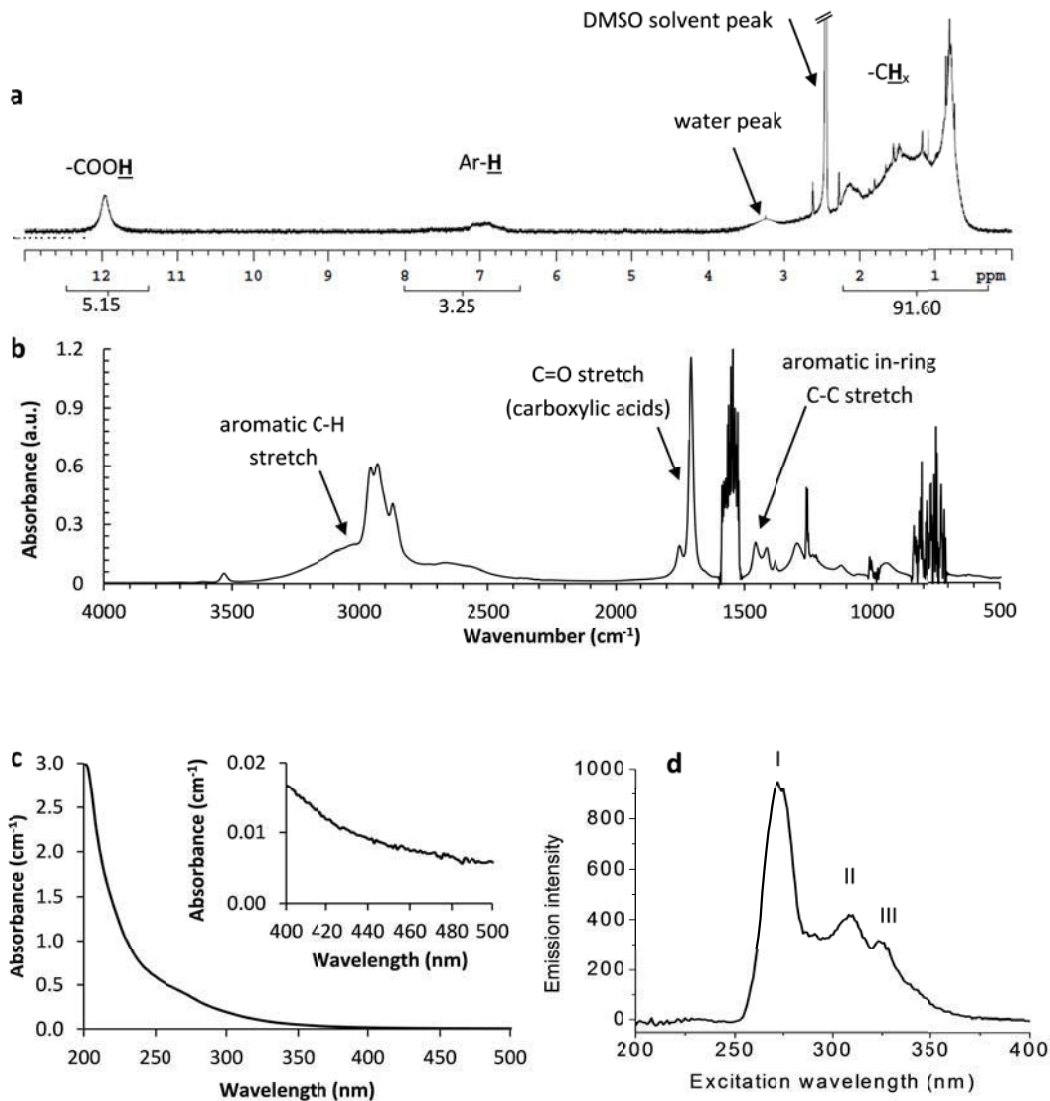


**Figure 3.1** Spectroscopic analyses of raw OSPW: (a)  $^1\text{H}$  NMR spectrum (the numbers below the scale are the integrated peak area for each fraction with a total of 100), (b) FT-IR spectrum, (c) UV-Visible light absorption spectrum, and (d) SFS

broad, indicating that aromatic organic matter in OSPW is a complex mixture; it might include benzene rings with aliphatic branches, oxygen or sulfur-containing

heteroatomic aromatics, and even small amount of humic and fulvic acids (Allen 2008, Clayden et al. 2012). So far there is no quantitative information about the total concentration of the aromatics in OSPW. However, based on the peak area shown in the  $^1\text{H}$  NMR spectrum, the molar ratio of total aromatic compounds over total organic acids (including classical NAs, oxy-NAs, and other organic acids) in OSPW can be roughly estimated to be in the range of 0.08-0.32 depending on the number of carboxyl functional groups in each organic acid and the number of hydrogen atoms on each aromatic ring (detailed calculation is provided in Appendix E). FT-IR spectrum is an effective way to study functional groups by detecting the stretching and bending of bonds. FT-IR spectrum (Figure 3.1b) confirms the existence of both organic acids and aromatics in OSPW: the sharp peak at  $1706\text{ cm}^{-1}$  was assigned to the C=O stretch of carboxyl functional groups, while the peaks at  $3100\text{-}3000\text{ cm}^{-1}$  and at  $1400\text{-}1500\text{ cm}^{-1}$  are the signals of the aromatic C-H stretch and aromatic in-ring C-C stretch, respectively (Clayden et al. 2012). The UV-Vis absorption spectrum (Figure 3.1c) shows low absorption above 400 nm, consistent with our previous report of the low color of OSPW (Wang et al. 2015). SFS of OSPW (Figure 3.1d) provides more specific information of fluorescing compounds: peak I at 267 nm is assigned to one-ring aromatics (which refer to not only aromatics containing one aromatic ring but also aromatics containing two or more unfused aromatic rings), while peak II at 310 nm and peak III at 330 nm are assigned to aromatics with two and three fused rings respectively (Pourrezaei et al. 2014, Tuan Vo 1978). Considering that the peaks for two-ring and three-ring aromatics are weaker than one-ring aromatics

and the quantum yield for fluorescence of two-ring and three-ring aromatics is much higher than one-ring aromatics (e.g. the quantum yield of anthracene is ten times that of benzene) (Williams et al. 1983), it can be concluded that one-ring aromatics predominate in OSPW.

### **3.3.2 Consumption of potassium ferrate(VI) in OSPW**

The reaction of ferrate(VI) with organic compounds in OSPW was a slow process and it took around 2-3 hours to consume more than 95% of ferrate(VI) depending on the initial doses. The consumption rate of ferrate(VI) was the highest at the first five minutes of the reaction, with 1 mg/(L·min) for a dose of 25 mg/L and 5 mg/(L·min) for a dose of 200 mg/L Fe(VI); the consumption rate decreased to values of 0.002-0.087 mg/(L·min) at the end of the reaction, depending on the initial doses (Figure 3.2a). This can be explained from two aspects: (1) Ferrate(VI) oxidation is a second-order reaction as reported by Jiang (2014), which means that the reaction rate is proportional to the concentrations of both oxidants and reductants; with increasing reaction time, the concentration of ferrate(VI) and contaminants in OSPW decreased, leading to low consumption rate. (2) The pH in OSPW increased from pH 8.6 to pH 8.7-10.9 (depending on the doses) during the course of the experiments after ferrate(VI) was added (Figure 3.2b-c), which was mainly due to the generation of hydroxide ions during the reaction and the self-decomposition of ferrate(VI) (Sharma 2002). Due to the increase of pH, the proportion of protonated ferrate(VI) ions, which had a higher redox potential than unprotonated ferrate(VI), was lower, thus decreasing the reactivity of ferrate(VI) in OSPW.

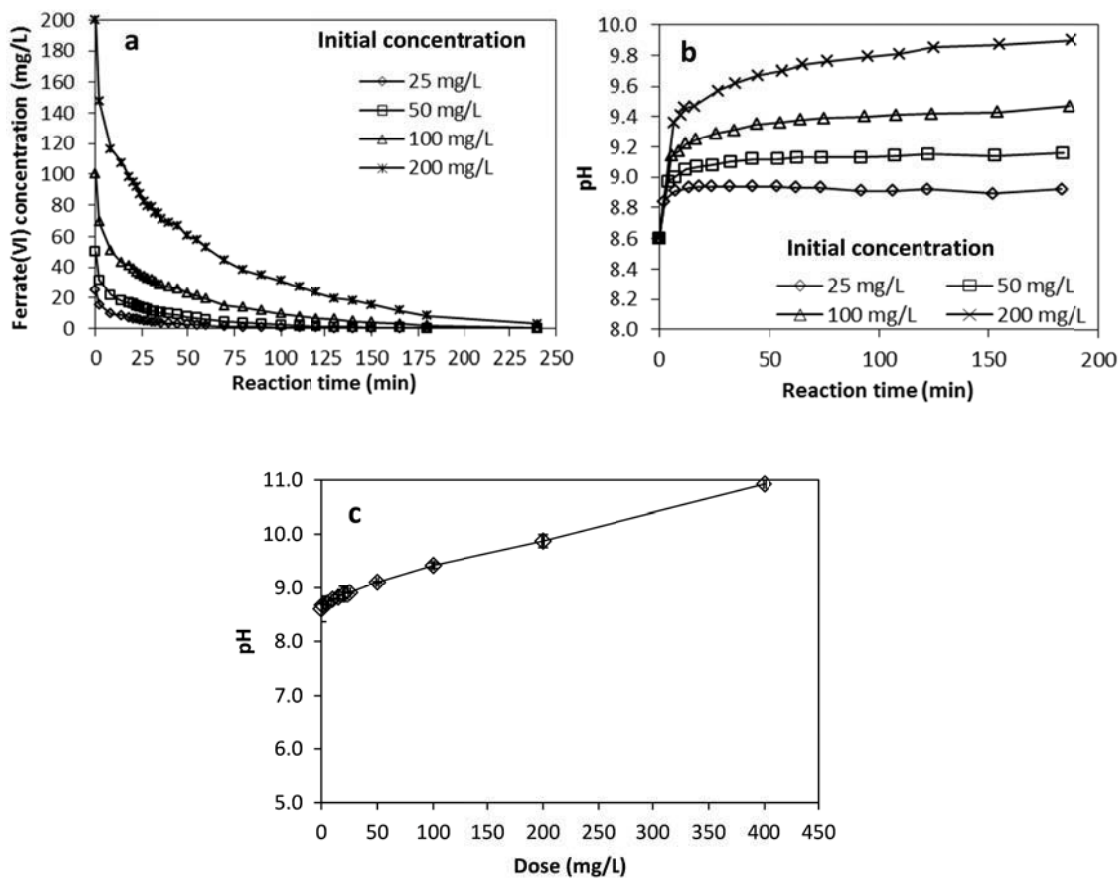


**Figure 3.2** Change of (a) residual ferrate(VI) concentration and (b) pH with reaction time, and (c) final pH of oxidized OSPW at different doses of ferrate(VI)

### 3.3.3 Organic matter removal

#### 3.3.3.1 Removal of aromatics

As mentioned in section 3.1, there are several ways to characterize the aromaticity of the organic matters in OSPW such as UV-vis spectrum, SFS, FT-IR spectrum, and  $^1\text{H}$  NMR spectrum. To investigate the removal of aromatics in OSPW, we employed only SFS and  $^1\text{H}$  NMR spectra, because SFS is a more selective and sensitive method to measure the aromaticity of the water than UV-vis spectrum

(Wakeham 1977), and  $^1\text{H}$  NMR spectrum provides qualitative and quantitative information of both aromatics and organic acids (Clayden et al. 2012).

Applying ferrate doses lower than 100 mg/L Fe(VI) removed two and three ring aromatic compounds while no removal of one ring compounds was observed (Figure 3.3). By increasing the ferrate(VI) dose from 100 to 400 mg/L Fe(VI), one

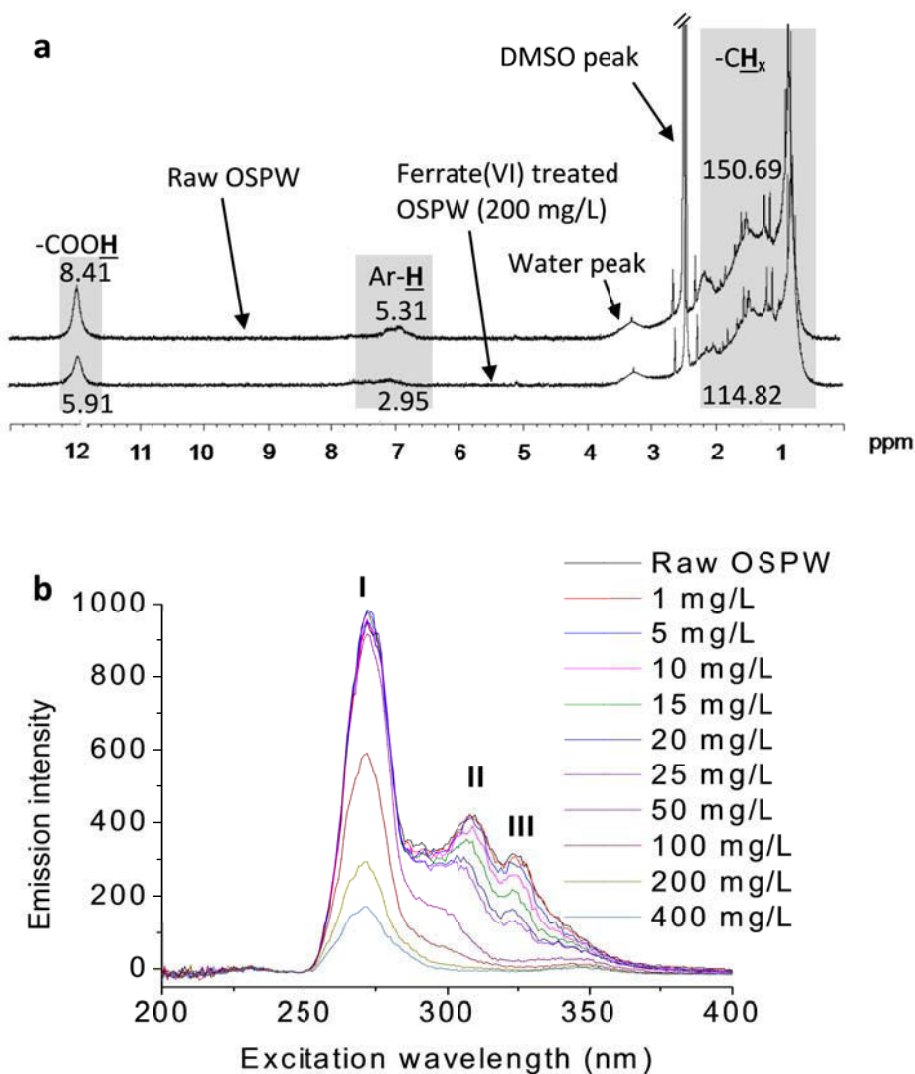


**Figure 3.3** (a)  $^1\text{H}$  NMR spectra for 200 mg/L Fe (VI)-treated OSPW (the numbers besides the peaks indicate the relative peak area when the DMSO solvent peak was set to be 100 as internal standard) and (b) SFS of raw and treated OSPW

ring aromatic compounds were also significantly removed, while two and three ring aromatic compounds were almost completely removed as can be seen in Figure 3.3b. This might be due to the fact that aromatic compounds with two or more fused rings had a higher electron density and thus were more reactive towards ferrate(VI) attack while the single benzene ring was usually unactivated and thus more stable to oxidation (Larson and Weber 1994). Additionally, the degradation of two and three ring compounds led to the formation of one ring compounds, which might explain the apparent stability of one ring aromatic compounds.

The significant removal of aromatic organic matter was confirmed by  $^1\text{H}$  NMR spectra (Figure 3.3a), which was acquired for samples treated at a representative dose of 200 mg/L Fe(VI). The peak assigned to hydrogen atoms on aromatic rings at the shift of 6.5-8.0 ppm decreased by 44.4% after ferrate(VI) oxidation, indicating that 44.4% of aromatic hydrogen atoms disappeared after treatment. However, this does not mean that only 44.4% aromatics were oxidized, because some aromatics can keep their aromaticity after oxidation. For example, fluorescing aromatics might be oxidized to other non-fluorescing aromatics with partial or all the aromaticity preserved. This also explains why SFS showed an almost complete decrease of peak areas while  $^1\text{H}$  NMR spectrum only showed 44.4% removal of aromatic hydrogens at 200 mg/L Fe(VI). Similar phenomenon was found in the oxidization of NAs, namely a high removal of NAs was achieved while only a moderate removal of the carboxyl functional groups was observed (29.7% removal of carboxyl functional groups at 200 mg/L Fe(VI)).

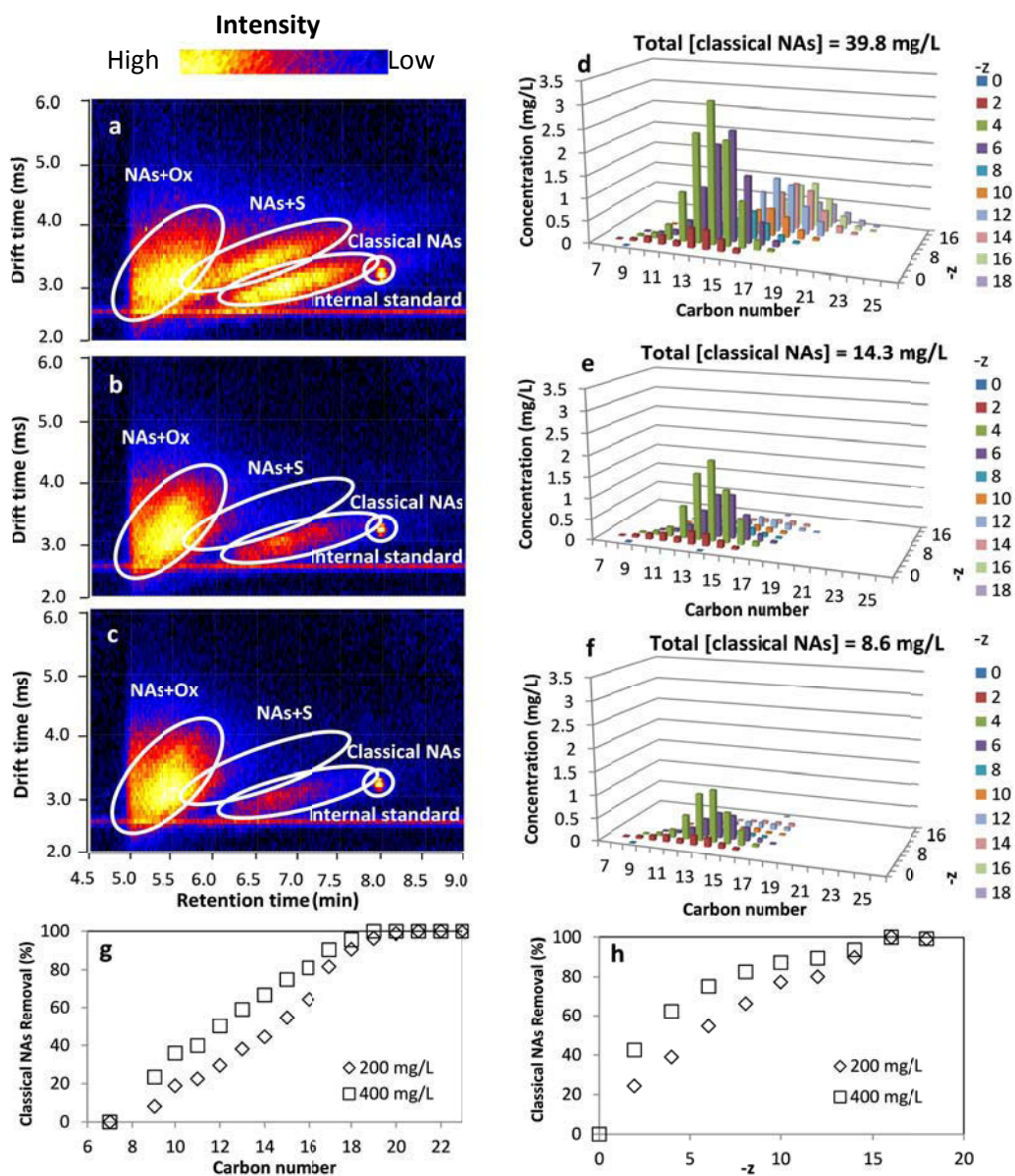


**Figure 3.4** Ion mobility spectra for (a) raw OSPW, (b) ferrate(VI)-treated OSPW (200 mg/L), and (c) ferrate(VI)-treated OSPW (400 mg/L); classical NAs distribution in (d) raw OSPW, (e) ferrate(VI)-treated OSPW (200 mg/L) and (f) ferrate(VI)-treated OSPW (400 mg/L); and classical NAs removal with respect to (g) carbon number and (h)  $-z$  number

### 3.3.3.2 Removal of NAs

Analysis of OSPW with ion mobility provides qualitative information about the present NAs. Three different regions according to retention and drift time can be distinguished: classical NAs, oxy-NAs, and heteroatomic NAs (Sun et al. 2014, Wang et al. 2013). High intensities of all three clusters can be seen in raw OSPW (Figure 3.4a). After treatment with 200 and 400 mg/L of ferrate(VI), the classical NAs were significantly reduced, and heteroatomic NAs were completely removed (Figure 3.4b&c). The preferential removal of heteroatomic NAs can be attributed to the electron-rich moieties that usually come with the heteroatoms (Jones et al. 2012, Pereira et al. 2013). No significant removal of oxy-NAs can be seen, this however can be attributed to the fact that oxy-NAs are removed but also produced during treatment. This finding is further confirmed by UPLC-TOF-MS.

Analysis by UPLC-TOF-MS showed that the initial concentration of classical NAs was 39.8 mg/L which changed to 14.3 mg/L and 8.6 mg/L after treatment by 200 mg/L Fe(VI) and 400 mg/L Fe(VI), corresponding to the removal of 64.0% and 78.4%, respectively (Figure 3.4d-2f). NAs+O (oxy-NAs with one additional oxygen) had an initial concentration of 12.5 mg/L and it changed to 14.8 and 15.6 mg/L after 200 mg/L Fe(VI) treatment and 400 mg/L Fe(VI) treatment, corresponding to a negative removal of -18.4% and -24.8%, respectively; NAs+O<sub>2</sub> (oxy-NAs with two additional oxygens) had an initial concentration of 13.3 mg/L, and the concentration changed to 15.7 and 14.4 mg/L after 200 mg/L Fe(VI) treatment and 400 mg/L Fe(VI) treatment, corresponding to a negative removal of -18.0% and -8.3%, respectively. Again this can be attributed to the fact that oxy-NAs are produced during treatment.

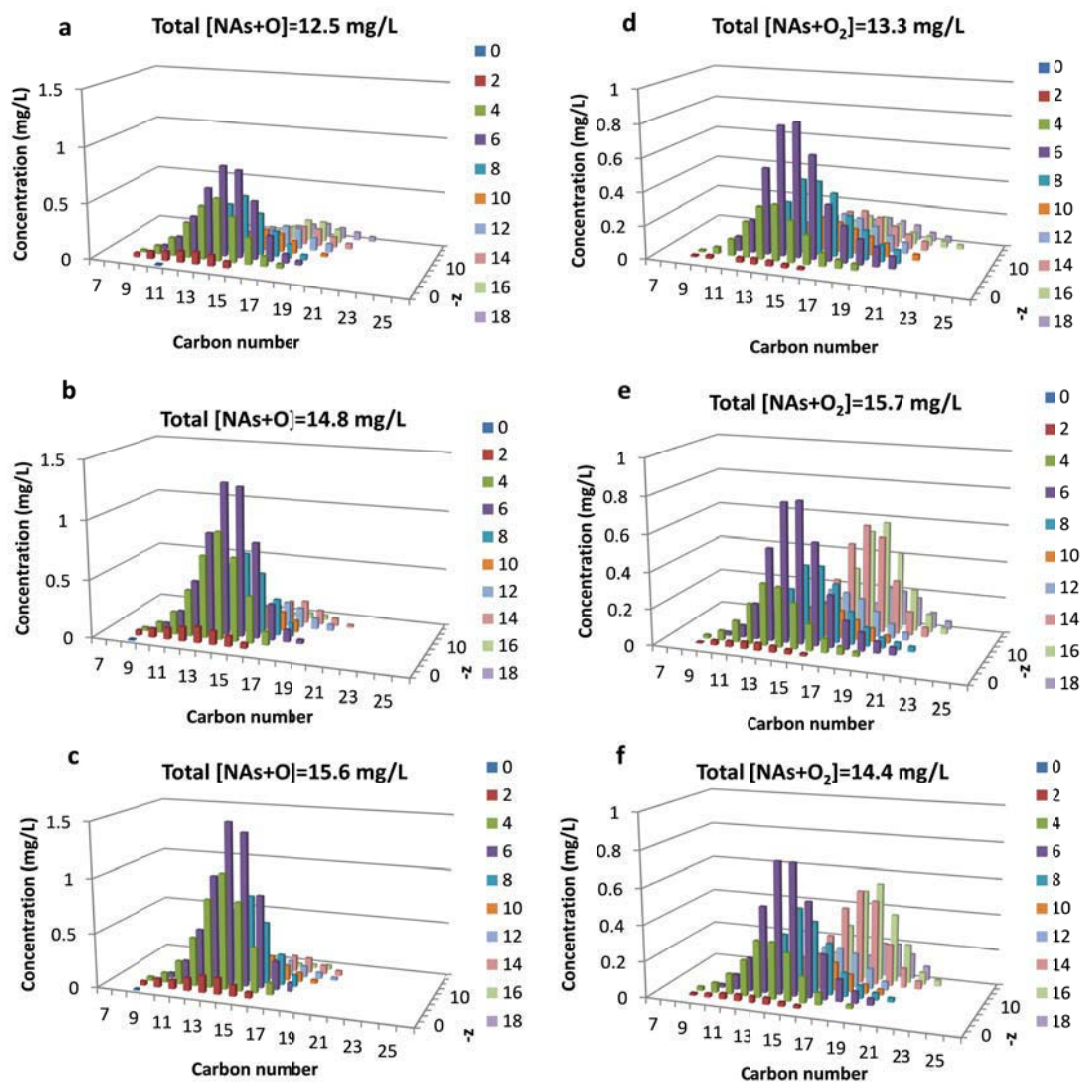


**Figure 3.5** Concentration of NAs+O in (a) raw OSPW, (b) 200 mg/L Fe(VI)-treated OSPW, (c) 400 mg/L Fe(VI) treated-OSPW; and concentration of NAs+O<sub>2</sub> in (d) raw OSPW, (e) 200 mg/L Fe(VI)-treated OSPW, and (f) 400 mg/L Fe(VI)-treated OSPW

In order to investigate the impact of carbon number and hydrogen-deficiency on the oxidation process, classical NAs removal versus carbon number and hydrogen-deficiency was plotted in Figure 3.4g and 3.4h. There was a clear trend that a high carbon number led to a high removal (Figure 3.4g), with complete

classical NAs removal when  $n \geq 18$ . The reason is that larger carbon skeleton structure means more potential sites for the attack of ferrate(VI), resulting in preferential removal of NAs with high carbon number, which is in accordance with work done by Pérez-Estrada et al. (2011). Similarly, as shown in Figure 3.4h, high hydrogen-deficiency also leads to high NAs removal, as higher -z number NAs have a higher reactivity for the following two reasons: first, high -z number might lead to higher number of rings, branches, and thus increasing number of tertiary carbons, which tend to be more reactive than primary and secondary carbons (Clayden et al. 2012); in addition, high hydrogen-deficiency might also imply more double bonds, which are more reactive than the saturated hydrocarbons (Pérez-Estrada et al. 2011).

For NAs+O, their concentration increase at low n and -z number outweighed their concentration decrease at the region of high n and -z number (Figure 3.5a-c). This is due to the fact that in general NAs+O with higher n and -z numbers are more reactive towards oxidation. This leads to degradation of oxy-NAs together with NAs resulting in lower n and -z number oxy-NAs (Figure 3.5) and is confirmed by other research (Klamerth et al. 2015). For NAs+O<sub>2</sub> an additional high n and -z number cluster in the range of -z=12-18 and n=15-24 was observed (Figure 3.5d-f). This leads to the conclusion that NAs+O<sub>2</sub> were another main group of transformed products from NAs oxidation, which was also confirmed by the fact that classical NAs in this range were almost completely removed. In general, during the ferrate(VI) oxidation process, there were both oxygen insertion which led to more “NAs+O<sub>x</sub>” species and the breakdown of the large molecules which

led to more small molecules (i.e. molecules with small carbon number  $n$ ). Both processes actually increased the solubility of the total NAs fraction in oxidized OSPW, which was confirmed by Figure 3.6 showing the OSPW before and after ferrate(VI) oxidation: the ferrate(VI)-treated OSPW was transparent when pH was adjusted to 2.5, while colloids formed in the untreated OSPW after pH adjustment.

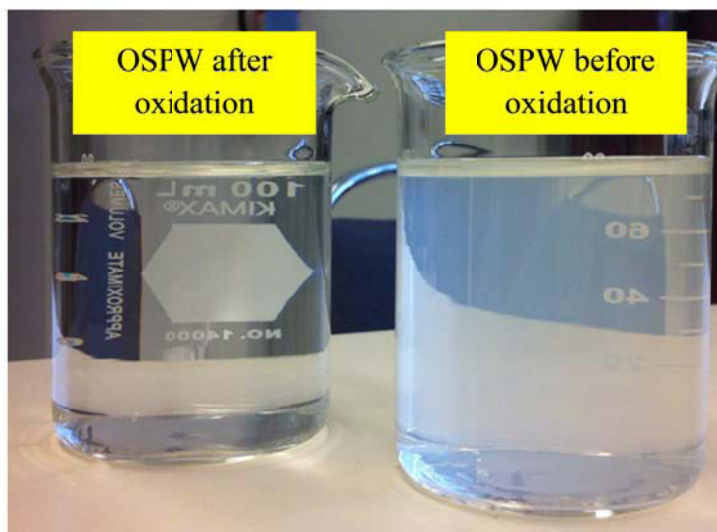


**Figure 3.6** Raw OSPW and 200 mg/L ferrate(VI)-treated OSPW (pH adjusted to 2.5)

### 3.3.4 Removal mechanisms

#### 3.3.4.1 Oxidation vs coagulation

Although ferrate(VI) is a dual agent as both oxidant and coagulant, the removal of organic matter can mainly be attributed to the oxidation process. In order to separate the contributions of these two processes, a comparison experiment was conducted with ferric chloride and potassium ferrate(VI). At  $\text{FeCl}_3$  concentrations between 1 and 400 mg/L calculated as iron, coagulation/flocculation achieved negligible removal of fluorescing organic matter (no peak decrease in the SFS),

UV<sub>254</sub>-absorbing organic matter (0-0.7%), and organic acids (0-1.7%) (Figure 3.7a-c), indicating that both aromatic and NA compounds were not removed through the coagulation/flocculation process. This negligible removal of organic matter by the coagulation in OSPW treatment was also reported by Alpatova et al. (2014). The reasons behind this limited removal of organic matter by the coagulation process are the follows: firstly, OSPW has a high pH of 8.6 (Figure 3.2b), making the floc surface highly negative. Organic acids in OSPW exist mostly in the anion form which is also negatively charged, and therefore electrostatic repulsion exists between the organic ions and the flocs; secondly, organic matter in OSPW has low molecular weight in the range of 150-350 Da (Wang et al. 2015), and the physical adsorption through van der Waals force is not enough to overcome the electrostatic repulsion; thirdly, the surface of ferric hydroxide flocs is too hydrophilic to be a good adsorbent for organic matter removal. Therefore, we can conclude that the organic matter removal in the ferrate(VI) process predominantly comes from the oxidation process, with the coagulation process making negligible contribution.

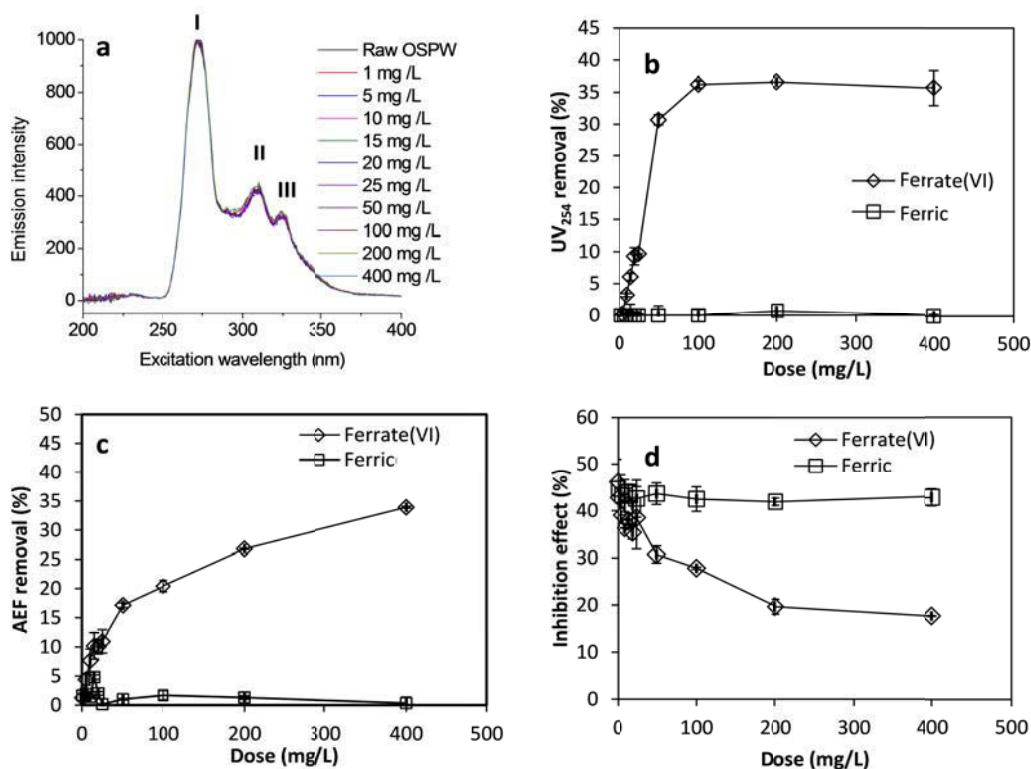


**Figure 3.7** Ferrate(VI) vs ferric in OSPW treatment: (a) SFS of raw OSPW and ferric-treated OSPW, (b) UV<sub>254</sub> removal, (c) AEF removal, and (d) inhibition effect on *Vibrio fischeri*

### 3.3.4.2 Oxidative species

At a pH above 8.6, the predominant ferrate(VI) species are  $\text{FeO}_4^{2-}$  and  $\text{HFeO}_4^-$  (Figure 3.8). Increasing the pH from 8.6 to 10.0, the  $\text{FeO}_4^{2-}$  percentage increases from 95.2% to 99.8%, and  $\text{HFeO}_4^-$  decreases from 4.8% to 0.2%. Although the concentration of  $\text{FeO}_4^{2-}$  is 20 times higher than  $\text{HFeO}_4^-$  initially, the main contributor to the oxidation in OSPW treatment is hypothesized to be  $\text{HFeO}_4^-$  for the following reasons. (1) The redox potential of  $\text{HFeO}_4^-$  is around 1.4 V; compared with unprotonated form  $\text{FeO}_4^{2-}$ , protonated form  $\text{HFeO}_4^-$  has a higher spin density on the oxo ligands which makes the metal center more electron

deficient, and thus increases the oxidation ability of  $\text{HFeO}_4^-$  (Hu et al. 2009, Sharma et al. 1997).  $\text{FeO}_4^{2-}$ , on the other hand, has a redox potential of only 0.7 V, and its contribution to the oxidation of organic matter especially classical NAs might be insignificant (Ho and Lau 2000, Zimmermann et al. 2012), although having a high concentration in the solution. (2) Reported specific rate constants for the reaction between organic compounds and  $\text{HFeO}_4^-$  are two to four orders of magnitude higher than those between organic compounds and  $\text{FeO}_4^{2-}$  (Hu et al. 2009, Sharma et al. 2006). (3) At pH range of the OSPW, the concentration of  $\text{HFeO}_4^-$  was high enough to make the oxidation process proceed because  $\text{HFeO}_4^-$  and the abundant  $\text{FeO}_4^{2-}$  exist in equilibrium; more  $\text{HFeO}_4^-$  will be generated from  $\text{FeO}_4^{2-}$  once consumed.

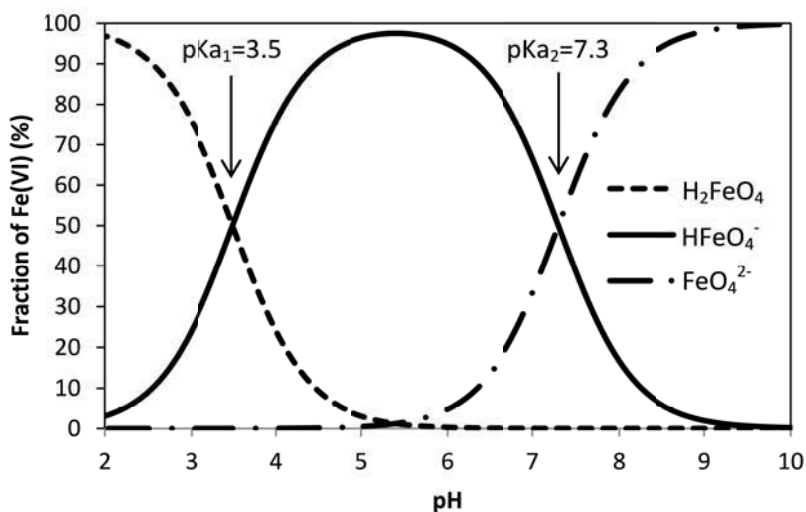


**Figure 3.8** Distribution diagram of Fe(VI) species

### 3.3.4.3 Oxidation mechanisms of aromatics and NAs

As the mechanisms of ferrate(VI) oxidation varies with different organic compounds, the focus in the following discussion will be on three groups of organics which were significantly removed in the ferrate(VI) oxidation process: aromatics, heteroatomic naphthenic acids, and classical NAs. (1) The reduction of aromaticity of the treated OSPW arose from the transformation of the aromatic rings. The opening of the aromatic rings was reported by Sharma et al. (2008) and Anquandah et al. (2013). It might occur through 1,3-dipolar cycloaddition and result in two aldehyde groups (Anquandah et al. 2013), which can be further oxidized by ferrate(VI) to acid groups. (2) The most likely pathway for the removal of NAs with heteroatoms is through the formation of a complex between the ferrate(VI) and target compounds, followed by inner-sphere electron transfer (Sharma et al. 2006). Heteroatoms such as sulfur constitute electron-rich moieties, which are good ligands for ferrate(VI) to form inner-sphere complexes, where electron transfer occurs between the electron-rich moieties and the electron-deficient iron center of ferrate(VI). Rate constants of reactions between  $\text{HFeO}_4^-$  and organosulfur compounds range from  $10^3$ - $10^6 \text{ M}^{-1}\text{s}^{-1}$  (Sharma 2013), which is high enough to lead to preferential removal of heteroatomic NAs. (3) For the removal of classical NAs by ferrate(VI), the mechanisms have not been reported. Classical NAs lack electron-rich moieties, and are relatively more stable to oxidation than the other two organic fractions mentioned above. The most probable attack sites for ferrate(VI) are reported to be  $\alpha$  and  $\beta$  carbons at the acid branches (Drzewicz et al. 2010, Sharma and Mishra 2006, Sharma and Bielski

1991) and tertiary carbons on the rings and the branches (Pérez-Estrada et al. 2011).  $^1\text{H}$  NMR spectra of raw OSPW and ferrate(VI)-treated OSPW showed that there was reduction of the  $\alpha$ -C hydrogen (Figure 3.3a), which indicates the attack on the  $\alpha$  carbon as one of the possible oxidation pathways for NAs by ferrate(VI). However, we cannot quantify the reduction as the peak was overlapped with other peaks. In addition, consistent with the order of reactivity of C-H (tertiary hydrogen > secondary hydrogen > primary hydrogen), other studies also showed that the bridgehead position of bicyclic aliphatic organics was vulnerable to the oxidation by metal oxidants (Wiberg and Foster 1961). To elucidate the oxidation mechanism of NAs by ferrate(VI), more studies with model compounds are needed.

#### 3.3.4.4 Electron paramagnetic resonance analysis

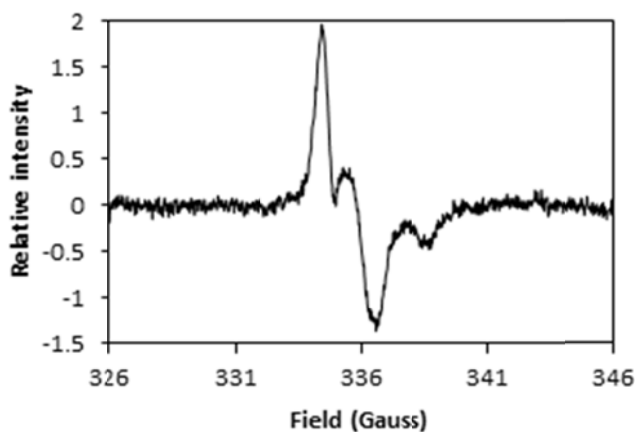


**Figure 3.9** EPR spectrum of the reaction mixture of OSPW, 100 mg/L Fe(VI) and 10g/L POBN

EPR analysis of the reaction mixture of POBN (the spin trap agent), OSPW and ferrate(VI) detected triplet signals at  $g_1=1.992$ ,  $g_2=2.001$  and  $g_3=2.015$ . On the

other hand, no such signals were detected with POBN/ferrate(VI) mixture or with POBN/OSPW mixture (Figure 3.9). It is safe to assume that these signals derive from the generated radicals from the reaction between OSPW and ferrate(VI). Due to the high g values, it can be stated that these radicals are of organic nature (Huang et al. 2001b). The existence of organic radicals as oxidation intermediates indicates that one of the probable reaction mechanisms is one-electron transfer, which often occurs via hydrogen abstraction by ferrate(VI) and results in organic radicals and ferrate(V). These organic radicals can react with dissolved oxygen in the water, generating intermediate species such as alcohols and aldehydes which can be further oxidized by ferrate(VI) or ferrate(V) until all oxidative iron species are reduced to Fe(III) (Ho and Lau 2000). Similar “Fe(VI)→Fe(V)→Fe(III)” oxidation sequence was also reported in ferrate(VI) oxidation of phenol (Huang et al. 2001a).

#### *3.3.4.5 Model compound study*

Three different model compounds which show a different structure to evaluate structure reactivity were selected for this study: CHA, with the carboxylic acid group directly attached to the ring; CHPA, in the same homologous series with CHA but with four more CH<sub>2</sub> increments between the acid group and the ring; and ADA, a dicarboxylic acids with tricyclic diamond-like structure and reported to exist in OSPW.(Scarlett et al. 2013) As shown in Figure 3.10, CHA exhibited the highest persistence towards ferrate(VI) oxidation, and its concentration only decreased by 26.3% during the 3-hour experiment. In the first 30 minutes of ferrate (VI) oxidation, the concentration decreased by 13.5% for CHA, 29.3% for



Analysis of degradation by-products was also attempted with high resolution HPLC TOF-MS (the mass spectra are provided in Appendix, Figure A4-6). With oxidized CHPA ( $C_{11}H_{20}O_2$ ) solution, a CHPA peak was detected at 4.82 min with  $m/z$  being 183.13849, and a composite product peak was detected at 4.22 min. The product peak contained two ions with corresponding  $m/z$  being 199.13352 and 197.11835, which fit molecular ions of  $C_{11}H_{20}O_3$  and  $C_{11}H_{18}O_3$  respectively. Most likely, after ferrate(VI) oxidation, a tertiary hydroxyl group was generated on the tertiary carbon, corresponding to the generation of  $C_{11}H_{20}O_3$ . Tertiary alcohols are stable to ferrate(VI) oxidation (Green 2001) and can thus be detected. The  $\alpha$  carbon reaction might also generate a hydroxyl group in the intermediate product, but it will soon be further oxidized by ferrate(VI) to ketones, which might be the second product we detected as  $C_{11}H_{18}O_3$ . Additionally, a ketone group on the  $\beta$  carbon might also contribute to the formation of  $C_{11}H_{18}O_3$  (this is supported by the fact that the ketone peak is a composite peak combining at least two distinct peaks (Figure A4)). Ketone groups are also resistant to ferrate(VI) oxidation, and can therefore survive and be detected at the end of the reaction (Green 2001). Similarly, two products,  $C_7H_{12}O_2$  and  $C_7H_{10}O_3$ , were identified as oxidized products of CHA (Figure A5); another two products,  $C_{12}H_{16}O_5$  and  $C_{12}H_{14}O_5$  were detected as oxidized products of ADA (Figure A6). Most likely, these products keep the carboxylic acid groups intact and have additional hydroxyl or ketone groups generated as discussed in CHPA oxidation. However, we cannot rule out the possibilities of the generation of other products, including

products that are not carboxylic acids (which might not be detected under the negative ESI mode). Nevertheless, these results are consistent with our previous conclusion from OSPW study that more “NAs+O<sub>x</sub>” were generated after classical NAs were oxidized.

### 3.3.5 Toxicity

As a prescreening tool for acute toxicity, Microtox<sup>®</sup> 81.9% screening test was adopted to evaluate the toxicity of OSPW on *Vibrio fischeri*. The inhibition level of raw OSPW was 42.8±0.6%, which was close to the previously reported values of 40-45% (Afzal et al. 2012, Shu et al. 2014). Overall, ferrate(VI) oxidation decreased the inhibition effect significantly to 19.6±1.6% at 200 mg/L Fe(VI) but a further increase of ferrate(VI) dose to 400 mg/L Fe(VI) only reduced the inhibition to 17.6±0.1% (Figure 3.11a). At the same time, NAs removal increased from 64.0% to 78.4%, indicating poor correlation between NAs removal and acute toxicity reduction. Klammerth et al. (2015)'s study also showed that low concentration of residual NAs after ozonation did not guarantee low toxicity. Similar poor correlation was reported by Zhang et al. (2015) in biological treatment of OSPW: after treatment, toxicity was reduced by 49.3% although there was no significant NAs removal. On the other hand, there is a linear correlation (empirical) between toxicity reduction and SFS (fluorescing compounds) peak area decrease (Figure 3.12). At low doses of 1-50 mg/L of Fe(VI) the inhibition effect decreased from 42.8±1.6% at 1 mg/L to 30.7±1.8% at 50 mg/L with decreasing peak area II and III (peak area decrease was calculated

to be 2% at 1 mg/L Fe(VI) and 75% at 50 mg/L Fe(VI)), while no significant decrease in peak area I was observed. At higher ferrate(VI) doses from 200

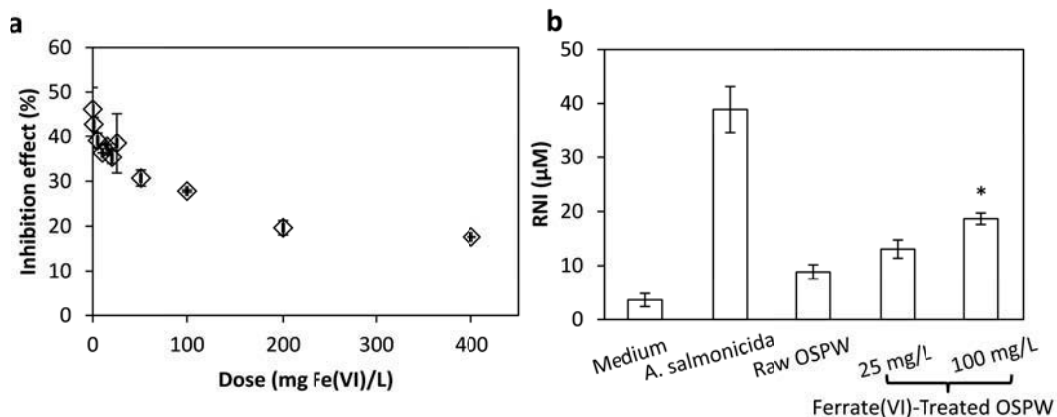


**Figure 3.11** (a) Acute toxicity to *Vibrio fischeri* of raw OSPW and ferrate(VI)-treated OSPW (Note: error bars indicate mean $\pm$ SD with n=3); (b) Nitrite production by PKMs exposed to medium control, raw OSPW, and OSPW treated with ferrate (VI) with the dose of 25 mg/L and 100 mg/L Fe(VI). Positive and negative controls were heat killed *A. sal monicida* and culture medium, respectively. Nitric oxide production was determined using the Griess reaction and RNI concentration was determined using RNI standard curve. Data are represented as RNI production by macrophages from separate cultures established from three individual fish. Statistical analysis was done using one-way ANOVA with a Dunnett's post hoc test. Asterisks (\*) indicate statistically significant increases ( $p < 0.05$ ) of RNI production in treated compared to raw OSPW

mg/L to 400 mg/L Fe(VI), there was no further decrease of peak II and III while only 10% more decrease of peak area I was observed, resulting in no significant reduction of toxicity (Figure 3.11a). Therefore, it can be concluded that although the concentration of the fluorescing compounds is relatively low compared to that

of NAs, the toxicity effect from them might be significant. This conclusion is consistent with the widely reported toxicity of the aromatics especially PAHs (Kupryianchyk et al. 2012, Lee et al. 2002, Sayles et al. 1999). In OSPW studies, Rowland et al. (2011) found that the estrogenic effect of OSPW arose from the aromatics in the water, and Scarlett et al. (2013) also suggested that aromatics in OSPW were at least as toxic as NAs. Further studies are needed to compare the toxic effects of aromatics and NAs in OSPW.

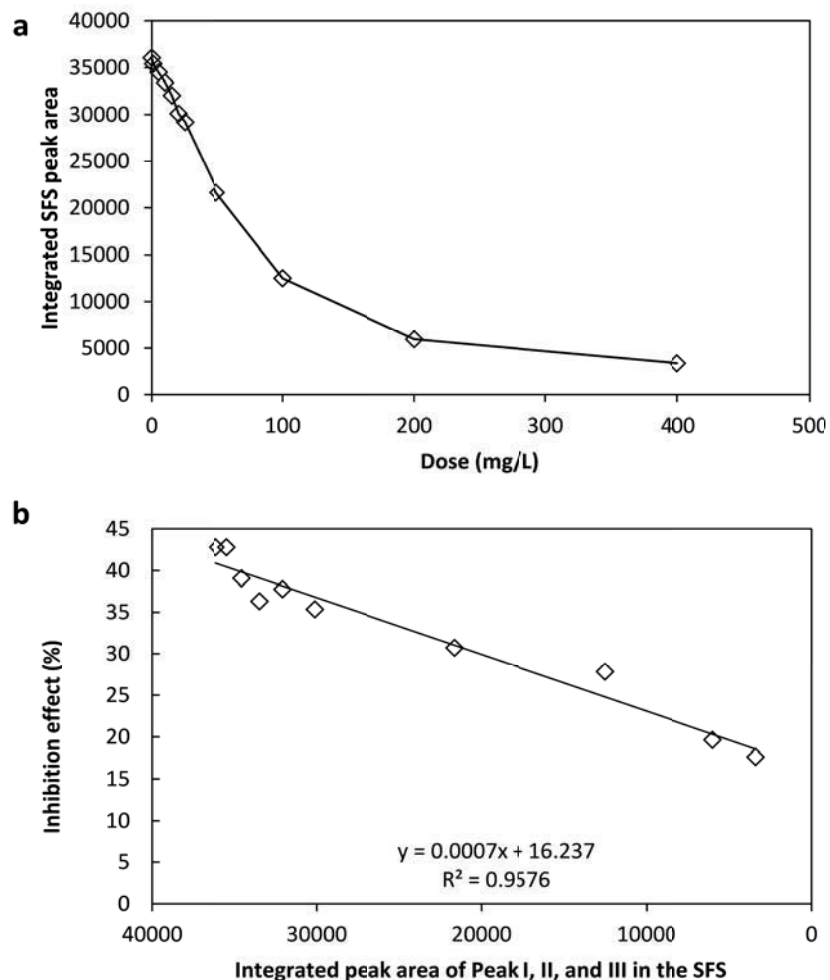


**Figure 3.12** (a) Integrated peak area of SFS at different ferrate(VI) dose; (b) Linear relationship between inhibition effect and integrated peak area in the SFS

The effects of the OSPW treated samples on goldfish primary kidney macrophages (PKMs) were examined by measuring the production of reactive nitrogen intermediates (RNIs) as shown in Figure 3.11b. Macrophages are large immune cells capable of destroying pathogens by producing toxic RNIs, such as nitric oxide; the production of RNI by macrophages was quantified using the Griess reaction (Stone et al. 2005). High RNI production indicates high functional activity of PKMs and correspondingly, low toxicity of the test sample. The exposure of PKMs to the raw and ferrate(VI)-treated OSPW samples caused a reduction in RNI production compared to positive control (heat-killed *A. salmonicida*) ( $38.9 \pm 4.3 \mu\text{M}$  RNI), showing higher toxicity induced by raw OSPW ( $8.8 \pm 1.3 \mu\text{M}$  RNI) and significantly lower toxicity induced by treated OSPW ( $18.7 \pm 1.1 \mu\text{M}$  RNI at 100 mg/L Fe(VI)). This results, together with the Microtox results, indicate that ferrate(VI) treatment is effective at reducing toxicity towards prokaryotic organisms such as *Vibrio fischeri* and eukaryotic cells such as goldfish PKMs.

### **3.3.6 pH adjustment**

To study the pH effect on ferrate(VI) oxidation, the initial pH of OSPW was adjusted to 6 and the oxidation experiments were repeated as at natural pH. The results were summarized in Figure 3.13. This adjustment improved the performance of the ferrate(VI) oxidation in terms of both aromatics removal (Figure 3.13a&b) and NAs removal (Figure 3.13c). The trend of the SFS peak reduction was similar to that achieved at natural pH: peak II and III were preferentially removed, and peak I was only significantly reduced at high doses.

At the same dose of ferrate(VI), oxidation at initial pH 6 achieved higher removal of fluorescing aromatics than at natural pH, which was mainly caused by the higher removal of single-ring aromatics (peak I) at initial pH 6 (Figure 3.13a&b). At the same time, inhibition effect on *Vibrio fischeri* was also reduced to  $16.3\pm 0.8\%$  at initial pH 6 at the dose of 400 mg/L Fe(VI), lower than achieved at natural pH ( $17.6\pm 0.1\%$ ) (Figure 3.13d). However, these improvements on removal of aromatics and reduction of toxicity were not significant compared with the

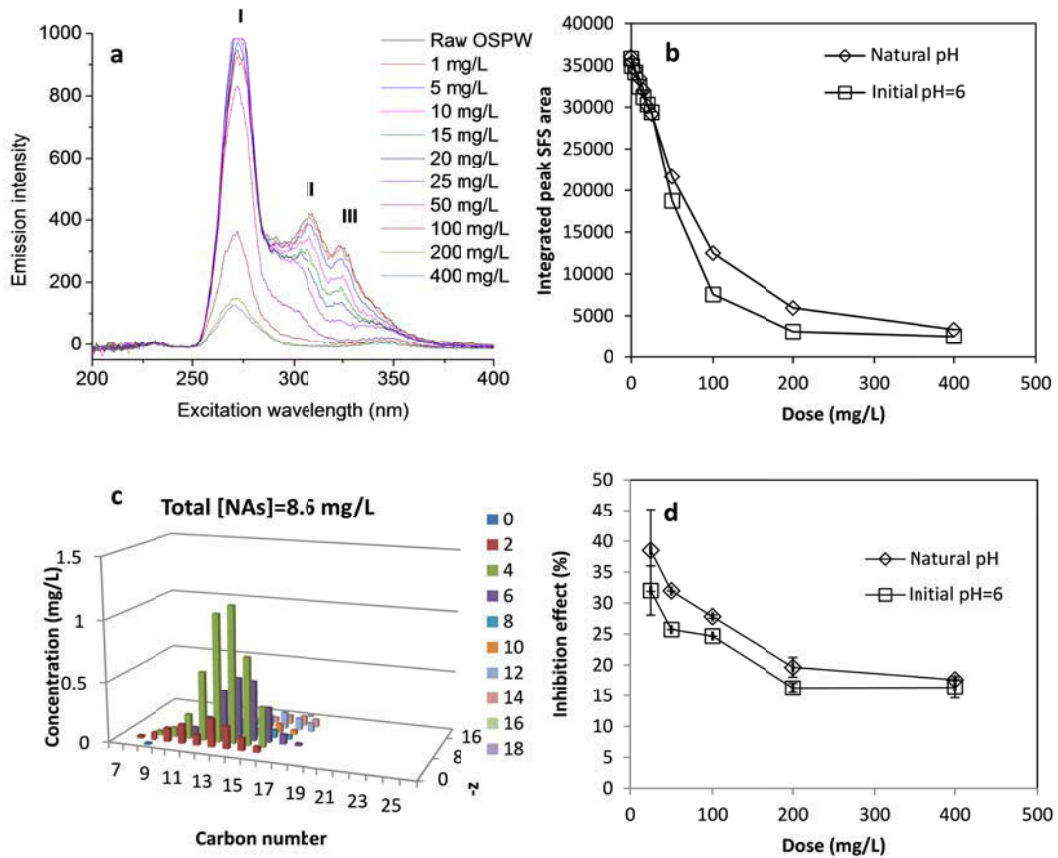


**Figure 3.13** Oxidation performance by ferrate(VI) at initial pH 6: (a) SFS, (b) SFS peak area, (c) NAs distribution (dose: 200 mg/L Fe(VI)), and (c) inhibition effect on *Vibrio fische ri* (For comparison reason, oxidation performance by ferrate(VI) at natural pH was replotted in b and d)

enhancement of NAs removal. At initial pH of 6, ferrate(VI) achieved 78.4% removal of NAs at 200 mg/L Fe(VI), equivalent to the removal at 400 mg/L Fe(VI) at natural pH. As mentioned in section 3.4, this also indicates the poor correlation between toxicity effect and NAs removal.

### **3.3.7 Environmental implications**

Although NAs and aromatics are two main fractions of organic matter in OSPW, most of the current studies of OSPW treatment focus on the removal of NAs; the toxicity of OSPW has been presumably attributed to NAs. However, as shown in this study, the toxicity effect of the aromatics might also be significant. More work is warranted to investigate the concentrations, species, and the environmental impact of the aromatics in OSPW. The results of this study demonstrated that ferrate(VI) oxidation is an effective process in transforming NAs and the aromatics and reducing the acute toxicity of OSPW. However, when high doses of ferrate(VI) (e.g. 200 mg/L and 400 mg/L Fe(VI)) are applied, large quantity of sludge will be generated. The disposal of the sludge in an environmentally and economically feasible way is a challenging topic to be addressed.

### 3.4 References

- Afzal, A., Drzewicz, P., Perez-Estrada, L.A., Chen, Y., Martin, J.W. and Gamal El-Din, M. (2012) Effect of molecular structure on the relative reactivity of naphthenic acids in the UV/H<sub>2</sub>O<sub>2</sub> advanced oxidation process. *Environmental Science & Technology* 46(19), 10727-10734.
- Alberta Government (2014) 2013-2014 Energy annual report, Edmonton, Alberta, Canada.
- Allen, E.W. (2008) Process water treatment in Canada's oil sands industry: I. Target pollutants and treatment objectives. *Journal of Environmental Engineering and Science* 7(2), 123-138.
- Alpatova, A., Kim, E.-S., Dong, S., Sun, N., Chelme-Ayala, P. and Gamal El-Din, M. (2014) Treatment of oil sands process-affected water with ceramic ultrafiltration membrane: Effects of operating conditions on membrane performance. *Separation and Purification Technology* 122(0), 170-182.
- Alsheyab, M., Jiang, J.Q. and Stanford, C. (2009) On-line production of ferrate with an electrochemical method and its potential application for wastewater treatment - A review. *Journal of Environmental Management* 90(3), 1350-1356.
- Anquandah, G.A.K., Sharma, V.K., Panditi, V.R., Gardinali, P.R., Kim, H. and Oturan, M.A. (2013) Ferrate(VI) oxidation of propranolol: Kinetics and products. *Chemosphere* 91(1), 105-109.
- Barrow, M.P., Witt, M., Headley, J.V. and Peru, K.M. (2010) Athabasca oil sands process water: characterization by atmospheric pressure photoionization

- and electrospray ionization Fourier transform ion cyclotron resonance mass spectrometry. *Analytical Chemistry* 82(9), 3727-3735.
- Brient, J.A., Wessner, P.J. and Doyle, M.N. (2000) *Kirk-Othmer encyclopedia of chemical technology*, John Wiley & Sons, Inc., New Jersey.
- Clayden, J., Greeves, N. and Warren, S. (2012) *Organic chemistry*, Oxford University Press, New York.
- Drzewicz, P., Afzal, A., Gamal El-Din, M. and Martin, J.W. (2010) Degradation of a model naphthenic acid, cyclohexanoic acid, by vacuum UV (172 nm) and UV (254 nm)/H<sub>2</sub>O<sub>2</sub>. *Journal of Physical Chemistry A* 114(45), 12067-12074.
- Frank, R.A., Kavanagh, R., Kent Burnison, B., Arsenault, G., Headley, J.V., Peru, K.M., Van Der Kraak, G. and Solomon, K.R. (2008) Toxicity assessment of collected fractions from an extracted naphthenic acid mixture. *Chemosphere* 72(9), 1309-1314.
- Gheraout, D. and Naceur, M.W. (2011) Ferrate(VI): In situ generation and water treatment - A review. *Desalination and Water Treatment* 30(1-3), 319-332.
- Green, J. R. (2011), Potassium ferrate. In *Encyclopedia of Reagents for Organic Synthesis*, John Wiley & Sons Inc., New Jersey.
- Grewer, D.M., Young, R.F., Whittal, R.M. and Fedorak, P.M. (2010) Naphthenic acids and other acid-extractables in water samples from Alberta: What is being measured? *Science of The Total Environment* 408(23), 5997-6010.
- Headley, J.V., Barrow, M.P., Peru, K.M., Fahlman, B., Frank, R.A., Bickerton, G., McMaster, M.E., Parrott, J. and Hewitt, L.M. (2011) Preliminary

fingerprinting of Athabasca oil sands polar organics in environmental samples using electrospray ionization Fourier transform ion cyclotron resonance mass spectrometry. *Rapid Communications in Mass Spectrometry* 25(13), 1899-1909.

Headley, J.V., Peru, K.M., Armstrong, S.A., Han, X., Martin, J.W., Mapolelo, M.M., Smith, D.F., Rogers, R.P. and Marshall, A.G. (2009) Aquatic plant-derived changes in oil sands naphthenic acid signatures determined by low-, high- and ultrahigh-resolution mass spectrometry. *Rapid Communications in Mass Spectrometry* 23(4), 515-522.

Headley, J.V., Peru, K.M., Fahlman, B., McMartin, D.W., Mapolelo, M.M., Rodgers, R.P., Lobodin, V.V. and Marshall, A.G. (2012) Comparison of the levels of chloride ions to the characterization of oil sands polar organics in natural waters by use of Fourier transform ion cyclotron resonance mass spectrometry. *Energy & Fuels* 26(5), 2585-2590.

Hirsch, T. (2005) *Treasure in the sand : an overview of Alberta's oil sands resources*. Canada West Foundation, Calgary, Alberta

Ho, C.M. and Lau, T.C. (2000) Lewis acid activated oxidation of alkanes by barium ferrate. *New Journal of Chemistry* 24(8), 587-590.

Hu, L., Martin, H.M., Arce-Bulted, O., Sugihara, M.N., Keating, K.A. and Strathmann, T.J. (2009) Oxidation of carbamazepine by Mn(VII) and Fe(VI): Reaction kinetics and mechanism. *Environmental Science & Technology* 43(2), 509-515.

- Huang, H., Sommerfeld, D., Dunn, B.C., Eyring, E.M. and Lloyd, C.R. (2001a) Ferrate(VI) oxidation of aqueous phenol: Kinetics and mechanism. *Journal of Physical Chemistry A* 105(14), 3536-3541.
- Huang, H., Sommerfeld, D., Dunn, B.C., Lloyd, C.R. and Eyring, E.M. (2001b) Ferrate(VI) oxidation of aniline. *Journal of the Chemical Society, Dalton Transactions* (8), 1301-1305.
- Huang, R., McPhedran, K.N. and Gamal El-Din, M. (2015) Ultra performance liquid chromatography ion mobility time-of-flight mass spectrometry characterization of naphthenic acids species from oil sands process-affected water. *Environmental Science & Technology* 49(19):11737-45
- Jiang, J.Q. (2014) Advances in the development and application of ferrate(VI) for water and wastewater treatment. *Journal of Chemical Technology & Biotechnology* 89(2), 165-177.
- Jones, D., Scarlett, A.G., West, C.E. and Rowland, S.J. (2011) Toxicity of individual naphthenic acids to *Vibrio fischeri*. *Environmental Science & Technology* 45(22), 9776-9782.
- Jones, D., West, C.E., Scarlett, A.G., Frank, R.A. and Rowland, S.J. (2012) Isolation and estimation of the aromatic' naphthenic acid content of an oil sands process-affected water extract. *Journal of Chromatography A* 1247, 171-175.
- Kavanagh, R.J., Frank, R.A., Burnison, B.K., Young, R.F., Fedorak, P.M., Solomon, K.R. and Van, D.K.G. (2012) Fathead minnow (*Pimephales*

- promelas*) reproduction is impaired when exposed to a naphthenic acid extract. *Aquatic Toxicology* 116-117, 34-42.
- Klamerth, N., Moreira, J., Li, C., Singh, A., McPhedran, K.N., Chelme-Ayala, P., Belosevic, M. and Gamal El-Din, M. (2015) Effect of ozonation on the naphthenic acids' speciation and toxicity of pH-dependent organic extracts of oil sands process-affected water. *Science of The Total Environment* 506–507(0), 66-75.
- Kupryianchyk, D., Rakowska, M.I., Grotenhuis, J.T.C. and Koelmans, A.A. (2012) Modeling trade-off between PAH toxicity reduction and negative effects of sorbent amendments to contaminated sediments. *Environmental Science & Technology* 46(9), 4975-4984.
- Larson, R. and Weber, E. (1994) Reaction mechanisms in environmental organic chemistry, pp. 275-358, Lewis Publishers, Florida.
- Lee, J.H., Landrum, P.F. and Koh, C.H. (2002) Toxicokinetics and time-dependent PAH toxicity in the amphipod *Hyaella azteca*. *Environmental Science & Technology* 36(14), 3124-3130.
- Leishman, C., Widdup, E.E., Quesnel, D.M., Chua, G., Gieg, L.M., Samuel, M.A. and Muench, D.G. (2013) The effect of oil sands process-affected water and naphthenic acids on the germination and development of *Arabidopsis*. *Chemosphere* 93(2), 380-387.
- Licht, S.; Yu, X. (2008) Recent Advances in Fe(VI) Synthesis. In *Ferrates*, American Chemical Society; Vol. 985, pp 2-51.

- Luo, Z., Strouse, M., Jiang, J.Q. and Sharma, V.K. (2011) Methodologies for the analytical determination of ferrate(VI): A Review. *Journal of Environmental Science and Health - Part A Toxic/Hazardous Substances and Environmental Engineering* 46(5), 453-460.
- Mackinnon, M. and Zubot, W. (2013) Handbook on theory and practice of bitumen recovery from Athabasca oil sands Volume II: Industrial practices. Czarnecki, J., Masliyah, J., Xu, Z. and Dabros, M. (eds), Kingsley Knowledge Publishing, Alberta.
- Martin, J.W., Barri, T., Han, X., Fedorak, P.M., Gamal El-Din, M., Perez, L., Scott, A.C. and Jiang, J.T. (2010) Ozonation of oil sands process-affected water accelerates microbial bioremediation. *Environmental Science and Technology* 44(21), 8350-8356.
- Nero, V., Farwell, A., Lee, L.E.J., Van, M.T., MacKinnon, M.D. and Dixon, D.G. (2006) The effects of salinity on naphthenic acid toxicity to yellow perch: Gill and liver histopathology. *Ecotoxicology and Environmental Safety* 65(2), 252-264.
- Ninane, L., Kanari, N., Criado, C., Jeannot, C., Evrard, O. and Neveux, N. (2008) New processes for alkali ferrate synthesis. In *Ferrates*, pp. 102-111, American Chemical Society.
- Nyakas, A., Han, J., Peru, K.M., Headley, J.V. and Borchers, C.H. (2013) Comprehensive analysis of oil sands processed water by direct-infusion fourier-transform ion cyclotron resonance mass spectrometry with and

without offline UHPLC sample prefractionation. *Environmental Science and Technology* 47(9), 4471-4479.

Pereira, A.S., Islam, M.s., Gamal El-Din, M. and Martin, J.W. (2013) Ozonation degrades all detectable organic compound classes in oil sands process-affected water; an application of high-performance liquid chromatography/obitrap mass spectrometry. *Rapid Communications in Mass Spectrometry* 27(21), 2317-2326.

Pérez-Estrada, L.A., Han, X., Drzewicz, P., Gamal El-Din, M., Fedorak, P.M. and Martin, J.W. (2011) Structure-reactivity of naphthenic acids in the ozonation process. *Environmental Science & Technology* 45(17), 7431-7437.

Pourrezaei, P., Alpatova, A., Khosravi, K., Drzewicz, P., Chen, Y., Chelme-Ayala, P. and Gamal El-Din, M. (2014) Removal of organic compounds and trace metals from oil sands process-affected water using zero valent iron enhanced by petroleum coke. *Journal of Environmental Management* 139(0), 50-58.

Reinardy, H.C., Scarlett, A.G., Henry, T.B., West, C.E., Hewitt, L.M., Frank, R.A. and Rowland, S.J. (2013) Aromatic naphthenic acids in oil sands process-affected water, resolved by GCxGC-MS, only weakly induce the gene for vitellogenin production in zebrafish (*Danio rerio*) larvae. *Environmental Science & Technology* 47(12), 6614-6620.

Ross, M.S., Pereira, A.d.S., Fennell, J., Davies, M., Johnson, J., Sliva, L. and Martin, J.W. (2012) Quantitative and qualitative analysis of naphthenic

- acids in natural waters surrounding the Canadian oil sands industry. *Environmental Science & Technology* 46(23), 12796-12805.
- Rowland, S.J., West, C.E., Jones, D., Scarlett, A.G., Frank, R.A. and Hewitt, L.M. (2011) Steroidal aromatic 'naphthenic acids' in oil sands process-affected water: structural comparisons with environmental estrogens. *Environmental Science & Technology* 45(22), 9806-9815.
- Sayles, G.D., Acheson, C.M., Kupferle, M.J., Shan, Y., Zhou, Q., Meier, J.R., Chang, L. and Brenner, R.C. (1999) Land treatment of PAH-contaminated soil: Performance measured by chemical and toxicity assays. *Environmental Science & Technology* 33(23), 4310-4317.
- Scarlett, A.G., Reinardy, H.C., Henry, T.B., West, C.E., Frank, R.A., Hewitt, L.M. and Rowland, S.J. (2013) Acute toxicity of aromatic and non-aromatic fractions of naphthenic acids extracted from oil sands process-affected water to larval zebrafish. *Chemosphere* 93(2), 415-420.
- Sharma, V.K., Noorhasan, N.N., Mishra, S.K. and Nesnas, N. (2008) Ferrate(VI) oxidation of recalcitrant compounds: Removal of biological resistant organic molecules by ferrate(VI). In *Ferrates*, pp. 339-349, American Chemical Society.
- Sharma, V.K. and Mishra, S. (2006) Ferrate(VI) oxidation of ibuprofen: A kinetic study. *Environmental Chemistry Letters* 3(4), 182-185.
- Sharma, V.K. (2002) Potassium ferrate(VI): An environmentally friendly oxidant. *Advances in Environmental Research* 6(2), 143-156.

- Sharma, V.K. (2013) Ferrate(VI) and ferrate(V) oxidation of organic compounds: Kinetics and mechanism. *Coordination Chemistry Reviews* 257(2), 495-510.
- Sharma, V.K. and Bielski, B.H.J. (1991) Reactivity of ferrate(VI) and ferrate(V) with amino acids. *Inorganic Chemistry* 30(23), 4306-4310.
- Sharma, V.K., Mishra, S.K. and Nesnas, N. (2006) Oxidation of sulfonamide antimicrobials by ferrate(VI) [FeVIO<sub>4</sub><sup>2-</sup>]. *Environmental Science & Technology* 40(23), 7222-7227.
- Sharma, V.K., Smith, J.O. and Millero, F.J. (1997) Ferrate(VI) oxidation of hydrogen sulfide. *Environmental Science & Technology* 31(9), 2486-2491.
- Shu, Z., Li, C., Belosevic, M., Bolton, J.R. and Gamal El-Din, M. (2014) Application of a solar UV/chlorine advanced oxidation process to oil sands process-affected water remediation. *Environmental Science & Technology* 48(16), 9692-9701.
- Stone, W., Yang, H. and Qui, M. (2005) Assays for nitric oxide expression. In *Mast Cells*. Krishnaswamy, G. and Chi, D. (eds), pp. 245-256, Humana Press, New York.
- Sun, N., Chelme-Ayala, P., Klammerth, N., McPhedran, K.N., Islam, M.S., Perez-Estrada, L., Drzewicz, P., Blunt, B.J., Reichert, M., Hagen, M., Tierney, K.B., Belosevic, M. and Gamal El-Din, M. (2014) Advanced analytical mass spectrometric techniques and bioassays to characterize untreated and ozonated oil sands process-affected water. *Environmental Science & Technology* 48(19), 11090-11099.

- Thompson, G.W., Ockerman, L.T. and Schreyer, J.M. (1951) Preparation and purification of potassium Ferrate(VI). *Journal of the American Chemical Society* 73(3), 1379-1381.
- Tuan Vo, D. (1978) Multicomponent analysis by synchronous luminescence spectrometry. *Analytical Chemistry* 50(3), 396-401.
- Wakeham, S.G. (1977) Synchronous fluorescence spectroscopy and its application to indigenous and petroleum-derived hydrocarbons in lacustrine sediments. *Environmental Science & Technology* 11(3), 272-276.
- Wang, C., Alpatova, A., McPhedran, K.N. and Gamal El-Din, M. (2015) Coagulation/flocculation process with polyaluminum chloride for the remediation of oil sands process-affected water: Performance and mechanism study. *Journal of Environmental Management* 160, 254-262.
- Wang, N., Chelme-Ayala, P., Perez-Estrada, L., Garcia-Garcia, E., Pun, J., Martin, J.W., Belosevic, M. and Gamal El-Din, M. (2013) Impact of ozonation on naphthenic acids speciation and toxicity of oil sands process-affected water to *Vibrio fischeri* and mammalian immune system. *Environmental Science & Technology* 47(12), 6518-6526.
- Wiberg, K.B. and Foster, G. (1961) The stereochemistry of the chromic acid oxidation of tertiary hydrogens<sup>1</sup>. *Journal of the American Chemical Society* 83(2), 423-429.

- Williams, A.T.R., Winfield, S.A. and Miller, J.N. (1983) Relative fluorescence quantum yields using a computer-controlled luminescence spectrometer. *Analyst* 108(1290), 1067-1071.
- Zhang, Y., McPhedran, K.N. and Gamal El-Din, M. (2015) Pseudomonads biodegradation of aromatic compounds in oil sands process-affected water. *Science of The Total Environment* 521-522, 59-67.
- Zimmermann, S.G., Schmukat, A., Schulz, M., Benner, J., Gunten, U.V. and Ternes, T.A. (2012) Kinetic and mechanistic investigations of the oxidation of tramadol by ferrate and ozone. *Environmental Science & Technology* 46(2), 876-884.

## 4 COMPARISON OF UV/HYDROGEN PEROXIDE, POTASSIUM FERRATE(VI), AND OZONE IN OXIDIZING THE ORGANIC FRACTION OF OIL SANDS PROCESS-AFFECTED WATER (OSPW)<sup>3</sup>

### 4.1 Introduction

Oil sands process-affected water (OSPW) is the water produced in the bitumen extraction and the following upgrading processes (Mackinnon and Zubot 2013). Although nearly 80% OSPW is reused, a sustained oil sands production requires fresh water withdrawal from surface water, leading to an increasing quantity of OSPW stored in the tailing ponds (Mackinnon and Zubot 2013). OSPW is a type of water with high salinity and alkalinity, and it contains varieties of metal cations, anions, and organic compounds as well as suspended particles (Bauer 2013, Wang et al. 2015). The organic fraction of OSPW contains naphthenic acids (NAs), sulfur and nitrogen containing species, and aromatic compounds including trace amount of polyaromatic hydrocarbon (PAH) (Jones et al. 2013, Mohamed et al. 2013, Quagraine et al. 2005). NAs refers to a mixture of alkyl-substituted acyclic and cycloaliphatic carboxylic acids, with a general formula  $C_nH_{2n+z}O_x$ , where n indicates the number of carbon atoms, z specifies the hydrogen deficiency arising

---

<sup>3</sup> A version of this chapter has been published: Wang, C., Klammerth, N., Messele, S. A., Singh, A., Belosevic, M., and Gamal El-Din, M., Comparison of UV/hydrogen peroxide, potassium ferrate(VI), and ozone in oxidizing the organic fraction of oil sands process-affected water (OSPW). *Water Research* 100, 476-485.

from double bonds and/or rings, and  $x$  is the number of oxygen atoms (Jones et al. 2013, Mohamed et al. 2013). So far focus of OSPW treatment has been put on removing classical NAs (NAs with  $x=2$ ) (Gamal El-Din et al. 2011, Shu et al. 2014, Wang et al. 2015, Zhang et al. 2015) which was reported to be “the most acutely toxic chemical classes in OSPW” (Morandi et al. 2015). NAs with more oxygens (oxy-NAs,  $x>2$ ) were reported to be less toxic than the classical NAs due to the increase of hydrophilicity after oxidation (i.e., less affinity to cell membrane) (Frank et al. 2009, Frank et al. 2008, He et al. 2010).

The high concentration and low biodegradability of the organic matter in OSPW prompted extensive chemical oxidation research in OSPW treatment. So far, chlorine oxidation (Shu et al. 2014), ozonation (Gamal El-Din et al. 2011), and various advanced oxidation processes (AOPs) including UV/chlorine (Shu et al. 2014), UV/H<sub>2</sub>O<sub>2</sub> (Afzal et al. 2012, Liang et al. 2012), and peroxydisulfate oxidation (Drzewicz et al. 2012) have been investigated in treating OSPW. Although many treatment processes have been studied, very few studies have done well-defined performance comparison among these different oxidation processes. Furthermore, a direct comparison between selective oxidation and unselective oxidation has not been carried out. The difference between those two oxidative reactions leads to variations in efficiency of transforming the two main organic fractions in OSPW, NAs and aromatics, and will further impact the toxicity of the treated OSPW.

To close the abovementioned research gap, this study investigated three different oxidation processes for the treatment of OSPW: UV/H<sub>2</sub>O<sub>2</sub> oxidation (unselective),

ferrate(VI) oxidation (selective), and ozonation (selective and/or unselective depending on the pathway and pH). To further elucidate the reaction mechanism of ozonation, the hydroxyl radical ( $\bullet\text{OH}$ ) scavenger tert-butyl alcohol (TBA) was applied. A brief overview of each process is provided as follows.

UV/H<sub>2</sub>O<sub>2</sub> oxidation: the generation of  $\bullet\text{OH}$  in the UV/H<sub>2</sub>O<sub>2</sub> process relies on the homolytic cleavage of the H<sub>2</sub>O<sub>2</sub> molecule by UV photons. The  $\bullet\text{OH}$  is a strong oxidant with a redox potential of 2.6-2.9 V at acidic pH and 1.8-1.9 V at basic pH (Ghernaout and Naceur 2011, Wardman 1989), transforming almost all organics indiscriminately mainly by hydrogen abstraction and by electrophilic addition to double bonds (Larson and Weber 1994a).

Ferrate(VI) oxidation: ferrate(VI) is a strong oxidant with a redox potential of  $\sim 2.2$  V at acidic pH and  $\sim 0.7$ -1.4 V at neutral and basic pHs (Ghernaout and Naceur 2011). Although ferrate(VI) is a selective oxidant, which preferentially targets amines and alcohols, it also reacts with unreactive species such as alkanes and carboxylic acids, but at a relatively slow rate (e.g., rate constant =  $1.11 \pm 0.22$  M<sup>-1</sup>s<sup>-1</sup> for ibuprofen) (Sharma et al. 2008, Sharma and Mishra 2006).

Ozonation: the redox potential of ozone is  $\sim 2.1$  V at acidic pH and 1.2-1.8 at basic pH (Ghernaout and Naceur 2011, Wardman 1989). Ozonation effectively decreased the concentration of classical NAs in OSPW, increased the biodegradability of the organics, and reduced the toxicity towards *Vibrio fischeri* (Gamal El-Din et al. 2011), *Chironomus dilutu* (Anderson et al. 2012) and fathead minnow (He et al. 2012). However, the separate contributions of ozone oxidation

and •OH oxidation to organics transformation and toxicity reduction have not been clearly illustrated. One of the commonly used methods to investigate direct ozone reaction is to inhibit •OH reaction with the radical scavenger (e.g., TBA) (Gottschalk et al. 2010).

The specific objectives of this study were as follows: (1) to compare the oxidation processes including UV/H<sub>2</sub>O<sub>2</sub>, potassium ferrate(VI), and ozone (with and without radical scavenger TBA) in transforming NAs and aromatics in OSPW; (2) to investigate the toxicity of the OSPW treated by different processes; and (3) to explore the oxidation mechanisms behind the performance differences.

## **4.2 Materials and methods**

### **4.2.1 OSPW and chemicals**

Raw OSPW was collected from an active oil sands tailings pond in Fort McMurray, Alberta, Canada, and was stored in HDPE barrels at 4°C in a cold storage room prior to use. Water quality of raw OSPW is summarized in Table 4.1. Potassium ferrate(VI) with purity of 92% was prepared by wet method (Thompson et al. 1951). The 30% hydrogen peroxide (H<sub>2</sub>O<sub>2</sub>) solution was purchased from Fisher Scientific (ON, Canada), and 99.5% extra pure TBA was purchased from Acros Organics (NJ, USA). Ozone was generated from extra-dry and high-purity oxygen using an ozone generator (Model GLS-7, PCI-WEDECO, Herford, Germany). All other chemicals were of analytical grade unless specified otherwise.

**Table 4.1** Water quality of raw OSPW

<b>Parameter</b>	<b>Value</b>
pH	8.4±0.2
Alkalinity (mg/L as CaCO <sub>3</sub> )	650±15
Total dissolved solids (mg/L)	2620.6±24.9
Conductivity (mS/cm)	3.5±0.3
<i>Organic parameters</i>	
COD (mg/L)	245.3±1.2
TOC (mg/L)	60.1±5.0
UV <sub>254</sub> (cm <sup>-1</sup> ) <sup>a</sup>	0.597±0.011
Naphthenic acids (NAs) (mg/L)	36.4
NAs+O (mg/L)	13.6
NAs+O <sub>2</sub> (mg/L)	15.3
Acid extractible fraction (AEF) (mg/L) <sup>b</sup>	78.3±1.2

Note: <sup>a</sup> Specific UV<sub>254</sub> absorbance (SUVA)=100\*(UV<sub>254</sub>/DOC).

<sup>b</sup> AEF analysis was done with the same method described by Gamal El-Din et al.

#### **4.2.2 Experimental design**

All experiments were done in duplicates. The dosage of potassium ferrate(VI), ozone, and H<sub>2</sub>O<sub>2</sub> investigated in this study ranged from 0.1 mM to 4.0 mM, which covered the most typical doses applied in previous studies (Anderson et al. 2012, Drzewicz et al. 2010, Shu et al. 2013, Singh et al. 2015). All treated OSPW

samples were filtered through 0.45  $\mu\text{m}$  nylon filter (Supelco Analytical, PA, USA) and preserved in amber glass bottles.

UV/H<sub>2</sub>O<sub>2</sub> process: a quasi-collimated beam UV apparatus equipped with a 1 kW medium pressure mercury lamp (Model PSI-I-120, Calgon Carbon Corporation, PA, USA) (Figure 4.1) was used to generate polychromatic UV light (Bolton and Linden 2003). The irradiance spectrum of the lamp is provided in Figure 4.2. The irradiance was measured by a calibrated UV detector (Model SED 240, International Light, MA, USA) connected to a radiometer (Model IL 1400A, International Light, USA). The samples were held in an 80 mL glass beaker with a diameter of 5.4 cm, and the water path length was 3.5 cm. The distance from the lamp to the top of the water surface was 31 cm. UV dose was fixed as 950  $\text{mJ}/\text{cm}^2$ , which was at the high end of the reported UV dose range but still comparable to many studies (Afzal et al. 2012, Chelme-Ayala et al. 2010, Shu et al. 2013). After UV exposure, sodium thiosulfate (Fisher Scientific, NJ, USA) was added to the beaker to quench residual H<sub>2</sub>O<sub>2</sub>.

Ferrate(VI) oxidation: dry potassium ferrate(VI) was added into 200 mL OSPW at the rapid mixing with RT 15 power IKAMAG stirrers (IKA Works, Inc., NC, USA). After 3 hours, the mixing was stopped, and sodium thiosulfate (Fisher Scientific, NJ, USA) was added to quench residual ferrate(VI).

Ozonation: an ozone flow of 1 L/min was fed into a 4-L glass reactor filled with 3.8 L OSPW via a gas diffuser on the bottom. The utilized ozone dose was calculated as the difference of the ozone quantity in the feed and off-gas lines.

Ozone concentrations in the feed gas and off-gas were continuously monitored by two identical ozone monitors (Model HC-500, PCI-WEDECO, Herford, Germany). Ozonation was done with both raw OSPW and TBA-spiked OSPW (TBA concentration was 100 mM). More details about the ozonation process were reported by Wang et al. (2013).



**Figure 4.1** Quasi-collimated beam UV apparatus

#### **4.2.3 Water quality analyses**

Synchronous fluorescence spectra (SFS) of the filtered water were recorded using a Varian Cary Eclipse fluorescence spectrometer (ON, Canada). Excitation wavelengths ranged from 200 to 600 nm, and emission wavelengths were recorded from 218 to 618 nm. Scanning speed was 600 nm/min and the photomultiplier (PMT) voltage was 800 mV.

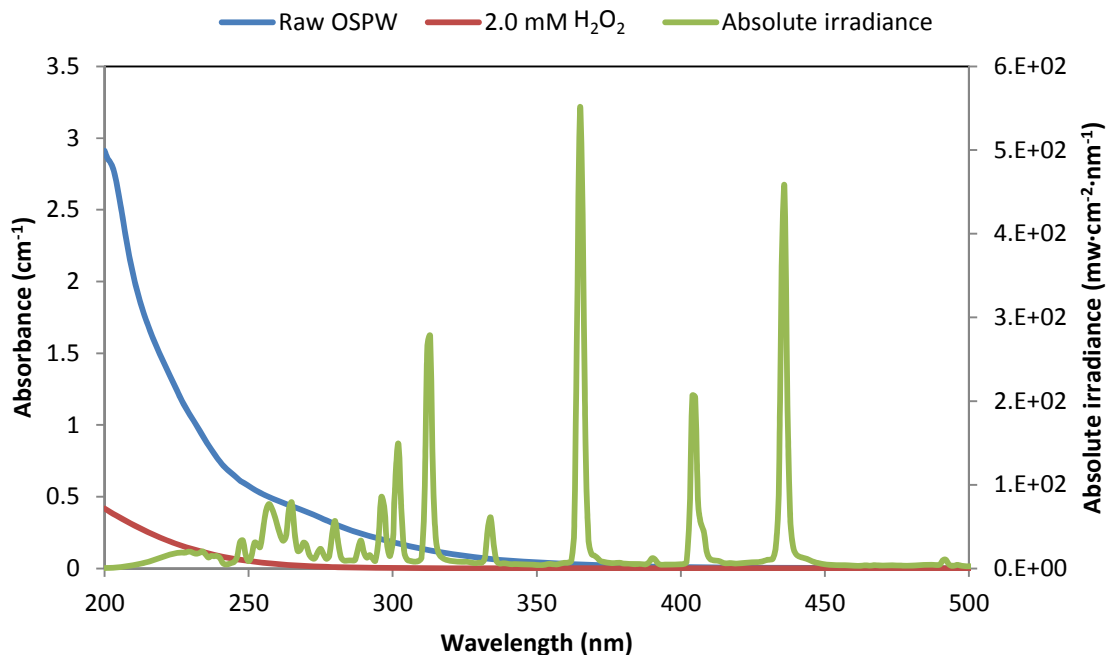


**Figure 4.2** Absorption spectra of the raw OSPW and 2.0 mM H<sub>2</sub>O<sub>2</sub> in Milli-Q water, and irradiance spectrum of the medium pressure mercury lamp

<sup>1</sup>H nuclear magnetic resonance (<sup>1</sup>H NMR) spectra of the organic extracts in deuterated dimethyl sulfoxide (DMSO) were acquired using 700 MHz Varian VNMRS spectrometer with a z-gradient HCN indirect detection cold probe (Agilent Technologies, CA, USA). Spectra were recorded with a 13300 Hz sweep width, a 5.0 s acquisition time, and a 0.1 s relaxation delay. <sup>13</sup>C nuclear magnetic resonance (<sup>13</sup>C NMR) spectra were acquired using 400 MHz Varian spectrometer with a broadband z-gradient probe (Agilent Technologies, CA, USA). They were recorded with a 27000 Hz sweep width, a 2.5 s acquisition time, and a 0.1 s relaxation time delay. Data for both <sup>1</sup>H and <sup>13</sup>C NMR were recorded with a 30 degree flip angle. Detailed sample preparation procedure is as follows: 200 mL water sample was used for each analysis. The pH of the water was adjusted to 2.0-

2.5 with 6 M sulfuric acid, and then the organic fraction was extracted with 50 mL dichloromethane (DCM). Then the extract was evaporated to dryness through the air drying process. The dried organic fraction was then reconstituted in 1 mL DMSO and transferred into the NMR tubes for analysis.

NAs were quantified by ultra-performance liquid chromatography time-of-flight mass spectrometer (UPLC-TOF-MS). 500  $\mu$ L sample was mixed with 100  $\mu$ L internal standard (myristic acid- $^{13}\text{C}$ , 4 mg/L) and 400  $\mu$ L methanol. Chromatographic separations were performed using a Waters UPLC Phenyl BEH column (1.7  $\mu\text{m}$ , 150 mm  $\times$  1 mm) (Waters, MA, USA). Samples were analyzed with a high resolution TOF-MS with electrospray ionization in negative mode (Synapt G2, Waters, MA, USA) and TOF analyzer in high-resolution mode (Huang et al. 2015a, Martin et al. 2010, Sun et al. 2014). The UPLC-TOF-MS quantification method was developed previously and has been verified in a number of publications (Huang et al. 2015a, Ross et al. 2012, Sun et al. 2014, Wang et al. 2013). The method for acquisition of ion mobility spectra (IMS) was the same as described by Wang et al. (2013).

Acute toxicity towards *Vibrio fischeri* was measured with the Microtox 81.9% screening test protocol. *In vitro* toxicity assessment was done using goldfish primary kidney macrophages (PKMs), and detailed assessment procedure can be found in Shu et al. (2014). Briefly, goldfish were anesthetized using tricaine methanesulfonate (TMS) and killed by spinal severance. The PKMs were isolated and cultivated in complete medium (C-MGFL-15) supplemented with 10% newborn calf and 5% carp serum. Six-day-old PKMs were harvested, enumerated

and used from nitric oxide assay. These PKMs were then seeded into 96-well plates in 50  $\mu$ L of C-MGFL-15. Cells were exposed to samples for 18 h and then were stimulated with heat-killed *A. salmonicida* ( $3.6 \times 10^7$  cfu/well) for 72 h. Cells in the negative and positive controls were exposed to 50  $\mu$ L of C-MGFL-15 and heat killed *A. salmonicida*, respectively. The production of reactive nitrogen intermediates (RNIs) was determined via the Griess reaction by adding 1% sulfanilamide and 0.1% N-naphthylethylenediamine to supernatants from the treated cells, measuring absorbance at 540 nm, and the amount of nitrite in supernatants was determined using a nitrite standard curve.

## **4.3 Results and discussion**

### **4.3.1 SFS analysis**

SFS as a selective analytical method requires the detectable molecule to have a low-energy  $\pi \rightarrow \pi^*$  transition or  $n \rightarrow \pi^*$  transition to be able to fluoresce under UV irradiation (Williams et al. 1983). SFS was mainly employed in OSPW analysis to detect single-ring and fused-ring aromatics. As displayed in Figure 4.3, the SFS showed three distinct peaks at 267 nm (peak I, one aromatic ring), 310 nm (peak II, two fused aromatic rings) and 330 nm (peak III, three fused aromatic rings) (Shu et al. 2014, Tuan Vo 1978). One-ring aromatics predominated in OSPW as indicated by the highest intensity of peak I, in spite of the much lower fluorescence quantum yield of one-ring aromatics than fused-ring aromatics (Williams et al. 1983).

In all the three oxidation processes a general decrease in peak areas was observed, but to the different extent and with different selectivity (see Figure 4.3).

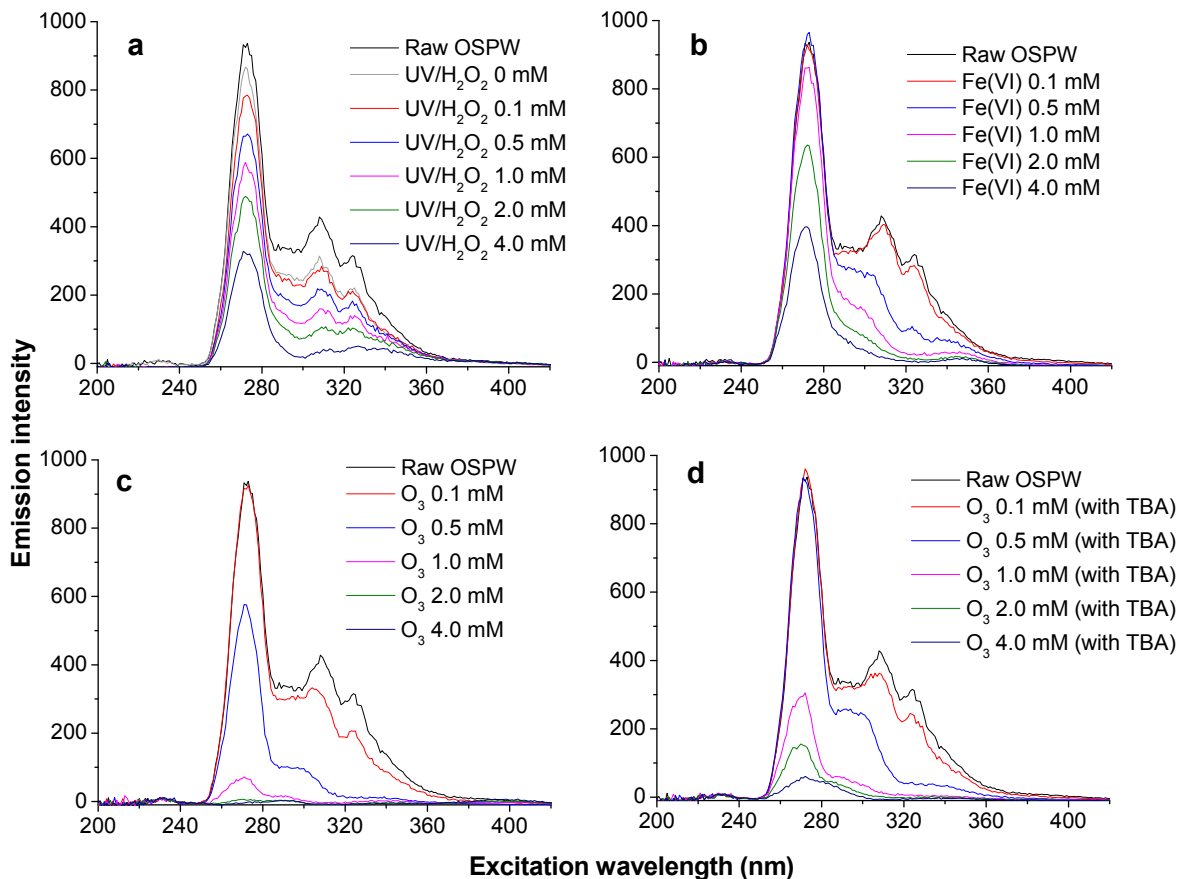


**Figure 4.3** SFS of raw OSPW and OSPW oxidized by UV/H<sub>2</sub>O<sub>2</sub> (a), ferrate(VI) (b), O<sub>3</sub> with and without TBA (c and d)

The generation of •OH in the UV/H<sub>2</sub>O<sub>2</sub> process led to a simultaneous removal of all the three peaks as the oxidation of the aromatic moieties occurs through both electrophilic addition reaction on the aromatic rings and hydrogen abstraction at the branches, which leads to either aromatic ring opening (the loss of aromaticity) or the generation of electron-withdrawing groups on or near the aromatic rings

(the weakening of the aromaticity) (von Sonntag and von Gunten 2012). In addition, direct photolysis and sensitized photolysis with polyaromatics as photosensitizing agent contributed to the removal of fluorescing aromatics, as UV radiation alone also achieved peak reduction in the absence of H<sub>2</sub>O<sub>2</sub> (Figure 4.3a) (Larson and Weber 1994b).

For ferrate(VI) oxidation, peak II and peak III were preferentially reduced at doses <2.0 mM Fe(VI), while peak I was only significantly reduced at high ferrate doses (i.e., ≥2.0 mM Fe(VI)), indicating the high selectivity of ferrate(VI) oxidation. The reason behind this selectivity lies in the fact that fused-ring aromatics contain sites with high electron density and are thus susceptible to oxidative attack (Larson and Weber 1994c). One of the reaction pathways was reported to be 1,3-dipolar cycloaddition, resulting in the opening of the aromatic rings (Anquandah et al. 2013). Similar ring opening reaction by ferrate(VI) was reported by Sharma et al. (2008).

Ozonated OSPW showed different SFS profiles from ferrate(VI)-treated OSPW and UV/H<sub>2</sub>O<sub>2</sub>-treated OSPW. Ozonation is a much more effective process in removing fluorescing aromatics due to the fact that it is a combination of selective process via direct ozone oxidation and unselective process via radical oxidation. At doses ≥1.0 mM O<sub>3</sub>, nearly all the fluorescing aromatics were degraded by ozonation. Although all the three peaks were reduced at low doses (e.g., 0.5 mM O<sub>3</sub>), the preferential removal of peaks II and III could also be observed in Figures 4.3a and 4.3c. Even when the ·OH was scavenged by TBA, ozonation also achieved high removal of fluorescing aromatics and showed preferential reduction

of peaks II and III (Figure 4.3d), indicating the high efficiency of the selective oxidation by molecular ozone. Comparing Figures 4.3c and 4.3d, there was a significant decrease of oxidation efficiency after TBA was added, indicating that radical reaction was also an important pathway for the transformation of fluorescing aromatics.

#### **4.3.2 IMS analysis**

Ion mobility spectrometry coupled with UPLC is a powerful analytical technique that can separate different classes of NAs in OSPW based on the UPLC retention time and the drift-gas selectivity. The IMS of OSPW shows three clusters of NAs: classical NAs, oxy-NAs, and other heteroatomic NAs (mainly sulfur containing NAs, noted as “NAs+S”) (Sun et al. 2014, Wang et al. 2013). As displayed in Figure 4.4, the oxy-NAs cluster showed the highest intensity in raw OSPW indicating that they were the most abundant NA species in raw OSPW, which agreed with previous reports (Klamerth et al. 2015, Sun et al. 2014, Wang et al. 2013).

UV/H<sub>2</sub>O<sub>2</sub> process removed NAs+S and classical NAs indiscriminately, while ferrate(VI) preferentially removed NAs+S over classical NAs (Figures 4.4a-f). Similar to the removal of fluorescing aromatics, this result was expected due to the unselective reaction by •OH and selective reactions by ferrate(VI). As IMS is a qualitative measurement, a quantification of the NAs removal is not possible as there are thousands of NA species not identified so far; however, the selective

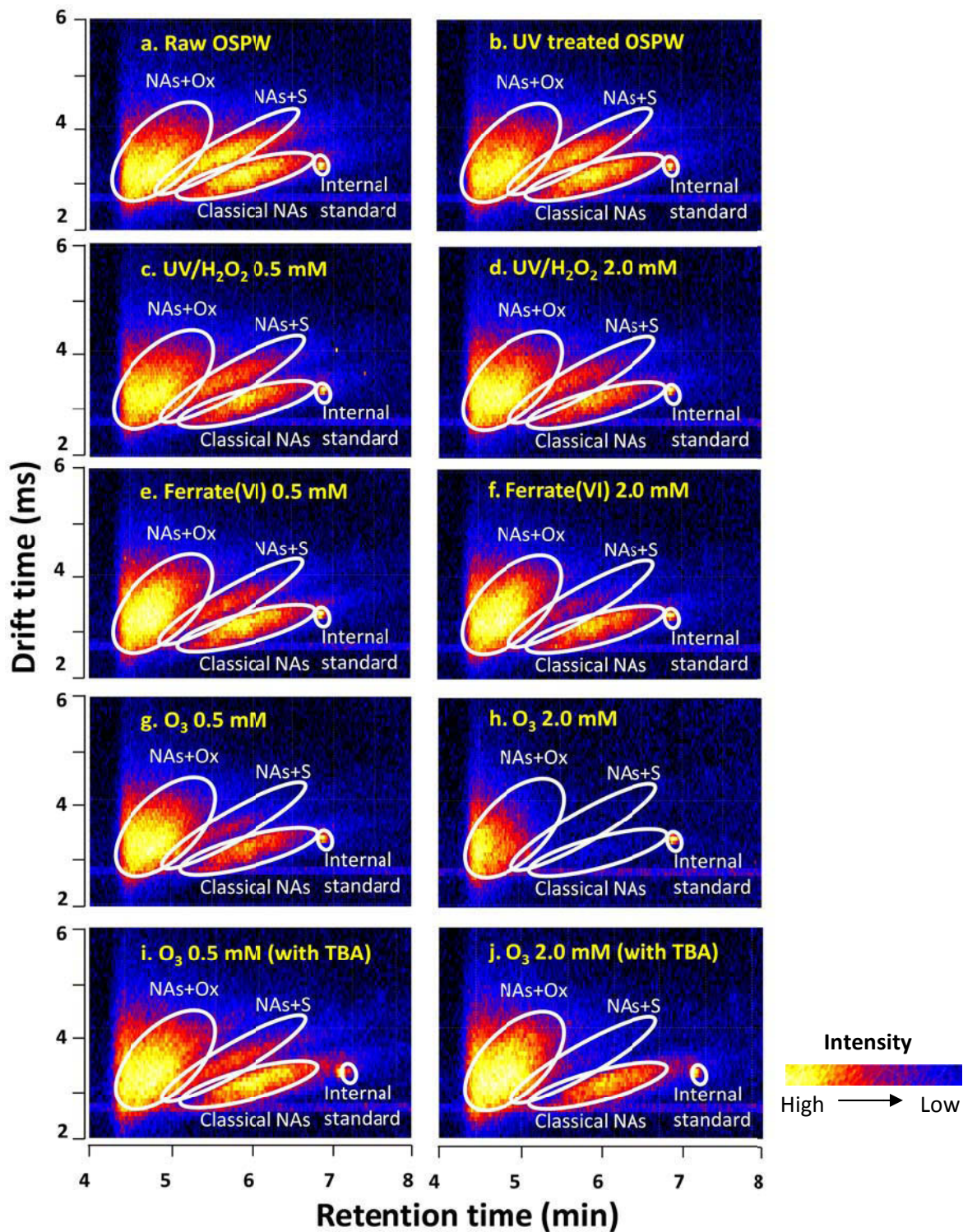


**Figure 4.4** Ion mobility spectra for raw OSPW (a), UV-treated OSPW (no H<sub>2</sub>O<sub>2</sub>) (b), UV/H<sub>2</sub>O<sub>2</sub>- treated OSPW (c, d), ferrate(VI)-treated OSPW (e, f), O<sub>3</sub>-treated OSPW with and without TBA (g, h, i, and j)

oxidation by ferrate(VI) is clearly represented by the changes of cluster intensity. At the dose of 0.5 mM Fe(VI), ferrate(VI) achieved high removal of NAs+S but limited removal of classical NAs; when the doses increased to 2.0 mM Fe(VI), ferrate(VI) also achieved significant removal of classical NAs and almost complete removal of NAs+S. The preferential removal of NAs+S by ferrate(VI) can be attributed to the possible existence of sulfur-containing electron rich moieties (ERMs) such as low oxidation state thiols and sulfides (Jones et al. 2012, Pereira et al. 2013, Zhang et al. 2015).

Compared with ferrate(VI) and UV/H<sub>2</sub>O<sub>2</sub> processes, ozone achieved significantly higher removal of both NAs+S and classical NAs (Figures 4.4g-h). At the dose of 2.0 mM, these two fractions were almost completely removed while oxy-NAs were also removed to a great extent, indicating that the oxidation products of classical and NAs+S were also further oxidized. With the addition of TBA (Figures 4.4i-j), the performance of ozonation was significantly weakened, especially for the removal of classical NAs, indicating the importance of •OH reaction in ozonation. As a result, the IMS of ozonated TBA-spiked OSPW showed a preferential removal of NAs+S, similar to that exhibited by ferrate(VI) oxidation, indicating the selectivity of molecular ozone reaction. Based on IMS, it can be concluded that ozonation is the most effective process in the removal of classical NAs, NAs+S as well as oxy-NAs.

### **4.3.3 Quantification of NAs by UPLC-TOF-MS**

#### *4.3.3.1 Classical NAs*

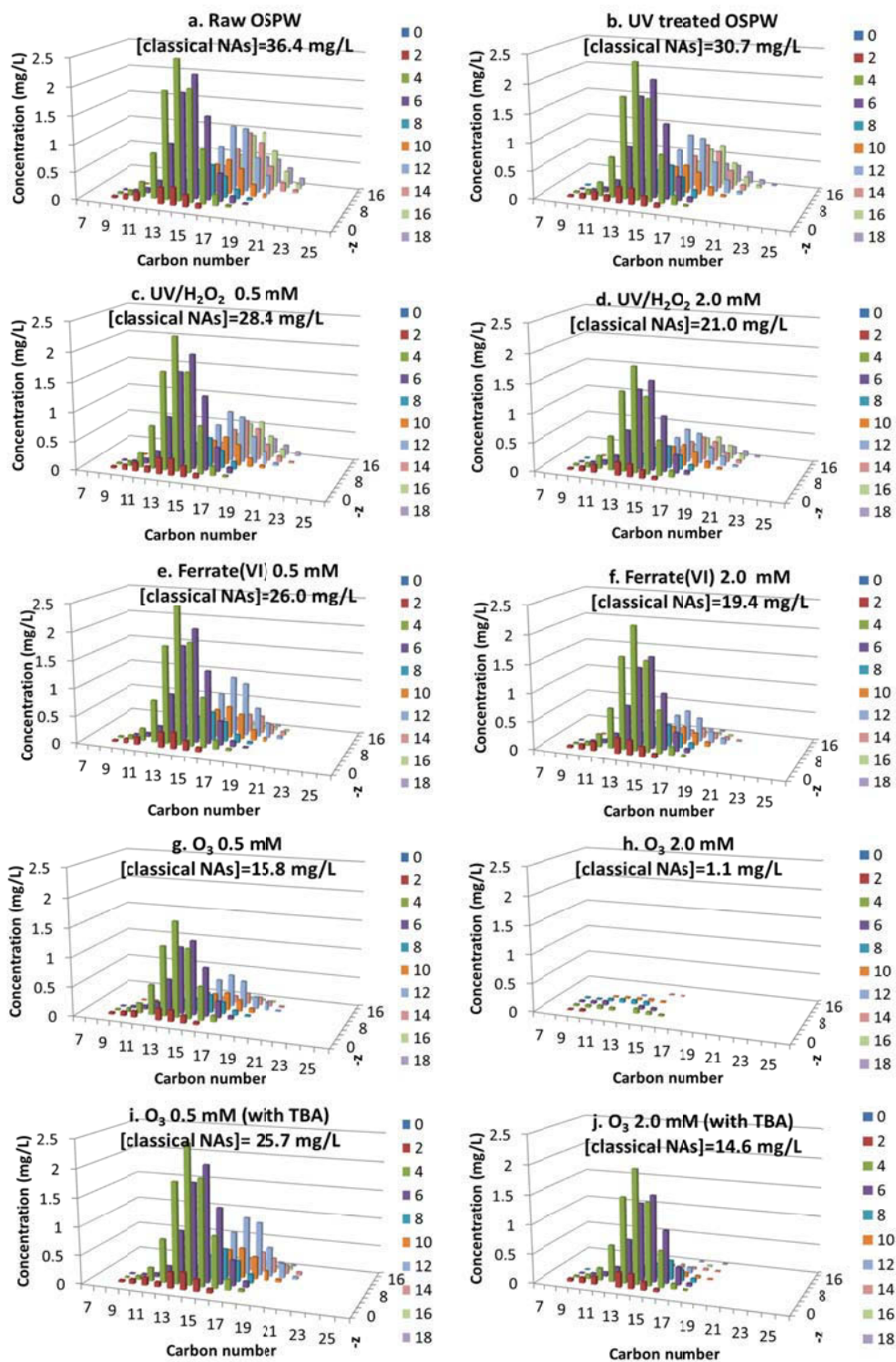


**Figure 4.5** Classical NAs distribution in raw OSPW (a), UV treated OSPW (b), ferrate(VI)-treated OSPW (c,d), UV/H<sub>2</sub>O<sub>2</sub>- treated OSPW (e, f), and O<sub>3</sub>-treated OSPW with and without TBA (g, h, i and j)

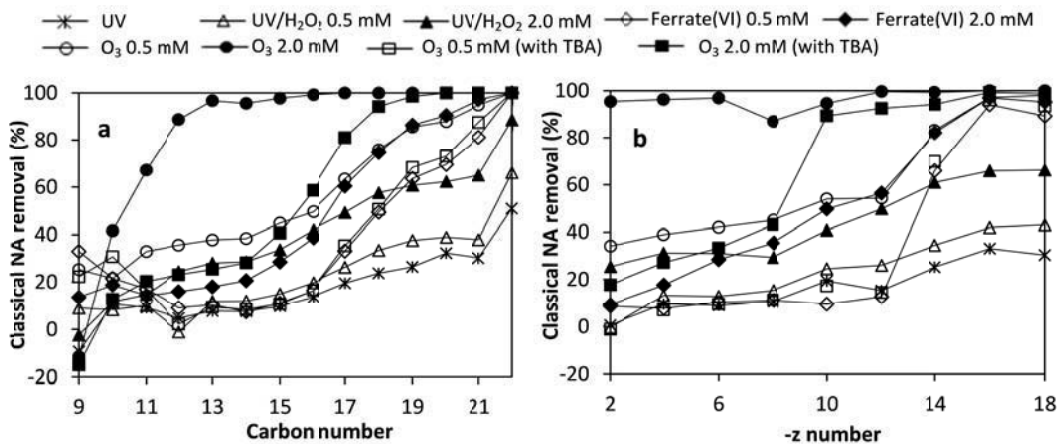


**Figure 4.6** Classical NA removal with respect to carbon number (a) and  $-z$  number (b)

The total concentration of classical NAs in OSPW was 36.4 mg/L, with classical NAs of  $n=15$  and  $-z=4$  being the most abundant (Figure 4.5, Table 4.2). This concentration decreased by 21.9% and 42.4% after UV/H<sub>2</sub>O<sub>2</sub> treatment at doses of 0.5 and 2.0 mM H<sub>2</sub>O<sub>2</sub>, respectively (Figure 4.5, Table 4.2), while UV alone removed 15.7%, signifying that NAs removal in the UV/H<sub>2</sub>O<sub>2</sub> process was contributed by both  $\bullet\text{OH}$  oxidation and UV photolysis. This can be explained by the fact that most of the UV irradiation was absorbed by the OSPW constituents instead of H<sub>2</sub>O<sub>2</sub> (see Figure 4.2 which showed that about 90% of the absorbed UV was from OSPW constituent absorption at H<sub>2</sub>O<sub>2</sub> dose of 2.0 mM); in addition, classical NAs with high hydrogen deficiency (e.g.,  $-z \geq 8$ ) were very likely to be UV-absorbing aromatics, which can be transformed by photo-chemical reaction or can function as photosensitizing agents. Further addition of H<sub>2</sub>O<sub>2</sub> as photosensitizing agents further promoted the oxidation performance, but the enhancement of the performance by H<sub>2</sub>O<sub>2</sub> was unexpectedly low, which was

caused by the low extinction coefficient of  $\text{H}_2\text{O}_2$  and the high alkalinity ( $650 \pm 15$  mg/L as  $\text{CaCO}_3$ , see Table 4.1). The former factor resulted in low generation of  $\bullet\text{OH}$  and the later factor led to strong  $\bullet\text{OH}$  scavenging effect. After ferrate oxidation, 28.5% and 46.7% of the classical NAs were removed at ferrate(VI) doses of 0.5 and 2.0 mM, respectively. Classical NAs with higher -z and n number were preferentially removed (Figures 4.6a and 4.6b). This preferential removal of classical NAs by ferrate(VI) was especially obvious with a sharp increase of the removal of NAs with -z higher than 12 (Figure 4.6b), due to the high number of rings, branches, the increasing number of tertiary carbons, and even possible aromaticity. The most likely mechanism for the degradation of aliphatic classical NAs by ferrate(VI) is the attack on the  $\alpha$  carbons at carboxylic acid branches (Drzewicz et al. 2010, Sharma and Mishra 2006, Sharma and Bielski 1991) and tertiary carbons (Pérez-Estrada et al. 2011). For example, the bridgehead position of bicyclic aliphatic organics, which exists in two-ring NAs, is reported to be vulnerable to the oxidation by metal oxidants Cr(VI) (Wiberg and Foster 1961). However, this selectivity of ferrate(VI), combined with its self-decomposition (i.e., reaction with water) without generating active oxidative species, makes ferrate(VI) not as effective as ozone in oxidizing classical NAs.

After ozonation, classical NAs were removed by 56.5% and 97.1% at doses of 0.5 and 2.0 mM  $\text{O}_3$ , respectively. With the addition of TBA, the removal of classical NAs by ozonation decreased to 29.4% and 59.9% at the dose of 0.5 and 2.0 mM, respectively. This meant that  $\bullet\text{OH}$  driven reaction pathway in ozonation removed about 27.1% and 37.2% of NAs, respectively. These results indicated that both

oxidations by ozone and oxidation via  $\cdot\text{OH}$  contributed significantly to the oxidation of classical NAs. Similar results were reported by Wang et al. (2013). There are several reasons behind this phenomenon: (1) ozone itself is a strong oxidant with high redox potentials, and it is thermodynamically feasible for ozone to oxidize a variety of organics including aliphatic carbons (Hoigné and Bader 1983a). The possible pathways of ozone reaction on aliphatic C-H bonds were complicated and still unresolved; von Sonntag and von Gunten 2012 suggested that both hydrogen abstraction (ozone receives a  $\text{H}\cdot$ ) and hydride transfer (ozone receives a  $\text{H}:\cdot$ ) contributed to the reaction. (2) Although direct reaction between ozone and aliphatic carbon is a slow process, it is still kinetically competitive to the radical reaction due to the concentration advantage. For example, the reported rate constants of direct ozone reactions with carboxylic acids is  $10^{-3}$ - $10\text{ M}^{-1}\text{s}^{-1}$  (Francis 1987, Hoigné and Bader 1983b), much lower than the rate constants of radical reactions with carboxylic acids ( $10^7$ - $10^9\text{ M}^{-1}\text{s}^{-1}$ ) (Gottschalk et al. 2010); however, typically ozone concentration is  $10^7$ - $10^9$  times higher than that of  $\cdot\text{OH}$  (e.g., utilized dose in this studies was 0.1-4.0 mM, much higher than the typical steady concentration of  $<10^{-9}$  mM for  $\cdot\text{OH}$ ) (Elovitz and von Gunten 1999, Oppenländer 2007). Therefore, both pathways are kinetically active in oxidizing classical NAs. (3) The scavenging effect of the carbonate/bicarbonate system decreased the radical exposure to the classical NAs, which further promoted the relative importance of molecular ozone reaction.

#### 4.3.3.2 *NAs+O and NAs+O<sub>2</sub>*

The concentrations of NAs+O (NAs with x=3) and NAs+O<sub>2</sub> (NAs with x=4) in OSPW were 13.6 mg/L and 15.3 mg/L, respectively (Figures 4.7-4.10, Table 4.2). The change of NAs+O and NAs+O<sub>2</sub> concentrations during the oxidation process was more complicated to follow, as oxy-NAs were both consumed and generated simultaneously. First, after UV/H<sub>2</sub>O<sub>2</sub> oxidation, the concentration of NAs+O increased while the concentration of NAs+O<sub>2</sub> decreased. Second, with ferrate(VI), an opposite oxidation pattern was achieved: the concentration of NAs+O decreased while the concentration of NAs+O<sub>2</sub> increased. The increase of NAs+O<sub>2</sub> was featured by the emerging of a new cluster in the range of z=12-18 and n=15-24 (Figure 4.9e&f), consistent with the high removal of classical NAs in this region (Figure 4.5e&f). The difference between UV/H<sub>2</sub>O<sub>2</sub> oxidation and ferrate(VI) oxidation could be explained by the selectivity of ferrate(VI) oxidation and the lack of selectivity of •OH oxidation: as intermediate products, newly generated NAs+O are usually more susceptible to oxidation than the parent classical NAs, and will be preferentially transformed to NAs+O<sub>2</sub> by ferrate(VI) oxidation once they are generated (Carey and Sundberg 2010). Therefore, there was no accumulation of the intermediate products NAs+O in ferrate(VI) oxidation as supported by their concentration decrease. On the other hand, •OH oxidation in the UV/H<sub>2</sub>O<sub>2</sub> process did not have such selectivity, which means that the newly generated NAs+O was not specially targeted by •OH and some of them survived the oxidation process, resulting in their concentration increase. Third, with ozonation, concentrations of both NAs+O and NAs+O<sub>2</sub> were significantly reduced (Figures 4.7-4.10, Table 4.2). Due to the high efficiency of ozonation, molecule

breakdown and transformation of NAs+O and NAs+O<sub>2</sub> to more oxygen-rich species might be the cause of their concentration decrease. When TBA was added as •OH scavenger, the performance of ozonation in transforming oxy-NAs was similar to that of ferrate(VI) oxidation in the following two aspects: (1) NA+O concentration decreased at 2.0 mM and (2) a new cluster of NAs+O<sub>2</sub> emerged in the range of -z=12-18 and n=15-24 at 2.0 mM. This similarity between direct ozone reaction and ferrate(VI) oxidation was probably also due to that both of these processes are selective oxidation.

**Table 4. 2** Summary of NA removal by different oxidation processes

	Raw OSPW	OSPW treated by different processes								
		UV	UV/H <sub>2</sub> O <sub>2</sub>	Ferrate(VI)		Ozonation		Ozonation (with TBA)		
Chemical dose <sup>a</sup> (mM)	- <sup>b</sup>	0	0.5	2.0	0.5	2.0	0.5	2.0	0.5	2.0
Classical NAs (mg/L)	36.4	30.7	28.4	21.0	26.0	19.4	15.8	1.1	25.7	14.6
Removal (%)	-	15.7	22.0	42.3	28.6	46.7	56.5	97.1	29.4	59.9
NAs+O (mg/L)	13.6	13.2	14.3	14.5	10.9	11.6	13.4	4.3	13.6	11.7
Removal (%)	-	2.9	-5.1	-6.6	19.9	14.7	1.5	68.4	0.0	14.0
NAs+O <sub>2</sub> (mg/L)	15.3	14.2	14.3	13.1	16.5	17.7	11.4	5.1	12.7	15.1
Removal (%)	-	7.2	6.5	14.4	-7.8	-15.7	25.5	66.7	17.0	1.3

Note: <sup>a</sup>For UV/H<sub>2</sub>O<sub>2</sub> process, the UV dose was fixed to be 950 mJ/cm<sup>2</sup>, and H<sub>2</sub>O<sub>2</sub> dose was provided in the table. <sup>b</sup>“-” means no data.

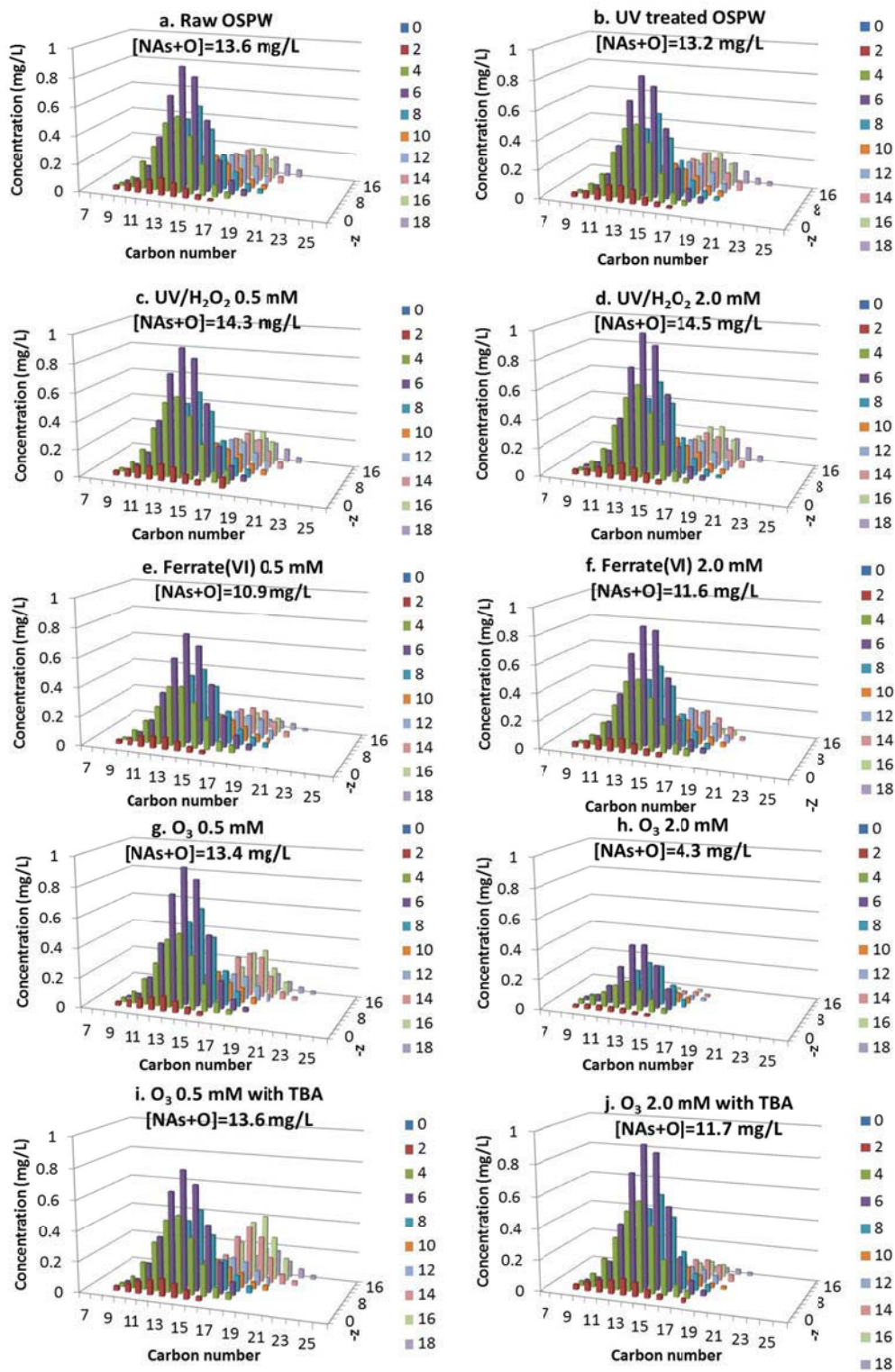


**Figure 4.7** NAs+O distribution in raw OSPW (a), UV treated OSPW (b), ferrate(VI)-treated OSPW (c,d), UV/H<sub>2</sub>O<sub>2</sub>- treated OSPW (e, f), and O<sub>3</sub>-treated OSPW with and without TBA (g, h, i and j)

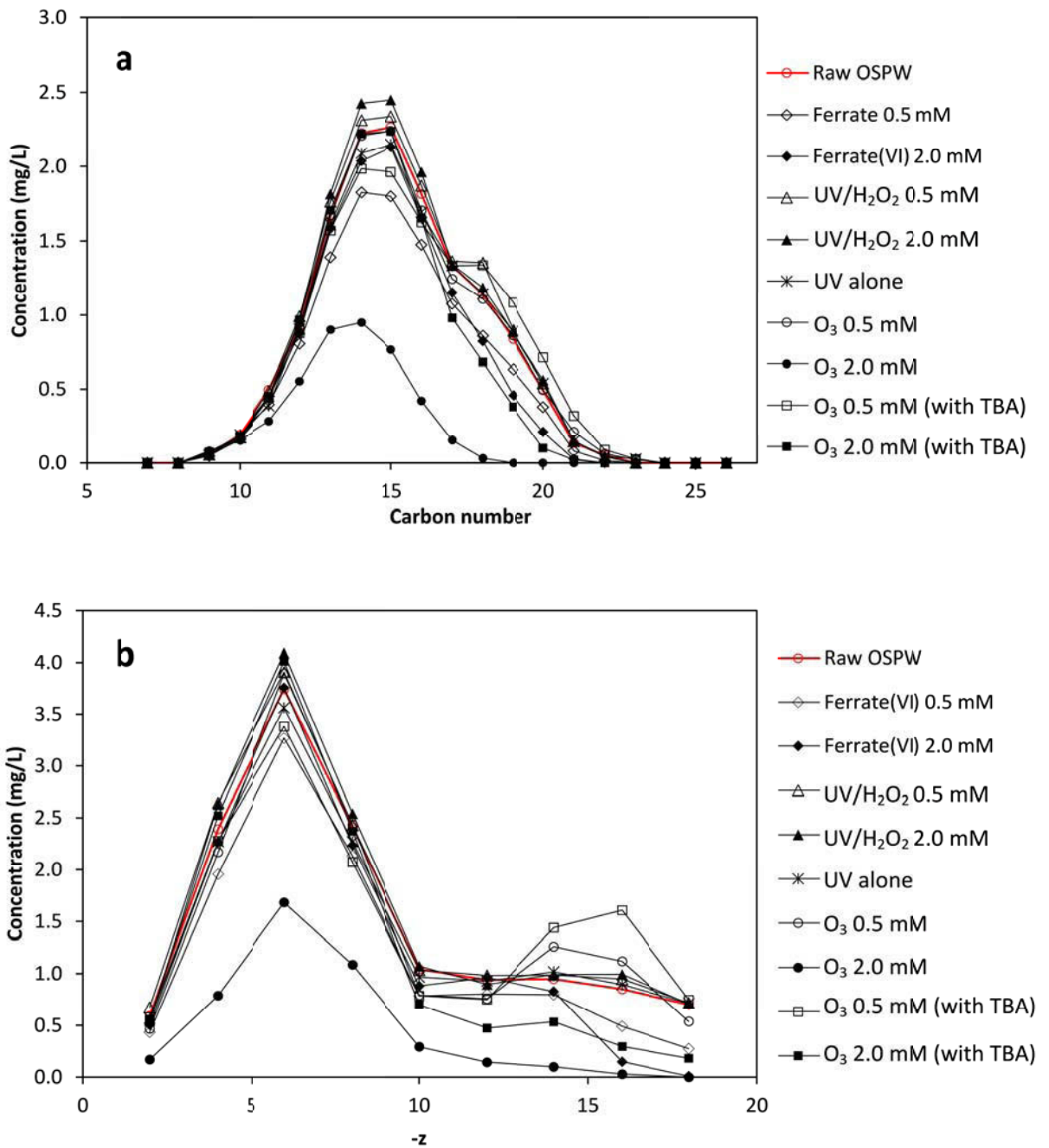


**Figure 4.8** NAs+O distribution in raw OSPW and treated OSPW with respect to carbon number (a) and  $-z$  number (b)

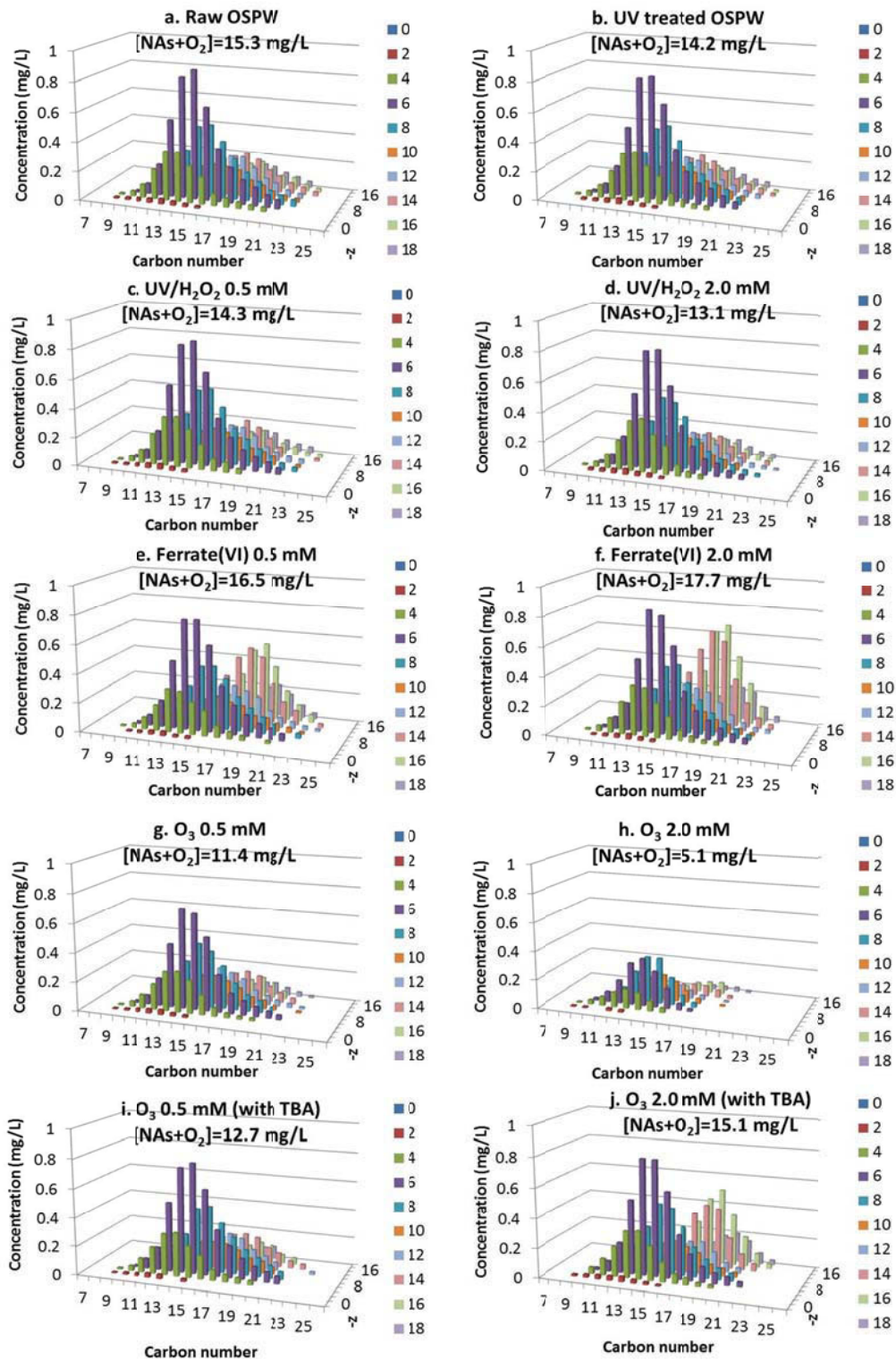


**Figure 4.9** NAs+O<sub>2</sub> distribution in raw OSPW (a), UV treated OSPW (b), ferrate(VI)-treated OSPW (c,d), UV/H<sub>2</sub>O<sub>2</sub>- treated OSPW (e, f), and O<sub>3</sub>-treated OSPW with and without TBA (g, h, i and j)

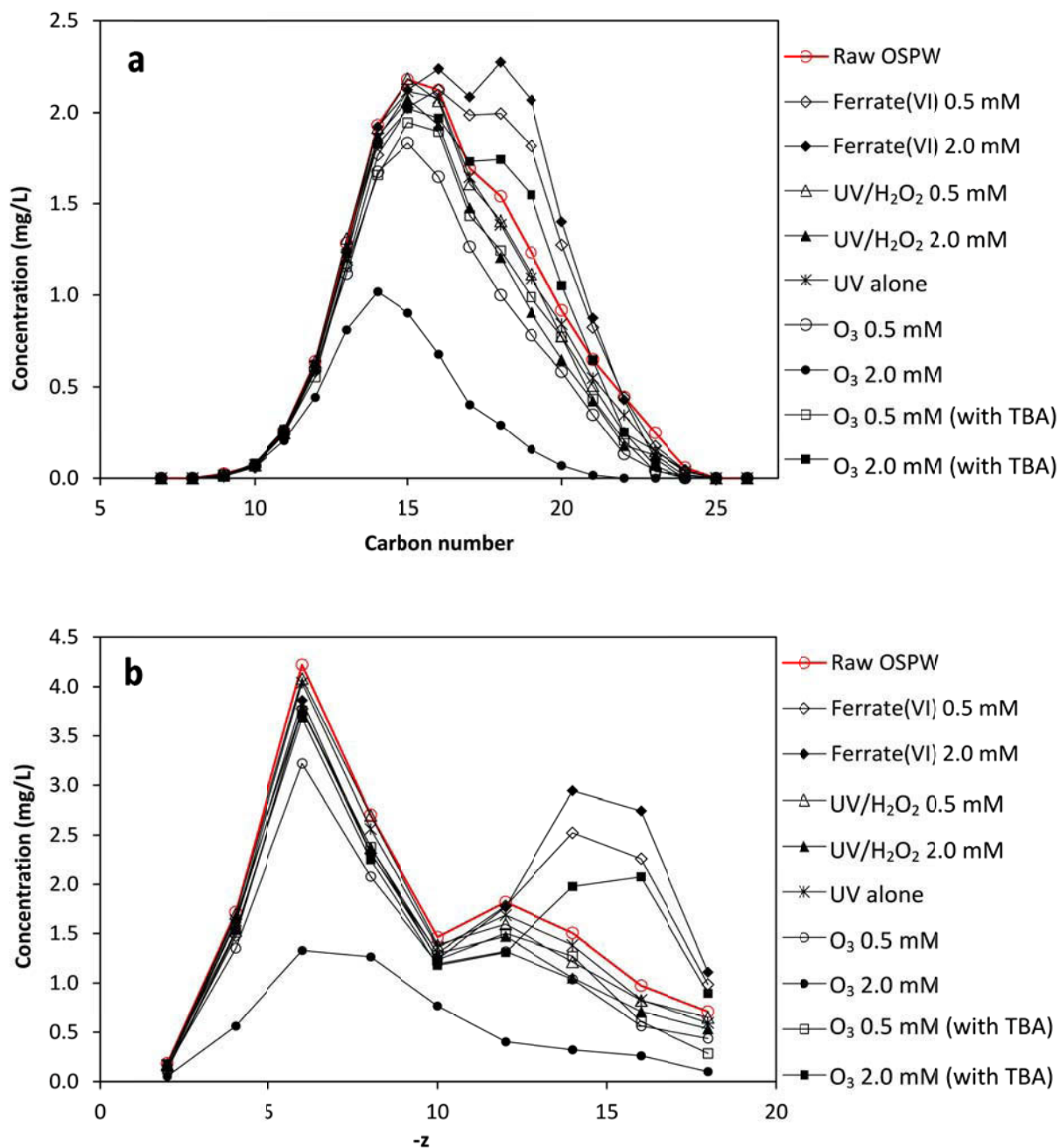


**Figure 4.10** NAs+O<sub>2</sub> distribution in raw OSPW and treated OSPW with respect to carbon number (a) and  $-z$  number (b)

#### 4.3.4 NMR

<sup>1</sup>H and <sup>13</sup>C NMR spectra can provide both qualitative and quantitative information of the hydrocarbon skeleton and functional groups in the organic molecules in

OSPW. Due to the low natural abundance of  $^{13}\text{C}$  (1.1%) and its low magnetogyric ratio, the signal-to-noise ratio in  $^{13}\text{C}$  NMR spectra was relatively low and the resolution of the spectra was compromised (Kishore Nadkarni 2011, Larson and Weber 1994d). Both the  $^1\text{H}$  and the  $^{13}\text{C}$  NMR spectra of OSPW showed three main peaks (Figure 4.11): for  $^1\text{H}$  NMR these were: 0-3.0 ppm for aliphatic hydrogens (Region 1), 6.5-8.5 ppm for hydrogens on the aromatic rings (Region 2), 11.5-12.5 ppm for hydrogens in the carboxyl functional groups (Region 3) (Larson and Weber 1994d). Weak peaks were also detected from 4.5 to 5.5 ppm, which represented organics containing carbon-carbon double bonds. Due to the very low concentrations, these alkenyl functional groups will not be covered in the following discussion.

Among the three main regions in  $^1\text{H}$  NMR spectra, the most abundant one was for aliphatic hydrogens (Region 1), accounting for 93% of all hydrogens. This was expected as the organics in OSPW came from oil sands and the aliphatic part was the high energy containing components (Majid and Pihillagawa 2014). Region 1 contained four peaks: hydrogens in terminal  $\text{CH}_3$  at 0.9 ppm, hydrogens in  $\text{CH}_2$  chains at 1.2 ppm, hydrogens in  $\text{CH}$  at 1.4 ppm, and hydrogens  $\alpha$  to aromatic rings or carboxylic acid groups at 2.2 ppm (Dutta Majumdar et al. 2013, Larson and Weber 1994d). The highest peak of terminal  $\text{CH}_3$  at 0.9 ppm and relative low

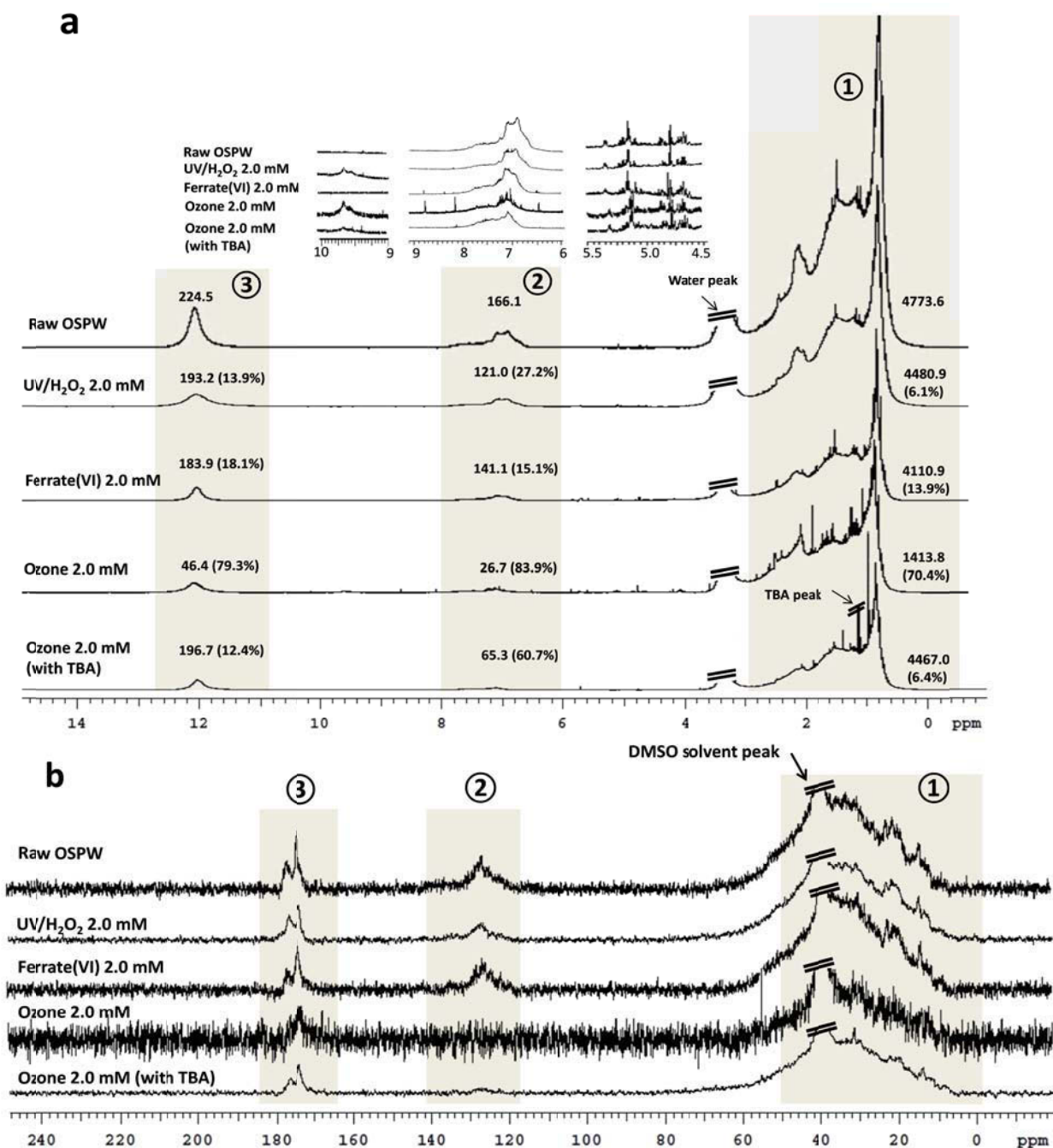


**Figure 4.11** <sup>1</sup>H NMR spectra (a) and <sup>13</sup>C NMR spectra (b) for the organics in raw OSPW and treated OSPW (Note: the numbers besides the peaks indicate the relative peak area as the DMSO solvent peak was set to be 100 as internal standard, and the numbers in the brackets are the peak reduction relative to the corresponding raw OSPW peak area)

peak of CH<sub>2</sub> at 1.2 ppm suggested that unbranched long CH<sub>2</sub> chains or alicyclic rings did not predominate in OSPW. Instead, carbon chains, rings or fused rings with short branches ended with CH<sub>3</sub> might be the most abundant organics. For the aromatics, monoaromatic CH peaks predominated from 6.5 to 7.3 ppm, while relatively small amounts of diaromatic and triaromatic CH were detected from 7.3 to 8.5 ppm (Kishore Nadkarni 2011), which was consistent with the results from SFS. Region 3 only contained one symmetrical peak for hydrogens in carboxyl functional groups, which stands for 4% of the total organic hydrogens in OSPW.

The three main Regions for <sup>13</sup>C NMR spectra in raw OSPW were (Figure 4.11b): Region 1 for aliphatic carbons at 0-50 ppm, Region 2 for aromatic carbons at 120-140 ppm, and Region 3 for carbonyl carbons at 170-180 ppm. The broad bands in Region 1 and Region 2 confirmed a wide variety of aliphatic and aromatic carbons. The lack of peaks at around 150 ppm indicated there was no phenolic carbon (Larson and Weber 1994d). For carbonyl carbon, there were two peaks at 174 ppm and 177 ppm, respectively, indicating that the carbonyl carbons existed in two different environments. More work is needed to elucidate the causes of these two environments, which include but are not limited to different carbonyl types (e.g. ketone versus carboxyl groups), hydrogen bonding, and neighboring effects (Breitmaier and Voelter 1987).

Based on the reduction of the peak area in <sup>1</sup>H NMR spectra, UV/H<sub>2</sub>O<sub>2</sub> process achieved 13.9% removal of hydrogens in carboxyl groups, 27.2% removal of hydrogens on aromatic rings, and 6.1% removal of aliphatic hydrogens at the 2.0 mM H<sub>2</sub>O<sub>2</sub> dose. Ferrate(VI) oxidation only achieved 18.1% removal of hydrogens

in carboxyl functional groups, 15.1% removal of hydrogens on aromatic rings, and 13.9% removal of aliphatic hydrogens at the same molar dose. The removals of the aliphatic hydrogens by ferrate(VI) and UV/H<sub>2</sub>O<sub>2</sub> were supposed to come from hydrogen abstraction; as aliphatic hydrogens consisted of more than 90% of the organic hydrogens, the low removals of the aliphatic hydrogens confirmed that NAs were mostly transformed instead of being mineralized. The relatively lower removal of aromatic hydrogens by ferrate(VI) than by UV/H<sub>2</sub>O<sub>2</sub> was due to that ferrate(VI) preferentially removed two-ring and three-ring aromatics which only constituted a minor part of the total aromatics, and did not remove as much single-ring aromatics (predominant in OSPW) as did by UV/H<sub>2</sub>O<sub>2</sub>. In addition, the profile of the aromatic peaks of UV/H<sub>2</sub>O<sub>2</sub>-treated OSPW remained identical to that of raw OSPW, which further confirmed the unselective reaction by •OH. On the other hand, low removals of carboxyl functional groups by ferrate(VI) and UV/H<sub>2</sub>O<sub>2</sub> confirmed the typical phenomenon in OSPW treatment, chemical or biological: the removal of total organic acids was always lower than the removal of classical NAs (Dong et al. 2015, Gamal El-Din et al. 2011, Huang et al. 2015b, Shi et al. 2015). Although some carboxyl functional groups were mineralized as supported by the peak decrease in Region 3, NA removal was mainly achieved by local hydrogen abstraction, local oxidization of EMRs, and oxidation on the aromatic rings, which only transformed NAs to other organic acids.

As shown previously, among the three oxidation processes, ozonation achieved the most significant transformation of the organics in OSPW. At the dose of 2.0 mM, ozone achieved 79.3% removal of hydrogens in carboxyl functional groups,

83.9% removal of hydrogens on aromatic rings, and 70.4% removal of aliphatic hydrogens (Figure 4.11a). In Region 2, the profile of the aromatic peaks was also transformed, with the peaks below 7 ppm being reduced more than those above 7 ppm. This is understandable because low values of chemical shift usually come from the electron-donating effect of neighboring atoms attached to the aromatic rings; it is the same electron-donating effect that makes these monoaromatics easy targets of ozonation. Downfield from Region 2, new peaks emerged at 9.6-9.8 ppm, which were assigned to hydrogens in aldehydes (Larson and Weber 1994d). As intermediate products, although most of the aldehydes were further oxidized, some aldehydes existed as end products. Similar aldehyde peaks were also observed in the spectra of UV/H<sub>2</sub>O<sub>2</sub> treated OSPW. However, aldehydes were not detected in ferrate(VI)-treated OSPW, mainly because ferrate(VI) oxidation was selective and aldehyde was preferentially oxidized by ferrate(VI) immediately after its generation. For ozonation with the addition of TBA, the removal of hydrogens in carboxyl functional groups, hydrogens on aromatic rings, and aliphatic hydrogens significantly decreased to 12.4%, 60.7%, and 6.4%, respectively. The results indicated that the removal of carboxyl groups and the transformation of aliphatic hydrogens by ozonation mainly came from the radical reaction. Comparing the <sup>1</sup>H NMR spectra of UV/H<sub>2</sub>O<sub>2</sub>-treated OSPW and ozone-treated OSPW, it could be concluded that •OH exposure in UV/H<sub>2</sub>O<sub>2</sub> oxidation was much lower than in ozonation.

Similarly to <sup>1</sup>H NMR spectra, the general profiles of <sup>13</sup>C NMR spectra did not change significantly after UV/H<sub>2</sub>O<sub>2</sub> oxidation, ferrate(VI) oxidation, and

ozonation with TBA, mainly because in these processes hydrogen abstraction only occurred at some relative active positions on the aliphatic branches and the reaction was not enough to change the shape of the profiles of Region 1. On the other hand, the transformation of aromatics and organic acids did not guarantee the opening of the aromatic rings and the mineralization of carboxyl groups, leaving Regions 2 and 3 maintaining the shape of profiles similar to that of raw OSPW spectrum.

#### **4.3.5 Toxicity**

As shown in Figure 4.12, the raw OSPW showed  $45.1 \pm 1.7$  % inhibition effect on *Vibrio fischeri*. All the three processes reduced the inhibition effect; for each process, more reduction in toxicity was observed when higher doses of chemicals were applied (Figure 4.12a). For UV/H<sub>2</sub>O<sub>2</sub> and ferrate (VI) processes, the inhibition effects were reduced to  $31.6 \pm 1.9$  % and  $27.5 \pm 0.5$  % at the doses of 4.0 mM of H<sub>2</sub>O<sub>2</sub> and ferrate(VI), respectively. The ferrate (VI) process was more effective than UV/H<sub>2</sub>O<sub>2</sub> in reducing toxicity, as supported by its higher removal of NAs. In addition, two-ring and three-ring aromatics, which are considered more toxic than single-ring aromatics (Lee et al. 2002, Sayles et al. 1999), were preferentially removed by ferrate(VI) process. Ozonation significantly reduced the OSPW toxicity, which paralleled the highest removal of aromatics and NAs. The inhibition effect decreased to  $15.9 \pm 0.8$ % and  $14.5 \pm 0.1$ % after treatment with ozone doses of 2.0 mM and 4.0 mM, respectively. The remaining toxicity after treatments may be due to unoxidized aromatics and NAs, oxidation products, and heavy metals in OSPW (Pourrezaei et al. 2011, Wang et al. 2013).

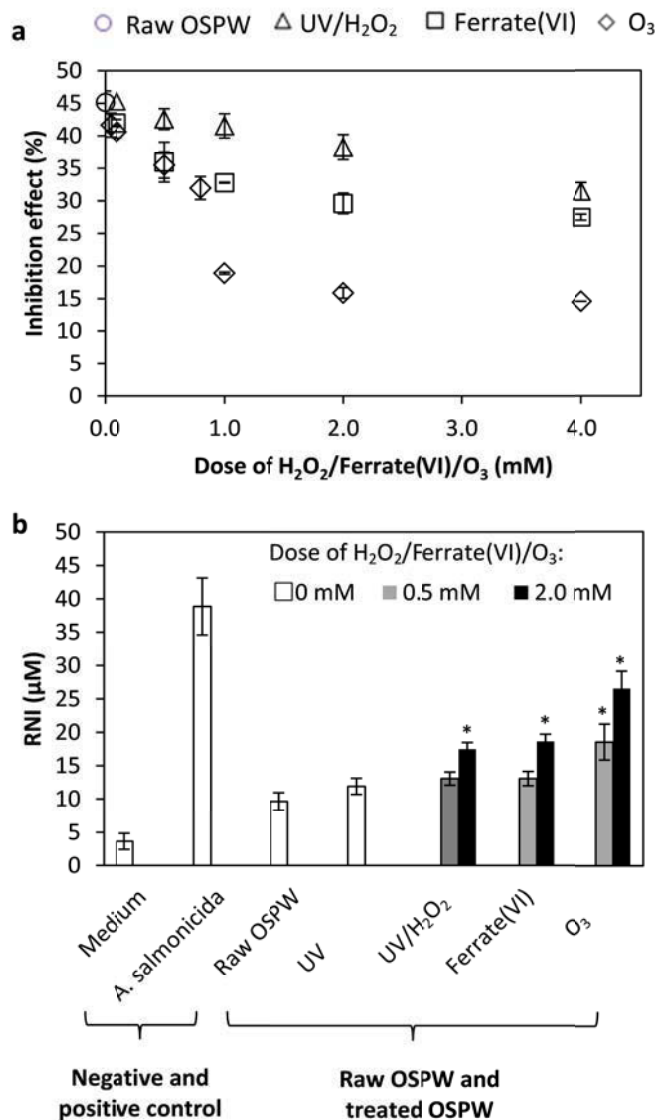


**Figure 4.12** (a) Inhibition effect on *Vibrio fischeri* caused by raw OSPW and OSPW treated with UV/H<sub>2</sub>O<sub>2</sub> ferrate (VI) and ozone, (b) Nitrite production by PKMs exposed to medium control, raw OSPW, and OSPW treated with UV/H<sub>2</sub>O<sub>2</sub>, ferrate (VI), and ozone (data for ozonation with TBA is not shown due to the interference on inhibition effect from TBA). Positive and negative controls were heat killed *A. salmonicida* and culture medium, respectively. Nitric oxide production was determined using the Griess reaction and RNI concentration was determined using RNI standard curve. Data are represented as mean  $\pm$  SEM RNI production by macrophages from separate cultures established from three individual fish ( $n = 3$ ). Statistical analysis was done using one-way ANOVA with a Dunnett's post hoc test. Asterisks (\*) indicate statistically significant increases ( $p < 0.05$ ) of RNI production in treated compared to raw OSPW

The effects of raw and treated OSPW on goldfish primary kidney macrophages (PKMs) were examined by measuring the production of RNIs (Figure 4.12b). High RNI production means high functional activity of PKMs and low toxicity of the tested sample. The higher production of nitrite by PKMs in cultures exposed to treated OSPW, compared to those exposed to raw OSPW ( $9.6 \pm 1.2 \mu\text{M}$  nitrite), indicates reduction in toxicity for all oxidation processes investigated in this study. Significant reduction in toxicity was observed after UV/H<sub>2</sub>O<sub>2</sub> at 2.0 mM H<sub>2</sub>O<sub>2</sub> ( $17.5 \pm 1.0 \mu\text{M}$ ), ferrate (VI) oxidation at 2.0 mM ( $18.6 \pm 1.1 \mu\text{M}$ ), and ozonation at both 0.5 and 2.0 mM ( $18.5 \pm 1.8 \mu\text{M}$  and  $26.5 \pm 2.7 \mu\text{M}$ ), respectively. Consistent with the Microtox results, ozonation was the most efficient process for the reduction of toxicity. However, toxicity assessment using PKMs did not confirm the advantage of ferrate (VI) over UV/H<sub>2</sub>O<sub>2</sub> indicated by Microtox assay. This discrepancy might be due to the differences in the mechanisms that induce toxic effects in prokaryotic organisms *Vibrio fischeri*, and eukaryotic cell goldfish PKMs. Toxicity assessment using goldfish PKMs was also done by Shu et al. (2014) evaluating UV/chlorine oxidation of OSPW. The researchers reported that treated OSPW was more toxic than raw OSPW, and speculated that increased toxicity may be due to formation of toxic by-products. Taken together, our results indicate that ferrate (VI) oxidation, UV/H<sub>2</sub>O<sub>2</sub> oxidation, and especially ozonation, are all potential treatment options for OSPW remediation regarding toxicity reduction.

### 4.3.6 Cost comparison

Rough cost estimates were done with assumptions (e.g., capacity, service life, interest rate, etc.) listed in Table 4.3. The costs of treating 1 m<sup>3</sup> of OSPW at chemical dose of 2.0 mM were estimated to be \$0.5, \$1.8, and \$0.4 for UV/H<sub>2</sub>O<sub>2</sub> oxidation (UV dose: 950 mJ/cm<sup>2</sup>), ferrate(VI) oxidation, and ozonation, respectively (Table 4.4). The high cost of the ferrate(VI) process is mainly caused by the high cost of chemical production, which might be considerably reduced if production is optimized and fully commercialized. When NA removal is correlated to the chemical cost, it is apparent that ozonation is the most cost-efficient process in OSPW treatment.

**Table 4.3** Assumptions for cost estimate

Parameters	Value
Capacity, m <sup>3</sup> /d	10000
Service life, yr	15
Interest rate	6%
Electricity price, \$/ (kW·h)	0.08 <sup>a</sup>
H <sub>2</sub> O <sub>2</sub> (100%) chemical cost, \$/kg	0.9 <sup>b</sup>
K <sub>2</sub> FeO <sub>4</sub> chemical cost, \$/kg	4.4 <sup>c</sup>

Notes:

<sup>a</sup> Based on the electricity price in Edmonton, Alberta, Canada.

<sup>b</sup> Obtained from industrial sources.

<sup>c</sup> Obtained from [http://cfpub.epa.gov/ncer\\_abstracts/index.cfm/fuseaction/display.highlight/abstract/8338](http://cfpub.epa.gov/ncer_abstracts/index.cfm/fuseaction/display.highlight/abstract/8338).

**Table 4.4** CapEx<sup>a</sup> and OpEx<sup>b</sup> analyses for the oxidation processes (chemical dose: 2.0 mM)

	UV/H <sub>2</sub> O <sub>2</sub> <sup>c</sup>	K <sub>2</sub> FeO <sub>4</sub> <sup>d</sup>	O <sub>3</sub> <sup>e</sup>
Estimated CapEx, \$/yr	48,999	30,495	523,081
Estimated OpEx, \$/yr	1,852,056	6,359,760	872,927
Total annual cost, \$/yr	1,901,055	6,390,255	1,396,008
Estimated cost per volume of processed water, \$/m <sup>3</sup>	0.5	1.8	0.4

Notes:

<sup>a</sup> CapEx: capital expenditures.

<sup>b</sup> OpEx: operational and maintenance expenditures. Both CapEx and OpEx values are present worth (PW) in the year 2016, adjusted with Engineering News Record (ENR) index.

<sup>c</sup> Estimated with cost equations for UV disinfection systems by Qasim et al. (1998). The cost was modified by considering additional chemical cost of H<sub>2</sub>O<sub>2</sub> and a UV dose of 950 mJ/cm<sup>2</sup>. Reference: Qasim S.R. (1998) Wastewater Treatment Plants: Planning, Design, and Operation, Second Edition, Taylor & Francis.

<sup>d</sup> Cost of the feed system was estimated with the same equation developed for potassium permanganate (McGivney and Kawamura, 2008). The OpEx cost was estimated mainly based on the chemical cost. Reference: McGivney W.T. and Kawamura S. (2008) Cost estimating manual for water treatment facilities, John Wiley & Sons, Inc.

<sup>e</sup> Estimated with cost equations for ozonation systems by Sharma et al. (2013). Reference: Sharma, J.R., Najafi M., and Qasim S.R., Preliminary cost estimation models for construction, operation, and maintenance of water treatment plants. Journal of Infrastructure Systems, 2013. 19(4): p. 451-464.

## 4.4 Conclusions

This study compared the performance of UV/H<sub>2</sub>O<sub>2</sub> oxidation, ferrate(VI) oxidation, and ozonation in OSPW remediation. The following conclusions could be drawn:

(1) Ozonation was the most effective process in treating OSPW, achieving almost complete removal of fluorescing aromatics, NAs+S, and classical NAs (97.1%) at the dose of 2.0 mM O<sub>3</sub>. Both reactions by ozone and •OH were important in transforming the organics.

(2) UV/H<sub>2</sub>O<sub>2</sub> oxidation was a combination of direct UV photolysis and •OH reaction. The efficiency of this process was compromised by the low molar extinction coefficient of hydrogen peroxide. 42.4% classical NAs were removed at a 2.0 mM H<sub>2</sub>O<sub>2</sub> dose and 950 mJ/cm<sup>2</sup> UV dose.

(3) Ferrate(VI) oxidation showed high selectivity in removing two-ring and three-ring fluorescing aromatics, NAs+S, and NAs with high carbon number and high hydrogen deficiency. 46.7% classical NA removal was achieved at 2.0 mM Fe(VI).

(4) <sup>1</sup>H NMR analyses showed that high removal of fluorescing aromatics and NAs did not necessarily mean equally high removal of hydrogens on aromatic rings and in carboxyl groups. Only ozonation at high dose (e.g., 2.0 mM) achieved significant removal of these hydrogens.

(5) Acute toxicity towards *Vibrio fischeri* was reduced, with the order of efficiency as “O<sub>3</sub> > ferrate (VI) > UV/H<sub>2</sub>O<sub>2</sub>” at the same molar doses of the

oxidants. In addition, toxicity on goldfish PKMs was also mitigated after all the treatment, with the order of efficiency as “O<sub>3</sub> > ferrate (VI) ≈ UV/H<sub>2</sub>O<sub>2</sub>”.

## References

- Afzal, A., Drzewicz, P., Perez-Estrada, L.A., Chen, Y., Martin, J.W. and Gamal El-Din, M. (2012) effect of molecular structure on the relative reactivity of naphthenic acids in the UV/H<sub>2</sub>O<sub>2</sub> advanced oxidation process. *Environmental Science & Technology* 46(19), 10727-10734.
- Anderson, J.C., Wiseman, S.B., Wang, N., Moustafa, A., Perez-Estrada, L., Gamal El-Din, M., Martin, J.W., Liber, K. and Giesy, J.P. (2012) Effectiveness of ozonation treatment in eliminating toxicity of oil sands process-affected water to *Chironomus dilutus*. *Environmental Science & Technology* 46(1), 486-493.
- Anquandah, G.A.K., Sharma, V.K., Panditi, V.R., Gardinali, P.R., Kim, H. and Oturan, M.A. (2013) Ferrate(VI) oxidation of propranolol: Kinetics and products. *Chemosphere* 91(1), 105-109.
- Bauer, A.E. (2013) Identification of oil sands naphthenic acid structures and their associated toxicity to *Pimephales promelas* and *Oryzias latipes*. M.S., University of Waterloo, Waterloo, Ontario.
- Bolton, J. and Linden, K. (2003) Standardization of methods for fluence (UV dose) determination in bench-scale UV experiments. *Journal of Environmental Engineering* 129(3), 209-215.
- Breitmaier, E. and Voelter, W. (1987) Carbon-13 NMR spectroscopy: high-resolution methods and applications in organic chemistry and biochemistry, VCH Publishers, Weinheim.

- Carey, F.A. and Sundberg, R.J. (2010) *Advanced organic chemistry: part B: reaction and synthesis*, Springer New York.
- Chelme-Ayala, P., Gamal El-Din, M. and Smith, D.W. (2010) Degradation of bromoxynil and trifluralin in natural water by direct photolysis and UV plus H<sub>2</sub>O<sub>2</sub> advanced oxidation process. *Water Research* 44(7), 2221-2228.
- Dong, T., Zhang, Y., Islam, M.S., Liu, Y. and Gamal El-Din, M. (2015) The impact of various ozone pretreatment doses on the performance of endogenous microbial communities for the remediation of oil sands process-affected water. *International Biodeterioration & Biodegradation* 100, 17-28.
- Drzewicz, P., Afzal, A., Gamal El-Din, M. and Martin, J.W. (2010) Degradation of a model naphthenic acid, cyclohexanoic acid, by vacuum UV (172 nm) and UV (254 nm)/H<sub>2</sub>O<sub>2</sub>. *Journal of Physical Chemistry A* 114(45), 12067-12074.
- Drzewicz, P., Perez-Estrada, L., Alpatova, A., Martin, J.W. and Gamal El-Din, M. (2012) Impact of peroxydisulfate in the presence of zero valent iron on the oxidation of cyclohexanoic acid and naphthenic acids from oil sands process-affected water. *Environmental Science & Technology* 46(16), 8984-8991.
- Dutta Majumdar, R., Gerken, M., Mikula, R. and Hazendonk, P. (2013) Validation of the Yen–Mullins model of Athabasca Oil-Sands asphaltenes using solution-state <sup>1</sup>H NMR relaxation and 2D HSQC spectroscopy. *Energy Fuels* 27(11), 6528-6537.

- Elovitz, M.S. and von Gunten, U. (1999) Hydroxyl radical/ozone ratios during ozonation processes. I. the  $R_{ct}$  concept. *Ozone: Science & Engineering* 21(3), 239-260.
- Francis, P.D. (1987) Oxidation by UV and ozone of organic contaminants dissolved in deionized and raw mains water. *Ozone: Science & Engineering* 9(4), 369-390.
- Frank, R.A., Fischer, K., Kavanagh, R., Burnison, B.K., Arsenault, G., Headley, J.V., Peru, K.M., Van, D.K.G. and Solomon, K.R. (2009) Effect of carboxylic acid content on the acute toxicity of oil sands naphthenic acids. *Environmental Science & Technology* 43(2), 266-271.
- Frank, R.A., Kavanagh, R., Kent Burnison, B., Arsenault, G., Headley, J.V., Peru, K.M., Van Der Kraak, G. and Solomon, K.R. (2008) Toxicity assessment of collected fractions from an extracted naphthenic acid mixture. *Chemosphere* 72(9), 1309-1314.
- Gamal El-Din, M., Fu, H., Wang, N., Chelme-Ayala, P., Pérez-Estrada, L., Drzewicz, P., Martin, J.W., Zubot, W. and Smith, D.W. (2011) Naphthenic acids speciation and removal during petroleum-coke adsorption and ozonation of oil sands process-affected water. *Science of the Total Environment* 409(23), 5119-5125.
- Gheraout, D. and Naceur, M.W. (2011) Ferrate(VI): In situ generation and water treatment - A review. *Desalination and Water Treatment* 30(1-3), 319-332.

- Gottschalk, C., Libra, J.A. and Saupe, A. (2010) Ozonation of water and waste water: A practical guide to understanding ozone and its applications, Wiley, Weinheim.
- He, Y., Patterson, S., Wang, N., Hecker, M., Martin, J.W., Gamal El-Din, M., Giesy, J.P. and Wiseman, S.B. (2012) Toxicity of untreated and ozone-treated oil sands process-affected water (OSPW) to early life stages of the fathead minnow (*Pimephales promelas*). *Water Research* 46(19), 6359-6368.
- He, Y., Wiseman, S.B., Zhang, X., Hecker, M., Jones, P.D., Gamal El-Din, M., Martin, J.W. and Giesy, J.P. (2010) Ozonation attenuates the steroidogenic disruptive effects of sediment free oil sands process water in the H295R cell line. *Chemosphere* 80(5), 578-584.
- Hoigné, J. and Bader, H. (1983a) Rate constants of reactions of ozone with organic and inorganic compounds in water—I. *Water Research* 17(2), 173-183.
- Hoigné, J. and Bader, H. (1983b) Rate constants of reactions of ozone with organic and inorganic compounds in water—II. *Water Research* 17(2), 185-194.
- Huang, C., Shi, Y., Gamal El-Din, M. and Liu, Y. (2015b) Treatment of oil sands process-affected water (OSPW) using ozonation combined with integrated fixed-film activated sludge (IFAS). *Water Research* 85, 167-176.
- Huang, R., McPhedran, K.N. and Gamal El-Din, M. (2015a) Ultra performance liquid chromatography ion mobility time-of-flight mass spectrometry

- characterization of naphthenic acids species from oil sands process-affected water. *Environmental Science & Technology* 49(19), 11737-11745.
- Jones, D., Scarlett, A.G., West, C.E., Frank, R.A., Gieleciak, R., Hager, D., Pureveen, J., Tegelaar, E. and Rowland, S.J. (2013) Elemental and spectroscopic characterization of fractions of an acidic extract of oil sands process water. *Chemosphere* 93(9), 1655-1664.
- Jones, D., West, C.E., Scarlett, A.G., Frank, R.A. and Rowland, S.J. (2012) Isolation and estimation of the 'aromatic' naphthenic acid content of an oil sands process-affected water extract. *Journal of Chromatography A* 1247, 171-175.
- Kishore Nadkarni, R.A. (2011) *Spectroscopic analysis of petroleum products and lubricants*, ASTM International, Pennsylvania.
- Klamerth, N., Moreira, J., Li, C., Singh, A., McPhedran, K.N., Chelme-Ayala, P., Belosevic, M. and Gamal El-Din, M. (2015) Effect of ozonation on the naphthenic acids' speciation and toxicity of pH-dependent organic extracts of oil sands process-affected water. *Science of the Total Environment* 506–507(0), 66-75.
- Larson, R. and Weber, E. (1994a) Chapter 4. Environmental oxidations. In: *Reaction mechanisms in environmental organic chemistry*, pp. 217-274, Lewis Publishers, Florida.

- Larson, R. and Weber, E. (1994b) Chapter 6. Environmental photochemistry. In: Reaction mechanisms in environmental organic chemistry, pp. 359-414, Lewis Publishers, Florida.
- Larson, R. and Weber, E. (1994c) Chapter 5. Reactions with disinfectants. In: Reaction mechanisms in environmental organic chemistry, pp. 275-358, Lewis Publishers, Florida.
- Larson, R. and Weber, E. (1994d) Chapter 1. Organic chemicals in the environment. In: Reaction mechanisms in environmental organic chemistry, pp. 1-102, Lewis Publishers, Florida.
- Lee, J.H., Landrum, P.F. and Koh, C.H. (2002) Toxicokinetics and time-dependent PAH toxicity in the amphipod *Hyalella azteca*. *Environmental Science & Technology* 36(14), 3124-3130.
- Liang, X., Zhu, X. and Butler, E.C. (2011) Comparison of four advanced oxidation processes for the removal of naphthenic acids from model oil sands process water. *Journal of Hazardous Materials* 190(1-3), 168-176.
- Mackinnon, M. and Zubot, W. (2013) Chapter 10: Water management. In: Handbook on theory and practice of bitumen recovery from Athabasca oil sands Volume II: Industrial practices. Czarnecki, J., Masliyah, J., Xu, Z. and Dabros, M. (eds), Kingsley Knowledge Publishing, Alberta.
- Majid, A. and Pihillagawa, I. (2014) Potential of NMR Spectroscopy in the Characterization of Nonconventional Oils. *Journal of Fuels* Volume 2014, Article ID 390261.

- Martin, J.W., Barri, T., Han, X., Fedorak, P.M., Gamal El-Din, M., Perez, L., Scott, A.C. and Jiang, J.T. (2010) Ozonation of oil sands process-affected water accelerates microbial bioremediation. *Environmental Science & Technology* 44(21), 8350-8356.
- Mohamed, M.H., Wilson, L.D., Peru, K.M. and Headley, J.V. (2013) Colloidal properties of single component naphthenic acids and complex naphthenic acid mixtures. *Journal of Colloid and Interface Science* 395(0), 104-110.
- Oppenländer, T. (2007) Photochemical purification of water and air: advanced oxidation processes (AOPs) - principles, reaction mechanisms, reactor concepts, Wiley, Weinheim.
- Pereira, A.S., Islam, M.s., Gamal El-Din, M. and Martin, J.W. (2013) Ozonation degrades all detectable organic compound classes in oil sands process-affected water; an application of high-performance liquid chromatography/obitrap mass spectrometry. *Rapid Communications in Mass Spectrometry* 27(21), 2317-2326.
- Pérez-Estrada, L.A., Han, X., Drzewicz, P., Gamal El-Din, M., Fedorak, P.M. and Martin, J.W. (2011) Structure-reactivity of naphthenic acids in the ozonation process. *Environmental Science & Technology* 45(17), 7431-7437.
- Pourrezaei, P., Drzewicz, P., Wang, Y., Gamal El-Din, M., Perez-Estrada, L.A., Martin, J.W., Anderson, J., Wiseman, S., Liber, K. and Giesy, J.P. (2011) The impact of metallic coagulants on the removal of organic compounds

from oil sands process-affected water. *Environmental Science & Technology* 45(19), 8452-8459.

Quagraine, E.K., Peterson, H.G. and Headley, J.V. (2005) *In situ* bioremediation of naphthenic acids contaminated tailing pond waters in the Athabasca oil sands region - Demonstrated field studies and plausible options: A review. *Journal of environmental science and health. Part A, Toxic/hazardous substances & environmental engineering* 40(3), 685-722.

Ross, M.S., Pereira, A.d.S., Fennell, J., Davies, M., Johnson, J., Sliva, L. and Martin, J.W. (2012) Quantitative and qualitative analysis of naphthenic acids in natural waters surrounding the Canadian oil sands industry. *Environmental Science & Technology* 46(23), 12796-12805.

Sayles, G.D., Acheson, C.M., Kupferle, M.J., Shan, Y., Zhou, Q., Meier, J.R., Chang, L. and Brenner, R.C. (1999) Land treatment of PAH-contaminated soil: performance measured by chemical and toxicity assays. *Environmental Science & Technology* 33(23), 4310-4317.

Sharma, V.K., Noorhasan, N.N., Mishra, S., K. and Nesnas, N. (2008) Ferrate(VI) oxidation of recalcitrant compounds: removal of biological resistant organic molecules by ferrate(VI). In: *Ferrates: synthesis, properties, and applications in water and wastewater treatment*. Sharma, V., K. (ed), American Chemical Society, Washington, DC

Sharma, V.K. and Mishra, S. (2006) Ferrate(VI) oxidation of ibuprofen: A kinetic study. *Environmental Chemistry Letters* 3(4), 182-185.

- Sharma, V.K. and Bielski, B.H.J. (1991) Reactivity of ferrate(VI) and ferrate(V) with amino acids. *Inorganic Chemistry* 30(23), 4306-4310.
- Shi, Y., Huang, C., Rocha, K.C., Gamal El-Din, M. and Liu, Y. (2015) Treatment of oil sands process-affected water using moving bed biofilm reactors: With and without ozone pretreatment. *Bioresource Technology* 192(0), 219-227.
- Shu, Z., Bolton, J.R., Belosevic, M. and Gamal El-Din, M. (2013) Photodegradation of emerging micropollutants using the medium-pressure UV/H<sub>2</sub>O<sub>2</sub> advanced oxidation process. *Water Research* 47(8), 2881-2889.
- Shu, Z., Li, C., Belosevic, M., Bolton, J.R. and Gamal El-Din, M. (2014) Application of a solar UV/chlorine advanced oxidation process to oil sands process-affected water remediation. *Environmental Science & Technology* 48(16), 9692-9701.
- Singh, A., Havixbeck, J.J., Smith, M.K., Shu, Z., Tierney, K.B., Barreda, D.R., Gamal El-Din, M. and Belosevic, M. (2015) UV and hydrogen peroxide treatment restores changes in innate immunity caused by exposure of fish to reuse water. *Water Research* 71, 257-273.
- Sun, N., Chelme-Ayala, P., Klammerth, N., McPhedran, K.N., Islam, M.S., Perez-Estrada, L., Drzewicz, P., Blunt, B.J., Reichert, M., Hagen, M., Tierney, K.B., Belosevic, M. and Gamal El-Din, M. (2014) Advanced analytical mass spectrometric techniques and bioassays to characterize untreated and ozonated oil sands process-affected water. *Environmental Science & Technology* 48(19), 11090-11099.

- Thompson, G.W., Ockerman, L.T. and Schreyer, J.M. (1951) Preparation and purification of potassium ferrate (VI). *Journal of the American Chemical Society* 73(3), 1379-1381.
- Tuan Vo, D. (1978) Multicomponent analysis by synchronous luminescence spectrometry. *Analytical Chemistry* 50(3), 396-401.
- von Sonntag, C. and von Gunten, U. (2012) *Chemistry of ozone in water and wastewater treatment: from basic principles to applications*, IWA Publishing, London
- Wang, C., Alpatova, A., McPhedran, K.N. and Gamal El-Din, M. (2015) Coagulation/flocculation process with polyaluminum chloride for the remediation of oil sands process-affected water: Performance and mechanism study. *Journal of Environmental Management* 160, 254-262.
- Wang, N., Chelme-Ayala, P., Perez-Estrada, L., Garcia-Garcia, E., Pun, J., Martin, J.W., Belosevic, M. and Gamal El-Din, M. (2013) Impact of ozonation on naphthenic acids speciation and toxicity of oil sands process-affected water to *Vibrio fischeri* and mammalian immune system. *Environmental Science & Technology* 47(12), 6518-6526.
- Wardman, P. (1989) Reduction potentials of one-electron couples involving free radicals in aqueous solution. *Journal of Physical and Chemical Reference Data* 18(4), 1637-1755.
- Wiberg, K.B. and Foster, G. (1961) The stereochemistry of the chromic acid oxidation of tertiary hydrogens. *Journal of the American Chemical Society* 83(2), 423-429.

Williams, A.T.R., Winfield, S.A. and Miller, J.N. (1983) Relative fluorescence quantum yields using a computer-controlled luminescence spectrometer. *Analyst* 108(1290), 1067-1071.

Zhang, K., Pereira, A.S. and Martin, J.W. (2015) Estimates of octanol-water partitioning for thousands of dissolved organic species in oil sands process-affected water. *Environmental Science & Technology* 49(14), 8907-8913.

## 5 ANALYSES OF THE ORGANIC FRACTIONS IN RAW AND OXIDIZED OIL SANDS PROCESS-AFFECTED WATER WITH FOURIER TRANSFORM ION CYCLOTRON RESONANCE MASS SPECTROMETRY AND ULTRA-PERFORMANCE LIQUID CHROMATOGRAPHY TIME-OF-FLIGHT MASS SPECTROMETRY<sup>4</sup>

### 5.1 Introduction

Bitumen extraction from oil sands and the following upgrading processes produces large amounts of wastewater, commonly known as oil sands process-affected water (OSPW). This type of water features high concentration of inorganic ions (e.g., sodium, potassium, chloride, sulfate, bicarbonate), and thousands of dissolved organic species such as naphthenic acids (NAs), sulfur/nitrogen-containing organic species, and aromatics (Allen 2008, Barrow et al. 2010, Headley et al. 2014, Zhang et al. 2015a). The toxicity of OSPW has been widely reported (Alharbi et al. 2016, Anderson et al. 2012, Gamal El-Din et al. 2011, He et al. 2012, Morandi et al. 2015), which warrants the current non-release policy on the OSPW and prompts extensive studies on OSPW treatment.

---

<sup>4</sup> A version of this chapter has been submitted to Environmental Science & Technology as “Wang, C., Huang, R., Klamerth, N., Chelme-Ayala, P., and Gamal El-Din, M., Analyses of the organic fractions in raw and oxidized oil sands process-affected water with Fourier transform ion cyclotron resonance mass spectrometry (FTICR-MS) and ultra-performance liquid chromatography time-of-flight mass spectrometry (UPLC-TOF-MS)”.

So far, the focus of OSPW treatment was on the removal of classical NAs (Garcia-Garcia et al. 2011, Wang et al. 2015, Zhang et al. 2015b), which are reported to be the “most acutely toxic chemical classes in OSPW” (Morandi et al. 2015). NAs with a higher number of oxygens (oxy-NAs) are generally less toxic than the classical NAs due to the increase of hydrophilicity (i.e., less affinity to cell membrane) (Frank et al. 2009, Frank et al. 2008, He et al. 2010). However, these “NAs-centered” ideas have been challenged by studies incorporating other organic species into the research scope or applying different toxicity tests. For example, a recent study by Alharbi et al. (2016) concluded that NAs “did not appear to be the cause of the inhibition” of the ATP-binding cassette (ABC) transport proteins; instead, sulfur and nitrogen-containing species detected by Orbitrap mass spectrometry (MS) in positive ionization mode might be the culprits. Similarly, Quesnel et al.’s research attributed the reduced toxicity towards *S. pombe* cells to the removal of O<sub>3</sub>S species. These diverse and sometimes controversial conclusions from OSPW toxicity studies have warranted the inclusion of sulfur and nitrogen-containing species in evaluating the OSPW remediation processes.

The existence of sulfur/nitrogen-containing species in OSPW has been reported for years (Barrow et al. 2010, Headley et al. 2011, Headley et al. 2009). However, research on OSPW remediation did not include them as target compounds until Wang et al. (2013) and Pereira et al. (2013b) initiated such studies. Wang et al. (2013) employed ion mobility spectroscopy (IMS) to identify the nitrogen/sulfur-containing species as one general group and compared their intensity before and

after ozonation. However, IMS is essentially a qualitative method with no differentiation of the specific nitrogen/sulfur-containing species, and therefore, was far less informative than the high resolution mass spectrometry with Orbitrap MS results achieved by Pereira et al. (2013b) on raw and ozonated OSPWs. Besides Pereira et al.'s study, Fourier transform ion cyclotron resonance MS (FTICR-MS) has also been employed to characterize the transformation of nitrogen/sulfur-containing species by ozonation and ultrasonication (Headley et al. 2015a), bioremediation with indigenous algae (Quesnel et al. 2015), and solar photocatalysis over TiO<sub>2</sub> (Leshuk et al. 2016). Moreover, among these studies, only Pereira et al.'s study investigated the species composition in both positive and negative ionization modes. As more species can be detected in positive mode than in negative mode (Barrow et al. 2010, Pereira et al. 2013b), another knowledge gap exists regarding how the species detected in positive mode will be transformed with the various treatments. At last, ultra-performance liquid chromatography time-of-flight mass spectrometry (UPLC-TOF-MS) coupled with negative electrospray ionization (ESI) has been extensively used to estimate the concentration of O<sub>x</sub> species in OSPW, especially NAs and oxy-NAs (Gamal El-Din et al. 2011, Shu et al. 2014, Sun et al. 2014, Wang et al. 2015, Zhang et al. 2015b) and thus a comparison of the UPLC-TOF-MS results with the FTICR-MS results is also warranted.

Therefore, in this study, we selected three oxidation processes to treat OSPW as representatives of selective and unselective oxidation processes, including ferrate(VI) oxidation, UV/H<sub>2</sub>O<sub>2</sub> oxidation, and ozonation with and without radical

scavenger at representative dose. These treated OSPW, together with raw OSPW, were analyzed by FTICR-MS and UPLC-TOF-MS in both negative and positive ESI modes. The objectives of this study are as follows: (1) to investigate the abundance of organic species in raw and oxidized OSPWs; (2) to compare the performance of the different oxidation processes in transforming the organic species; and (3) to compare the organic species detected by UPLC-TOF-MS and those detected by FTICR-MS.

## **5.2 Materials and methods**

### **5.2.1 Raw OSPW and chemicals**

Raw OSPW was collected in 2014 from an active oil sands tailings pond in Fort McMurray, Alberta, Canada, and was stored at 4°C prior to use. Potassium ferrate(VI) with purity of 92% was prepared by wet method (Thompson et al. 1951). 30% hydrogen peroxide solution was purchased from Fisher Scientific (ON, Canada), and 99.5% extra pure tert-butyl alcohol (TBA) was purchased from Acros Organics (NJ, USA). Ozone was generated from extra-dry and high-purity oxygen using an ozone generator (Model GLS-7, PCI-WEDECO, Herford, Germany). All other chemicals were of analytical grade unless specified otherwise.

### **5.2.2 Experimental design**

The dosage of potassium ferrate(VI), ozone, and hydrogen peroxide investigated in this study was selected to be 2.0 mM, which was one of the typical doses applied in previous studies (Anderson et al. 2012, Drzewicz et al. 2010, Shu et al. 2013, Singh et al. 2015). Ferrate(VI) oxidation was done by adding potassium

ferrate(VI) into OSPW at rapid mixing and the reaction time was maintained for three hours before adding sodium thiosulfate (Fisher Scientific, NJ, USA) to quench residual ferrate(VI). UV/H<sub>2</sub>O<sub>2</sub> oxidation was achieved with a quasi-collimated beam UV apparatus equipped with a 1 kW medium pressure mercury lamp (Model PSI-I-120, Calgon Carbon Corporation, PA, USA). UV dose was fixed as 950 mJ/cm<sup>2</sup>, which is within the typical dose range reported by other studies (Afzal et al. 2012, Chelme-Ayala et al. 2010, Shu et al. 2013). After UV exposure, sodium thiosulfate (Fisher Scientific, NJ, USA) was added to quench residual H<sub>2</sub>O<sub>2</sub>. Ozonation was done with both raw OSPW and TBA-spiked OSPW (TBA concentration was 100 mM), following the procedure described by Wang et al. (2013). All samples were filtered through 0.45 μm nylon filter (Supelco Analytical, PA, USA) and preserved in amber glass bottles.

### **5.2.3 FTICR-MS analysis**

The samples were analyzed by direct infusion to the ESI source on a Bruker 9.4 T Apex-Qe FTICR mass spectrometer (Bruker Daltonics, Billerica, MA, USA) at a flow rate of 2.0 μL/min. Samples were pre-treated with liquid-liquid extraction using dichloromethane (DCM). Briefly, the pH of 100 mL sample was adjusted to 2.0 using diluted 1.0 M H<sub>2</sub>SO<sub>4</sub>, and then extracted twice with 50 mL DCM. The combined 100 mL extracted fractions were dried completely under air flow at room temperature and weighed (Table S1) precisely prior to use.

For negative ESI analysis, each dried fraction was re-dissolved in DCM (1000 mg/L) and then diluted 500 times in isopropyl alcohol (IPA) to give a final concentration of 2 mg/L with 0.1% (v/v) NH<sub>4</sub>OH added. The internal standard

(myristic acid-1-<sup>13</sup>C) was added at a final concentration of 0.088 μM. For positive ESI analysis, each dried fraction was re-dissolved in DCM (1000 mg/L) and then diluted 50 times in methanol (IPA gives background in the positive mode) to give a final concentration of 20 mg/L with 0.1% (v/v) formic acid added. No internal standard was used in positive mode.

Data were collected over the range of 145-2000 m/z with an ion-accumulation time in the external hexapole collision-cell of 10 s prior to injection to the ICR cell using side-kick trapping. Time-domain data sets (4M data points) were summed (16 acquisitions) to enhance the signal-to-noise ratio. Mass accuracy across the full mass range was less than 0.1 ppm root-mean-square (RMS) error. Bruker Daltonics Data Analysis version 4.0 was used to process the raw data. The formulae were generated using the “Smart formula” algorithm within Bruker Daltonics Data Analysis.

#### **5.2.4 UPLC-TOF-MS analysis**

The ESI source was operated in negative ion mode to measure NAs and in positive mode to measure other species in addition to NAs (Pereira et al. 2013a). Analysis in negative ESI mode was done as follows. The samples were prepared with centrifugation at 10000 rpm for 10 min. The injection solution was prepared with 500 μL of the centrifuged supernatant, 100 μL of 4.0 mg/L internal standard (myristic acid-1-<sup>13</sup>C) in methanol, and 400 μL methanol to reach a final sample volume of 1 mL. Chromatographic separations were performed using a Waters UPLC Phenyl BEH column (1.7 μm, 150 mm × 1 mm), with mobile phases of 10 mM ammonium acetate in water (A), 10 mM ammonium acetate in 50/50

methanol/acetonitrile (B), the injection volume of 10  $\mu\text{L}$  and a column temperature of 50°C. The elution gradient was 0–2 min, 1% B; 2–3 min, increased from 1% to 60% B; 3–7 min, from 60% to 70% B; 7–13 min, from 70% to 95% B; 13–14 min, from 95% to 1% B, and hold 1% B until 20 min to equilibrate column with a flow rate of 100  $\mu\text{L min}^{-1}$ . Samples were analyzed with the UPLC-TOF-MS (Synapt G2, Waters, ON, Canada) with the TOF analyzer in high-resolution mode (mass resolution is 40000) and the investigated mass range of 100-600 ( $m/z$ ). Data acquisition was controlled using MassLynx (Waters Corp., Milford, MA, USA) and data extraction from spectra was performed using TargetLynx (Waters Corp., Milford, MA, USA). Analysis in positive ESI mode: same procedure was used as described above except that no internal standard was employed due to the lack of information on the molecular structures of the species detected in positive ESI mode.

### 5.3 Results and discussion

As the species detected by FTICR-MS and UPLC-TOF-MS were not necessarily carboxylic acids, we employed the following general formula of  $\text{C}_n\text{H}_{2n+2+z}\text{O}_x$ ,  $\text{C}_n\text{H}_{2n+2+z}\text{O}_x\text{S}_y$ ,  $\text{C}_n\text{H}_{2n+2+y+z}\text{O}_x\text{N}_y$  for  $\text{O}_x$  species, sulfur-containing species (e.g.,  $\text{O}_x\text{S}$  and  $\text{O}_x\text{S}_2$ ), and nitrogen-containing species (e.g.,  $\text{O}_x\text{N}$  and  $\text{O}_x\text{N}_2$ ), respectively, in which  $n$  is carbon number,  $z$  is hydrogen deficiency (including the deficiency caused by carboxyl groups),  $x$  is oxygen number, and  $y$  is sulfur number or nitrogen number. In addition, there were also species containing both sulfur and nitrogen, and will be noted as  $\text{O}_x\text{S}_{y_1}\text{N}_{y_2}$  ( $y_1$  and  $y_2$  are sulfur number and nitrogen number respectively) in the following discussion.

### 5.3.1 FTICR-MS results

393 and 759 compounds were detected by FTICR-MS in negative and positive ESI respectively from the organic fractions of raw OSPW. The change of ionization mode significantly altered the relative abundance ( $A_{rel}$ ) of  $O_x$ ,  $O_xS_y$ ,  $O_xN_y$  and  $O_xS_{y1}N_{y2}$  species (Figure 5.1). Therefore, the transformation of these species is discussed based on results in negative ESI mode and positive mode, respectively.

#### 5.3.1.1 Transformation of $O_x$ species

##### *Negative ESI mode*

$O_x$  species predominated in raw OSPW, accounting for 82.3% of total intensity in negative ESI mode (Figure 5.1a; numerical information of Figure 5.1 is provided in Appendix F). Generally,  $O_x$  species remained the dominant species after all the treatments, accounting for 71.6%, 86.7%, 84.8%, and 78.8% of the total intensity after ferrate(VI) oxidation, UV/H<sub>2</sub>O<sub>2</sub> oxidation, ozonation, ozonation with the addition of TBA, respectively (Figure 5.1a). This might suggest that transformation from  $O_xS_y$  or  $O_xN_y$  to  $O_x$  did not prevail in the oxidation processes.

Among the  $O_x$  species detected in raw OSPW in negative ESI mode,  $O_2$  (38.2% out of the total  $O_x$  species, the same applies to  $A_{rel}$  of the other specific  $O_x$ ),  $O_4$  (30.5%), and  $O_3$  (24.4%) were the most abundant, followed by  $O_5$  (6.1%) and  $O_6$  (0.6%), and other species (Figure 5.1c). The dominance of the  $O_2$ ,  $O_4$ , and  $O_3$  species was consistent with previous analyses with FTICR-MS (Zhang et al. 2015a). The distribution of specific  $O_x$  species,  $O_2$ ,  $O_3$ ,  $O_4$ ,  $O_5$ ,  $O_6$ , and  $O_7$ , was

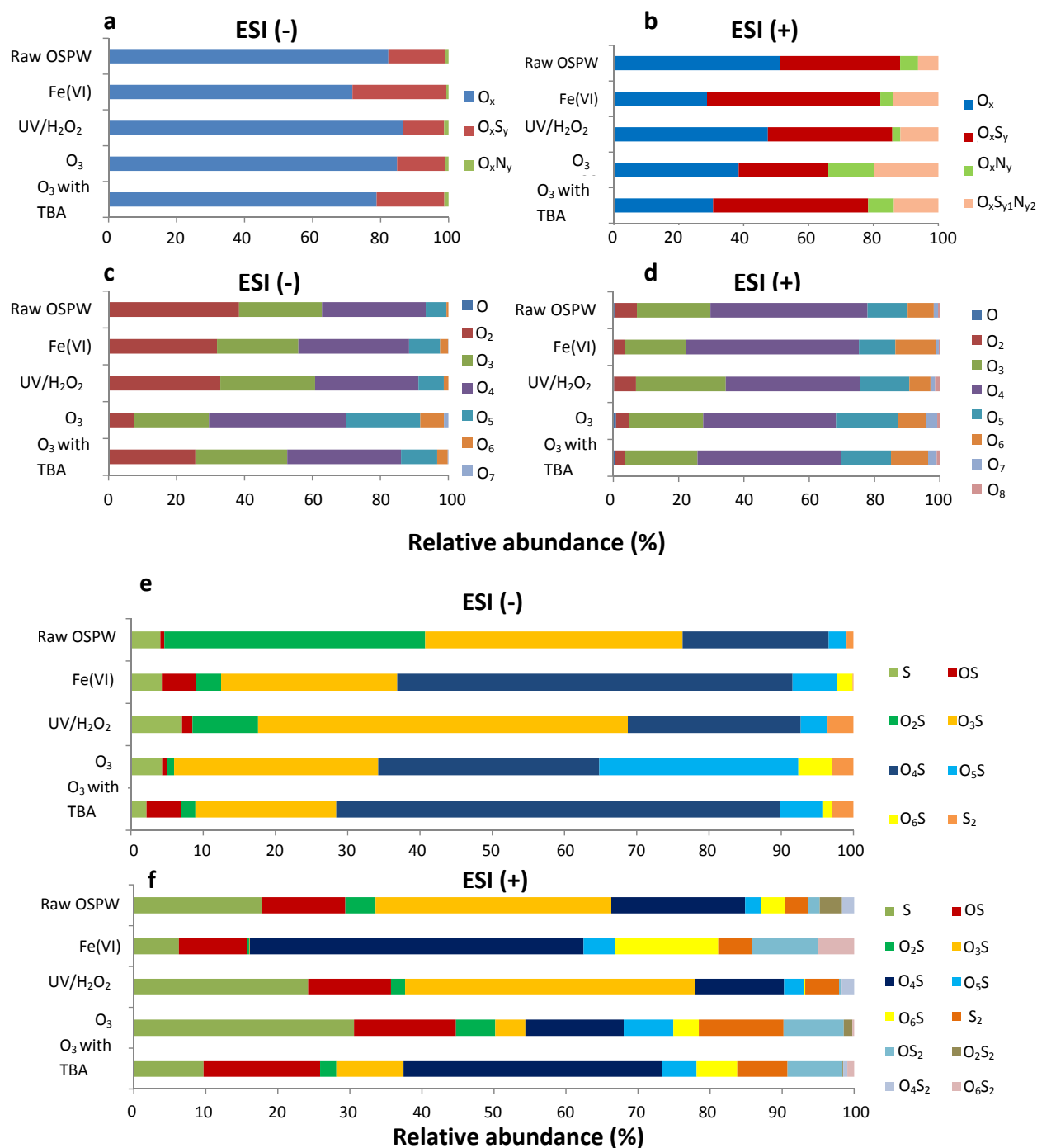


**Figure 5.1** Fractions of organics in raw and treated OSPWs detected by FTICR-MS: relative abundance of  $O_x$ ,  $O_xS_y$ , and  $O_xN_y$  out of the total organic species detected in negative ESI mode (a) and positive ESI mode (b), and relative abundance of O,  $O_2$ ,  $O_3$ ,  $O_4$ ,  $O_5$ ,  $O_6$ ,  $O_7$ , and  $O_8$  species out of the total  $O_x$  species detected in negative ESI mode (c) and positive ESI mode (d), and relative abundance of S, OS,  $O_2S$ ,  $O_3S$ ,  $O_4S$ ,  $O_5S$ ,  $O_6S$ ,  $S_2$ ,  $OS_2$ ,  $O_2S_2$ ,  $O_4S_2$ , and  $O_6S_2$  species out of the total sulfur containing species detected by FTICR-MS in negative ESI mode (e) and positive ESI mode (f)

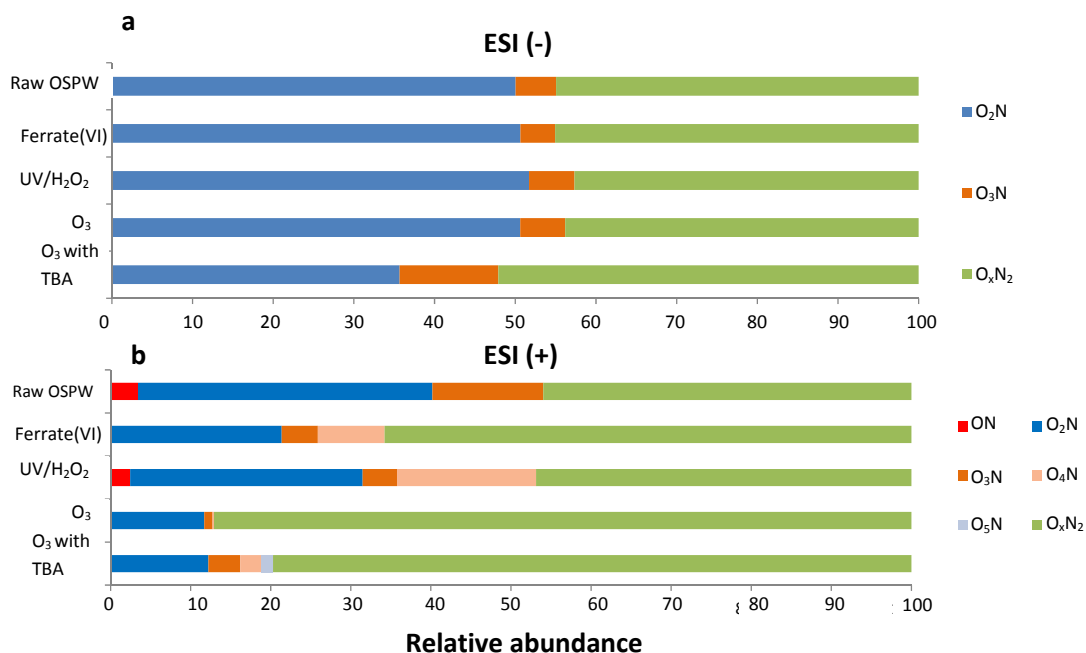


**Figure 5.2** Relative abundance of ON, O<sub>2</sub>N, O<sub>3</sub>N, O<sub>4</sub>N, O<sub>5</sub>N, O<sub>x</sub>N<sub>2</sub> species out of total nitrogen containing species in raw and treated OSPWs measured by FTICR-MS in negative ESI mode (a) and positive ESI mode (b)

also altered after oxidation. All treatments reduced the proportion of O<sub>2</sub> species, corresponding to the removal of classical NAs; other O<sub>x</sub> species showed either increase or decrease of their A<sub>rel</sub> after oxidation depending on the selectivity of the oxidants. Ferrate(VI) oxidation decreased the A<sub>rel</sub> of O<sub>2</sub> and O<sub>3</sub> to 31.7% and 23.9% respectively, and increased the A<sub>rel</sub> of O<sub>4</sub>, O<sub>5</sub> and O<sub>6</sub> to 32.6%, 9.1%, and 2.4%, respectively. The decrease in the A<sub>rel</sub> of O<sub>3</sub>, although very limited, was possibly due to the selectivity of ferrate(VI) oxidation: some of the newly generated O<sub>3</sub> species (especially those with additional hydroxyl group or aldehyde group) are more reactive than the parent compounds and were, therefore, preferentially oxidized by ferrate(VI) to O<sub>4</sub> species or more oxygen-rich (i.e.,

molecules have higher oxygen number) species depending on the oxidation extent. UV/H<sub>2</sub>O<sub>2</sub> oxidation resulted in a comparable O<sub>2</sub> A<sub>rel</sub> of 32.6%, but was accompanied by an increase of the O<sub>3</sub> A<sub>rel</sub> to 27.9%. UV/H<sub>2</sub>O<sub>2</sub> oxidation mainly relies on the reactions with ·OH which oxidize all the O<sub>x</sub> species indiscriminately. Therefore, some of the newly generated O<sub>3</sub> species were not preferentially targeted and survived the radical oxidation, resulting in its A<sub>rel</sub> increase.

Ozonation is the most effective process in transforming the O<sub>x</sub> species in OSPW. After ozonation, O<sub>2</sub> and O<sub>3</sub> abundances were reduced to 7.3% and 22.0%, while O<sub>4</sub>, O<sub>5</sub>, and O<sub>6</sub> species increased to 40.5%, 21.8% and 6.9%, indicating that a significant shift of organic species distribution to more oxygen-rich species. Ozonation of TBA-spike OSPW showed that molecular ozone oxidation also transformed the NAs distribution to 25.4% O<sub>2</sub>, 27.0% O<sub>3</sub>, 33.5% O<sub>4</sub>, 10.7% O<sub>5</sub>, and 3.1% O<sub>6</sub> species, indicating the efficiency of molecular ozone in removing classical NAs. The performance difference of ozonation with and without TBA can be attributed to the ·OH oxidation. Most likely, both molecular ozone reaction and ·OH oxidation played important roles in transforming the organics in OSPW.

No obvious change of the carbon number distribution of the total O<sub>x</sub> species and the major O<sub>x</sub> species such as O<sub>2</sub>, O<sub>3</sub>, O<sub>4</sub>, and O<sub>5</sub> was observed after oxidation except for ozonated OSPW (Figures 5.3-5.4, panels a, c, e, g, and i). The reason is that partial oxidation, for example, transformation of O<sub>2</sub> species to O<sub>3</sub> species, hardly changed the carbon number. Carbon number changes only when molecule breakdown occurs, and the detection of small hydrophilic molecules was not

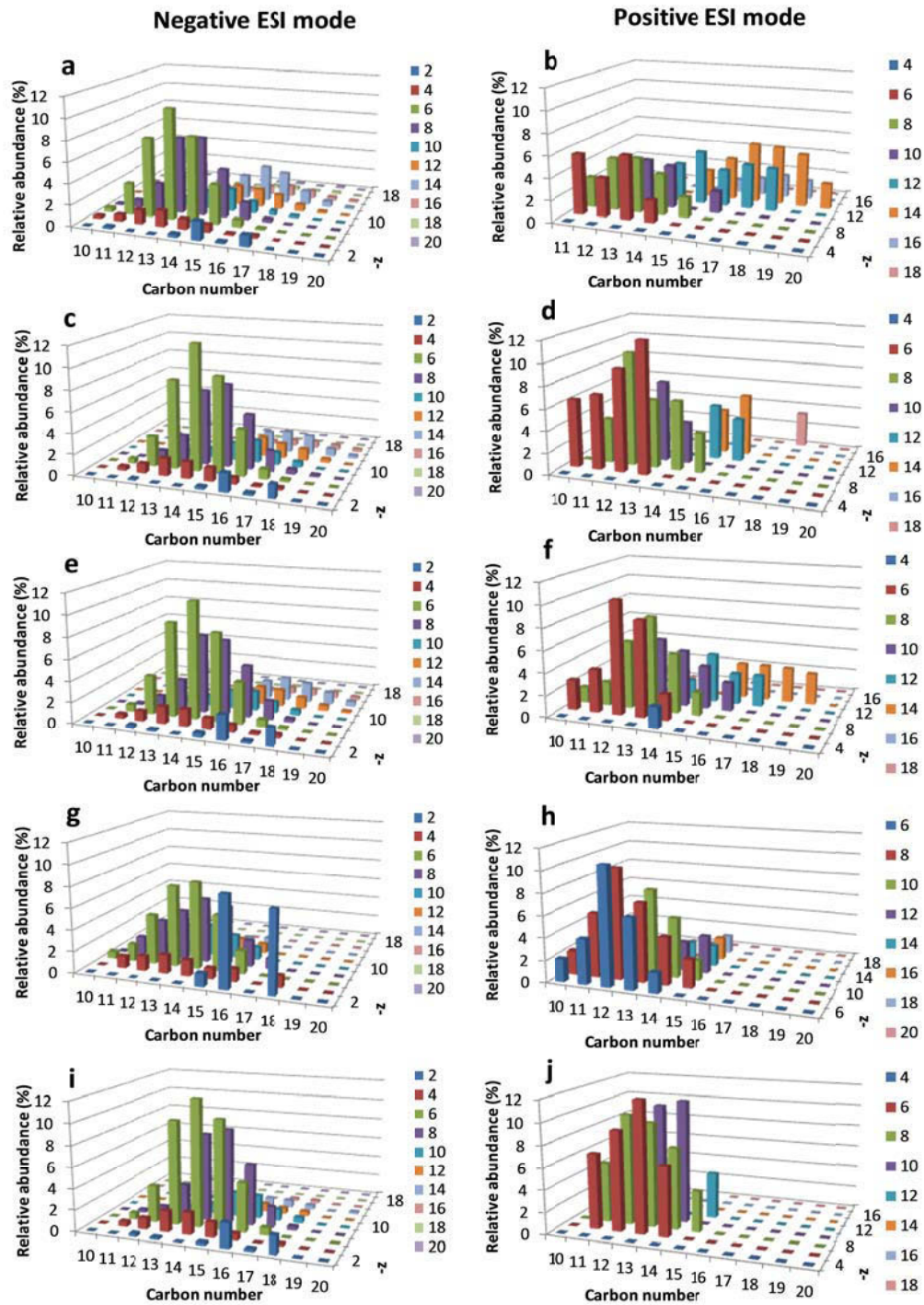


**Figure 5.3** Carbon number and  $-z$  number distribution of  $O_2$  species in raw OSPW (a,b), ferrate(VI)-treated OSPW (c,d), UV/ $H_2O_2$ -treated OSPW (e,f), ozonated OSPW (g,h), and ozonated TBA-spiked OSPW (i,j) detected by FTICR-MS in negative and positive ESI modes

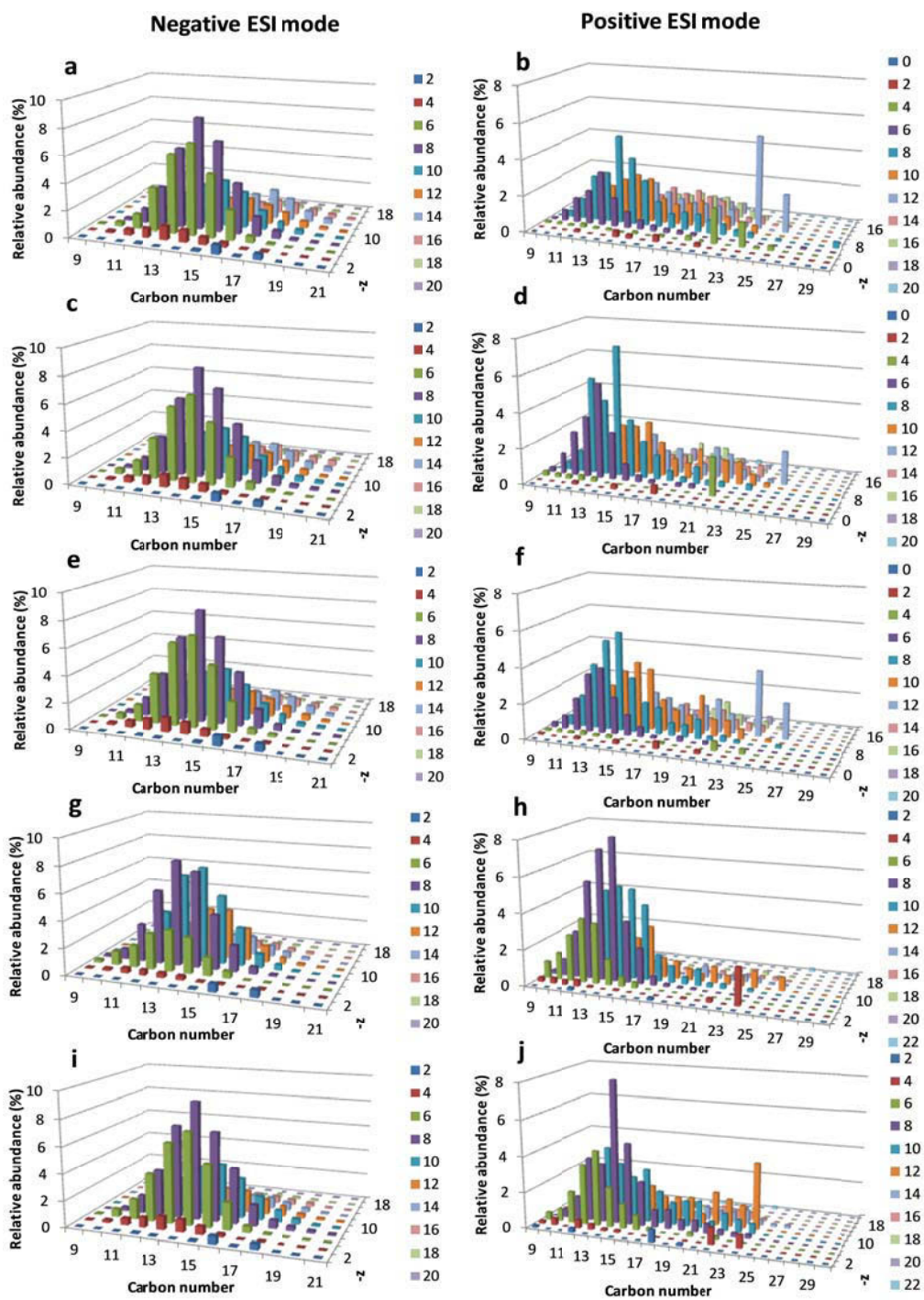


**Figure 5.4** Carbon number and -z number distribution of total  $O_x$  species in raw OSPW (a,b), ferrate(VI)-treated OSPW (c,d), UV/ $H_2O_2$ -treated OSPW (e,f), ozonated OSPW (g,h), and ozonated TBA-spiked OSPW (i,j) detected by FTICR-MS in negative and positive ESI modes



**Figure 5.5** DCM extracted organic fractions of OSPW

achieved with current method. Only ozonation achieved a shift of the distribution profile to lower carbon numbers, which was due to the cleavage of larger molecules on reactive sites and oxidative abstraction of the terminal carbons.

Hydrogen deficiency distribution of the total  $O_x$  species in raw OSPW showed two peaks: one peak at  $-z=8$  and the other at  $-z=14$  (Figure 5.4a). The first peak was caused by the existence of alicyclic rings or double bonds (as aromatic rings require essentially at least  $-z \geq 10$  for aromatic carboxylic acids). On the other hand, the second peak at  $-z=14$  is very likely to be related to aromatic rings considering the high value of the hydrogen deficiency. The existence of aromatic NAs was also previously reported by Rowland et al. (2011) and Scarlett et al. (2013), and was indicated by the yellow-orange color of the extracted organic fractions (Figure 5.5) and the fluorescing properties of the OSPW (Shu et al. 2014, Zhang et al. 2015b). The oxidation processes (including ferrate(VI), UV/ $H_2O_2$ , and molecular ozone oxidation) preferentially decreased the  $A_{rel}$  of  $O_x$  species

with  $-z > 12$ , probably due to the higher reactivity of the aromatics than that of aliphatic hydrocarbons. However, these oxidation processes did not significantly alter the  $-z$  distribution profiles as the organics were only mildly transformed. On the other hand, ozonation transformed the organics to a higher extent, resulting in a notable change of the distribution curve. Interestingly, it shifted the curve towards higher hydrogen deficiency, which might be caused by the newly generated carbonyl groups such as ketone, aldehyde, and carboxyl groups after ozonation.

#### *Positive ESI mode*

The  $A_{\text{rel}}$  of  $O_x$  species decreased from 51.3% in raw OSPW notably to 28.7% after ferrate(VI) oxidation, 47.4% after UV/ $H_2O_2$  oxidation, 38.5% and 30.5% after ozonation without and with TBA (Figure 5.1b). The change in  $A_{\text{rel}}$  of the species detected in positive mode was more evident than in negative mode, except for UV/ $H_2O_2$  oxidation, which is understandable as UV/ $H_2O_2$  is an unselective process. As suggested by Pereira et al. (2013a), dihydroxy, diketo, or ketohydroxy functional groups might be the species detected in positive ESI mode. These functional groups were less oxidized than carboxylic acids detected in negative ESI mode, and further oxidation to carboxylic acids was likely to occur during the oxidation processes, after which some of them might not be detected in the positive mode any more. This might contribute to the  $A_{\text{rel}}$  decrease of the  $O_x$  species.

Positive mode  $O_x$  species are more oxygen-rich than those detected in negative mode. The dominant  $O_x$  species in raw OSPW was  $O_4$  (48.1%), followed by  $O_3$

(22.5%) and O<sub>5</sub> (12.3%) (Figure 5.1d). Similar to the results acquired in negative ESI mode, all the oxidation process decreased the A<sub>rel</sub> of O<sub>2</sub> species, with the least decrease achieved by UV/H<sub>2</sub>O<sub>2</sub> process. Ferrate(VI) oxidation resulted in O<sub>3</sub> A<sub>rel</sub> decrease and O<sub>4</sub> A<sub>rel</sub> increase, while UV/H<sub>2</sub>O<sub>2</sub> process achieved the opposite pattern (i.e., O<sub>3</sub> A<sub>rel</sub> increase and O<sub>4</sub> A<sub>rel</sub> decrease). In addition, as the most efficient process, ozonation did not change the profile as much as it did for negative mode species although it achieved the highest decrease of O<sub>4</sub> species and highest increase of O<sub>5</sub> species among all the treatment investigated. The addition of TBA did not alter the general trend of the species increase or decrease, but all the changes of the A<sub>rel</sub> occurred to a less extent.

The carbon number of species detected in positive mode ranged from 9 to 30, broader than 9-21 in negative mode (Figure 5.4a and b). The broad range of carbon number and the rugged distribution might imply more complex composition detected in positive mode than in negative mode. As shown in Figure 5.4, the oxidation process preferentially removed the high carbon number (e.g., 17-25) O<sub>x</sub> species and increased the A<sub>rel</sub> of species with carbon number from 7 to 16, with ozonation achieving the highest extent change. The -z number distribution showed two maxima at -z=8 and 12 (Figure 5.4 and Table A8) and the A<sub>rel</sub> of the species around the second maximum was much higher than that detected in negative mode, implying more rings and double bonds detected in positive mode. Therefore, the preferential removal of species with -z>10 was clearly observed in positive mode, as embodied by A<sub>rel</sub> increase of species with -z ≤10 and A<sub>rel</sub> decrease of species with -z>10. This preferential removal of species

with high  $-z$  number was also observed with the transformation of the  $O_2$  species (Figure 5.3, panel b, d, f, h, and j).

### 5.3.1.3 Transformation of sulfur-containing species

#### *Negative ESI mode*

The  $A_{rel}$  of sulfur-containing species in raw OSPW detected in negative mode was only 16.6%, which increased to 27.6% after ferrate(VI) oxidation and 19.9% after ozonation with TBA, and decreased to 12.0% after UV/ $H_2O_2$  oxidation and 14.1% after ozonation without TBA. The increase of  $O_xS$   $A_{rel}$  by selective oxidation and limited decrease of  $O_xS$   $A_{rel}$  by unselective oxidation indicated that the sulfur-containing species as a whole were not preferentially *eliminated* by the oxidation processes. However, this did not mean that sulfur-containing species were unreactive and were not transformed. On the contrary, the transformation of sulfur-containing species significantly changed the distribution profile of specific  $O_xS$  species (Figure 5.1e). One explanation was that the possible existence of electron-rich moieties in sulfur-containing species could only facilitate the localized *oxidation/transformation* of sulfur-containing functional groups but not guarantee the *removal/elimination* of them.

$O_2S$  (36.1% out of the total  $O_xS_y$  species, and the same applies to the  $A_{rel}$  of other specific  $O_xS_y$  species),  $O_3S$  (35.6%), and  $O_4S$  (20.2%) were the major sulfur-containing species in raw OSPW. As selective processes, ferrate(VI) and molecular ozone oxidations performed in similar ways in transforming  $O_xS$  species:  $O_2S$  and  $O_3S$  were significantly transformed, as indicated by their low

abundance in ferrate(VI) treated OSPW (3.5% for O<sub>2</sub>S and 24.4% for O<sub>3</sub>S) and ozone (with TBA)-treated OSPW (2.0% for O<sub>2</sub>S and 19.5% for O<sub>3</sub>S). Simultaneously, the percentage of O<sub>4</sub>S species increased to 54.7% and 61.5% respectively after ferrate(VI) oxidation and ozonation with TBA, becoming the predominate species in the oxidized OSPW. As an unselective oxidation process, UV/H<sub>2</sub>O<sub>2</sub> performed in a different way. While the A<sub>rel</sub> of O<sub>2</sub>S species decreased notably (9.1%), the O<sub>3</sub>S (51.2%) and O<sub>4</sub>S (23.9%) species both increased, with O<sub>3</sub>S being the most abundant sulfur-containing species. This different performance between selective oxidation and unselective oxidation can also be explained as follows: the newly generated O<sub>3</sub>S species as reaction intermediates were preferentially transformed by selective oxidants to O<sub>4</sub>S, while these same O<sub>3</sub>S can survive the ·OH reaction as they were not specially targeted after their generation. Ozonation without radical scavenger was again the most effective process in transforming the sulfur-containing species, as confirmed by the almost complete removal of O<sub>2</sub>S species and the increase of the O<sub>4</sub>S (30.6%), O<sub>5</sub>S (27.5%) and O<sub>6</sub>S (4.7%) species.

The significant transformation of sulfur-containing species probably indicated that sulfur-containing species was more reactive than O<sub>x</sub> species. Preferential removal of sulfur-containing species over O<sub>x</sub> species was also achieved by remediation studies with ozonation (Wang et al. 2013), ozonation and ultrasonication (Headley et al. 2015a), and solar photocatalytic degradation (Leshuk et al. 2016). Previous studies suggested that sulfur-containing species in OSPW not only contained highly oxidized sulfurs such as sulfoxides (Pereira et al. 2013a), sulphone

(Rowland et al. 2014), and sulfonate (Quesnel et al. 2015), but also low oxidation state sulfurs containing non-bonding electrons (Leshuk et al. 2016), such as sulfides in sulfur-containing carboxylic acid (Rowland et al. 2014) and sulfurs in thiophenic compounds (Bowman et al. 2014, Headley et al. 2015b, Stanford et al. 2007), which were reactive towards oxidation.

#### *Positive ESI mode*

Higher  $A_{\text{rel}}$  of total  $O_xS$  species (36.9%) was detected in the positive ESI mode than in negative ESI mode (16.6%), and the  $A_{\text{rel}}$  distribution of different  $O_xS$  species was quite different in these two ionization modes. Raw OSPW for example showed that the S and OS species increased from 4.1% and 0.6% in negative mode to 17.8% and 11.6% in positive mode, respectively;  $O_2S$  species was only a minor species with a  $A_{\text{rel}}$  of 4.2% in positive mode, a sharp decrease from 36.1% detected in negative mode. No  $O_6S$  was detected in negative ESI mode, while 3.3%  $A_{\text{rel}}$  of  $O_6S$  was observed in positive mode. The predominant species in positive mode was the  $O_3S$  species (32.7%), which was consistent with the results acquired with positive mode APPI (atmospheric pressure photoionization) FTICR-MS (Barrow et al. 2010) and GC APCI (atmospheric pressure chemical ionization) FTICR-MS (Barrow et al. 2014).  $A_{\text{rel}}$  of  $O_4S$  and  $O_5S$  detected in positive ESI mode was similar to that detected in negative mode. Other  $O_xS_2$  species such as  $OS_2$ ,  $O_2S_2$ ,  $O_4S_2$ , and  $O_6S_2$  were also detected in positive mode, but only at very low  $A_{\text{rel}}$ .

Ferrate(VI) oxidation decreased the  $A_{\text{rel}}$  of low oxygen containing species such as S (6.3%), OS (9.5%),  $O_2S$  (0.2%),  $O_3S$  (0.1%), and increased the  $A_{\text{rel}}$  of higher

oxygen containing species such as  $O_4S$  (46.3%),  $O_5S$  (4.4%),  $O_6S$  (14.3%). This trend was consistent with the results in negative ESI mode. Similar trend was achieved by molecular ozone reaction. Interestingly, after UV/ $H_2O_2$  oxidation and ozonation, both of which contained radical reaction, there was  $A_{rel}$  increase of low oxygen containing species (e.g., S,  $O_3S$  for UV/ $H_2O_2$  treated OSPW; S, OS,  $O_2S$  for ozonated OSPW), which might come from the breakdown of other sulfur-containing species and/or even particulate sulfur-containing organics.

#### *5.3.1.4 Transformation of nitrogen-containing species*

In negative mode,  $O_xN_y$  only accounted for 1.1% of the total intensity, and no  $O_xS_{y1}N_{y2}$  species were detected. However, in positive mode, the  $A_{rel}$  increased to 5.5% for  $O_xN_y$  species and 6.3% for  $O_xS_{y1}N_{y2}$  species in raw OSPW, again confirming the more complex organic fractions detected in positive mode than negative mode. As shown in Figure 5.6,  $O_xN_2$  species was the most abundant nitrogen-containing species, accounting for 45.0% of  $O_xN_y$  species detected in negative ESI mode and 46.0% of  $O_xN_y$  species detected in positive ESI mode in raw OSPW. The existence of  $O_xN_2$  species was reported by Headley et al. (2014) and was suggested to be proton-bound dimer of  $O_xN$  species. Based on the positive mode results, oxidation processes decreased the  $A_{rel}$  of low-oxygen containing species such as ON,  $O_2N$ , and  $O_3N$ , and increased that of  $O_4N$ ,  $O_5N$ , and  $O_xN_2$  species.

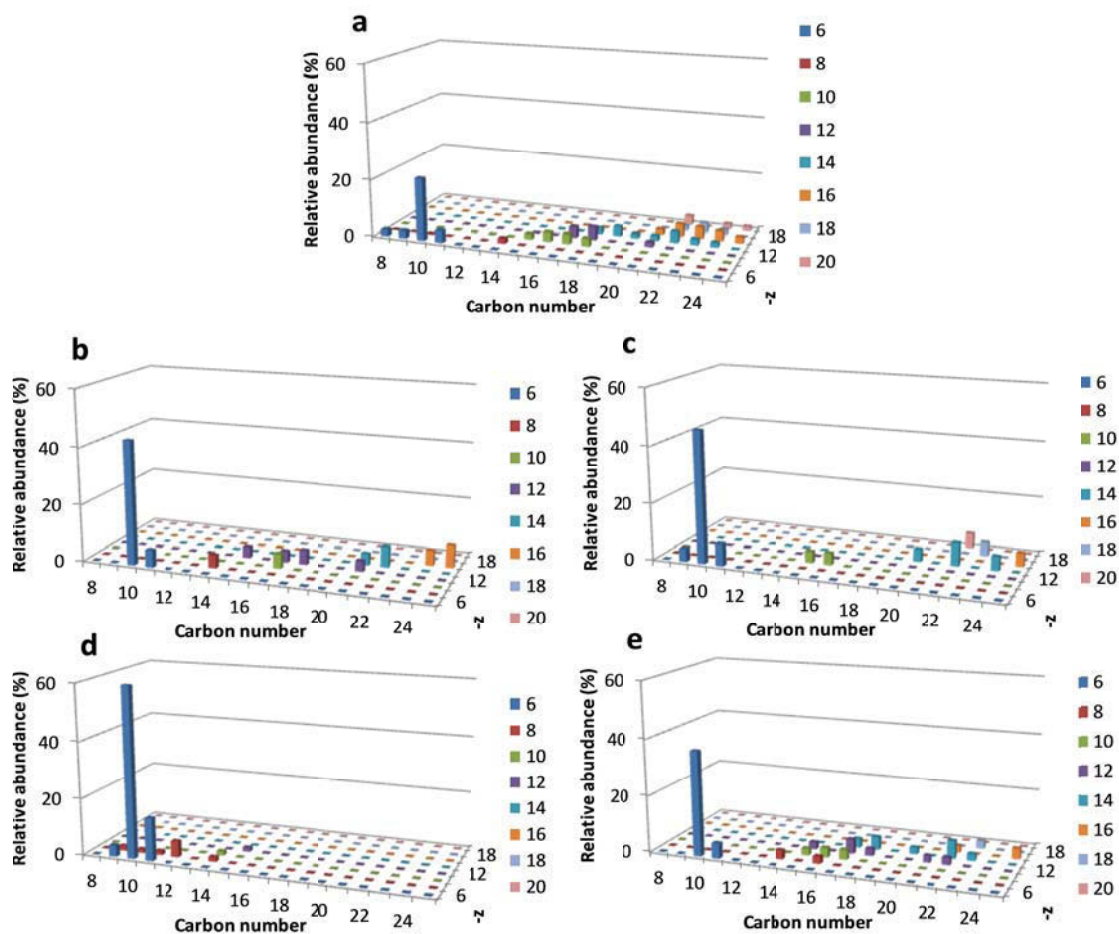


**Figure 5.6** Carbon number and -z number distribution of  $O_xN$  species in raw OSPW (a), ferrate(VI)-treated OSPW (b), UV/ $H_2O_2$ -treated OSPW (c), ozonated OSPW (d), and ozonated TBA-spiked OSPW (e) detected by FTICR-MS in positive ESI mode

In raw OSPW, the carbon number distribution of  $O_xN$  species showed three maximums at  $n=10$ , 18, and 22. After oxidation, the maximum at  $n=10$  prevailed, while the other ones decreased. The most significant change was achieved with ozonation, after which the maxima at  $n=18$  and 22 almost vanished. The hydrogen deficiency of the  $O_xN$  species in raw OSPW started and also peaked at 6, one double bond equivalent less than the peak at 8 detected for  $O_x$  and  $O_xS_y$ . This

might indicate two interesting properties of the  $O_xN$  species detected in the positive ESI mode. First, the  $-z$  peak at 6 ruled out the possibility that the predominant species had pyridinic nature (which required at least  $-z = 8$ ); however, Barrow et al. (2010)'s previous speculation of a pyridinic nature of the  $O_xN$  species might still be valid for species with higher  $-z$  number in the range of 10-20. Second, the fact that  $O_xN$  has one double bond equivalent less than  $O_x$  and  $O_xS$  species might indicate that these  $O_xN$  species was not carboxylic acids (lack of the  $C=O$  double bond), which was also consistent that these  $O_xN$  species was not detected in negative ESI mode. After oxidation, the  $A_{rel}$  of species with low hydrogen deficiency (e.g., 6) increased while those with high hydrogen deficiency (10-20) decreased, indicating the preferential removal of  $O_xN$  species with more rings or double bonds.

### **5.3.2 UPLC-TOF-MS results**

#### *5.3.2.1 Total ion chromatograms (TICs)*

TICs obtained for raw OSPW in negative and positive ESI modes showed different shapes (Figure 5.7a). In negative mode TIC two maxima at 4.6 min and 5.7 min respectively (excluding the internal standard peak at 6.8 min) were observed. If the intensity of each detected species was plotted against retention time as in Figure 5.7b, it was clear that most of the species were included in the first broad peak from 4.0 to 5.3 min, and the second peak from 5.3 to 8.0 min mainly contained high-intensity  $O_2$  species. The relatively longer retention time of  $O_2$  species was expected as they were less hydrophilic than the more oxygen-rich species. In positive mode, no second maximum was observed; the retention time

of all the O<sub>2</sub> species also concentrated between 4.3 min and 5.5 min, which again indicated that different O<sub>2</sub> species were detected at the two ionization modes. As alcohols, ketones or hydroxy-ketones detected in positive mode were less hydrophilic than carboxylic acids, the influence of oxygen number on the retention time in positive mode was less apparent than that exhibited in negative mode.

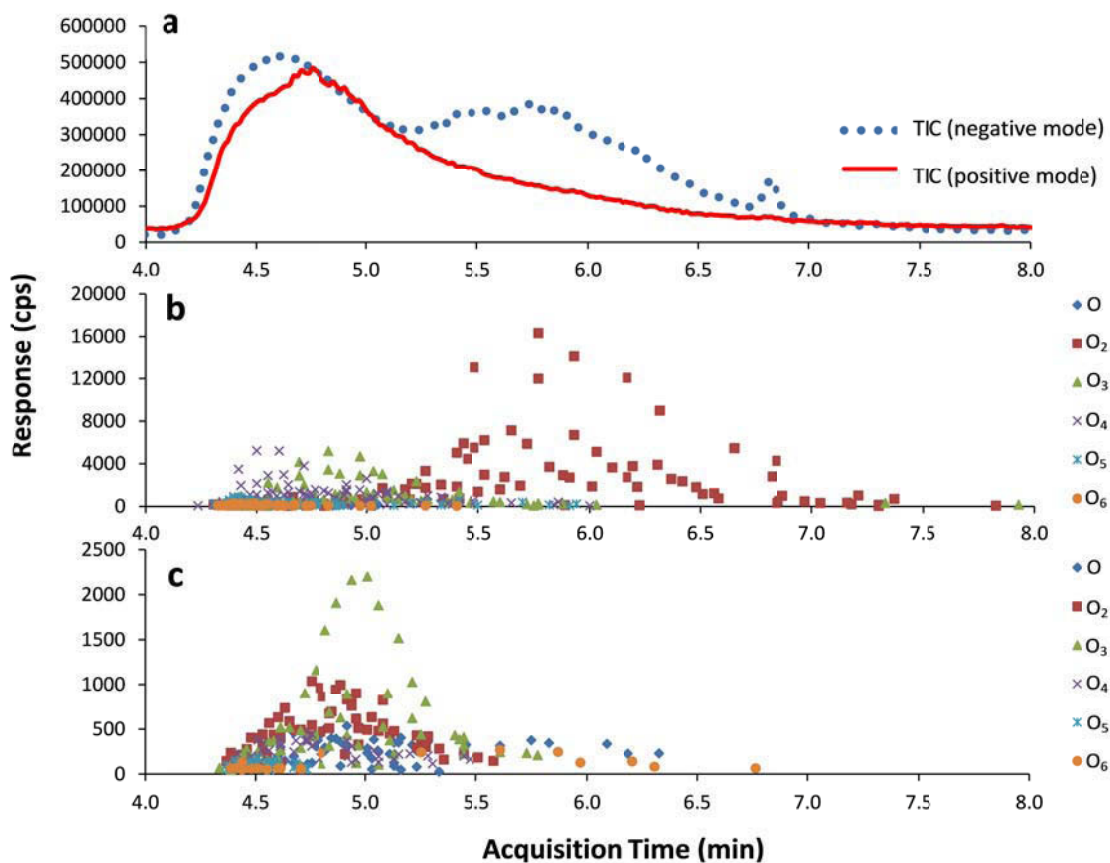


**Figure 5.7** TICs of the raw OSPW acquired in negative and positive ESI modes (a), and the retention time distribution of the species detected by UPLC-TOF-MS in negative ESI mode (b) and positive ESI mode (c)

### 5.3.2.2 Negative mode results

In raw OSPW, the total concentration of  $O_x$  species was 78.5 mg/L. It decreased to 63.4 mg/L after ferrate(VI) oxidation (equalling to 19.2% removal), 66.3 mg/L after UV/H<sub>2</sub>O<sub>2</sub> treatment (equalling to 15.5% removal), 55.7 mg/L after ozonation with TBA (equalling to 29.0% removal), and 21.0 mg/L after ozonation without TBA (equalling to 73.2% removal) (Figure 5.8a). Except ozonation without TBA, the oxidation process achieved low removal (i.e., <30%) of the total carboxylic acids. But as one of the main targets in OSPW remediation, classical NAs ( $O_2$  species) were removed in each oxidation process significantly: 40.7% removal with ferrate(VI), 32.7% with UV/H<sub>2</sub>O<sub>2</sub>, 54.0% with ozonation (with TBA), and 95.1% with ozonation (without TBA). For ferrate(VI) oxidation and molecular ozone reaction, the concentration of  $O_3$  species was decreased and that of  $O_4$  species was increased, and this pattern was reversed to be  $O_3$  species being increased and  $O_4$  species being decreased with UV/H<sub>2</sub>O<sub>2</sub> oxidation (Figure 5.8a). These patterns were consistent with the FTICR-MS results, and can be explained by the selectivity in ferrate(VI) oxidation and molecular ozone reaction and the lack of selectivity in  $\cdot OH$  oxidation. Species with more oxygens such as  $O_5$  and  $O_6$  species existed in relatively low concentration (4.4 mg/L and 1.5 mg/L respectively in raw OSPW), and their concentrations did not change very much (within 0.5 and 1.0 mg/L respectively) after oxidation as they were both removed and generated in the oxidation processes.

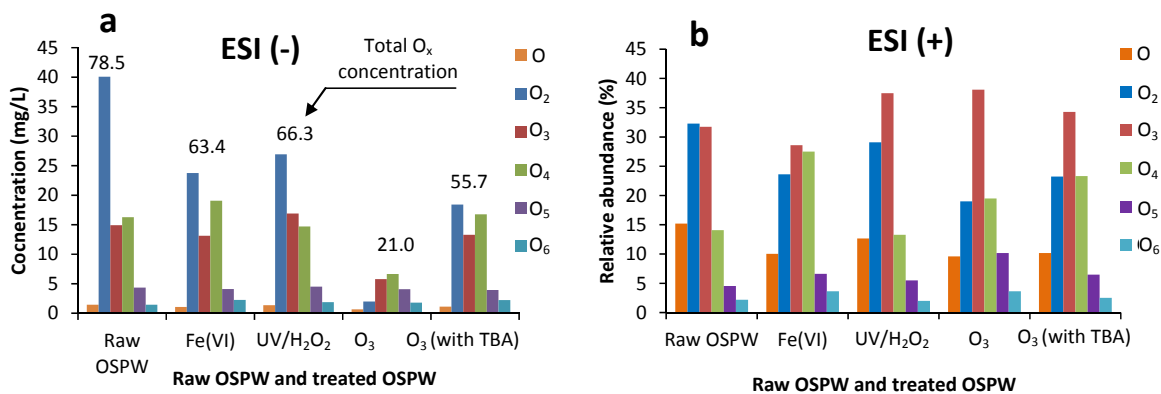


**Figure 5.8** Concentrations of O<sub>x</sub> species in raw OSPW and treated OSPW detected by UPLC-TOF-MS in negative ESI mode (a), and relative abundance of O<sub>x</sub> species detected in positive ESI mode (b)

The carbon number of O<sub>x</sub> species ranged from 7 to 22, with 15 corresponding to the most abundant species (Figure 5.9-5.10). This range was consistent with that detected with FTICR-MS, but one significant difference was that the A<sub>rel</sub> of species with carbon number ≤15 detected by FTICR-MS was higher than those detected by UPLC-TOF-MS, although the difference was always within ~15% (Figure 5.11). This difference can be explained by the high hydrophilicity of small molecules (e.g., molecules with carbon number ≤15) some of which were eluted in a very short time from UPLC column and were not detected by UPLC-TOF-MS. On the other hand, the FTICR-MS did not include a chromatographic separation process and thus had more small molecules detected.

The hydrogen deficiency ranged from 0 to 18, with 8 corresponding to the most abundant species (Figure 5.10 and Table A13). Similar to the carbon number distribution, the -z distribution detected by UPLC-TOF-MS featured lower A<sub>rel</sub> of species with low -z number than that detected by FTICR-MS (Figure 5.12),

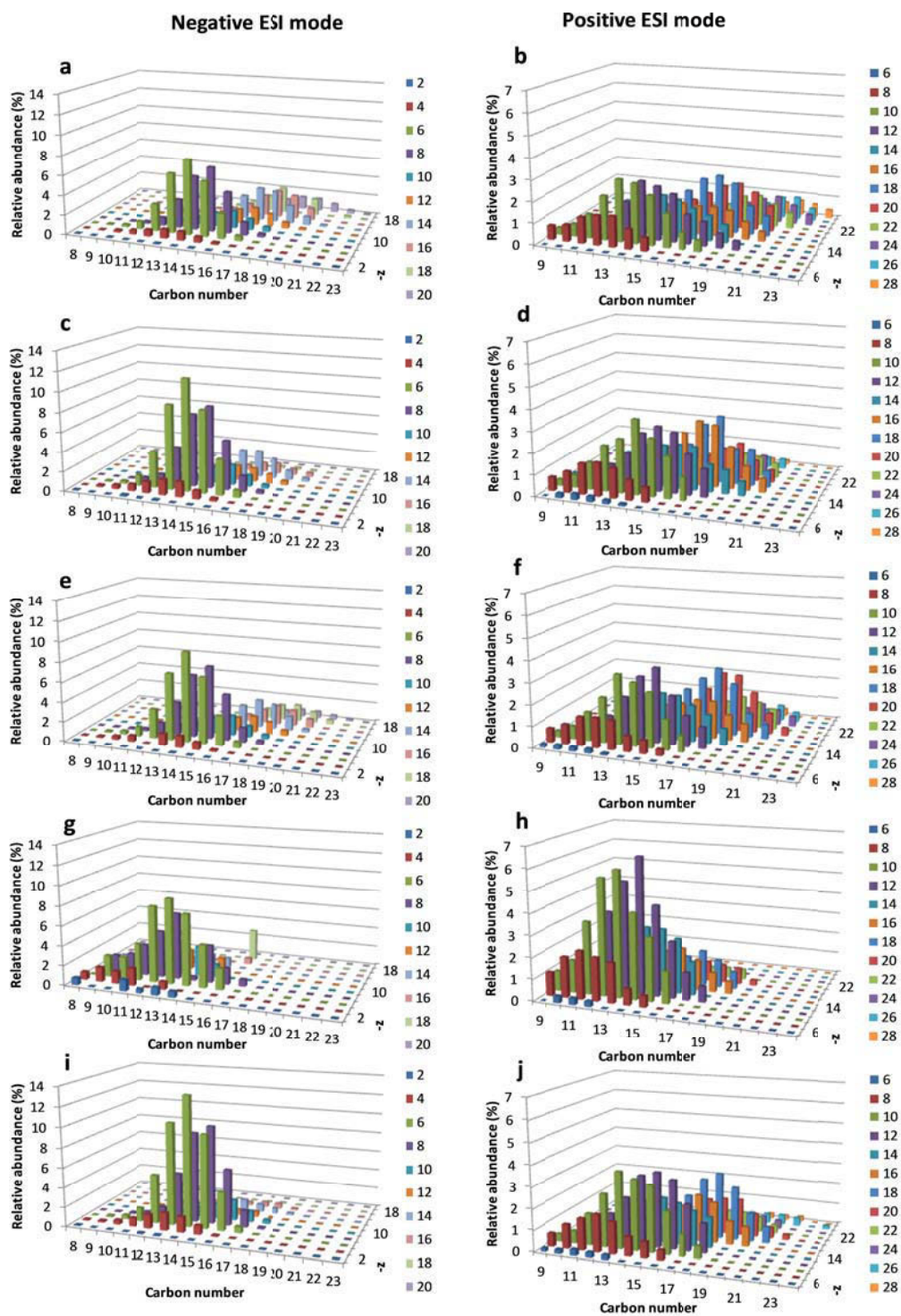


**Figure 5.9** Carbon number and -z number distribution of O<sub>2</sub> species in raw OSPW (a,b), ferrate(VI)-treated OSPW (c,d), UV/H<sub>2</sub>O<sub>2</sub>-treated OSPW (e,f), ozonated OSPW (g,h), and ozonated TBA-spiked OSPW (i,j) detected by UPLC TOF-MS in negative and positive ESI mode

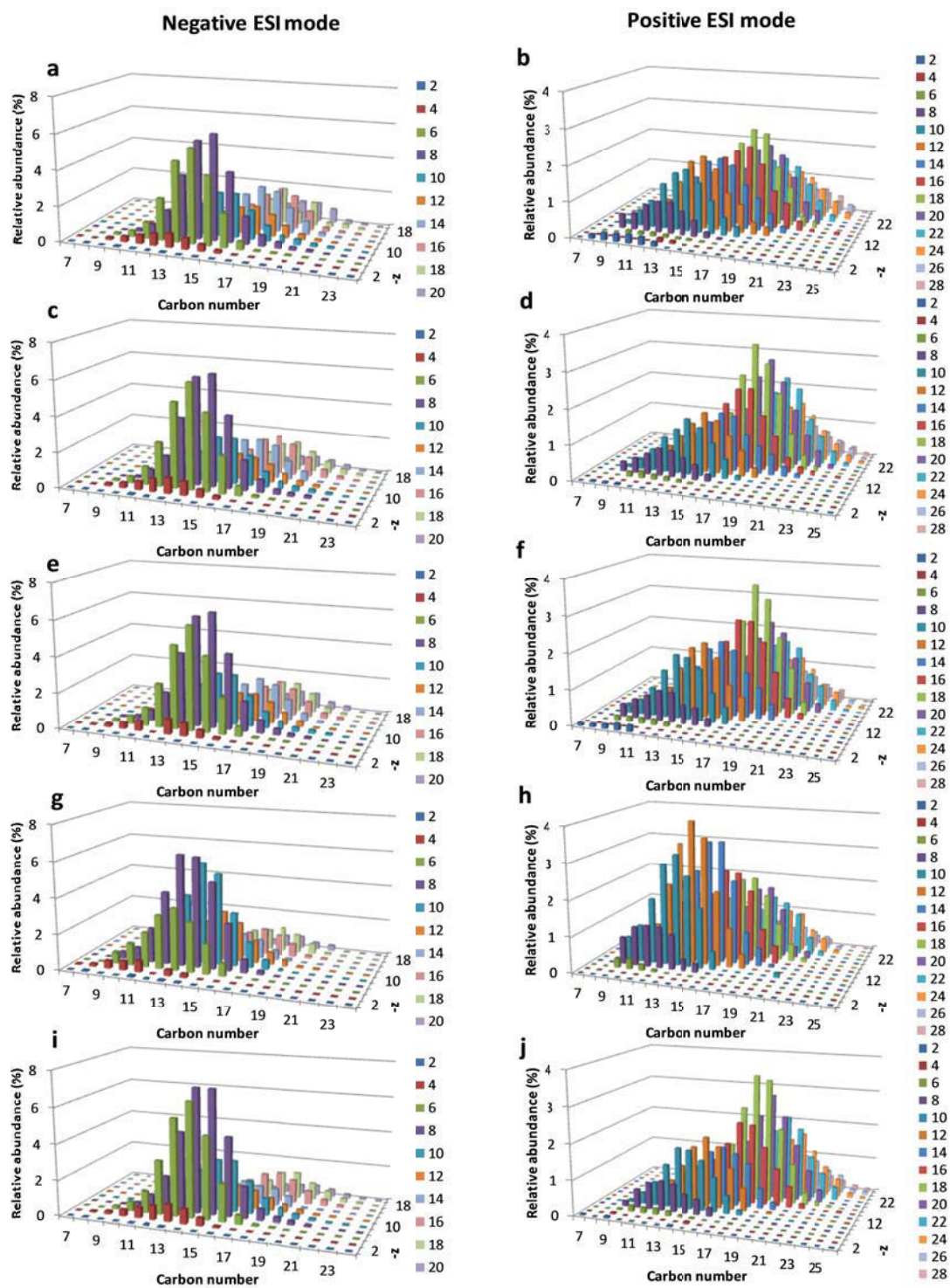


**Figure 5.10** Carbon number and -z number distribution of total  $O_x$  species in raw OSPW (a,b), ferrate(VI)-treated OSPW (c,d), UV/ $H_2O_2$ -treated OSPW (e,f), ozonated OSPW (g,h), and ozonated TBA-spiked OSPW (i,j) detected by UPLC-TOF-MS in negative and positive ESI mode

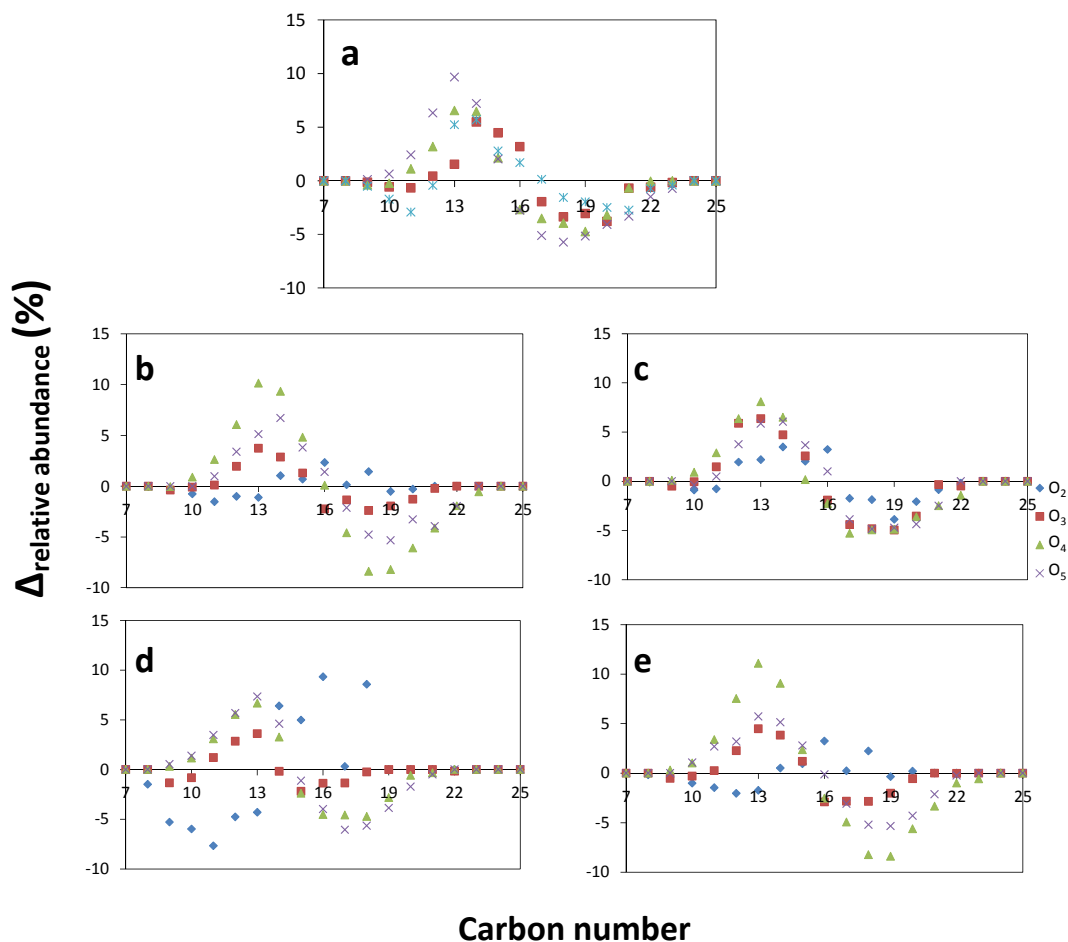


**Figure 5.11** The difference of relative abundance of  $O_x$  species with different carbon number detected with negative mode FTICR-MS and UPLC-TOF-MS in raw OSPW (a), OSPW treated by ferrate(VI) (b), UV/ $H_2O_2$  (c), ozonation without TBA (d), and ozonation with TBA (e) ( $\Delta_{\text{Relative abundance}} = \text{Relative abundance detected with FTICR-MS} - \text{Relative abundance detected with UPLC-TOF-MS}$ , and the relative abundance is out of the total  $O_x$  species. Only results based on major species  $O_2$ ,  $O_3$ ,  $O_4$ , and  $O_5$  were plotted)

which can also be explained by the fast eluting of species with low hydrogen deficiency, as confirmed by Barrow et al. (2014) that retention times decreased with decreasing double bond equivalent. Two peaks were observed in the

distribution curve of the hydrogen deficiency in raw OSPW: one at  $-z=6$  corresponding to alicyclic rings or double bonds (as aromatic rings require  $-z\geq 8$ ); the second peak was at  $-z=12$  (different from 14 in the FTICR-MS results), which might be related to aromatic rings (Figure 5.10 and Table A13).

Despite all these differences, negative ESI UPLC-TOF-MS results were consistent with the negative ESI FTICR-MS results in two aspects: (1) the  $A_{rel}$  of specific  $O_x$  species detected with these two methods was linearly correlated with an  $R^2$  of 0.84 (Figure 5.13). Similar good correlation was reported by Sun et al. (2014); (2) both methods revealed that only ozonation without TBA notably shifted the carbon number distribution to the low end and shifted the  $-z$  number distribution to the high end, all other processes transformed the distribution curve to a less extent (Figures 5.3&5.4 and Figures 5.9&5.10).

### 5.3.2.3 Positive mode results

The positive mode results from UPLC-TOF-MS analyses were different from those detected from FTICR-MS analyses significantly in the following aspects. (1) Compared with FTICR-MS, UPLC-TOF-MS detected a much higher  $A_{rel}$  of O and  $O_2$  species and lower abundance of  $O_4$  and  $O_5$  species. For example, in raw OSPW, the  $A_{rel}$  of O,  $O_2$ ,  $O_3$ ,  $O_4$ ,  $O_5$ , and  $O_6$  species detected by UPLC-TOF-MS in positive ionization mode was 15.2%, 32.3%, 31.7%, 14.1%, 4.5%, and 2.2%, respectively (Figure 5.10b), versus 0.4%, 6.9%, 22.5%, 48.1%, and 12.3% detected by FTICR-MS (Figure 5.4b). (2) Carbon number distribution obtained by UPLC-TOF-MS in positive mode featured higher number of carbons than FTICR-

MS, with the peak at 18 instead of 14 detected by FTICR-MS. (3)  $-z$  number distribution ranged from 0 to  $\sim 28$ , with the peak at 18, quite different from the

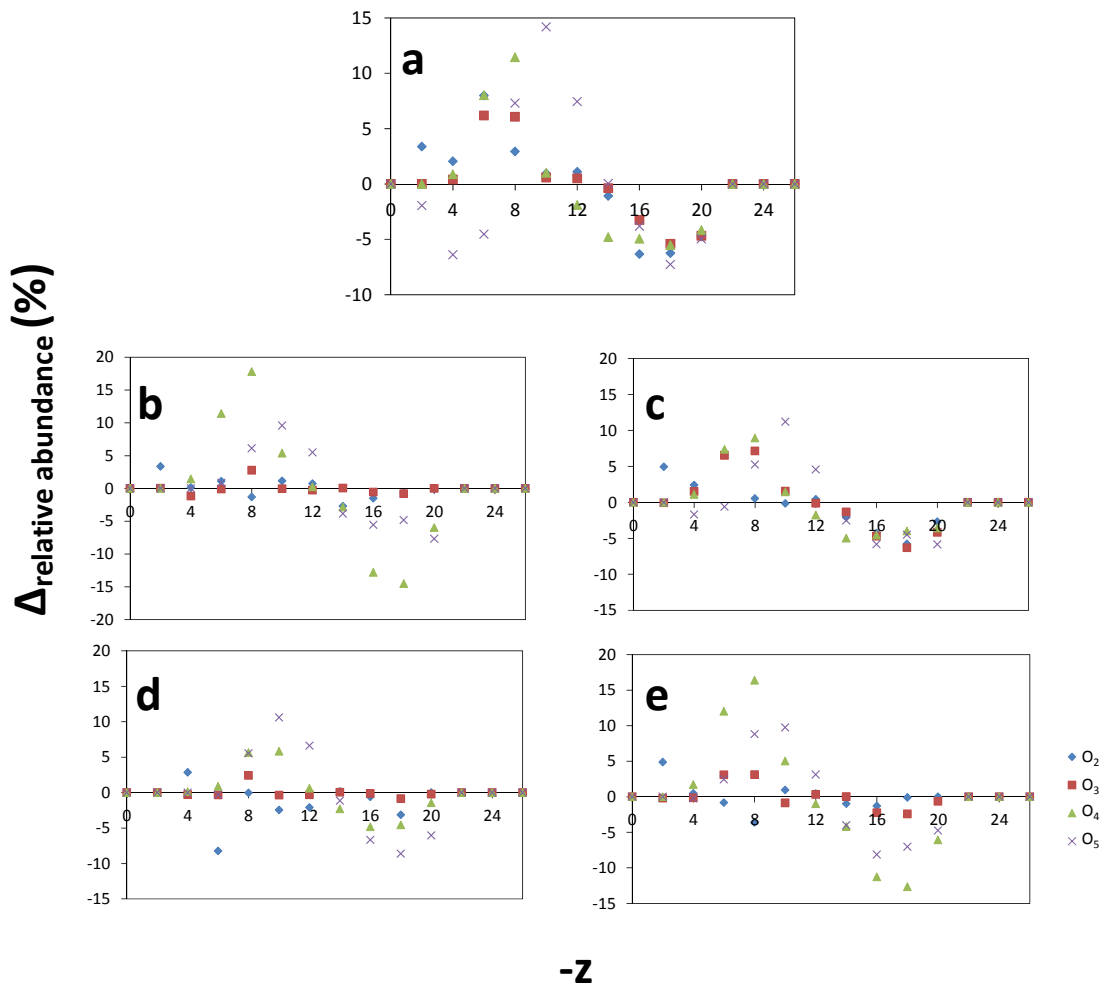


**Figure 5.12** The difference of relative abundance of O<sub>x</sub> species with different  $-z$  number detected with negative mode FTICR-MS and UPLC-TOF-MS in raw OSPW (a), OSPW treated by ferrate(VI) (b), UV/H<sub>2</sub>O<sub>2</sub> (c), ozonation without TBA (d), and ozonation with TBA (e) ( $\Delta$ Relative abundance = Relative abundance detected with FTICR-MS – Relative abundance detected with UPLC-TOF-MS, and the relative abundance is out of the total O<sub>x</sub> species. Only results based on major species O<sub>2</sub>, O<sub>3</sub>, O<sub>4</sub>, and O<sub>5</sub> were plotted)

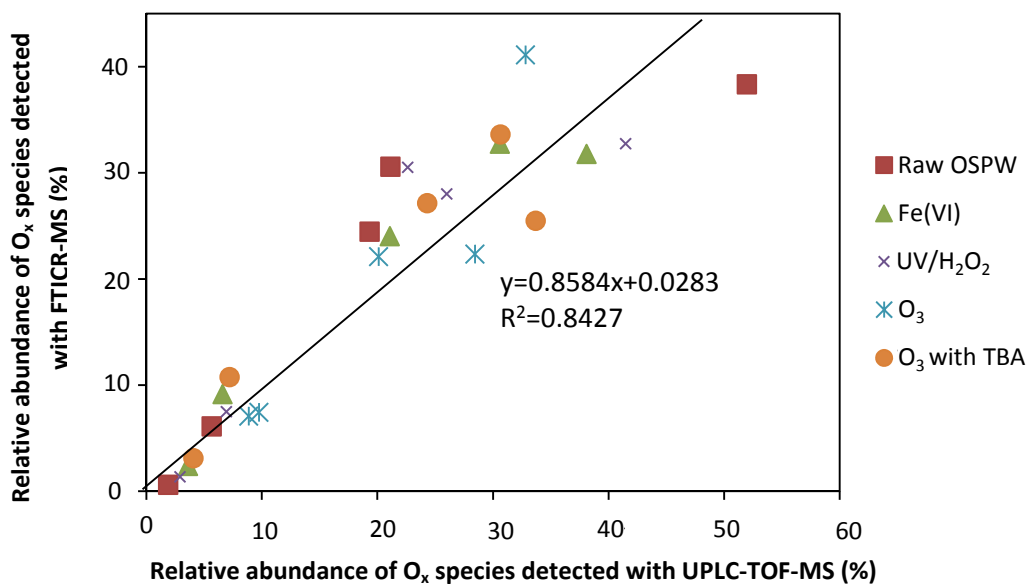


**Figure 5.13** Correlation between relative abundance of O<sub>x</sub> species detected by UPLC-TOF-MS and FTICR-MS (for each sample, the relative abundance of O<sub>2</sub>, O<sub>3</sub>, O<sub>4</sub>, O<sub>5</sub>, and O<sub>6</sub> out of total O<sub>x</sub> species was used)

peak at 8 detected in positive mode by FTICR-MS. These discrepancies between UPLC-TOF-MS results and FTICR-MS results in positive modes could be caused by factors such as solvent type (i.e., water in UPLC-TOF-MS and DCM in FTICR-MS) and ionization mechanism (i.e., proton addition in UPLC-TOF-MS and sodium addition in FTICR-MS). The sulfur/nitrogen-containing species were not identified using UPLC-TOF-MS due to its insufficient mass resolution. Specifically, typical resolution of >120000 is required for identification of O<sub>x</sub>S from O<sub>x</sub> species (Pereira et al. 2013b) and UPLC-TOF-MS resolution is 40000 in this work. Therefore, interference from sulfur/nitrogen-containing species on O<sub>x</sub> species detection by UPLC-TOF-MS is likely to occur, and it is supposed to be more severe in positive ESI mode than in negative ESI mode, as the A<sub>rel</sub> of sulfur/nitrogen-containing species was much higher than in negative mode (see

FTICR-MS results). In this sense, the positive results from UPLC-TOF-MS should be interpreted with extreme caution.

### **5.3.3 Environmental significance**

OSPW contains various organic fractions. Understanding its composition is the precondition to explore the mechanisms behind its toxicity and to evaluate the performance of the water treatment technologies. For example, the assumption that NA is the only species contributing to water toxicity and the main target of water treatment has been challenged by studies on sulfur-containing species, nitrogen-containing species, and other organic species in OSPW. This paper is the first study employing FTICR-MS to characterize OSPW treated by ferrate(VI), UV/H<sub>2</sub>O<sub>2</sub>, and molecular ozone (ozonation with TBA), which incorporated sulfur and nitrogen-containing species as an additional dimension besides O<sub>x</sub> species to evaluate the oxidation performance. Considering that the transformation of the O<sub>x</sub>, O<sub>x</sub>S<sub>y</sub>, and O<sub>x</sub>N<sub>y</sub> species will impact the OSPW toxicity, further research is warranted to explore the molecular structures of these organic species and their toxicity effects.

## 5.4 References

- Afzal, A., Drzewicz, P., Martin, J.W. and Gamal El-Din, M. (2012) Decomposition of cyclohexanoic acid by the UV/H<sub>2</sub>O<sub>2</sub> process under various conditions. *Science of The Total Environment* 426, 387-392.
- Alharbi, H.A., Saunders, D.M.V., Al-Mousa, A., Alcorn, J., Pereira, A.S., Martin, J.W., Giesy, J.P. and Wiseman, S.B. (2016) Inhibition of ABC transport proteins by oil sands process affected water. *Aquatic Toxicology* 170, 81-88.
- Allen, E.W. (2008) Process water treatment in Canada's oil sands industry: I. Target pollutants and treatment objectives. *Journal of Environmental Engineering & Science* 7(2), 123-138.
- Anderson, J.C., Wiseman, S.B., Wang, N., Moustafa, A., Perez-Estrada, L., Gamal El-Din, M., Martin, J.W., Liber, K. and Giesy, J.P. (2012) Effectiveness of ozonation treatment in eliminating toxicity of oil sands process-affected water to *Chironomus dilutus*. *Environmental Science & Technology* 46(1), 486-493.
- Barrow, M.P., Peru, K.M. and Headley, J.V. (2014) An added dimension: GC atmospheric pressure chemical Ionization FTICR MS and the Athabasca oil sands. *Analytical Chemistry* 86(16), 8281-8288.
- Barrow, M.P., Witt, M., Headley, J.V. and Peru, K.M. (2010) Athabasca oil sands process water: characterization by atmospheric pressure photoionization and electrospray ionization Fourier transform ion cyclotron resonance mass spectrometry. *Analytical Chemistry* 82(9), 3727-3735.

- Bowman, D.T., Slater, G.F., Warren, L.A. and McCarry, B.E. (2014) Identification of individual thiophene-, indane-, tetralin-, cyclohexane-, and adamantane-type carboxylic acids in composite tailings pore water from Alberta oil sands. *Rapid Communications in Mass Spectrometry* 28(19), 2075-2083.
- Chelme-Ayala, P., Gamal El-Din, M., and Smith, D.W. (2010) Degradation of bromoxynil and trifluralin in natural water by direct photolysis and UV plus H<sub>2</sub>O<sub>2</sub> advanced oxidation process. *Water Research* 44(7), 2221-2228.
- Drzewicz, P., Afzal, A., Gamal El-Din, M., and Martin, J.W. (2010) Degradation of a model naphthenic acid, cyclohexanoic acid, by vacuum UV (172 nm) and UV (254 nm)/H<sub>2</sub>O<sub>2</sub>. *The Journal of Physical Chemistry A* 114(45), 12067-12074.
- Frank, R.A., Fischer, K., Kavanagh, R., Burnison, B.K., Arsenault, G., Headley, J.V., Peru, K.M., Van, D.K.G. and Solomon, K.R. (2009) Effect of carboxylic acid content on the acute toxicity of oil sands naphthenic acids. *Environmental Science & Technology* 43(2), 266-271.
- Frank, R.A., Kavanagh, R., Kent Burnison, B., Arsenault, G., Headley, J.V., Peru, K.M., Van Der Kraak, G. and Solomon, K.R. (2008) Toxicity assessment of collected fractions from an extracted naphthenic acid mixture. *Chemosphere* 72(9), 1309-1314.
- Gamal El-Din, M., Fu, H., Wang, N., Chelme-Ayala, P., Pérez-Estrada, L., Drzewicz, P., Martin, J.W., Zubot, W. and Smith, D.W. (2011) Naphthenic acids speciation and removal during petroleum-coke

adsorption and ozonation of oil sands process-affected water. *Science of The Total Environment* 409(23), 5119-5125.

Garcia-Garcia, E., Ge, J.Q., Oladiran, A., Montgomery, B., Gamal El-Din, M., Perez-Estrada, L.C., Stafford, J.L., Martin, J.W. and Belosevic, M. (2011) Ozone treatment ameliorates oil sands process water toxicity to the mammalian immune system. *Water Research* 45(18), 5849-5857.

He, Y., Patterson, S., Wang, N., Hecker, M., Martin, J.W., Gamal El-Din, M., Giesy, J.P. and Wiseman, S.B. (2012) Toxicity of untreated and ozone-treated oil sands process-affected water (OSPW) to early life stages of the fathead minnow (*Pimephales promelas*). *Water Research* 46(19), 6359-6368.

He, Y., Wiseman, S.B., Zhang, X., Hecker, M., Jones, P.D., Gamal El-Din, M., Martin, J.W. and Giesy, J.P. (2010) Ozonation attenuates the steroidogenic disruptive effects of sediment free oil sands process water in the H295R cell line. *Chemosphere* 80(5), 578-584.

Headley, J.V., Barrow, M.P., Peru, K.M., Fahlman, B., Frank, R.A., Bickerton, G., McMaster, M.E., Parrott, J. and Hewitt, L.M. (2011) Preliminary fingerprinting of Athabasca oil sands polar organics in environmental samples using electrospray ionization Fourier transform ion cyclotron resonance mass spectrometry. *Rapid Communications in Mass Spectrometry* 25(13), 1899-1909.

Headley, J.V., Kumar, P., Dalai, A., Peru, K.M., Bailey, J., McMartin, D.W., Rowland, S.M., Rodgers, R.P. and Marshall, A.G. (2015a) Fourier

transform ion cyclotron resonance mass spectrometry characterization of treated Athabasca oil sands processed waters. *Energy & Fuels* 29(5), 2768-2773.

Headley, J.V., Peru, K.M., Armstrong, S.A., Han, X., Martin, J.W., Mapolelo, M.M., Smith, D.F., Rogers, R.P. and Marshall, A.G. (2009) Aquatic plant-derived changes in oil sands naphthenic acid signatures determined by low-, high- and ultrahigh-resolution mass spectrometry. *Rapid Communications in Mass Spectrometry* 23(4), 515-522.

Headley, J.V., Peru, K.M. and Barrow, M.P. (2015b) Advances in mass spectrometric characterization of naphthenic acids fraction compounds in oil sands environmental samples and crude oil—a review. *Mass Spectrometry Reviews, In progress.*

Headley, J.V., Peru, K.M., Mohamed, M.H., Wilson, L., McMartin, D.W., Mapolelo, M.M., Lobodin, V.V., Rodgers, R.P. and Marshall, A.G. (2014) Atmospheric pressure photoionization Fourier transform ion cyclotron resonance mass spectrometry characterization of tunable carbohydrate-based materials for sorption of oil sands naphthenic acids. *Energy & Fuels* 28(3), 1611-1616.

Leshuk, T., Wong, T., Linley, S., Peru, K.M., Headley, J.V. and Gu, F. (2016) Solar photocatalytic degradation of naphthenic acids in oil sands process-affected water. *Chemosphere* 144, 1854-1861.

Morandi, G.D., Wiseman, S.B., Pereira, A., Mankidy, R., Gault, I.G.M., Martin, J.W. and Giesy, J.P. (2015) Effects-directed analysis of dissolved organic

- compounds in oil sands process-affected water. *Environmental Science & Technology* 49(20), 12395-12404.
- Pereira, A.S., Bhattacharjee, S. and Martin, J.W. (2013a) Characterization of oil sands process-affected waters by liquid chromatography orbitrap mass spectrometry. *Environmental Science & Technology* 47(10), 5504-5513.
- Pereira, A.S., Islam, M.s., Gamal El-Din, M. and Martin, J.W. (2013b) Ozonation degrades all detectable organic compound classes in oil sands process-affected water; an application of high-performance liquid chromatography/orbitrap mass spectrometry. *Rapid Communications in Mass Spectrometry* 27(21), 2317-2326.
- Quesnel, D.M., Oldenburg, T.B.P., Larter, S.R., Gieg, L.M. and Chua, G. (2015) Biostimulation of oil sands process-affected water with phosphate yields removal of sulfur-containing organics and detoxification. *Environmental Science & Technology* 49(21), 13012-13020.
- Rowland, S.J., Pereira, A.S., Martin, J.W., Scarlett, A.G., West, C.E., Lengger, S.K., Wilde, M.J., Pureveen, J., Tegelaar, E.W., Frank, R.A. and Hewitt, L.M. (2014) Mass spectral characterisation of a polar, esterified fraction of an organic extract of an oil sands process water. *Rapid Communications in Mass Spectrometry* 28(21), 2352-2362.
- Rowland, S.J., West, C.E., Jones, D., Scarlett, A.G., Frank, R.A. and Hewitt, L.M. (2011) Steroidal aromatic 'naphthenic acids' in oil sands process-affected water: Structural comparisons with environmental estrogens. *Environmental Science & Technology* 45(22), 9806-9815.

- Scarlett, A.G., Reinardy, H.C., Henry, T.B., West, C.E., Frank, R.A., Hewitt, L.M. and Rowland, S.J. (2013) Acute toxicity of aromatic and non-aromatic fractions of naphthenic acids extracted from oil sands process-affected water to larval zebrafish. *Chemosphere* 93(2), 415-420.
- Shu, Z., Bolton, J.R., Belosevic, M. and Gamal El-Din, M. (2013) Photodegradation of emerging micropollutants using the medium-pressure UV/H<sub>2</sub>O<sub>2</sub> Advanced Oxidation Process. *Water Research* 47(8), 2881-2889.
- Shu, Z., Li, C., Belosevic, M., Bolton, J.R. and Gamal El-Din, M. (2014) Application of a solar UV/chlorine advanced oxidation process to oil sands process-affected water remediation. *Environmental Science & Technology* 48(16), 9692-9701.
- Singh, A., Havixbeck, J.J., Smith, M.K., Shu, Z., Tierney, K.B., Barreda, D.R., Gamal El-Din, M. and Belosevic, M. (2015) UV and hydrogen peroxide treatment restores changes in innate immunity caused by exposure of fish to reuse water. *Water Research* 71, 257-273.
- Stanford, L.A., Kim, S., Klein, G.C., Smith, D.F., Rodgers, R.P. and Marshall, A.G. (2007) Identification of water-soluble heavy crude oil organic-acids, bases, and neutrals by electrospray ionization and field desorption ionization Fourier transform ion cyclotron resonance mass spectrometry. *Environmental Science & Technology* 41(8), 2696-2702.
- Sun, N., Chelme-Ayala, P., Klammerth, N., McPhedran, K.N., Islam, M.S., Perez-Estrada, L., Drzewicz, P., Blunt, B.J., Reichert, M., Hagen, M., Tierney, K.B., Belosevic, M. and Gamal El-Din, M. (2014) Advanced analytical

mass spectrometric techniques and bioassays to characterize untreated and ozonated oil sands process-affected water. *Environmental Science & Technology* 48(19), 11090-11099.

Thompson, G.W., Ockerman, L.T. and Schreyer, J.M. (1951) Preparation and purification of potassium ferrate(VI) *Journal of the American Chemical Society* 73(3), 1379-1381.

Wang, C., Alpatova, A., McPhedran, K.N. and Gamal El-Din, M. (2015) Coagulation/flocculation process with polyaluminum chloride for the remediation of oil sands process-affected water: Performance and mechanism study. *Journal of Environmental Management* 160, 254-262.

Wang, N., Chelme-Ayala, P., Perez-Estrada, L., Garcia-Garcia, E., Pun, J., Martin, J.W., Belosevic, M. and Gamal El-Din, M. (2013) Impact of ozonation on naphthenic acids speciation and toxicity of oil sands process-affected water to *Vibrio fischeri* and mammalian immune system. *Environmental Science & Technology* 47(12), 6518-6526.

Zhang, K., Pereira, A.S. and Martin, J.W. (2015a) Estimates of octanol-water partitioning for thousands of dissolved organic species in oil sands process-affected water. *Environmental Science & Technology* 49(14), 8907-8913.

Zhang, Y., McPhedran, K.N. and Gamal El-Din, M. (2015b) Pseudomonads biodegradation of aromatic compounds in oil sands process-affected water. *Science of The Total Environment* 521-522, 59-67.

## 6 CONCLUSIONS AND RECOMMENDATIONS

### 6.1 Thesis overview

OSPW generated during bitumen production from oil sands is a complex mixture of suspended solids, dissolved organic matter, metals, and anions. The potential environmental risks estimated with model plant, bacteria, algae, fish, and mammals warrant the current non-release measure adopted by the oil sand companies. Natural remediation processes such as biodegradation by indigenous microorganisms and solar UV-driven oxidation are too slow for OSPW remediation. Therefore, extensive research projects have been done to actively target the pollutants in OSPW, especially the recalcitrant organic fractions, using physical, chemical, and biological processes.

As one of these research projects, the present study focused on coagulation and flocculation (CF) with PACl and oxidation with potassium ferrate(VI), both of which have unique merits but have not been investigated in OSPW remediation. The  $Al_{13}$  species in PACl is a polycation with stable Keggin structure, high positive charge, and potential surface adsorption sites. PACl with high  $Al_{13}$  abundance was, therefore, synthesized in the laboratory. The CF performance of  $Al_{13}$ -rich synthetic PACl was compared with that of commercial PACl in OSPW remediation.

Potassium ferrate(VI) is a strong oxidant at acidic pH; although it becomes a mild oxidant at basic pH. The selective ferrate(VI) oxidation can be used as a tool to “chemically fractionate” the organics in OSPW (i.e., at low applied ferrate(VI)

doses, it preferentially targets organics containing ERMs such as fused ring aromatics) and can, to a certain degree, untangle the toxicity effects of the complex organic mixture. In addition, the ferric product generated from ferrate(VI) oxidation is a commonly used coagulant in water and wastewater treatment and promotes a CF process after oxidation. The ferric product will deposit in the sediment and leave little residual iron in the water. In our study, ferrate(VI) oxidation was investigated with both OSPW and model compounds to evaluate its performance and explore the reaction mechanisms. We also extended our ferrate(VI) study to a comparison experiment on different oxidation processes including ferrate(VI) oxidation, UV/H<sub>2</sub>O<sub>2</sub> advanced oxidation, and ozonation with and without radical scavenger. The comparison experiments not only targeted NAs and aromatics, but also sulfur and nitrogen containing species by employing FTICR-MS.

## **6.2 Conclusions**

In general, the following conclusions were drawn from this research: both synthetic and commercial PACls were efficient at reducing turbidity and metal cations with low pK<sub>a</sub> values, and synthetic PACl achieved higher removal of dissolved organics than commercial PACl at low dose range; ferrate(VI) and molecular ozone exhibited high selectivity, and UV/H<sub>2</sub>O<sub>2</sub> did not show such selectivity; ozonation was the most efficient in organics removal and toxicity reduction. Both molecular ozone reaction and hydroxyl radical reaction contributed to the removal of NAs and aromatics; and UPLC-TOF-MS results were consistent with FTICR-MS results in negative ESI mode, but showed high

discrepancy in positive ESI mode. Specifically, the following conclusions were reached.

### 6.2.1 New findings on OSPW composition

- Based on  $^1\text{H}$  NMR results, the molar concentration of aromatics was about 8-25% of that of total organic acids (not necessarily NAs) in OSPW.
- Very few aliphatic carbon-carbon double bonds existed in the OSPW organic fraction as indicated by the lack of peaks in its  $^1\text{H}$  NMR spectrum from 4.5 to 5.5 ppm.
- Unbranched long  $\text{CH}_2$  carbon chains or alicyclic rings did not predominate in OSPW. Instead, carbon chains, rings or fused rings with short branches ended with  $\text{CH}_3$  might be the most abundant organics. This was supported by the highest peak of terminal  $\text{CH}_3$  at 0.9 ppm and relative low peak of  $\text{CH}_2$  at 1.2 ppm in the  $^1\text{H}$  NMR spectrum of OSPW organic fraction.
- The aromatics with unfused aromatic rings had a much higher abundance than aromatics with two or three fused aromatic rings, supported by the  $^1\text{H}$  NMR spectrum and SFS.
- Detected by FTICR-MS,  $\text{O}_x$  species predominated in raw OSPW, accounting for 82.3% of total intensity in negative ESI mode and 51.3% of the total intensity in positive mode. Among the  $\text{O}_x$  species detected in negative ESI mode,  $\text{O}_2$  (38.2% out of  $\text{O}_x$ ),  $\text{O}_4$  (30.5%), and  $\text{O}_3$  (24.4%) were the most abundant species. On the other hand, in positive ESI mode, the most abundant  $\text{O}_x$  species were  $\text{O}_4$  (48.1%),  $\text{O}_3$  (22.5%), and  $\text{O}_5$  (12.3%), notably different from the abundance order detected in negative

mode. This difference of distribution profile also indicated that distinct species were detected in negative and positive ESI modes.

- Sulfur-containing species accounted for 16.6% of the total intensity in negative ESI mode, much less than 36.9% in positive mode. Among the  $O_xS$  species detected in negative ESI mode,  $O_2S$  (36.1% out of  $O_xS$ ),  $O_3S$  (35.6%), and  $O_4S$  (20.2%) were the dominant species, while in positive mode  $O_3S$  (32.7%),  $O_4S$  (18.6%),  $S$  (17.8%), and  $OS$  (11.6%) species were more abundant than other species.  $O_xN_y$  species were the least abundant species in raw OSPW, accounting for 1.1% and 5.5% of the total intensity in negative and positive ESI modes, respectively.

### **6.2.2 Coagulation and flocculation with PACl**

- According to  $^{27}Al$  NMR analysis, 83.6% and 30.5% of total aluminum atoms existed as  $Al_{13}$  in the synthetic and commercial PACl, respectively. Both coagulants were effective in removing suspended solids from OSPW, achieving more than 96% turbidity removal at the applied coagulants dose range of 0.5-3.0 mM Al. Based on zeta potential analysis, turbidity removal performance, and floc analysis, the dominant particle removal mechanism was sweep flocculation.
- Dissolved organic matter removal was <10% in terms of DOC and  $UV_{254}$  removals for both synthetic and commercial PACl. The DOC and  $UV_{254}$  removals for synthetic PACl were slightly higher at low doses (< 2.0 mM Al) than commercial PACl, which was attributed to the higher charge neutralization capacity of synthetic PACl reducing the electrostatic

repulsion and facilitating adsorption. NAs were not removed due to their negative charge and hydrophilic characteristics in the alkaline environment of OSPW.

- The removal efficiencies of metals varied among different metals depending on the  $pK_a$  values of their cations. Metal cations with  $pK_a$  values (Fe, Al, Ga, and Ti) below OSPW pH of 6.9-8.1 (dose dependent) were removed by more than 90%, while metal cations with higher  $pK_a$  values (K, Na, Ca, Mg and Ni) had removals of less than 40%. Surface complexation might be one of the main mechanisms for metal removal.
- At the highest applied coagulant dose of 3.0 mM Al, the synthetic PACl reduced *Vibrio fischeri* toxicity to  $43.3 \pm 3.0\%$  from  $49.5 \pm 0.4\%$  in raw OSPW. In contrast, no reduction of toxicity was found for OSPW treated with the commercial PACl.

### 6.2.3 Ferrate(VI) oxidation

- NAs with high carbon number and high hydrogen deficiency were preferentially removed, while fluorescing aromatics with two and three fused rings were preferentially removed. At 200 and 400 mg/L Fe(VI), 64.0% and 78.4% NAs were oxidized as quantified by UPLC-TOF-MS. At a dose of 200 mg/L Fe(VI), 44.4% hydrogens in aromatic rings and 27.9% hydrogens in carboxyl functional groups were removed, respectively, as quantified by  $^1\text{H}$  NMR.
- Ferrate(VI) oxidation reduced the acute toxicity on *Vibrio fischeri* from  $42.8 \pm 0.6\%$  inhibition effect to  $19.6 \pm 1.6\%$  and  $17.6 \pm 0.1\%$  inhibition effect

at the dose of 200 and 400 mg/L Fe(VI), respectively. The toxicity effect from aromatics might be significant as a linear relationship was empirically established between integrated SFS peak areas and inhibition effects.

- Oxidation, rather than coagulation, contributed to the organic matter removal. One of the reaction mechanisms was one-electron transfer, with organic radical intermediates generated.

#### **6.2.4 Comparison experiment with ferrate(VI), UV/H<sub>2</sub>O<sub>2</sub>, and ozonation**

- Among the oxidation processes investigated, ozonation was the most effective in transforming the organic fractions of OSPW, achieving almost complete removal of fluorescing aromatics, heteroatomic NAs, and classical NAs (97.1%) at the dose of 2.0 mM O<sub>3</sub>. Both direct reaction by ozone and indirect reaction by ·OH were important oxidation pathways.
- UV/H<sub>2</sub>O<sub>2</sub> oxidation achieved 42.4% classical NAs removal at a 2.0 mM H<sub>2</sub>O<sub>2</sub> dose and 950 mJ/cm<sup>2</sup> UV dose, and ferrate(VI) oxidation achieved 46.7% classical NA removal at 2.0 mM Fe(VI). Compared with UV/H<sub>2</sub>O<sub>2</sub>, ferrate(VI) oxidation showed high selectivity as indicated by the preferential removal of organics with two and three fused aromatic rings and preferential removal of NAs with high carbon number and high hydrogen deficiency. In addition, after ferrate(VI) oxidation, NA+O concentration decreased and NA+O<sub>2</sub> concentration increased. On the other hand, UV/H<sub>2</sub>O<sub>2</sub> oxidation led to the opposite results (i.e., NA+O concentration increased and NA+O<sub>2</sub> concentration decreased). This again

can be explained by the preferential removal by ferrate(VI) of the newly generated NA+O species which might be more reactive than the parent NAs.

- $^1\text{H}$  NMR analyses showed that the high removal of fluorescing aromatics and NAs did not necessarily mean an equally high removal of hydrogens on aromatic rings and in carboxyl groups. As confirmed by the high residual aromatic peak and carboxyl peak in the  $^1\text{H}$  NMR spectra of treated OSPW, the oxidation processes investigated in this study mainly resulted in partial oxidation, transforming the aromatics and NAs but not necessarily opening the aromatic rings or mineralizing the carboxyl groups.
- Acute toxicity towards *Vibrio fischeri* was reduced by oxidation, with the order of efficiency as “ $\text{O}_3 > \text{ferrate (VI)} > \text{UV}/\text{H}_2\text{O}_2$ ” at the same molar doses of the oxidants. In addition, toxicity on goldfish PKMs was also mitigated by all the treatment, with the order of efficiency as “ $\text{O}_3 > \text{ferrate (VI)} \approx \text{UV}/\text{H}_2\text{O}_2$ ”.

#### 6.2.5 FTICR-MS vs UPLC-TOF-MS

- FTICR-MS analyses showed that the oxidation processes transformed the distribution profiles of the specific species in each  $\text{O}_x$ ,  $\text{O}_x\text{S}_y$ ,  $\text{O}_x\text{N}_y$  fraction, with the most significant abundance changes occurring to the  $\text{O}_x\text{S}_y$  species. It was also noted that the selectivity of the oxidants impacted the transformation patterns, notably embodied by the different performance by the oxidants on transforming  $\text{O}_2$  to  $\text{O}_3$  and/or  $\text{O}_4$  and on transforming  $\text{O}_2\text{S}$  to  $\text{O}_3\text{S}$  and/or  $\text{O}_4\text{S}$  detected in negative ESI mode.

- Ferrate(VI) oxidation decreased the relative abundance of low oxygen containing  $O_xS$  species, and increased the relative abundance of oxygen-rich species such as  $O_4S$ ,  $O_5S$ ,  $O_6S$ . Similar trend was achieved by direct ozone reaction. Interestingly, after UV/ $H_2O_2$  oxidation and ozonation (without TBA) both of which contained radical reaction, there was an increase of the relative abundance of low oxygen containing species (e.g. S,  $O_3S$  for UV/ $H_2O_2$  treated OSPW; S, OS,  $O_2S$  for ozonated OSPW), which might come from the breakdown of other sulfur-containing species and/or even particulate sulfur-containing organics.
- Negative mode UPLC-TOF-MS confirmed the transformation of  $O_x$  species observed with FTICR-MS, but it detected lower abundance of species with carbon number  $\leq 15$  and hydrogen deficiency  $\leq 12$  than FTICR-MS. On the other hand, positive mode UPLC-TOF-MS results showed severe discrepancies with FTICR-MS results and should be used with caution.

### 6.3 Recommendations

Based on the findings obtained in this study, the following recommendations are proposed for future studies.

- Naphthenic acids are low-molecular-weight organics and exist in dissociative state at the pH range of OSPW, making it extraordinarily hydrophilic and difficult to be removed in the CF process. Future study can either try to decrease the pH with acids to make NAs less hydrophilic,

or to apply organic polymers and/or activated carbon to provide hydrophobic surface to promote physical adsorption. In a nutshell, to achieve NAs removal in the CF process, try to avoid the situation that both the adsorbate (i.e. NAs) and adsorbent (i.e. floc surface) are hydrophilic.

- Combination of the coagulation and oxidation processes may exhibit some unique advantages. For example, alum coagulation prior to ferrate(VI) oxidation might be promising: alum addition decreases the pH of the water, which makes the subsequent ferrate(VI) oxidation faster and more powerful. On the other hand, the generation of ferric coagulant after the ferrate(VI) oxidation will further enhance the coagulation process.
- OSPW is a complex water matrix with various organic fractions. Understanding its composition is the precondition to explore the mechanisms behind its toxicity and to evaluate the performance of the water treatment processes. As shown in the ferrate(VI) oxidation study, the total concentration of aromatics in OSPW should be at the mg/L level and the toxicity effect of the aromatics might be an important toxicity source in OSPW. It is advisable to work on exploring the concentrations, species, and the environmental impact of the aromatics in OSPW. Similarly, it is also essential for OSPW remediation to identify and quantify the sulfur and nitrogen containing species in OSPW.
- Considering the limitation of the mass spectrometry (e.g., mass spectrometer coupled with soft ionization cannot provide functional group information) and the complexity of the OSPW organic fractions (i.e.,

thousands of species with different molecular weight, functional groups, and configurations), it is recommended that future research diversify the analytical techniques. For example, NMR and FTIR are two powerful tools to characterize the molecular structures of the organic fractions, and can be employed to characterize the OSPW organic fractions both qualitatively and quantitatively.

## APPENDIX A. STANDARD CURVE FOR ALUMINUM SPECIES QUANTIFICATION BY $^{27}\text{Al}$ NMR

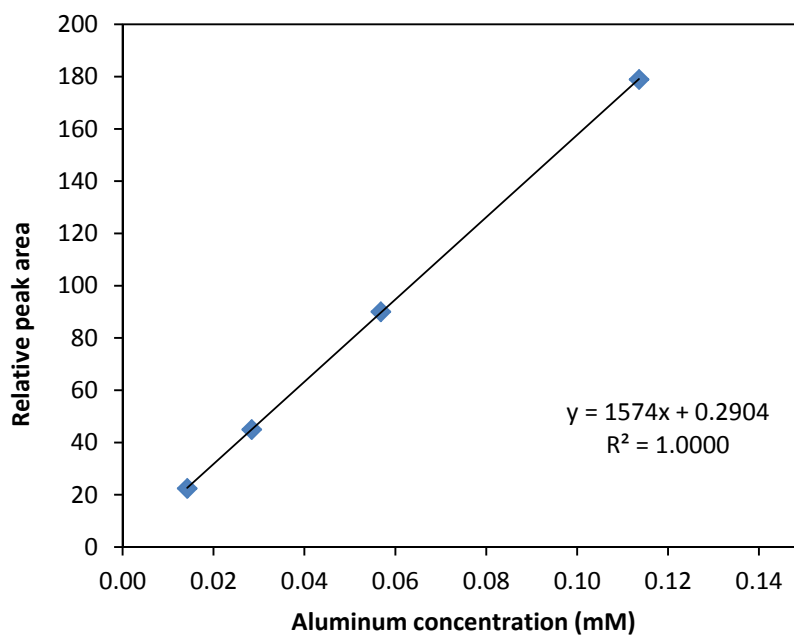


**Figure A1** Relative peak area of  $\text{Al}^{3+}$  versus its concentration (the peak area was relative to  $\text{AlO}_2^-$  peak area which was set to be 100;  $\text{AlO}_2^-$  solution was in the inner NMR tube with 3 mm OD and the  $\text{Al}(\text{NO}_3)_3$  solution was in the outer NMR tube with 5 mm OD)

Note: the NMR spectra based on which Figure A.1 was plotted was provided in Figure A.2.

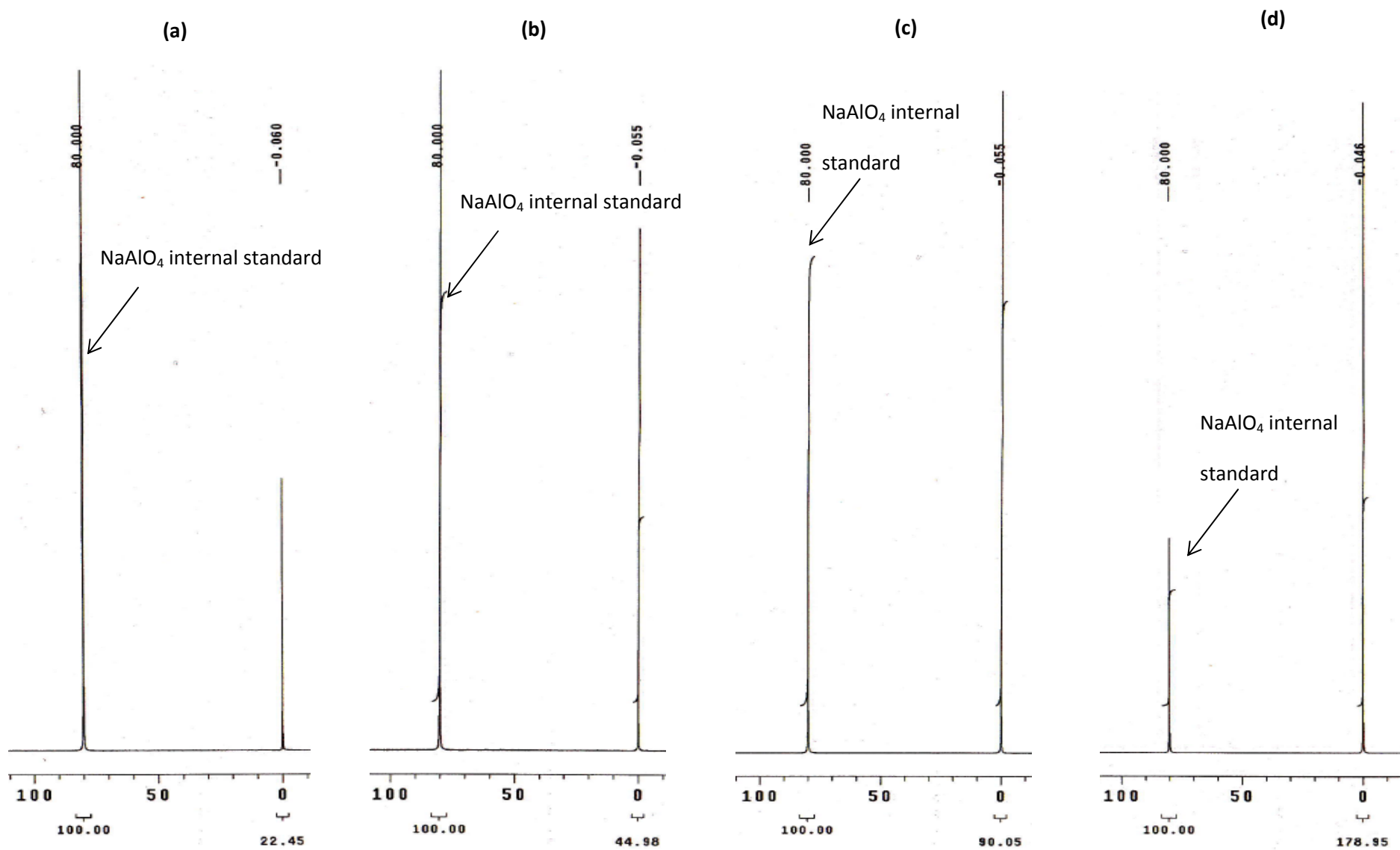


**Figure A2**  $^{27}\text{Al}$  NMR spectra for  $\text{Al}(\text{NO}_3)_3$  standard samples: (a) 0.0142 mM Al; (b) 0.0284 mM Al; (c) 0.0568 mM Al; and (d) 0.1136 mM Al ( $\text{NaAlO}_2$  was used as internal standard, and its peak area was set to be 100 in each spectrum)

## APPENDIX B. XRD SPECTRUM OF THE MINERALS IN RAW OSPW

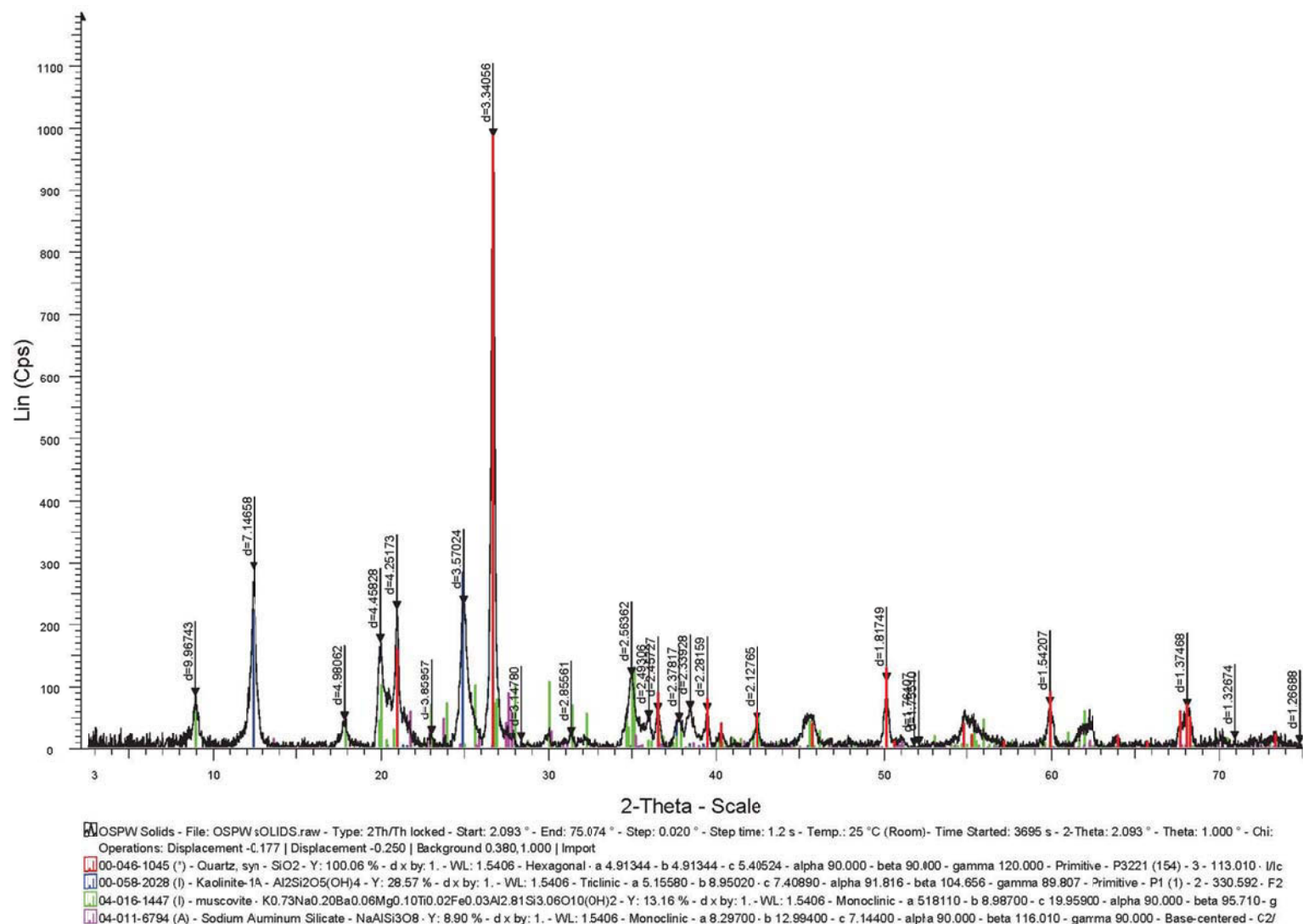


Figure A3 XRD spectrum of the minerals in raw OSPW

## APPENDIX C. IN VITRO ASSAY ON GOLDFISH PRIMARY KIDNEY MACROPHAGES

(1) Fish: Goldfish (8-12 cm in length) from Mt. Parnell Fisheries Inc. (Mercersburg, PA) were maintained at the Aquatic Facility of the Department of Biological Sciences, University of Alberta. The fish were kept at 17 °C in a flow-through water system with a 14 h light/10 h dark photoperiod, and fed to satiation daily with trout pellets. Fish were acclimated for at least 3 weeks prior to use in experiments and were handled according to the guidelines of the Canadian Council of Animal Care (CCAC-Canada).

(2) Goldfish macrophage cultures: Goldfish were anesthetized using Tricaine methanesulfonate (TMS), and sacrificed. The isolation and cultivation of goldfish primary kidney macrophages (PKMs) in complete medium (C-MGFL-15) supplemented with 10% newborn calf and 5% carp serum were performed. Six-day-old PKMs were harvested, enumerated and used for nitric oxide assay.

(3) Production of reactive nitrogen intermediates (RNI) by macrophages: Six-day-old PKMs ( $3 \times 10^5$  cells/well) were seeded into 96-well plates in 50  $\mu$ L of C-MGFL-15. Cells were exposed to samples for 18 h and then were stimulated with heat-killed *A. salmonicida* ( $3.6 \times 10^7$ cfu/well) for 72 h. Cells in the negative and positive control were exposed to 50  $\mu$ L of C-MGFL-15 and heat killed *A. salmonicida* respectively. RNI was determined via the Griess reaction by adding 1% sulfanilamide and 0.1% N-naphthylethylenediamine to supernatants from the

treated cells, measuring absorbance at 540 nm, and the amount of nitrite in supernatants determined using a nitrite standard curve.

(4) Statistical analysis was performed using a one-way ANOVA and a Dunnett's post hoc test. Asterisks (\*) denote significant differences compared to experimental control ( $p < 0.05$ ;  $n=3$ ).

## APPENDIX D. MEASUREMENT OF THE MODEL COMPOUND CONCENTRATION AND IDENTIFICATION OF THE END PRODUCTS IN THE FERRATE(VI) STUDY

The concentrations of the three model compounds, cyclohexanecarboxylic acid ( $C_7H_{12}O_2$ ), 3-methyl-octahydropentalene-1-carboxylic acid ( $C_{10}H_{16}O_2$ ), cyclohexanepentanoic acid ( $C_{11}H_{20}O_2$ ), were measured with Agilent 1100 binary HPLC coupled with G1946D MSD mass spectrometer (Santa Clara, CA, USA). End products were identified with Agilent 1200 HPLC coupled with Agilent 6220 oaTOF mass spectrometry (Santa Clara, CA, USA). Mass spectrometry was performed in negative scan/SIM mode. Integration of SIM mode signals were used for semi quantitation. Some details of the analysis are given below.

### **(1) Measurement of the concentration of model compound**

Sample volume injected: 20  $\mu$ L

HPLC column: Kinetex 2.6 $\mu$ m, XB-C18, 100 $\text{\AA}$ , 2.1x100mm

Column Thermostat temperature: 40  $^{\circ}$ C

Solvents: A: 4mM  $NH_4Ac$ , 0.1% acetic acid; B: acetonitrile

HPLC gradient table:

**Table A1** HPLC solvent gradient for the measurement of model compound concentration

Time (min)	The percentage of solvent B(%)	Flow (mL/min)
0.00	10	0.35
2.00	70	0.35
3.00	90	0.35
3.50	95	0.35
6.00	95	0.35

## (2) Identification of the end products

Sample volume injected: 5  $\mu$ L

HPLC column: Kinetex 2.6 $\mu$ m, XB-C18, 100 $\text{\AA}$ , 2.1x100mm

Column Thermostat temperature: 40  $^{\circ}$ C

Solvents: A: 4mM  $\text{NH}_4\text{Ac}$ , 0.1% acetic acid; B: acetonitrile

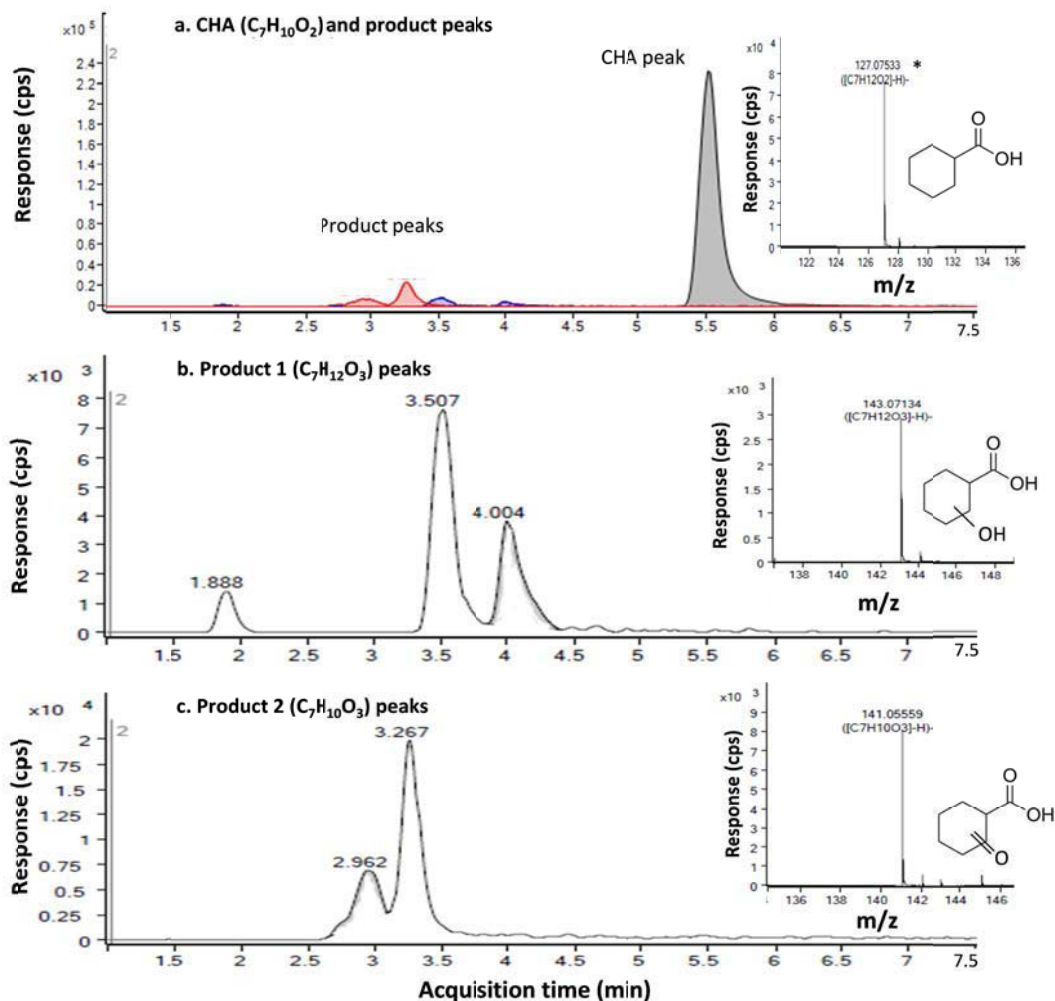
HPLC gradient table:

**Table A2** HPLC solvent gradient for detecting oxidation products of CHPA

Time (min)	The percentage of solvent B(%)	Flow (mL/min)
0.00	10	0.35
2.00	70	0.35
3.00	90	0.35
3.50	95	0.35
6.00	95	0.35

**Table A3** HPLC solvent gradient for detecting oxidation products of CHA and  
ADA

Time (min)	The percentage of solvent B(%)	Flow (mL/min)
0.00	2	0.35
1.00	2	0.35
8.00	95	0.35
11.0	95	0.35



\* The mass error for CHA was  $\sim 9$  ppm, relatively high due to CHA's much higher concentration than the calibrants, whose concentration was similar to that of the end products. The m/z shift occurred when the detector was overloaded.

**Figure A4** Extracted-ion chromatogram (EIC) of (a) model compound cyclohexanecarboxylic acid (C<sub>7</sub>H<sub>12</sub>O<sub>2</sub>, CHA), product 1 (C<sub>7</sub>H<sub>12</sub>O<sub>3</sub>, blue color), and product 2 (C<sub>7</sub>H<sub>10</sub>O<sub>3</sub>, red color) in ferrate(VI) oxidized CHA solution (200 mg/L Fe(VI), 180 min); product peaks were replotted with new scale in (b) for product 1 (C<sub>7</sub>H<sub>12</sub>O<sub>3</sub>), and (c) for product 2 (C<sub>7</sub>H<sub>10</sub>O<sub>3</sub>) (The peak composition regarding the m/z ratios was also provided in the inlaid figures for each peak)

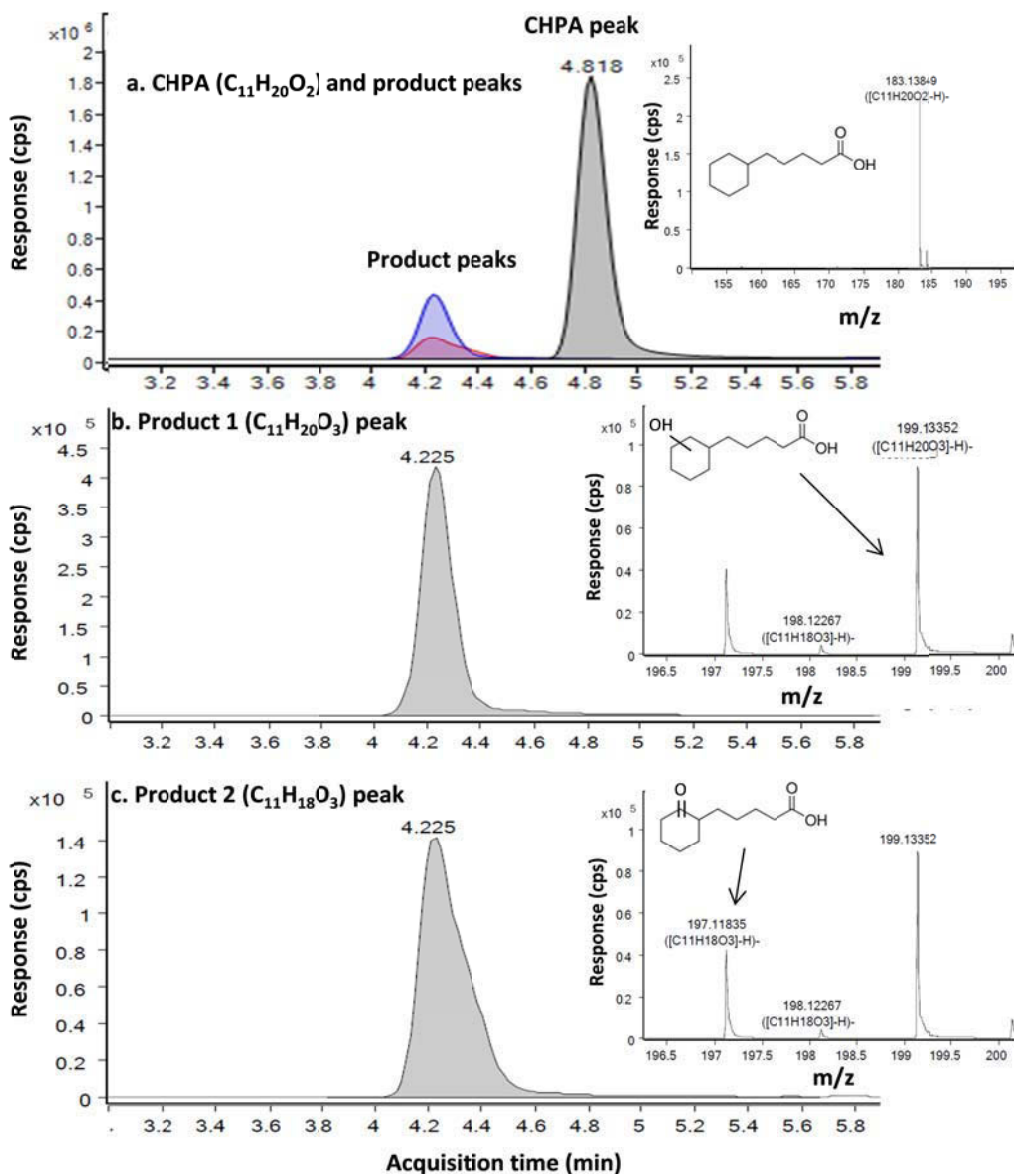


**Figure A5** Extracted-ion chromatogram (EIC) of (a) model compound cyclohexanepentanoic acid ( $C_{11}H_{20}O_2$ , CHPA), product 1 ( $C_{11}H_{20}O_3$ ), and product 2 ( $C_{11}H_{18}O_3$ ) in ferrate(VI) oxidized CHPA solution (200 mg/L Fe(VI), 180 min); product peaks were replotted with new scale in (b) for product 1 ( $C_{11}H_{20}O_3$ ), and (c) for product 2 ( $C_{11}H_{18}O_3$ ) (The peak composition regarding the  $m/z$  ratios was also provided in the inlaid figures for each peak)

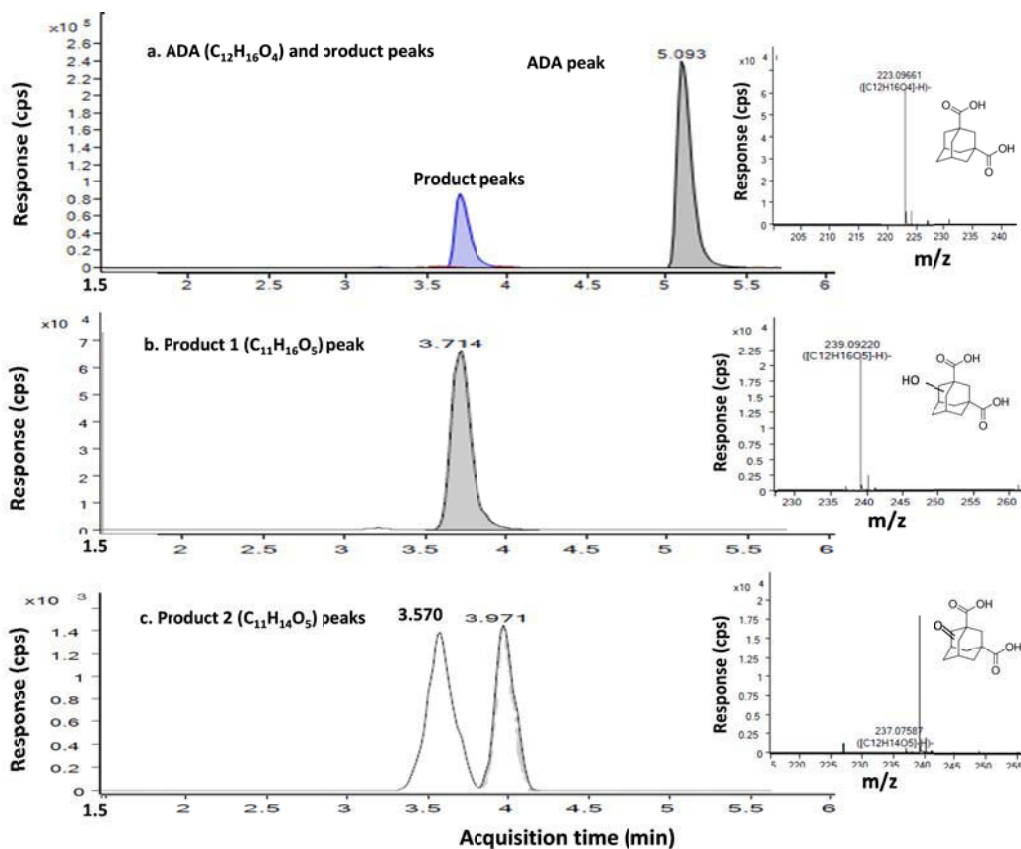


**Figure A6** Extracted-ion chromatogram (EIC) of (a) model compound 1,3-adamantanedicarboxylic acid ( $C_{12}H_{16}O_4$ , ADA), product 1 ( $C_{12}H_{16}O_5$ ), and product 2 ( $C_{12}H_{14}O_5$ ) in ferrate(VI) oxidized ADA solution (200 mg/L Fe(VI), 180 min); product peaks were replotted in (b) for product 1 ( $C_{12}H_{16}O_5$ ), and (c) for product 2 ( $C_{12}H_{14}O_5$ ) (The peak composition regarding the  $m/z$  ratios was also provided in the inlaid figures for each peak)

## APPENDIX E. ESTIMATION OF THE MOLAR RATIO OF AROMATIC ORGANIC MATTER OVER TOTAL NAS

Due to uncertainties in the number of aromatic hydrogen atoms in each aromatic molecule and the number of carboxyl functional groups in each organic acid molecule, we estimated the molar ratio of aromatic organic matter over total organic acid with several different assumptions. The results are summarized in Table S1. For the average number of carboxyl functional groups in each acid, we assumed it to be 1 or 1.5 because monoacids predominate in OSPW; for the average number of aromatic hydrogen in each aromatic molecule, 4, 5, 6, 8 are selected because fluorescing aromatics mainly contain one-ring, two-ring, and three-ring aromatics as verified by the SFS data. The following is a calculation sample.

Suppose there is 1 mole organic acid in OSPW, then there will be 1 mole hydrogen atoms attached to the carboxyl functional groups (assumption: average number of carboxyl functional groups in each acid = 1). Then there will be  $1/5.15 \times 3.25 = 0.63$  mole hydrogen atoms on aromatic rings (calculation is based on the relative peak area in Figure 1a in the main text). If we assume there are six hydrogen atoms in total on all the aromatic rings in each aromatic molecule (note: aromatics may contain more than one aromatic ring in one molecule, and these aromatic rings are not necessarily fused), then there will be  $0.63/6 = 0.105$  mole aromatic molecule. Therefore, the molar ratio of aromatic organic matter over total organic acid is estimated to be  $0.105:1 = 1:9.5 = 0.11$ . Note: for those aromatics containing more than one aromatic rings (not necessarily fused), there might be

high hydrogen number on aromatic rings in one molecule. To be conservative, we assume a broad the range of the hydrogen number on aromatic rings.

**Table A4 Estimation of molar ratio of aromatics over organic acids**

Average number of carboxyl functional groups in each acid	Average number of aromatic hydrogens in each aromatic molecule	Molar ratio of aromatics over organic acids
1	3	1:3.2 (0.32)
1	4	1:6.3 (0.16)
1	5	1:7.9 (0.13)
1	6	1:9.5 (0.11)
1	7	1:11.1 (0.09)
1	8	1:12.7 (0.08)
1.5	3	1:3.2 (0.32)
1.5	4	1:4.2 (0.24)
1.5	5	1:5.3 (0.19)
1.5	6	1:6.3 (0.16)
1.5	7	1:7.4 (0.14)
1.5	8	1:8.5 (0.12)

APPENDIX F. RELATIVE ABUNDANCE OF THE DETECTED SPECIES IN RAW AND OXIDIZED OSPW

**Table A5** Relative abundance (%) of  $O_x$ ,  $O_xS_y$ , and  $O_xN_y$  out of total organic species detected by FTICR-MS in negative ESI mode

	$O_x$	$O_xS_y$	$O_xN_y$	Total
Raw OSPW	82.3	16.6	1.1	100
Ferrate(VI)	71.6	27.6	0.8	100
UV/H <sub>2</sub> O <sub>2</sub>	86.7	12.0	1.3	100
Ozone	84.8	14.1	1.1	100
Ozone (with TBA)	78.8	19.9	1.2	100

**Table A6** Relative abundance (%) of  $O_x$ ,  $O_xS_y$ , and  $O_xN_y$  out of total organic species detected by FTICR-MS in positive ESI mode

	$O_x$	$O_xS_y$	$O_xN_y$	$O_xS_{y1}N_{y2}$	Total
Raw OSPW	51.3	36.9	5.5	6.3	100
Ferrate(VI)	28.7	53.4	4.0	13.9	100
UV/H <sub>2</sub> O <sub>2</sub>	47.4	38.4	2.5	11.7	100
Ozone	38.5	27.6	14.2	19.8	100
Ozone (with TBA)	30.5	47.9	7.9	13.7	100

**Table A7** Relative abundance (%) of specific  $O_x$  species out of total  $O_x$  species detected by FTICR-MS in negative ESI mode

	O	O <sub>2</sub>	O <sub>3</sub>	O <sub>4</sub>	O <sub>5</sub>	O <sub>6</sub>	O <sub>7</sub>	Total O <sub>x</sub>
Raw OSPW	0.2	38.2	24.4	30.5	6.1	0.6	0.0	100
Ferrate(VI)	0.3	31.7	23.9	32.6	9.1	2.4	0.1	100
UV/H <sub>2</sub> O <sub>2</sub>	0.2	32.6	27.9	30.4	7.5	1.3	0.0	100
Ozone	0.2	7.3	22.0	40.5	21.8	6.9	1.3	100
Ozone (with TBA)	0.2	25.4	27.0	33.5	10.7	3.1	0.2	100

**Table A8** Relative abundance (%) of specific O<sub>x</sub> species out of total O<sub>x</sub> species detected by FTICR-MS in positive ESI mode

	O	O <sub>2</sub>	O <sub>3</sub>	O <sub>4</sub>	O <sub>5</sub>	O <sub>6</sub>	O <sub>7</sub>	O <sub>8</sub>	Total O <sub>x</sub>
Raw OSPW	0.4	6.9	22.5	48.1	12.3	8.0	1.3	0.6	100
Ferrate(VI)	0.0	3.5	18.7	53.0	11.1	12.5	0.8	0.3	100
UV/H <sub>2</sub> O <sub>2</sub>	0.0	6.8	27.5	41.1	15.1	6.5	1.4	1.5	100
Ozone	0.8	3.9	22.7	40.7	19.0	8.7	3.3	0.8	100
Ozone (with TBA)	0.4	3.1	22.2	44.0	15.2	11.4	2.6	1.0	100

**Table A9** Relative abundance (%) of specific O<sub>x</sub>S<sub>y</sub> species out of total O<sub>x</sub>S<sub>y</sub> species detected by FTICR-MS in negative ESI mode

	S	OS	O <sub>2</sub> S	O <sub>3</sub> S	O <sub>4</sub> S	O <sub>5</sub> S	O <sub>6</sub> S	S <sub>2</sub>	Total O <sub>x</sub> S <sub>y</sub>
Raw OSPW	4.1	0.6	36.1	35.6	20.2	2.5	0.0	1.0	100
Ferrate(VI)	4.3	4.7	3.5	24.4	54.7	6.1	2.2	0.1	100
UV/H <sub>2</sub> O <sub>2</sub>	7.1	1.5	9.1	51.2	23.9	3.7	0.0	3.6	100
Ozone	4.3	0.7	1.0	28.2	30.6	27.5	4.7	3.0	100
Ozone (with TBA)	2.2	4.8	2.0	19.5	61.5	5.8	1.4	2.9	100

**Table A10** Relative abundance (%) of specific O<sub>x</sub>S<sub>y</sub> species out of total O<sub>x</sub>S<sub>y</sub> species detected by FTICR-MS in positive ESI mode

	S	OS	O <sub>2</sub> S	O <sub>3</sub> S	O <sub>4</sub> S	O <sub>5</sub> S	O <sub>6</sub> S	S <sub>2</sub>	OS <sub>2</sub>	O <sub>2</sub> S <sub>2</sub>	O <sub>4</sub> S <sub>2</sub>	O <sub>6</sub> S <sub>2</sub>	Total O <sub>x</sub>
Raw OSPW	17.8	11.6	4.2	32.7	18.6	2.2	3.3	3.2	1.6	3.1	1.7	0.0	100
Ferrate(VI)	6.3	9.5	0.2	0.1	46.3	4.4	14.3	4.6	9.3	0.0	0.0	5.0	100
UV/H <sub>2</sub> O <sub>2</sub>	23.6	11.2	1.9	39.2	12.1	2.7	0.1	4.6	0.4	2.2	1.7	0.3	100
Ozone	30.5	14.1	5.3	4.1	13.6	6.9	3.5	11.7	8.3	1.2	0.4	0.3	100
Ozone (with TBA)	9.6	16.1	2.3	9.3	35.9	4.8	5.7	6.9	7.6	0.1	0.6	1.0	100

**Table A11** Relative abundance (%) of specific O<sub>x</sub>N<sub>y</sub> species out of total O<sub>x</sub>N<sub>y</sub> species detected by FTICR-MS in negative ESI mode

	O <sub>2</sub> N	O <sub>3</sub> N	O <sub>x</sub> N <sub>2</sub>	Total O <sub>x</sub> N <sub>y</sub>
Raw OSPW	50.0	5.0	45.0	100
Ferrate(VI)	50.6	4.3	45.1	100
UV/H <sub>2</sub> O <sub>2</sub>	51.7	5.6	42.7	100
Ozone	50.6	5.6	43.8	100
Ozone (with TBA)	35.7	12.2	52.1	100

**Table A12** Relative abundance (%) of specific O<sub>x</sub>N<sub>y</sub> species out of total O<sub>x</sub>N<sub>y</sub> species detected by FTICR-MS in positive ESI mode

	ON	O <sub>2</sub> N	O <sub>3</sub> N	O <sub>4</sub> N	O <sub>5</sub> N	O <sub>x</sub> N <sub>2</sub>	Total O <sub>x</sub> N <sub>y</sub>
Raw OSPW	3.4	36.8	13.8	0.0	0.0	46.0	100
Ferrate(VI)	0	21.4	4.5	8.3	0.0	65.8	100
UV/H <sub>2</sub> O <sub>2</sub>	2.5	29.0	4.3	17.4	0.0	46.9	100
Ozone	0.0	11.7	1.0	0.2	0.0	87.1	100
Ozone (with TBA)	0.0	12.2	4.0	2.6	1.5	79.7	100

**Table A13** Relative abundance (%) of specific O<sub>x</sub> species out of total O<sub>x</sub> species detected by UPLC-TOF-MS in negative ESI mode

	O	O <sub>2</sub>	O <sub>3</sub>	O <sub>4</sub>	O <sub>5</sub>	O <sub>6</sub>	O <sub>7</sub>	Total O <sub>x</sub>
Raw OSPW	1.8	51.0	19.0	20.7	5.5	1.8	0.0	100
Ferrate(VI)	1.7	37.5	20.7	30.1	6.5	3.6	0.0	100
UV/H <sub>2</sub> O <sub>2</sub>	2.1	40.6	25.5	22.2	6.8	2.9	0.0	100
Ozone	3.1	9.5	27.6	31.8	19.5	8.6	0.0	100
Ozone (with TBA)	2.0	33.0	23.8	30.0	7.1	4.0	0.0	100

**Table A14** Relative abundance (%) of specific O<sub>x</sub> species out of total O<sub>x</sub> species detected by UPLC-TOF-MS in positive ESI mode

	O	O <sub>2</sub>	O <sub>3</sub>	O <sub>4</sub>	O <sub>5</sub>	O <sub>6</sub>	O <sub>7</sub>	Total O <sub>x</sub>
Raw OSPW	15.2	32.3	31.7	14.1	4.5	2.2	0.0	100
Ferrate(VI)	10.0	23.6	28.6	27.5	6.6	3.6	0.0	100
UV/H <sub>2</sub> O <sub>2</sub>	12.7	29.1	37.5	13.3	5.5	2.0	0.0	100
Ozone	9.6	19.0	38.1	19.5	10.2	3.6	0.0	100
Ozone (with TBA)	10.2	23.2	34.3	23.3	6.5	2.5	0.0	100

## BIBLIOGRAPHY

- Afzal, A., Drzewicz, P., Perez-Estrada, L.A., Chen, Y., Martin, J.W. and Gamal El-Din, M. (2012) Effect of molecular structure on the relative reactivity of naphthenic acids in the UV/H<sub>2</sub>O<sub>2</sub> advanced oxidation process. *Environmental Science & Technology* 46(19), 10727-10734.
- Al-Mutairi, N.Z. (2006) Coagulant toxicity and effectiveness in a slaughterhouse wastewater treatment plant. *Ecotoxicology and Environmental Safety* 65(1), 74-83.
- Alberta Government (2015) 2014-2015 Energy annual report, Edmonton, Alberta.
- Alharbi, H.A., Saunders, D.M.V., Al-Mousa, A., Alcorn, J., Pereira, A.S., Martin, J.W., Giesy, J.P. and Wiseman, S.B. (2016) Inhibition of ABC transport proteins by oil sands process affected water. *Aquatic Toxicology* 170, 81-88.
- Allen, E.W. (2008) Process water treatment in Canada's oil sands industry: I. Target pollutants and treatment objectives. *Journal of Environmental Engineering and Science* 7(2), 123-138.
- Alharbi, H.A., Saunders, D.M.V., Al-Mousa, A., Alcorn, J., Pereira, A.S., Martin, J.W., Giesy, J.P. and Wiseman, S.B. (2016) Inhibition of ABC transport proteins by oil sands process affected water. *Aquatic Toxicology* 170, 81-88.
- Alpatova, A., Kim, E.-S., Dong, S., Sun, N., Chelme-Ayala, P. and Gamal El-Din, M. (2014) Treatment of oil sands process-affected water with ceramic

ultrafiltration membrane: Effects of operating conditions on membrane performance. *Separation and Purification Technology* 122(0), 170-182.

Alpatova, A., Kim, E.-S., Sun, X., Hwang, G., Liu, Y. and Gamal El-Din, M. (2013) Fabrication of porous polymeric nanocomposite membranes with enhanced anti-fouling properties: Effect of casting composition. *Journal of Membrane Science* 444, 449-460.

Alpatova, A., Meshref, M., McPhedran, K.N. and Gamal El-Din, M. (2015) Composite polyvinylidene fluoride (PVDF) membrane impregnated with Fe<sub>2</sub>O<sub>3</sub> nanoparticles and multiwalled carbon nanotubes for catalytic degradation of organic contaminants. *Journal of Membrane Science* 490, 227-235.

Alsheyab, M., Jiang, J.Q. and Stanford, C. (2009) On-line production of ferrate with an electrochemical method and its potential application for wastewater treatment - A review. *Journal of Environmental Management* 90(3), 1350-1356.

Anderson, J.C., Wiseman, S.B., Wang, N., Moustafa, A., Perez-Estrada, L., Gamal El-Din, M., Martin, J.W., Liber, K. and Giesy, J.P. (2012) Effectiveness of ozonation treatment in eliminating toxicity of oil sands process-affected water to *Chironomus dilutus*. *Environmental Science & Technology* 46(1), 486-493.

Anquandah, G.A.K., Sharma, V.K., Panditi, V.R., Gardinali, P.R., Kim, H. and Oturan, M.A. (2013) Ferrate(VI) oxidation of propranolol: Kinetics and products. *Chemosphere* 91(1), 105-109.

- APHA (2005) Standard methods for the examination of water and wastewater. Eaton A.D., Clesceri L.S., Rice E.W., Greenberg A.E., Franson M.A.H. (Eds) 21<sup>st</sup> edition, American Public Health Association (APHA), American Water Works Association (AWWA), and the Water Environment Federation (WEF), Washington D.C.
- AWWA (1999) Water quality and treatment: a handbook of community water supplies, American Water Works Association (AWWA), McGraw-Hill, New York.
- Bard, S.M., Gagnon, G.A., Mortula, M. and Walsh, M.E. (2009) Aluminum toxicity and ecological risk assessment of dried alum residual into surface water disposal. *Canadian Journal of Civil Engineering* 36, 127.
- Barrow, M.P., Peru, K.M. and Headley, J.V. (2014) An added dimension: GC atmospheric pressure chemical ionization FTICR MS and the Athabasca oil sands. *Analytical Chemistry* 86(16), 8281-8288.
- Barrow, M.P., Peru, K.M., McMartin, D.W. and Headley, J.V. (2015) Effects of extraction pH on the fourier transform ion cyclotron resonance mass spectrometry profiles of Athabasca oil sands process water. *Energy & Fuels*, *in progress*.
- Barrow, M.P., Witt, M., Headley, J.V. and Peru, K.M. (2010) Athabasca oil sands process water: characterization by atmospheric pressure photoionization and electrospray ionization Fourier transform ion cyclotron resonance mass spectrometry. *Analytical Chemistry* 82(9), 3727-3735.

- Bauer, A.E. (2013) Identification of oil sands naphthenic acid structures and their associated toxicity to *Pimephales promelas* and *Oryzias latipes*. M.S., University of Waterloo, Waterloo, Ontario.
- Bolton, J. and Linden, K. (2003) Standardization of methods for fluence (UV dose) determination in bench-scale UV experiments. *Journal of Environmental Engineering* 129(3), 209-215.
- Bottero, J.Y., Cases, J.M., Fiessinger, F. and Polrier, J.E. (1980) Studies of hydrolyzed aluminum chloride solutions. 1. Nature of aluminum species and composition of aqueous solutions. *Journal of Physical Chemistry* 84(22), 2933-2939.
- Bowman, D.T., Slater, G.F., Warren, L.A. and McCarry, B.E. (2014) Identification of individual thiophene-, indane-, tetralin-, cyclohexane-, and adamantane-type carboxylic acids in composite tailings pore water from Alberta oil sands. *Rapid Communications in Mass Spectrometry* 28(19), 2075-2083.
- Breitmaier, E. and Voelter, W. (1987) Carbon-13 NMR spectroscopy: high-resolution methods and applications in organic chemistry and biochemistry, VCH Publishers, Weinheim.
- Brient, J.A., Wessner, P.J. and Doyle, M.N. (2000) *Kirk-Othmer encyclopedia of chemical technology*, John Wiley & Sons, Inc., New Jersey.
- Burgess, J. (1978) *Metal ions in solution*, Ellis Horwood, Chichester.
- Carey, F.A. and Sundberg, R.J. (2010) *Advanced organic chemistry: part B: reaction and synthesis*, Springer New York.

- Chalaturnyk, R.J., Don Scott, J. and Özüm, B. (2002) Management of oil sands tailings. *Petroleum Science and Technology* 20(9-10), 1025-1046.
- Chelme-Ayala, P., Gamal El-Din, M. and Smith, D.W. (2010) Degradation of bromoxynil and trifluralin in natural water by direct photolysis and UV plus H<sub>2</sub>O<sub>2</sub> advanced oxidation process. *Water Research* 44(7), 2221-2228.
- Clayden, J., Greeves, N. and Warren, S. (2012) *Organic chemistry*, Oxford University Press, New York.
- Crittenden, J.C., Trussell, R.R., Hand, D.W., Howe, K.J. and Tchobanoglous, G. (2012) *MWH's water treatment: principles and design*, Wiley, New Jersey.
- Debenest, T., Turcotte, P., Gagne, F., Gagnon, C. and Blaise, C. (2012) Ecotoxicological impacts of effluents generated by oil sands bitumen extraction and oil sands lixiviation on *Pseudokirchneriella subcapitata*. *Aquatic Toxicology* 112-113, 83-91.
- Delaude, L. and Laszlo, P. (1996) A novel oxidizing reagent based on potassium ferrate(VI). *Journal of Organic Chemistry* 61(18), 6360-6370.
- Dong, S., Kim, E.-S., Alpatova, A., Noguchi, H., Liu, Y. and Gamal El-Din, M. (2014) Treatment of oil sands process-affected water by submerged ceramic membrane microfiltration system. *Separation and Purification Technology* 138(0), 198-209.
- Dong, T., Zhang, Y., Islam, M.S., Liu, Y. and Gamal El-Din, M. (2015) The impact of various ozone pretreatment doses on the performance of endogenous microbial communities for the remediation of oil sands

- process-affected water. *International Biodeterioration & Biodegradation* 100, 17-28.
- Drzewicz, P., Afzal, A., Gamal El-Din, M. and Martin, J.W. (2010) Degradation of a model naphthenic acid, cyclohexanoic acid, by vacuum UV (172 nm) and UV (254 nm)/H<sub>2</sub>O<sub>2</sub>. *Journal of Physical Chemistry A* 114(45), 12067-12074.
- Drzewicz, P., Perez-Estrada, L., Alpatova, A., Martin, J.W. and Gamal El-Din, M. (2012) Impact of peroxydisulfate in the presence of zero valent iron on the oxidation of cyclohexanoic acid and naphthenic acids from oil sands process-affected water. *Environmental Science & Technology* 46(16), 8984-8991.
- Dutta Majumdar, R., Gerken, M., Mikula, R. and Hazendonk, P. (2013) Validation of the Yen–Mullins model of Athabasca oil-sands asphaltenes using solution-state <sup>1</sup>H NMR relaxation and 2D HSQC spectroscopy. *Energy Fuels* 27(11), 6528-6537.
- Elovitz, M.S. and von Gunten, U. (1999) Hydroxyl radical/ozone ratios during ozonation processes. I. the R<sub>ct</sub> concept. *Ozone: Science & Engineering* 21(3), 239-260.
- Faust, S.D. and Aly, O.M. (1998) *Chemistry of Water Treatment*, CRC Press, Florida.
- Fort, D.J. and Stover, E.L. (1995) Impact of toxicities and potential interactions of flocculants and coagulant aids on whole effluent toxicity testing. *Water Environment Research* 67(6), 921-925.

- Francis, P.D. (1987) Oxidation by UV and ozone of organic contaminants dissolved in deionized and raw mains water. *Ozone: Science & Engineering* 9(4), 369-390.
- Frank, R.A., Fischer, K., Kavanagh, R., Burnison, B.K., Arsenault, G., Headley, J.V., Peru, K.M., Van, D.K.G. and Solomon, K.R. (2009) Effect of carboxylic acid content on the acute toxicity of oil sands naphthenic acids. *Environmental Science & Technology* 43(2), 266-271.
- Frank, R.A., Kavanagh, R., Kent Burnison, B., Arsenault, G., Headley, J.V., Peru, K.M., Van Der Kraak, G. and Solomon, K.R. (2008) Toxicity assessment of collected fractions from an extracted naphthenic acid mixture. *Chemosphere* 72(9), 1309-1314.
- Gamal El-Din, M., Fu, H., Wang, N., Chelme-Ayala, P., Pérez-Estrada, L., Drzewicz, P., Martin, J.W., Zubot, W. and Smith, D.W. (2011) Naphthenic acids speciation and removal during petroleum-coke adsorption and ozonation of oil sands process-affected water. *Science of the Total Environment* 409(23), 5119-5125.
- Gao B., Chu Y., Yue Q., Wang, B., and Wang S. (2005) Characterization and coagulation of a polyaluminum chloride (PAC) coagulant with high Al<sub>13</sub> content. *Journal of Environmental Management* 76(2), 143-147.
- Garcia-Garcia, E., Ge, J.Q., Oladiran, A., Montgomery, B., Gamal El-Din, M., Perez-Estrada, L.C., Stafford, J.L., Martin, J.W. and Belosevic, M. (2011) Ozone treatment ameliorates oil sands process water toxicity to the mammalian immune system. *Water Research* 45(18), 5849-5857.

- Ghernaout, D. and Naceur, M.W. (2011) Ferrate(VI): In situ generation and water treatment - A review. *Desalination and Water Treatment* 30(1-3), 319-332.
- Gottschalk, C., Libra, J.A. and Saupe, A. (2010) *Ozonation of water and waste water: A practical guide to understanding ozone and its applications*, Wiley, Weinheim.
- Green, J. R. (2011), Potassium ferrate. In *Encyclopedia of Reagents for Organic Synthesis*, John Wiley & Sons Inc., New York.
- Grewer, D.M., Young, R.F., Whittal, R.M. and Fedorak, P.M. (2010) Naphthenic acids and other acid-extractables in water samples from Alberta: What is being measured? *Science of The Total Environment* 408(23), 5997-6010.
- Hagen, M.O., Garcia-Garcia, E., Oladiran, A., Karpman, M., Mitchell, S., Gamal El-Din, M., Martin, J.W. and Belosevic, M. (2012) The acute and sub-chronic exposures of goldfish to naphthenic acids induce different host defense responses. *Aquatic Toxicology* 109, 143-149.
- He, Y., Patterson, S., Wang, N., Hecker, M., Martin, J.W., Gamal El-Din, M., Giesy, J.P. and Wiseman, S.B. (2012) Toxicity of untreated and ozone-treated oil sands process-affected water (OSPW) to early life stages of the fathead minnow (*Pimephales promelas*). *Water Research* 46(19), 6359-6368.
- He, Y., Wiseman, S.B., Hecker, M., Zhang, X., Wang, N., Perez, L.A., Jones, P.D., Gamal El-Din, M., Martin, J.W. and Giesy, J.P. (2011) Effect of ozonation on the estrogenicity and androgenicity of oil sands process-affected water. *Environmental Science & Technology* 45(15), 6268-6274.

- He, Y., Wiseman, S.B., Zhang, X., Hecker, M., Jones, P.D., Gamal El-Din, M., Martin, J.W. and Giesy, J.P. (2010) Ozonation attenuates the steroidogenic disruptive effects of sediment free oil sands process water in the H295R cell line. *Chemosphere* 80(5), 578-584.
- Headley, J.V., Barrow, M.P., Peru, K.M., Fahlman, B., Frank, R.A., Bickerton, G., McMaster, M.E., Parrott, J. and Hewitt, L.M. (2011) Preliminary fingerprinting of Athabasca oil sands polar organics in environmental samples using electrospray ionization Fourier transform ion cyclotron resonance mass spectrometry. *Rapid Communications in Mass Spectrometry* 25(13), 1899-1909.
- Headley, J.V., Kumar, P., Dalai, A., Peru, K.M., Bailey, J., McMartin, D.W., Rowland, S.M., Rodgers, R.P. and Marshall, A.G. (2015a) Fourier transform ion cyclotron resonance mass spectrometry characterization of treated Athabasca oil sands processed waters. *Energy & Fuels* 29(5), 2768-2773.
- Headley, J.V., Peru, K.M., Armstrong, S.A., Han, X., Martin, J.W., Mapolelo, M.M., Smith, D.F., Rogers, R.P. and Marshall, A.G. (2009) Aquatic plant-derived changes in oil sands naphthenic acid signatures determined by low-, high- and ultrahigh-resolution mass spectrometry. *Rapid Communications in Mass Spectrometry* 23(4), 515-522.
- Headley, J.V., Peru, K.M. and Barrow, M.P. (2015b) Advances in mass spectrometric characterization of naphthenic acids fraction compounds in

oil sands environmental samples and crude oil—a review. *Mass Spectrometry Reviews*, *In progress*.

Headley, J.V., Peru, K.M., Fahlman, B., McMartin, D.W., Mapolelo, M.M., Rodgers, R.P., Lobodin, V.V. and Marshall, A.G. (2012) Comparison of the levels of chloride ions to the characterization of oil sands polar organics in natural waters by use of Fourier transform ion cyclotron resonance mass spectrometry. *Energy & Fuels* 26(5), 2585-2590.

Headley, J.V., Peru, K.M., Mohamed, M.H., Wilson, L., McMartin, D.W., Mapolelo, M.M., Lobodin, V.V., Rodgers, R.P. and Marshall, A.G. (2014) Atmospheric pressure photoionization Fourier transform ion cyclotron resonance mass spectrometry characterization of tunable carbohydrate-based materials for sorption of oil sands naphthenic acids. *Energy & Fuels* 28(3), 1611-1616.

Hirsch, T. (2005) *Treasure in the sand : an overview of Alberta's oil sands resources*. Canada West Foundation, Calgary, Alberta.

Ho, C.M. and Lau, T.C. (2000) Lewis acid activated oxidation of alkanes by barium ferrate. *New Journal of Chemistry* 24(8), 587-590.

Hoigné, J. and Bader, H. (1983a) Rate constants of reactions of ozone with organic and inorganic compounds in water—I. *Water Research* 17(2), 173-183.

Hoigné, J. and Bader, H. (1983b) Rate constants of reactions of ozone with organic and inorganic compounds in water—II. *Water Research* 17(2), 185-194.

- Holleman, A.F., Wiber, E. and Wiberg, N. (2001) Holleman-Wiberg's Inorganic Chemistry, Academic Press, California.
- Holowenko, F.M., MacKinnon, M.D. and Fedorak, P.M. (2002) Characterization of naphthenic acids in oil sands wastewaters by gas chromatography-mass spectrometry. *Water Research* 36(11), 2843-2855.
- Hu, C., Liu, H., Qu, J., Wang, D. and Ru, J. (2006) Coagulation behavior of aluminum salts in eutrophic water: Significance of  $Al_{13}$  species and pH control. *Environmental Science & Technology* 40(1), 325-331.
- Hu, L., Martin, H.M., Arce-Bulted, O., Sugihara, M.N., Keating, K.A. and Strathmann, T.J. (2009) Oxidation of carbamazepine by Mn(VII) and Fe(VI): Reaction kinetics and mechanism. *Environmental Science & Technology* 43(2), 509-515.
- Huang, C., Shi, Y., Gamal El-Din, M. and Liu, Y. (2015a) Treatment of oil sands process-affected water (OSPW) using ozonation combined with integrated fixed-film activated sludge (IFAS). *Water Research* 85, 167-176.
- Huang, H., Sommerfeld, D., Dunn, B.C., Eyring, E.M. and Lloyd, C.R. (2001) Ferrate(VI) oxidation of aqueous phenol: Kinetics and mechanism. *Journal of Physical Chemistry A* 105(14), 3536-3541.
- Huang, H., Sommerfeld, D., Dunn, B.C., Lloyd, C.R. and Eyring, E.M. (2001) Ferrate(VI) oxidation of aniline. *Journal of the Chemical Society, Dalton Transactions* (8), 1301-1305.
- Huang, R., McPhedran, K.N. and Gamal El-Din, M. (2015) Ultra performance liquid chromatography ion mobility time-of-flight mass spectrometry

- characterization of naphthenic acids species from oil sands process-affected water. *Environmental Science & Technology* 49(19):11737-45
- Hwang, G., Dong, T., Islam, M.S., Sheng, Z., Perez-Estrada, L.A., Liu, Y. and Gamal El-Din, M. (2013) The impacts of ozonation on oil sands process-affected water biodegradability and biofilm formation characteristics in bioreactors. *Bioresource Technology* 130, 269-277.
- Islam, M.S., Dong, T., Sheng, Z., Zhang, Y., Liu, Y. and Gamal El-Din, M. (2014) Microbial community structure and operational performance of a fluidized bed biofilm reactor treating oil sands process-affected water. *International Biodeterioration & Biodegradation* 91(0), 111-118.
- Islam, M.S., Zhang, Y., McPhedran, K.N., Liu, Y. and Gamal El-Din, M. (2016) Mechanistic investigation of industrial wastewater naphthenic acids removal using granular activated carbon (GAC) biofilm based processes. *Science of The Total Environment* 541, 238-246.
- Jiang, J.Q. (2014) Advances in the development and application of ferrate(VI) for water and wastewater treatment. *Journal of Chemical Technology & Biotechnology* 89(2), 165-177.
- Jones, D., Scarlett, A.G., West, C.E., Frank, R.A., Gieleciak, R., Hager, D., Pureveen, J., Tegelaar, E. and Rowland, S.J. (2013) Elemental and spectroscopic characterization of fractions of an acidic extract of oil sands process water. *Chemosphere* 93(9), 1655-1664.

- Jones, D., Scarlett, A.G., West, C.E. and Rowland, S.J. (2011) Toxicity of individual naphthenic acids to *Vibrio fischeri*. Environmental Science & Technology 45(22), 9776-9782.
- Jones, D., West, C.E., Scarlett, A.G., Frank, R.A. and Rowland, S.J. (2012) Isolation and estimation of the aromatic' naphthenic acid content of an oil sands process-affected water extract. Journal of Chromatography A 1247, 171-175.
- Kannel, P.R. and Gan, T.Y. (2012) Naphthenic acids degradation and toxicity mitigation in tailings wastewater systems and aquatic environments: A review. Journal of Environmental Science and Health, Part A 47(1), 1-21.
- Kavanagh, R.J., Frank, R.A., Burnison, B.K., Young, R.F., Fedorak, P.M., Solomon, K.R. and Van, D.K.G. (2012) Fathead minnow (*Pimephales promelas*) reproduction is impaired when exposed to a naphthenic acid extract. Aquatic Toxicology 116-117, 34-42.
- Kim, E.-S., Liu, Y. and Gamal, E.-D.M. (2013) An *in-situ* integrated system of carbon nanotubes nanocomposite membrane for oil sands process-affected water treatment. Journal of Membrane Science 429, 418-427.
- Kimura, M., Matsui, Y., Kondo, K., Ishikawa, T.B., Matsushita, T. and Shirasaki, N. (2013) Minimizing residual aluminum concentration in treated water by tailoring properties of polyaluminum coagulants. Water Research 47(6), 2075-2084.
- Kishore Nadkarni, R.A. (2011) Spectroscopic analysis of petroleum products and lubricants, ASTM International, Pennsylvania.

- Klamerth, N., Moreira, J., Li, C., Singh, A., McPhedran, K.N., Chelme-Ayala, P., Belosevic, M. and Gamal El-Din, M. (2015) Effect of ozonation on the naphthenic acids' speciation and toxicity of pH-dependent organic extracts of oil sands process-affected water. *Science of The Total Environment* 506–507(0), 66-75.
- Kupryianchyk, D., Rakowska, M.I., Grotenhuis, J.T.C. and Koelmans, A.A. (2012) Modeling trade-off between PAH toxicity reduction and negative effects of sorbent amendments to contaminated sediments. *Environmental Science & Technology* 46(9), 4975-4984.
- Larson, R. and Weber, E. (1994) Reaction mechanisms in environmental organic chemistry, pp. 275-358, Lewis Publishers, Florida.
- Lee, J.H., Landrum, P.F. and Koh, C.H. (2002) Toxicokinetics and time-dependent PAH toxicity in the amphipod *Hyaella azteca*. *Environmental Science & Technology* 36(14), 3124-3130.
- Leishman, C., Widdup, E.E., Quesnel, D.M., Chua, G., Gieg, L.M., Samuel, M.A. and Muench, D.G. (2013) The effect of oil sands process-affected water and naphthenic acids on the germination and development of Arabidopsis. *Chemosphere* 93(2), 380-387.
- Lengger, S.K., Scarlett, A.G., West, C.E. and Rowland, S.J. (2013) Diamondoid diacids ('O<sub>4</sub>' species) in oil sands process-affected water. *Rapid Communications in Mass Spectrometry* 27(23), 2648-2654.

- Leshuk, T., Wong, T., Linley, S., Peru, K.M., Headley, J.V. and Gu, F. (2016) Solar photocatalytic degradation of naphthenic acids in oil sands process-affected water. *Chemosphere* 144, 1854-1861.
- Li, M., Barbour, S.L. and Si, B.C. (2015) Measuring solid percentage of oil sands mature fine tailings using the dual probe heat pulse method. *Journal of Environmental Quality* 44(1), 293-298.
- Liang, X., Zhu, X. and Butler, E.C. (2011) Comparison of four advanced oxidation processes for the removal of naphthenic acids from model oil sands process water. *Journal of Hazardous Materials* 190(1-3), 168-176.
- Licht, S.; Yu, X. (2008) Recent Advances in Fe(VI) Synthesis. In *Ferrates*, American Chemical Society; Vol. 985, pp 2-51.
- Luo, Z., Strouse, M., Jiang, J.Q. and Sharma, V.K. (2011) Methodologies for the analytical determination of ferrate(VI): A Review. *Journal of Environmental Science and Health - Part A Toxic/Hazardous Substances and Environmental Engineering* 46(5), 453-460.
- Mackinnon, M.; Zubot, W., (2013) Chapter 10: Water management. In *Handbook on theory and practice of bitumen recovery from Athabasca oil sands Volume II: Industrial practices*, Czarnecki, J.; Masliyah, J.; Xu, Z.; Dabros, M., Eds. Kingsley Knowledge Publishing: Alberta.
- Majid, A. and Pihillagawa, I. (2014) Potential of NMR spectroscopy in the characterization of nonconventional Oils. *Journal of Fuels* Volume 2014, Article ID 390261.

- Marentette, J.R., Frank, R.A., Hewitt, L.M., Gillis, P.L., Bartlett, A.J., Brunswick, P., Shang, D. and Parrott, J.L. (2015) Sensitivity of walleye (*Sander vitreus*) and fathead minnow (*Pimephales promelas*) early-life stages to naphthenic acid fraction components extracted from fresh oil sands process-affected waters. *Environmental Pollution* 207, 59-67.
- Martin, J.W., Barri, T., Han, X., Fedorak, P.M., Gamal El-Din, M., Perez, L., Scott, A.C. and Jiang, J.T. (2010) Ozonation of oil sands process-affected water accelerates microbial bioremediation. *Environmental Science and Technology* 44(21), 8350-8356.
- Masliyah, J.H., Xu, Z. and Czarnecki, J.A. (2011) Handbook on theory and practice of bitumen recovery from Athabasca oil sands, Kingsley Publishing Services, Alberta.
- Mikula, R.J., Kasperski, K.L., Burns, R.D. and MacKinnorr, M.D. (1996) Nature and fate of oil sands fine tailings. *Advances in Chemistry Series* 251, 718-723.
- Mohamed, M.H., Wilson, L.D., Peru, K.M. and Headley, J.V. (2013) Colloidal properties of single component naphthenic acids and complex naphthenic acid mixtures. *Journal of Colloid and Interface Science* 395(0), 104-110.
- Morandi, G.D., Wiseman, S.B., Pereira, A., Mankidy, R., Gault, I.G.M., Martin, J.W. and Giesy, J.P. (2015) Effects-directed analysis of dissolved organic compounds in oil sands process-affected water. *Environmental Science & Technology* 49(20), 12395-12404.

- Moustafa, A.M.A., McPhedran, K.N., Moreira, J. and Gamal El-Din, M. (2014) Investigation of Mono/competitive adsorption of environmentally relevant ionized weak acids on graphite: impact of molecular properties and thermodynamics. *Environmental Science & Technology* 48(24), 14472-14480.
- Nero, V., Farwell, A., Lee, L.E.J., Van, M.T., MacKinnon, M.D. and Dixon, D.G. (2006) The effects of salinity on naphthenic acid toxicity to yellow perch: Gill and liver histopathology. *Ecotoxicology and Environmental Safety* 65(2), 252-264.
- Ninane, L., Kanari, N., Criado, C., Jeannot, C., Evrard, O. and Neveux, N. (2008) New processes for alkali ferrate synthesis. In *Ferrates*, pp. 102-111, American Chemical Society.
- Nyakas, A., Han, J., Peru, K.M., Headley, J.V. and Borchers, C.H. (2013) Comprehensive analysis of oil sands processed water by direct-infusion fourier-transform ion cyclotron resonance mass spectrometry with and without offline UHPLC sample prefractionation. *Environmental Science and Technology* 47(9), 4471-4479.
- Oppenländer, T. (2007) Photochemical purification of water and air: advanced oxidation processes (AOPs) - principles, reaction mechanisms, reactor concepts, Wiley, Weinheim.
- Pereira, A.S., Bhattacharjee, S. and Martin, J.W. (2013a) Characterization of oil sands process-affected waters by liquid chromatography orbitrap mass spectrometry. *Environmental Science & Technology* 47(10), 5504-5513.

- Pereira, A.S., Islam, M.S., Gamal El-Din, M. and Martin, J.W. (2013) Ozonation degrades all detectable organic compound classes in oil sands process-affected water; an application of high-performance liquid chromatography/obitrap mass spectrometry. *Rapid Communications in Mass Spectrometry* 27(21), 2317-2326.
- Pérez-Estrada, L.A., Han, X., Drzewicz, P., Gamal El-Din, M., Fedorak, P.M. and Martin, J.W. (2011) Structure-reactivity of naphthenic acids in the ozonation process. *Environmental Science & Technology* 45(17), 7431-7437.
- Pourrezaei, P., Alpatova, A., Khosravi, K., Drzewicz, P., Chen, Y., Chelme-Ayala, P. and Gamal El-Din, M. (2014) Removal of organic compounds and trace metals from oil sands process-affected water using zero valent iron enhanced by petroleum coke. *Journal of Environmental Management* 139(0), 50-58.
- Pourrezaei, P., Drzewicz, P., Wang, Y., Gamal El-Din, M., Perez-Estrada, L.A., Martin, J.W., Anderson, J., Wiseman, S., Liber, K. and Giesy, J.P. (2011) The impact of metallic coagulants on the removal of organic compounds from oil sands process-affected water. *Environmental Science & Technology* 45(19), 8452-8459.
- Pourrezaei, P., Drzewicz, P., Wang, Y., Gamal El-Din, M., Perez-Estrada, L.A., Martin, J.W., Anderson, J., Wiseman, S., Liber, K. and Giesy, J.P. (2011) The impact of metallic coagulants on the removal of organic compounds

- from oil sands process-affected water. *Environmental Science & Technology* 45(19), 8452-8459.
- Quagraine, E.K., Peterson, H.G. and Headley, J.V. (2005) *In situ* bioremediation of naphthenic acids contaminated tailing pond waters in the Athabasca oil sands region - Demonstrated field studies and plausible options: A review. *Journal of Environmental Science and Health - Part A Toxic/Hazardous Substances and Environmental Engineering* 40(3), 685-722.
- Quesnel, D.M., Oldenburg, T.B.P., Larter, S.R., Gieg, L.M. and Chua, G. (2015) Biostimulation of oil sands process-affected water with phosphate yields removal of sulfur-containing organics and detoxification. *Environmental Science & Technology* 49(21), 13012-13020.
- Reinardy, H.C., Scarlett, A.G., Henry, T.B., West, C.E., Hewitt, L.M., Frank, R.A. and Rowland, S.J. (2013) Aromatic naphthenic acids in oil sands process-affected water, resolved by GCxGC-MS, only weakly induce the gene for vitellogenin production in zebrafish (*Danio rerio*) larvae. *Environmental Science & Technology* 47(12), 6614-6620.
- Rogers, V.V., Wickstrom, M., Liber, K. and MacKinnon, M.D. (2002) Acute and subchronic mammalian toxicity of naphthenic acids from oil sands tailings. *Toxicological Sciences* 66(2), 347-355.
- Ross, M.S., Pereira, A.d.S., Fennell, J., Davies, M., Johnson, J., Sliva, L. and Martin, J.W. (2012) Quantitative and qualitative analysis of naphthenic acids in natural waters surrounding the Canadian oil sands industry. *Environmental Science & Technology* 46(23), 12796-12805.

- Rowland, S.J., Pereira, A.S., Martin, J.W., Scarlett, A.G., West, C.E., Lengger, S.K., Wilde, M.J., Pureveen, J., Tegelaar, E.W., Frank, R.A. and Hewitt, L.M. (2014) Mass spectral characterisation of a polar, esterified fraction of an organic extract of an oil sands process water. *Rapid Communications in Mass Spectrometry* 28(21), 2352-2362.
- Rowland, S.J., West, C.E., Jones, D., Scarlett, A.G., Frank, R.A. and Hewitt, L.M. (2011) Steroidal aromatic 'naphthenic acids' in oil sands process-affected water: structural comparisons with environmental estrogens. *Environmental Science & Technology* 45(22), 9806-9815.
- Sawyer, C., McCarty, P. and Parkin, G. (2003) *Chemistry for environmental engineering and science*, McGraw-Hill Education, New York.
- Sayles, G.D., Acheson, C.M., Kupferle, M.J., Shan, Y., Zhou, Q., Meier, J.R., Chang, L. and Brenner, R.C. (1999) Land treatment of PAH-contaminated soil: Performance measured by chemical and toxicity assays. *Environmental Science & Technology* 33(23), 4310-4317.
- Scarlett, A.G., Reinardy, H.C., Henry, T.B., West, C.E., Frank, R.A., Hewitt, L.M. and Rowland, S.J. (2013) Acute toxicity of aromatic and non-aromatic fractions of naphthenic acids extracted from oil sands process-affected water to larval zebrafish. *Chemosphere* 93(2), 415-420.
- Schindler, P.W. and Stumm, W. (1987) *Aquatic surface chemistry: chemical processes at the particle-water interface*. Stumm, W. (ed), pp. 83-110, John Wiley and Sons, New York.

- Sharma, V.K., Noorhasan, N.N., Mishra, S.K. and Nesnas, N. (2008) Ferrate(VI) oxidation of recalcitrant compounds: Removal of biological resistant organic molecules by ferrate(VI). In *Ferrates*, pp. 339-349, American Chemical Society.
- Sharma, V.K. and Mishra, S. (2006) Ferrate(VI) oxidation of ibuprofen: A kinetic study. *Environmental Chemistry Letters* 3(4), 182-185.
- Sharma, V.K. (2002) Potassium ferrate(VI): An environmentally friendly oxidant. *Advances in Environmental Research* 6(2), 143-156.
- Sharma, V.K. (2013) Ferrate(VI) and ferrate(V) oxidation of organic compounds: Kinetics and mechanism. *Coordination Chemistry Reviews* 257(2), 495-510.
- Sharma, V.K. and Bielski, B.H.J. (1991) Reactivity of ferrate(VI) and ferrate(V) with amino acids. *Inorganic Chemistry* 30(23), 4306-4310.
- Sharma, V.K., Mishra, S.K. and Nesnas, N. (2006) Oxidation of sulfonamide antimicrobials by ferrate(VI)  $[\text{Fe}^{\text{VI}}\text{O}_4^{2-}]$ . *Environmental Science & Technology* 40(23), 7222-7227.
- Sharma, V.K., Smith, J.O. and Millero, F.J. (1997) Ferrate(VI) oxidation of hydrogen sulfide. *Environmental Science & Technology* 31(9), 2486-2491.
- Shi, Y., Huang, C., Rocha, K.C., Gamal El-Din, M. and Liu, Y. (2015) Treatment of oil sands process-affected water using moving bed biofilm reactors: With and without ozone pretreatment. *Bioresource Technology* 192(0), 219-227.

- Shu, Z., Bolton, J.R., Belosevic, M. and Gamal El-Din, M. (2013) Photodegradation of emerging micropollutants using the medium-pressure UV/H<sub>2</sub>O<sub>2</sub> advanced oxidation process. *Water Research* 47(8), 2881-2889.
- Shu, Z., Li, C., Belosevic, M., Bolton, J.R. and Gamal El-Din, M. (2014) Application of a solar UV/chlorine advanced oxidation process to oil sands process-affected water remediation. *Environmental Science and Technology* 48(16), 9692-9701.
- Siefert, K.S. (2000) Polyaluminum chlorides. In *Kirk-Othmer encyclopedia of chemical technology*, John Wiley & Sons Inc., New York.
- Singh, A., Havixbeck, J.J., Smith, M.K., Shu, Z., Tierney, K.B., Barreda, D.R., Gamal El-Din, M. and Belosevic, M. (2015) UV and hydrogen peroxide treatment restores changes in innate immunity caused by exposure of fish to reuse water. *Water Research* 71, 257-273.
- Sobkowicz, J. (2010) History and developments in the treatment of oil sands fine tailings. In *Tailings and mine waste 2010*, The Organizing Committee of the 14th International Conference on Tailings and Mine Waste, Eds. CRC Press, Florida.
- Speight, J.G. (2000) *Kirk-Othmer encyclopedia of chemical technology*, John Wiley & Sons Inc., New York.
- Stanford, L.A., Kim, S., Klein, G.C., Smith, D.F., Rodgers, R.P. and Marshall, A.G. (2007) Identification of water-soluble heavy crude oil organic-acids, bases, and neutrals by electrospray ionization and field desorption

- ionization Fourier transform ion cyclotron resonance mass spectrometry. *Environmental Science & Technology* 41(8), 2696-2702.
- Stewart, T.A., Trudell, D.E., Alam, T.M., Ohlin, C.A., Lawler, C., Casey, W.H., Jett, S. and Nyman, M. (2009) Enhanced water purification: A single atom makes a difference. *Environmental Science & Technology* 43(14), 5416-5422.
- Stone, W., Yang, H. and Qui, M. (2005) Assays for nitric oxide expression. In *Mast Cells*. Krishnaswamy, G. and Chi, D. (eds), pp. 245-256, Humana Press, New York.
- Stumm, W. and Morgan, J.J. (1996) *Aquatic chemistry: chemical equilibria and rates in natural waters*, John Wiley & Sons Inc., New York.
- Sun, N., Chelme-Ayala, P., Klammerth, N., McPhedran, K.N., Islam, M.S., Perez-Estrada, L., Drzewicz, P., Blunt, B.J., Reichert, M., Hagen, M., Tierney, K.B., Belosevic, M. and Gamal El-Din, M. (2014) Advanced analytical mass spectrometric techniques and bioassays to characterize untreated and ozonated oil sands process-affected water. *Environmental Science & Technology* 48(19), 11090-11099.
- Tang, H. (2006) *Inorganic polymer flocculation theory and the flocculants*, China Architecture & Building Press, Beijing.
- Thompson, G.W., Ockerman, L.T. and Schreyer, J.M. (1951) Preparation and purification of potassium Ferrate(VI). *Journal of the American Chemical Society* 73(3), 1379-1381.

- Tuan Vo, D. (1978) Multicomponent analysis by synchronous luminescence spectrometry. *Analytical Chemistry* 50(3), 396-401.
- von Sonntag, C. and von Gunten, U. (2012) *Chemistry of ozone in water and wastewater treatment: from basic principles to applications*, IWA Publishing, London
- Wakeham, S.G. (1977) Synchronous fluorescence spectroscopy and its application to indigenous and petroleum-derived hydrocarbons in lacustrine sediments. *Environmental Science & Technology* 11(3), 272-276.
- Wang, C., Alpatova, A., McPhedran, K.N. and Gamal El-Din, M. (2015) Coagulation/flocculation process with polyaluminum chloride for the remediation of oil sands process-affected water: Performance and mechanism study. *Journal of Environmental Management* 160, 254-262.
- Wang, D., Sun, W., Xu, Y., Tang, H. and Gregory, J. (2004) Speciation stability of inorganic polymer flocculant-PACl. *Colloids and Surfaces A: Physicochemical and Engineering Aspects* 243(1-3), 1-10.
- Wang, D., Tang, H. and Gregory, J. (2002) Relative importance of charge neutralization and precipitation on coagulation of kaolin with PACl: Effect of sulfate ion. *Environmental Science & Technology* 36(8), 1815-1820.
- Wang, D., Wang, S., Huang, C. and Chow, C.W.K. (2011) Hydrolyzed Al(III) clusters: Speciation stability of nano-Al<sub>13</sub>. *Journal of Environmental Sciences* 23(5), 705-710.

- Wang, N., Chelme-Ayala, P., Perez-Estrada, L., Garcia-Garcia, E., Pun, J., Martin, J.W., Belosevic, M. and Gamal El-Din, M. (2013) Impact of ozonation on naphthenic acids speciation and toxicity of oil sands process-affected water to *Vibrio fischeri* and mammalian immune system. *Environmental Science & Technology* 47(12), 6518-6526.
- Wang, Y. (2011) Application of coagulation-flocculation process for treating oil sands process-affected water. M.Sc., University of Alberta, Edmonton, Alberta.
- Wardman, P. (1989) Reduction potentials of one-electron couples involving free radicals in aqueous solution. *Journal of Physical and Chemical Reference Data* 18(4), 1637-1755.
- Wiberg, K.B. and Foster, G. (1961) The stereochemistry of the chromic acid oxidation of tertiary hydrogens<sup>1</sup>. *Journal of the American Chemical Society* 83(2), 423-429.
- Williams, A.T.R., Winfield, S.A. and Miller, J.N. (1983) Relative fluorescence quantum yields using a computer-controlled luminescence spectrometer. *Analyst* 108(1290), 1067-1071.
- Wiseman, S.B., He, Y., Gamal El-Din, M., Martin, J.W., Jones, P.D., Hecker, M. and Giesy, J.P. (2013) Transcriptional responses of male fathead minnows exposed to oil sands process-affected water. *Comparative Biochemistry and Physiology Part C: Toxicology & Pharmacology* 157(2), 227-235.

- Wu, Z., Zhang, P., Zeng, G., Zhang, M. and Jiang, J. (2012) Humic acid removal from water with polyaluminum coagulants: effect of sulfate on aluminum polymerization. *Journal of Environmental Engineering* 138(3), 293-298.
- Xue, J., Zhang, Y., Liu, Y. and Gamal El-Din, M. (2016) Treatment of oil sands process-affected water (OSPW) using a membrane bioreactor with a submerged flat-sheet ceramic microfiltration membrane. *Water Research* 88, 1-11.
- Yan, M., Wang, D., Yu, J., Ni, J., Edwards, M. and Qu, J. (2008) Enhanced coagulation with polyaluminum chlorides: Role of pH/alkalinity and speciation. *Chemosphere* 71(9), 1665-1673.
- Yang, Z., Gao, B., Cao, B., Xu, W. and Yue, Q. (2011) Effect of  $\text{OH}^-/\text{Al}^{3+}$  ratio on the coagulation behavior and residual aluminum speciation of polyaluminum chloride (PAC) in surface water treatment. *Separation and Purification Technology* 80(1), 59-66.
- Zhang, K., Pereira, A.S. and Martin, J.W. (2015) Estimates of octanol-water partitioning for thousands of dissolved organic species in oil sands process-affected water. *Environmental Science & Technology* 49(14), 8907-8913.
- Zhang, Y., McPhedran, K.N. and Gamal El-Din, M. (2015) Pseudomonads biodegradation of aromatic compounds in oil sands process-affected water. *Science of The Total Environment* 521-522, 59-67.
- Zimmermann, S.G., Schmukat, A., Schulz, M., Benner, J., Gunten, U.V. and Ternes, T.A. (2012) Kinetic and mechanistic investigations of the

oxidation of tramadol by ferrate and ozone. *Environmental Science & Technology* 46(2), 876-884.

Zubot, W., MacKinnon, M.D., Chelme-Ayala, P., Smith, D.W. and Gamal El-Din, M. (2012) Petroleum coke adsorption as a water management option for oil sands process-affected water. *Science of The Total Environment* 427-428, 364-372.

Zubot, W.A. (2010) Removal of naphthenic acids from oil sands process water using petroleum coke. M.Sc., University of Alberta, Edmonton, Alberta.